Transdermal iontophoresis of dopaminergic (pro) drugs : from formulation to in vivo application

Ackaert, O.

Transdermal iontophoresis of dopaminergic (pro)drugs:

From formulation to *in vivo* application

Oliver Ackaert

Transdermal iontophoresis of dopaminergic (pro)drugs:

From formulation to *in vivo* application

Oliver Ackaert

PhD thesis with summary in Dutch

April 2010

ISBN: 978-90-9025318-3

Printed by Wöhrmann Print Service (Zutphen, The Netherlands)

Transdermal iontophoresis of dopaminergic (pro)drugs:

From formulation to *in vivo* application

Proefschrift

ter verkrijging van
de graad van Doctor aan de Universiteit Leiden,
op gezag van Rector Magnificus prof.mr. P.F. van der Heijden,
volgens besluit van het College van Promoties
te verdedigen op woensdag 28 april 2010
klokke 13.45 uur

door

Oliver Ackaert
geboren te Turnhout, België
in 1981

Promotiecommissie

Promotoren:	Prof. Dr. J.A. Bouwstra
	Prof. Dr. M. Danhof
Overige leden:	Prof. Dr. A.P. IJzerman
	Prof. Dr. J.J. van Hilten
	Prof. Dr. T. Hankemeier
	Prof. Dr. R.H. Guy (University of Bath)

The investigations described in this thesis were performed at the Division of Drug Delivery Technology of the Leiden/Amsterdam Center for Drug Research, Leiden University, Leiden, The Netherlands. The studies were financed by the Dutch Technology Foundation (STW LKG6507)

The publication of this thesis was financially supported by the Dutch Technology Foundation and the Leiden/Amsterdam Center for Drug Research

Table of contents

Chapter 1 Symptomatic treatment of Parkinson's disease: role of transdermal iontophoresis of dopamine agonists 1

Chapter 2 Objective and outline of the thesis 31

***Part I**-Optimizing the in vitro transdermal iontophoretic delivery of dopaminergic drugs*

Chapter 3 Mechanistic studies of the transdermal iontophoretic delivery of 5-OH-DPAT *in vitro* 41

Chapter 4 Comparing different salt forms of rotigotine to improve transdermal iontophoretic delivery 63

Chapter 5 Transdermal iontophoresis of a novel series of dopamine agonists: physicochemical considerations 85

***Part II**-In vivo assessment of controlling the iontophoretic delivery of (S)-5-OH-DPAT*

Chapter 6 Controlling the pharmacokinetics and the pharmacodynamic effect of (S)-5-OH-DPAT with transdermal iontophoresis 115

***Part III**-Transdermal iontophoretic delivery of ester prodrugs of 5-OH-DPAT: from synthesis to in vivo studies*

Chapter 7 Controlling the pharmacokinetics and the pharmacodynamic effect of (S)-5-OH-DPAT with transdermal iontophoresis 149

Chapter 8 Summary, conclusions and perspectives 181

Appendix

Samenvatting 203

List of abbreviations 215

List of publications 219

Curriculum Vitae 221

Nawoord 223

1

Symptomatic treatment of Parkinson's disease:

The role of transdermal iontophoretic delivery of dopamine agonists

1 Introduction

Parkinson's disease (Pd) is an age-related neurodegenerative disorder. Pharmacotherapy is the first line symptomatic treatment of this neurological disease [1]. Currently Levodopa is still considered the drug of first choice, but its suspected neurotoxicity and the induction of movement disability after chronic use demand for alternative therapies.

An attractive alternative is the use of (semi-)synthetic dopamine agonists. It has been suggested that continuous dopamine receptor stimulation is the best symptomatic treatment of Parkinson's disease [2-4]. Therefore the administration of dopamine agonists in a continuous, well-controlled manner by transdermal iontophoresis is an attractive therapeutic strategy in the symptomatic treatment of Parkinson's disease. In addition, by modulation of the current density and the donor concentration of the drug it will be possible to adjust the rate of administration to the requirements of the individual patient.

This thesis describes the investigation and optimization of the transdermal iontophoretic delivery of novel dopaminergic (pro)drugs for the symptomatic treatment of Parkinson's disease. In this chapter, firstly the current strategy for the treatment of Pd is discussed. Secondly the role of transdermal iontophoretic delivery of dopamine agonists in the symptomatic treatment of Pd is addressed. Thirdly, the use of compartmental modeling in drug development for transdermal iontophoresis is reviewed.

2 Current strategies for the treatment of Parkinson's disease

2.1 The condition

Parkinson's disease, first described in 1817 as 'shaking palsy' by James Parkinson, is an age-related neurodegenerative movement disorder with a prevalence in Europe of 1.28-1.50 % in the age group above 60 [6]. This number will increase in the coming decades, since the life expectancy is augmenting and the 'grey' population is expanding. Pd has a world-wide distribution and has no gender preference [4]. The mean age of onset of Pd is about 60 years, but in case of young-onset Pd and juvenile-onset Pd, symptoms already may occur at the age of 21 to 40 years, and occasionally even earlier [2].

The clinical character of Pd is described by four cardinal features: resting tremor, rigidity, bradykinesia or slowness of movement, and gait disturbance with postural

instability. In addition Pd, mainly considered as a movement disorder, is often accompanied by nonmotor features including autonomic dysfunction, sleep disturbances, depression, addiction, dementia, speech problems, dysphagia, micrographia and hyposmia…[1, 3].

The causes of Pd are still not fully understood, but several studies on inherited parkinsonisms and studies with transgenic Pd-like animal models suggest that the aetiology of this disease lies within the complex interaction between multiple cellular factors, including genetic influences on cellular mechanism, together with exposure to environmental toxins and the unique vulnerability of the dopamine neurons in the substantia nigra [7]. The understanding of the involvement of genetic factors in the aetiology of Pd has been strengthened by the discovery of 13 genetic loci and 9 pathogenic genes. Their involvement in Parkinson's disease, however, is not completely clear [8-10]. Moreover it is currently believed that only 5% of all cases of Parkinson's disease have a genetic cause [1, 9]. Several environmental factors, especially long-term exposure to pesticides have been reported as risk factors for Pd. Furthermore an excess of vitamine E and viral and bacteriological infection have been associated with Pd, however proving evidence is still lacking [1]. Intriguingly smoking and intake of caffeine are believed to reduce the prevalence of the disease [11].

For many years it is known that the basal ganglia are involved in controlling and regulating voluntary movement. The basal ganglia, a group of subcortical nuclei, consist of the striatum (caudate and putamen), globus pallidus (interna and externa), substantia nigra (pars compacta and recticularis) and the subthalamic nucleus. Pathways from these nuclei form loops between the motor cortex and the motor thalamus. The first neurological hallmark of Pd is a degeneration of nigrostriatal dopaminergic neurons in the substantia nigra pars compacta (SNc) [12]. Therefore in patients with Pd the balance of the excitatory and inhibitory loops, which is modulated by the dopaminergic pathway from the substantia nigra, will be disturbed and will result via a pathway of overexcitation and excessive inhibition of the different basal nuclei in a reduced activity towards the motor cortex (Figure 1). As a consequence the conscious control of the skeletal muscles, controlled by the long axons of the neurons of the motor cortex, which project to the spinal cord, is disturbed. The second neurological feature of Pd is the presence of Lewy bodies, predominantly present in the brainstem. The exact role of these proteinaceous intracellular inclusions is currently under debate. It is unclear if Lewy bodies are a result of the disease or are involved in the cause of the pathology. It has been suggested that Lewy bodies are a results of a failed attempt to protect the damaged

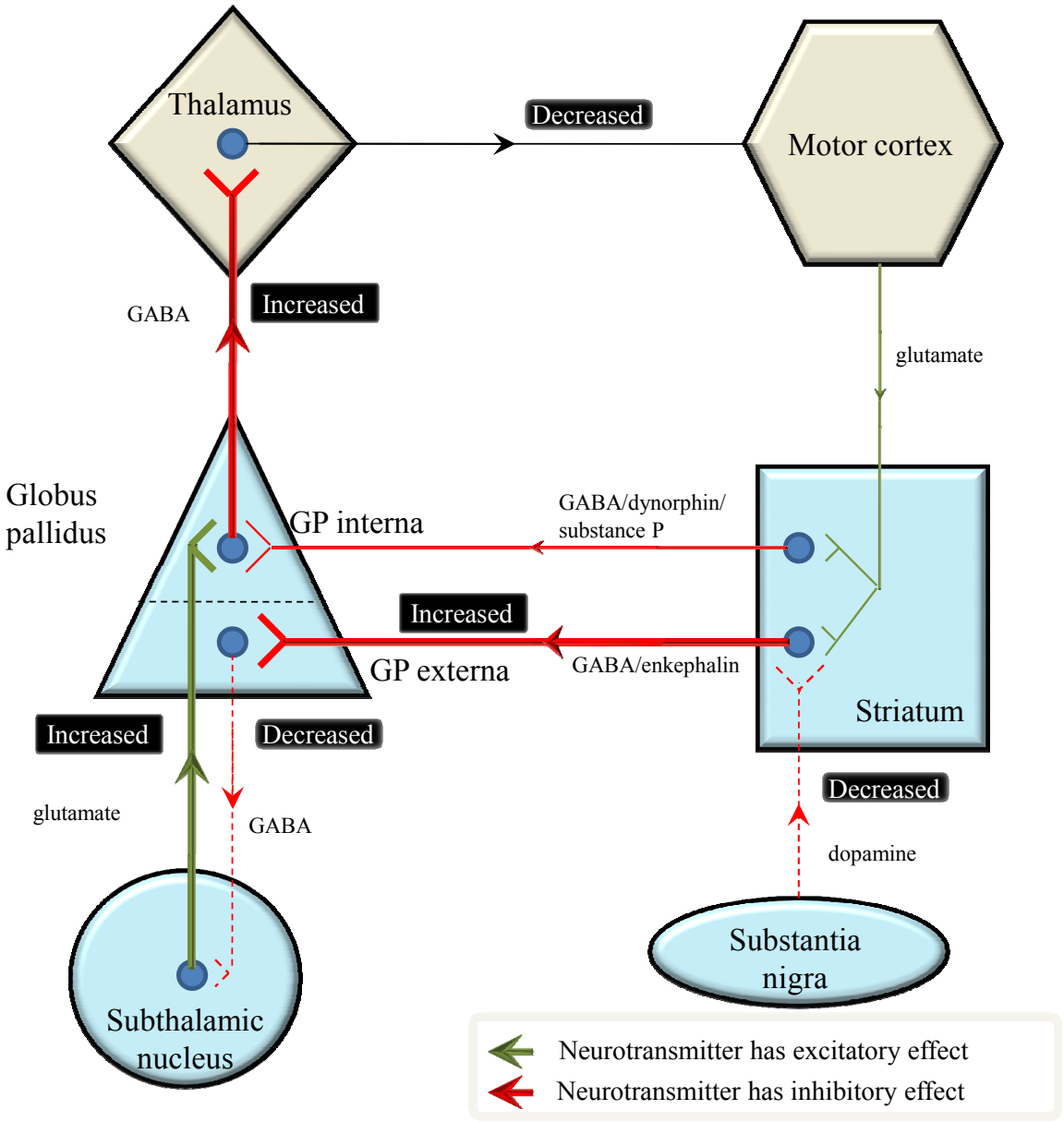

Figure 1: Diagram of the key neuronal pathways potentially involved in Parkinson's disease. Furthermore the changes in activity (increased activity: thick line; decreased activity: intermittent line) are indicated as a result of the reduction of the dopaminergic activity caused by Parkinson's disease. Figure was adapted from literature [1].

neurons against certain toxins [13]. Furthermore excessive quantities of toxic α-synuclein inside Lewy bodies may disturb the normal cell physiology, resulting in cell death [3, 14-15]. Contrastingly Lewy bodies may act as simple biomarker for neuronal cell loss, not actively involved in the pathophosiology of Pd. Lewy bodies are also found in patients with other neurodegenerative disorders, including

Alzheimer disease, progressive supranuclear palsy (PSP), multiple system atrophy (MSA) and dementia with Lewy Bodies (DLB).

The diagnosis of Pd is performed clinically and based on careful history taking and physical examination. Currently there are neither laboratory tests nor imaging techniques that can confirm with 100% certainty the diagnosis. The ultimate diagnosis can only be performed post mortem [16]. It can be very difficult to distinguish idiopathic Parkinson's disease from other certain neurological disorders, making the diagnosis of Pd very challenging. It has been estimated that around 10% of the patients are misdiagnosed [1, 17-18]. Especially in the early stages a lot of overlap can be observed between the features of Pd and other forms of parkinsonism. Since the proper diagnosis is essential for the prognosis and therapeutic treatment, the identification of a possible secondary cause of parkinsonian symptoms is essential. In practice 3 secondary causes of parkinsonian symptoms are considered for differentiation from Pd: essential tremor, drug induced parkinsonism and Parkinson's plus syndromes.

2.2 Current treatment of Parkinson's disease

The therapeutic strategy of Parkinson's disease is to minimize the effect of depletion of dopamine in the striatum. The two general approaches used in the clinic today for the symptomatic treatment of Pd are surgery and pharmacotherapy.

2.2.1 Surgical therapy

Because of the limitations of levodopa, improvements in stereotactic operative techniques, the use of microelectrode recording to more accurately define the target site, improved imaging and insights into the anatomical and physiological organization of the basal ganglia, surgery in the treatment of Pd has gained more interest in the last few years [4, 19]. Overactivity in the subthalamic nucleus, the globus pallidus and the thalamus results in inappropriate activity from the thalamus to the motor cortex and consequently development of the symptoms of Pd [1]. Two surgical approaches are currently applied to inactivate the particular region in the basal ganglia. Firstly ablation, a structural lesion in the brain, can provide some anti-dyskinetic benefits. Because of the irreversibility and the side effects (e.g. hemorrhage, damage to neighboring structures), associated with these techniques, physicians now prefer the second surgical approach, i.e. high-frequency deep brain stimulation (DBS). With this technique an electrode is implanted into the brain target. It is associated with marked benefits in reducing drug-induced motor fluctuations and dyskinesias. Furthermore a minimal morbidity is observed in

Parkinson patients that undergo this surgical procedure [20]. The use of DBS in patients with depression, dementia or other mental health problems is however not recommended. These therapies are only designed to compensate for damaged neuronal circuits and therefore used in advanced Pd [21].

The most recent evolution in surgery is the possible neuroprotective effect of cell based therapies and gene therapies. Cell based therapies aim to stimulate the production of intrinsic dopamine by transplanting dopamine-producing cells. Firstly, although the implantation of embryonic dopaminergic neurons has been proven to be successful in animal studies, up to now no double-blind trial has proven the benefit of cell based therapies over placebo [22-24]. Secondly though the use of stem cells may look promising, the research is still in an initial stage since stem cell transplantation in animal models did not show beneficial effects compared to fetal nigral transplantation [25-26]. Gene delivery, using viral vectors to introduce the desired protein DNA in the target region, is also actively being investigated as possible treatment for Pd [27]. In analogy to cell based therapies, no placebo controlled double-blind clinical trial, considered as the gold standard for evaluating a new therapy, can clearly confirm the safety and efficacy of gene therapy for the treatment of Pd [23, 28-29].

2.2.2 Pharmacological approach

As discussed above, surgery still compels certain risks and mostly is used only in the treatment of advanced Pd. This makes pharmacotherapy the first line treatment of Parkinson's disease. As no curative therapy has yet been discovered, the pharmacotherapeutic strategy is the symptomatic treatment of the disease. Usually pharmacotherapy is initiated with levodopa (combined with benserazide or cardidopa) as such or in combination with dopamine agonists. Although levodopa is most effective and still considered as the gold standard, it remains associated with serious motor complications after long term use [30-31]. This emphasizes the need for alternative therapies to treat the symptoms of Pd, certainly in the early stage of the disease. Up to date the most attractive alternative class of drugs are the dopamine agonists, which activate directly the dopamine receptor. Dopamine agonists can be divided into ergot derivatives (bromocriptine, pergolide, lisuride, cabergoline) and non-ergot derivatives (apomorphine, ropinirole, pramipexol, rotigotine) based on their molecular structure. Dopamine agonists have shown their efficacy as monotherapy and as adjunctive therapy for patients using levodopa. Several trials have shown that dopamine agonists can reduce the 'off' time and reduce or delay the use of levodopa [1]. In early stages of Pd, another class of drugs, monoamine oxidase

type (MAO-B) inhibitors, that stimulate the dopamine receptor indirectly by inhibiting the breakdown of dopamine, is also used. MAO-B inhibitors, such as selegiline, rasagaline and safinamide, can provide modest anti-parkinsonian effects and delay the use of levodopa [32-33]. Moreover this class of drugs gained more interest because of their possible, however not clinically proven, neuroprotection [34-36]. Less frequently used as monotherapy are catechol-O-methyltransferase (COMT) inhibitors, such as tolcapone and entecapone with the same working principle as MAO-B inhibitors. Finally because of their lack of efficacy and serious side effects, anticholinergics and amantadine are sparingly prescribed for Pd [1]. As Pd progresses, the need for therapy tailoring increases and becomes more challenging. Besides an increase in the severity of the symptoms, the management of the long term motor complications, caused by levodopa will play a central role in pharmacotherapy. For patients in an advanced state of Parkinson's disease a combination therapy of levodopa with dopamine agonists, MAO-B inhibitors or COMT inhibitors is used. Since levodopa and dopamine agonists are still the first choice in the treatment of early and advanced Pd, these compounds will be discussed in more detail in the next paragraphs.

2.3 Limitations of current pharmacotherapy

Since its introduction in the early 60's levodopa, a precursor for dopamine, remains the `gold standard` for the treatment of Pd [37]. To prevent side effects (such as nausea and vomiting), because of the peripheral metabolism of levodopa, levodopa is administered in combination with a peripheral decarboxylase inhibitor such as carbidopa or benserazide [38]. As mentioned earlier, levodopa is excellent in minimizing the symptoms of Pd and improves the activities of daily living, independence, employability and survival of the patient. However the use of levodopa has been put in question, because of its possible neurotoxicity and the induction of movement disorders after chronic long term use. Firstly *in vitro* toxicity studies showed that levodopa is able to degenerate cultured dopaminergic neurons, but in humans or animals no clear proof is given so far that levodopa is toxic [23, 39-40]. In some reports neuroprotection has even been suggested [40]. Secondly and more importantly it is generally believed that chronic treatment with L-dopa can cause dyskinesias and motor fluctuations, including a wearing off and on-off phenomenon in the later stages of the disease. 50-80 % of Pd patients, who have received this drug for 5 to 10 years, experience these complications following long term use [30-31]. A recent study Early *vs* Later Levodopa Therapy in Pd (ELLDOPA) showed that indeed higher doses result in greater clinical benefits, but pose a greater risk for developing motor complications [1, 23, 41]. These L-DOPA

associated complications are a source of severe disability for patients with Pd. Management of these motor complications is very difficult and requires individualized therapy [42]. Current strategy to manage these symptoms can be a combination of low and multiple doses of L-DOPA with or without a combination with dopamine agonists (DA) [42] or functional surgery [43]. Although dopamine agonist (e.g. bromocriptine, pergolide, cabergoline, pramipexole, ropinorole, rotigotine) may be less effective, these drugs are still less associated with motor complications after long term use when used as the initial treatment in early Pd [44-45]. This reduction in motor complication is associated with their increased half-lives and L-DOPA sparing effect.

2.4 Continuous dopaminergic stimulation

Under normal physiological conditions nigral neurons fire continuously, providing a constant level of dopamine in the striatum, resulting in a constant stimulation of the dopaminergic neurons [46-47]. In addition a re-uptake mechanism into pre-synaptic terminals functions as a buffer to external stimuli and ensures a constant extracellular dopamine concentration [46-47]. In Pd, there is a loss of nigral neurons and their striatal terminals that normally store and regulate the release of dopamine. As the disease progresses, the buffer capacity reduces and pulsatile stimulation of the dopamine receptors increases [47]. In addition to the pulsatile stimulation, the exposure to fluctuating levels of dopaminergic agents, is also believed to be responsible for the development of motor fluctuations[47-49]. This emphasizes the need for dopaminergic treatments that provide non-pulsatile stimulation and thus mimics the normal physiological state more closely. This therapeutic strategy is believed not only to reduce the dyskinesia and motor response disturbances, but also can provide a beneficial effect for other symptoms, like nocturnal disturbances [47].

2.5 Strategies for continuous dopaminergic stimulation

A continuous stimulation of dopamine receptors can be achieved by prolonging the activity of levodopa by modifying the release or the delivery of this short-acting dopaminergic agent. For this purpose oral sustained release formulations of levodopa Madopar HBS® and Sinemet CR®, were developed. These long-acting controlled release formulations showed improvement in activities of daily living of the patient, however not in controlling motor fluctuations [47, 50-51]. In addition the intake of small doses of a liquid formulation of levodopa/carbidopa improved the ’on’-time without worsening the dyskinesia, but did not affect the pulsatile levodopa plasma concentration or the motor response fluctuations [52]. In contrast clinical trials

showed an improvement in motor dysfunction after chronic IV infusion of levodopa [53]. A more recent small open-label clinical trial, in which continuous intravenous levodopa [54] was compared to oral administration, also shows a reduced risk of motor complications in the infusion group [55]. Besides IV infusion, duodenal infusion via a portable pump of low doses of levodopa ameliorates plasma fluctuations and dyskinesia with a satisfactory therapeutic window in advanced Pd patients [51, 56].

Dopamine agonists in general have significant longer half-lives compared to levodopa [57]. Several studies in patients have discovered that DA are less likely to induce motor fluctuations after chronic treatment. In addition some studies have suggested a neuroprotective effect of DA [50, 58-59]. Therefore this class of drugs has gained more popularity over the recent years as alternative to or in combination with levodopa. In accordance to the levodopa treatment, the current strategy is to achieve continuous stimulation of the dopamine receptors to reduce development of motor fluctuations. This led to the development of long-acting therapeutic formulations of DA. For instance the slow-release formulation of a dopamine agonist, bromocriptine, showed promising efficacy but has not been widely used in Parkinson's disease [51]. Furthermore ropinirole, formulated as extended release tablets, requires only one dose intake per day. The incidence of motor complications is reduced, while the adverse effects are comparable to other dopamine agonists [50, 60]. Although promising results were obtained with oral modified release formulations, other delivery routes were explored to achieve continuous drug delivery. Various routes of administration of apomorphine, a potent short acting dopamine agonist, have been investigated, but currently only subcutaneous infusion is used in clinical practice [61]. Apomorphine is useful in the treatment of acute and long term treatment of 'off'-periods and reduces the levodopa intake [50, 61]. Similar results were obtained with subcutaneous infusion of lisuride, an ergot dopamine agonist [62]. Skin nodules, however, were present in most patients after long term use, making this administration route for R-apomorhine and lisuride less attractive [63].

In summary there is a need for new delivery strategies for the symptomatic treatment of Pd that fulfill following requirements. Firstly, the drug delivery is continuous, resulting in continuous stimulation of the dopamine receptor. Secondly, the administration is non-invasive, reducing costs and inconvenience for the patient. Thirdly, the dose is easily adjustable to the demand of the therapy. Rapid dose changes are often required, certainly when initiating therapy. Fourthly, ideally the delivery device also includes a feedback system. During delivery, such a device also

monitors a relevant end-point/biomarker, which via a feedback system controls the drug delivery. As discussed earlier with oral delivery it is difficult to achieve a continuous administration. Moreover the aforementioned non-oral strategies to achieve a continuous delivery are invasive, cumbersome and inconvenient for the patient. This emphasizes the need for alternative non-invasive delivery methods that ideally can fulfill all the requirements stated in the previous paragraph.

3 Transdermal drug delivery of dopamine agonists

Transdermal iontophoretic delivery is an attractive alternative delivery technique to provide continuous delivery. Therefore transdermal iontophoretic delivery of dopamine agonist can be an interesting therapeutic strategy for the symptomatic treatment of Parkinson's disease.

3.1 Skin structure and skin barrier function

Transdermal delivery is the administration of the drug via the skin into the systemic circulation. Compared to oral and parental delivery, transdermal delivery has certain distinct advantages: 1) it offers the possibility for non-invasive delivery 2) it circumvents the first pass metabolism 3) this administration route can be beneficial for drugs that are sensitive to gastrointestinal degradation 4) transdermal delivery can be useful for therapeutics that are poorly absorbed via the GI tract, due to their physicochemical properties or due to disease progression 5) it can provide a sustained delivery during a longer period of time, increasing the applicability of the technique 6) it can deliver drugs with a zero order mass input, reducing plasma fluctuations.

However the barrier function of the skin challenges the design of transdermal therapeutic systems and limits the number of potential drug candidates for this administration route. The skin is the largest organ of the human body, comprises about 10% of the body mass and has a surface area of around 1.5 to 2.0 m^2 [64]. A typical square centimeter comprises 10 hair follicles, 12 nerves, 15 sebaceous glands, 100 sweat glands, 3 blood vessels with 92 cm total length, 360 cm of nerves and $3x10^6$ cells [65]. Two distinctive tissue layers can be found in human skin. The most upper layer is the stratified, avascular, cellular epidermis with the stratum basale, stratum spinosum, stratum granulosum, stratum lucidum and stratum corneum from the inner to the outermost layer. The epidermis is supported by a much thicker layer, the dermis. This layer consists of a matrix of connective tissue which is embedded in an amorphous substance of mucopolysaccharide. Blood vessels, nerves and

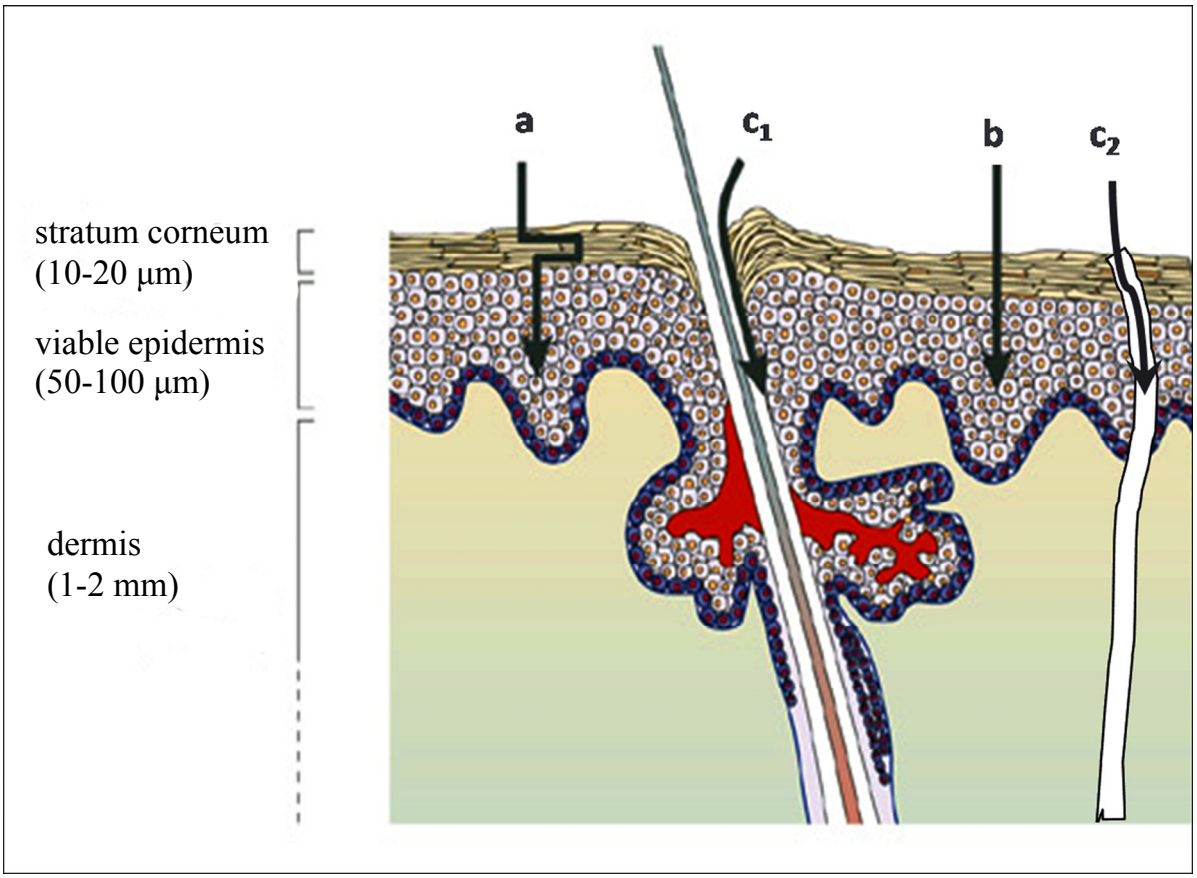

Figure 2: Graphical representation of the suggested transport pathways during transdermal transport: across the intact stratum cornuem via the intercellular route (a) or via the transcellular route (b) and the appendageal route via the hair follicles (c_1) or sweat pores (c_2). (This figure was adapted from ref. [5])

lymphatic vessels cross this matrix and skin appendages (sweat glands and pilosebaceous units) penetrate it. The lower side of the dermis is connected with the subcutaneous fat. Human skin displays two main types. The first type, hairy skin, encloses follicles and sebaceous glands, however no encapsulated sense organs. The second type, glabrous skin of the palms and the soles, consists mainly of thick epidermis with a compact and thick stratum corneum [65]. The stratum corneum, the outermost layer of the skin, is very lipophilic and forms the main barrier, protecting the body from water loss and penetration of exogenous agents. The stratum corneum or horny layer consists of corneocytes embedded in a highly organized lipid matrix

in a brick and mortar like structure [66]. Both the corneocytes and the lipid matrix are important for the transport of drugs across the stratum corneum [67].

3.2 Passive diffusion

3.2.1 Basic concepts

Different transport routes have been proposed for passive penetration of molecules through the stratum corneum, a thin (10-20 μm), relative impermeable layer, which provides the rate limiting step for percutaneous penetration. Several macroroutes for penetration from the surface of the human skin into the subepidermal tissue are displayed in Figure 2 [5, 65, 68]: 1) via the sweat ducts 2) through the hair follicles with their associated sebaceous glands or 3) across the continuous stratum corneum between these appendages. It is generally believed that transport of most small lipophilic molecules occurs mostly via the latter pathway. This pathway can be subdivided into the transcellular route, though the corneocytes and lipid lamellae, and the intercellular pathway, solely through the lipid regions [65, 67]. For larger hydrophilic molecules and ions the appendegeal route may play also a significant role [68].

3.2.2 Dopamine agonists

Due to the difficult permeability properties of the skin, the choice of potential candidates of dopamine agonists for passive transdermal delivery is limited. In order to penetrate the skin, the permeant should be potent, since the relative bioavailability is low and should have specific physicochemical properties: moderate hydrophilicity and low molecular weight (<500 Mw). Despite these restrictions several molecules have been investigated for the symptomatic treatment of Parkinson's disease with transdermal passive delivery. All the DA of which the feasibility of (passive and/or iontophoretic) transdermal delivery has been investigated together with the structure of levodopa are depicted in Figure 3.

In the 1980's naxagolide was identified as a very potent dopamine agonist and a potential candidate for transdermal delivery due to its moderate lipophilic nature. Despite the very promising results that were obtained *in vitro* and later *in vivo* in primates and humans [69-70], the further development was discontinued because of the lack of efficacy as monotherapy and concerns about the toxicity [71]. These results encouraged further investigations with other potential candidates.

A number of gel formulations for bromocriptine, an ergot derived dopamine agonist, were developed and transdermal delivery was compared with oral delivery in rabbits.

It was observed that a gel, formulated with chitosan showed similar plasma concentration profile as with a commercially available tablet [72]. An enhancement in transdermal transport *in vitro* of pergolide, another ergot derived dopamine agonist, was obtained using elastic vesicles, but further investigation *in vivo* is necessary [73]. Transdermal delivery of a third ergot derivative dopamine agonist, lisuride showed promising efficacy as add-on therapy for Pd. Axxonis Pharma, a pharmaceutical company in Germany, recently submitted a European marketing authorization application for the transdermal patch and subcutaneous infusion of lisuride [50, 74]. The non-ergot derivatives, such as piribedil, apomorphine and rotigotine do not cause serious fibrotic reactions, associated with the use of the older ergot-derived compounds, described above. For this reason the non-ergot derivatives are the preferred dopamine agonists to commence therapy, especially in younger patients [1]. A randomized double blind clinical study, including 72 patients with Pd, failed however to show clinical efficacy of transdermal delivery of piribedil, explained by low plasma concentrations [75]. However one year later a study was published on transdermal peribidil that demonstrated, a long-lasting effect (reversal of motor deficits) in MPTP-treated common marmosets [76].

Apomorphine is regarded as a potent dopamine agonist, since its introduction for the treatment for Pd in 1951. Different administration routes have been explored for this D_1/D_2 dopamine agonist, including transdermal delivery [1]. The transdermal delivery of apomorphine, formulated as a hydroxyl-propyl-methyl-cellulose gel and formulated in microemulsions was investigated in rabbits and mice, respectively. Both studies reported sufficient bioavailability and suggested potential use in humans [77-78]. One of the two microemulsions, used for the *in vivo* study in mice, was applied transdermally in 21 patients with Pd. The transdermal delivery of this micro-emulsion, containing apomorphine, provided a sustained release of apomorphine, resulting in stable therapeutic plasma levels and reduction of *off* periods [79]. However the clinical efficacy and tolerability has not been investigated in a placebo controlled double blind study.

Another potent dopamine agonist rotigotine, the (-)-enantiomer of the aminotetralin derivative, 2-(N-propyl-N-2-thienylethylamino)-5-hydroxytetralin, is the first transdermal delivery system (Neupro®) approved by the regulatory authorities for the symptomatic treatment of all stages of Pd in Europe and of early-stage Pd in USA [80]. Due to drug stability (crystallization inside the patch), compromising the bioavailability, the EMEA limited the supply of rotigotine and the FDA asked professionals and patients for a recall of Neupro® [80]. After adjustments concerning storage conditions, Neupro® is since June 2009 available in Europe for symptomatic

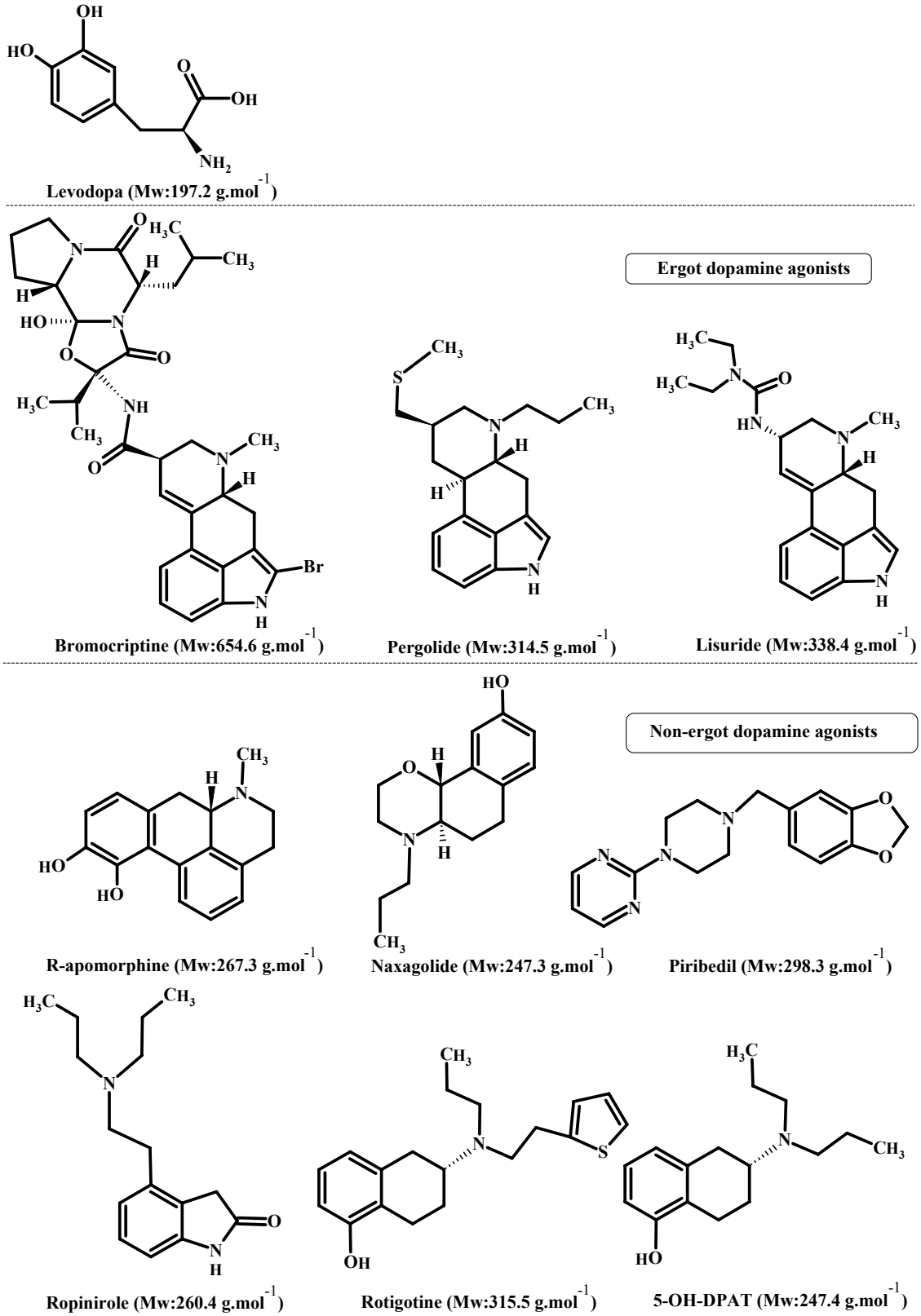

Figure 3: The chemical structures and Mw of levodopa and ergot and non-ergot dopamine agonists, that were investigated for administration with passive and/or iontophoretic transdermal delivery for the symptomatic treatment of Pd.

treatment of Pd. In the USA up to the present time Neupro® is not yet available on the market. In addition to approval for the symptomatic treatment of Pd, Neupro® has been approved for the treatment of moderate to severe restless leg syndrome in adult patients [81]. Patches releasing 1, 2, 4, 6, 8 mg of rotigotine during 24 h are available [82]. In 63 patients with early Pd after repeated daily administration of 8 mg/24h stable steady-state plasma concentrations were observed [83] and animal studies demonstrated that continuous plasma concentrations translate into continuous dopamine stimulation [47, 84]. Three large-scale placebo-controlled phase III trials investigated the efficacy of transdermal delivery of rotigotine as mono-therapy for early stage Pd. All three trials showed an improvement in UPDRS (unified Parkinson's disease rating scale)-ADL (activities daily living)-Motor subscores in baseline *vs* placebo [80, 85-87]. In addition the first phase III clinical trial reported that response reached a plateau when delivering between 6 and 8 mg/24h. This was the base to set the maximum approved dose as monotherapy in the USA and Europe to 6 and 8 mg rotigotine per 24h, respectively [80]. Furthermore a subgroup analysis in the second trial showed that the efficacy is independent of gender, age, disease severity and disease duration [80]. Finally the third trial, which compared transdermal rotigotine *vs* ropinirole over a 37-week period, reported that ropinirole resulted in a better symptomatic effect than rotigotine, which could be explained by possible under-dosing of the patients receiving rotigotine, compared to ropinirole [87]. Two large phase III trials (PREFER and CLEOPATRA PD-study) investigated the efficacy of transdermal rotigotine as adjunct therapy to L-dopa in advanced Pd [80, 88-89]. The phase III trials showed a significant improvement in the UPDRS-Motor score and one phase III trial did not show any reduction in the required L-dopa dose. However both phase III trials showed a significant reduction in daily *off* time and an increase in *on* time without dyskinesia after waking for rotigotine *vs* placebo [88-89]. Thus as monotherapy for early stage Pd and as adjunct therapy for advanced stage Pd, transdermal rotigotine has been proven to be efficacious and useful. In addition, continuous dopamine stimulation has been suggested to contribute to the prevention of motor complications later in the disease course. Moreover dopamine agonists have been less associated with motor complication than levodopa, emphasizing the potential of transdermal rotigotine to play an important role in the symptomatic treatment of Pd.

Although the passive delivery of dopamine agonist has great potential, investigations to improve the transdermal delivery are required to increase the delivery rate and to expand the number of potential candidates for continuous delivery via the skin. The first major approach to overcome the skin barrier and to improve transdermal

delivery is the use of chemical enhancers, such as azones, glycols, terpenes etc. They facilitate stratum corneum transport by interaction with the lipids in the skin and/or increase partitioning [90]. A second approach is the use of particulate systems (e.g. nano-particles, vesicles, liposomes). These systems can increase the skin transport by improving drug solubilization in the formulation, drug partitioning into the skin and skin permeability [91]. The use of chemical enhancers and particulate systems can cause skin irritation and therefore limit the number and concentration (in formulation) of enhancers used [90]. Finally a third approach for permeation increase is the use of physical enhancement methods, such as sonophoresis (ultrasound), electroporation, microneedles thermal ablation, microdermabrasion and iontophoresis [91]. Whereas ultrasound, microneedles and thermal ablation show potential for delivery of macromolecules, such as vaccines and therapeutic proteins [91], iontophoresis is promising method for the delivery of small and moderate hydrophilic molecules, such as dopamine agonists.

3.3 Iontophoresis

3.3.1 Basic concepts

Transdermal iontophoresis is one of the promising alternative techniques for non-invasive continuous delivery of dopamine agonists. By applying a small electrical current ($\leq$ 500 μA.cm-2) across the skin it is possible to enhance the transdermal delivery of small ionized therapeutic agents as illustrated in Figure 4. Besides a continuous administration and increased bioavailability, a particular advantage of iontophoresis is the possibility to adjust the delivery rate to the demand of the therapy. Especially in symptomatic treatment of Pd this can be very important, since individual titration is often required when administering dopaminergic agents. Three transport mechanisms are involved in transdermal iontophoretic delivery: 1) passive diffusion, resulting from a concentration gradient between the patch and the systemic circulation 2) the electromigration which is the result from the current flow from the anode (+ electrode) to the cathode (- electrode) across the skin and 3) electroosmosis, which can be attributed to the current induced solvent flow across the skin in the counter direction of the skin charge [92]. For small charged molecules the contribution of the passive flow is often negligible, making electromigration and electroosmosis the principle transport mechanisms with a dominating transport due to electromigration. With increasing molecular size, however, the contribution of the electroosmosis increases and may be really important for large peptides and proteins [92].

In addition for uncharged molecules electroosmosis is considered to be the only transporting mechanism involved in transdermal iontophoresis. Therefore marker molecules, such as mannitol and acetaminophen, are used to quantify the electroosmotic contribution during iontophoretic transport of various molecules. In the last few years acetaminophen has gained more interest over ^{14}C-mannitol, because of its practical advantages [93-97].

Current application across the skin will drive the molecules through the pathway of least electrical resistance. In case of iontophoresis of the three suggested penetration routes (transcellular, intercellular and transappendageal), transport is reported to occur primarily via the intercellular and transappendageal route (Figure 2). The major contribution is via the appendages in the skin, including hair follicles and sweat glands [98]. In addition ions can also migrate via the damaged structures in the skin [90]. These penetration pathways can exist in parallel [65], as was suggested for the percutaneous penetration of methothrexate [99]. The relative contribution of the different pathways is presumably dependent on the physicochemical properties of the permeant. For instance Jadoul et al. showed that fentanyl, a relatively lipophilic molecule, was distributed across the whole human stratum corneum (HSC), while the more hydrophilic thyrotropin releasing hormone was mainly localized in the pores after iontophoresis [100]. Confocal laser scanning microscopy studies with calcein, a

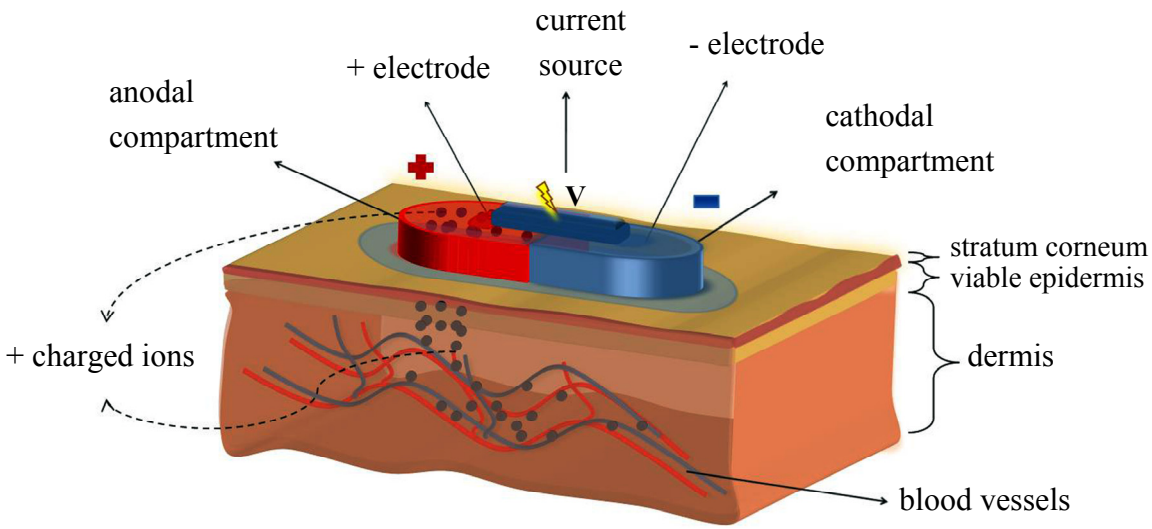

Figure 4: Iontophoresis set-up *in vivo* with the transport of positively charged ions across the skin during current application

charged hydrophilic dye and nile red, a neutral lipophilic dye, confirmed that the more lipophilic compound is transported via the lipid-filled intercellular regions of the stratum corneum, while iontophoresis enhanced the transcutaneous transport of calcein mainly in the follicular structures [101].

Up to today 2 iontophoretic delivery systems made it to the market. In 2007 EMEA approved IONSYS®, manufactured by ALZA corporation, a credit card system delivering fentanyl.HCl for analgesia [102]. However because of safety issues Janssen-Cilag withdrew IONSYS® voluntary from the market and as a consequence the EMEA suspended its registration [103]. Currently the only commercialized iontophoresis system on the market is Lidosite® from Vyteris, delivering the anesthetic lidocaine.HCl. Lidosite® can be applied for local analgesia prior to blood sampling, venipunctures or small dermatological procedures [104].

Instead of delivery of molecules, it is also possible with iontophoresis to extract molecules from the skin. Therefore so-called 'reverse iontophoresis' has been explored in the last two decades to monitor subdermal levels of several molecules like lithium [105], phenytoin [106], valproate [107], lactate [108], urea [109], amino acids [110] and glucose [111]. The GlucoWatch® Biographer (Johnson & Johnson, New Brunswick, NJ) was approved in 2002 by the FDA to monitor the glycaemia for up to 12h [111]. These results show the potential of reverse iontophoresis to monitor different molecules subdermally. By monitoring a relevant biomarker it may even be possible to design a feedback system that can control the delivery of the therapeutic drug.

3.3.2 Dopamine agonists

Transdermal iontophoresis of various non-ergot dopamine agonists have been studied *in vitro* and *in vivo* for symptomatic treatment of Pd. Several studies on the transdermal iontophoretic delivery of R-apomorphine have been reported. After promising results *in vitro* across human skin [112], in small scale clinical studies apomorphine was applied using transdermal iontophoresis in patients with Pd. After application of 2 different current densities (250 and 375 $\mu A.cm^{-2}$) for 1 hour, in all patients measurable plasma concentrations were observed. However these plasma levels were subtherapeutic in all patients, except one [113]. Li et al. showed an improvement of the transdermal iontophoretic delivery of this dopamine agonist after non-occlusive pretreatment of the skin with a surfactant formulations [114]. A 2-fold and 1.4 fold increase in flux was observed in studies across HSC and dermatomed human skin (DHS), respectively [115]. These findings led to further exploration of the feasibility of the transdermal iontophoretic delivery of apomorphine in a clinical

study including 16 patients. 2 groups of patients were compared receiving R-apomorphine using transdermal iontophoresis (250 $\mu A.cm^{-2}$, 3 hours) with or without pretreatment of with the surfactant formulation, respectively. With a similar enhancement ratio (1.3 times) as was observed for transport across DHS, the surfactant pretreatment increased the iontophoretic delivery. In this study 62.5% and 37.5% respectively, of the surfactant pretreated and control group, reported clinical improvement [116].

The feasibility of transdermal iontophoretic administration of ropinirole was explored, because of its suitable fysicochemical properties (Mw: 260.4 $g.mol^{-1}$; pKa: 9.68 and 12.43; logP=3.32) [117]. Studies, investigating *in vitro* transport across full piglet skin in the absence of competing co-ions, showed that the flux of ropinirole was independent of the donor concentration, however linearly dependent of the current density [118]. In a follow-up study with hairless rats, similar plasma profiles were observed, despite the 10-fold difference in donor concentration. The absence of competing co-ions results in a constant flux, independent of the donor concentration and dependent on the mobility of the drug, the skin diffusivity and the counterion in the skin (mainly Cl^-). The authors concluded that, based on the *in vitro* flux and *in vivo* plasma concentrations, therapeutic levels of ropinirole in humans can be achieved with transdermal iontophoresis, providing an alternative administration route for the drug, as a tablet available [117].

Finally several studies were conducted to investigate the iontophoretic delivery of 2 dopamine agonist of the 2-aminotetralin group. Most dopamine agonists of this group are shown to be very potent [119-125]. In addition the low molecular weight, the chargeability of the nitrogengroup and the moderate lipophilicity, make several members of the 2-aminotetralingroup interesting candidates for transdermal iontophoresis. Therefore Nugroho et al. studied the transdermal iontophoretic delivery of rotigotine.HCl (Mw: 351.9 $g.mol^{-1}$; pKa (nitrogen): 7.9; logP: 4.03) and of 5-OH-DPAT.HBr (Mw: 328.3 $g.mol^{-1}$; pKa (nitrogen): 8.12; logP: 2.19) [126-127]. *In vitro* transdermal iontophoresis studies of the potent dopamine receptor agonist rotigotine, currently on the market as passive delivery system (cf. supra), were performed. Increasing the pH of the donor phase increases the flux, doubling the NaCl concentration reduces the flux and lowering the pH of the acceptor phase does not affect the flux. Furthermore electroosmosis contributed only 2% to the total flux [128]. In a follow up assay it was shown that in the concentration range tested, the flux was linearly dependent on the donor concentration and the current density. Replacing HSC by DHS reduced, while higher temperatures increased it [126]. Although the maximum flux of 80 $nmol.cm^{-2}.h^{-1}$ is considered to be sufficient for

therapeutic levels, the limited solubility of this compound prevented the researchers to further increase the iontophoretic delivery.

The second 2-aminotetralin investigated was 5-hydroxy-2-(N,N,-di-n-propylamino)tetralin (5-OH-DPAT). This dopamine agonist has similar structure and potency as rotigotine [127]. The absence of the thienylgroup in the side chain of 5-OH-DPAT makes this compound less lipophilic, which could lead to increased solubility and a faster transdermal transport because of less retardation in the lipophilic environment of the skin. *In vitro* studies showed a higher flux for 5-OH-DPAT, compared to rotigotine. The flux was linearly dependent on the concentration in the given concentration range (0-7 mM) and on the current density. Increasing the salt concentration from 0.07 M to 0.14 M dramatically decreased the flux with almost 10 fold. In analogy to rotigotine, transport across DHS was less compared to transport across HSC [127]. Although the *in vitro* transport of this potent dopamine agonist has not yet been fully characterized, these results showed an improved transport compared to rotigotine. Therefore the authors continued with 5-OH-DPAT to explore the potential of transdermal iontophoresis in a series of *in vivo* studies. The pharmacodynamic effect of 5-OH-DPAT was investigated in an anaesthetized rat model with the dopamine level as pharmacodynamic end-point, measured by online microdialysis. Administration of 5-OH-DPAT with transdermal iontophoresis during 3 hours using a current density of 250 $\mu A.cm^{-2}$ resulted in a strong and long lasting effect, which was suggested to persist for 24 hours post-iontophoresis [129]. The pharmacokinetic and pharmacodynamic data were analyzed using compartmental modeling. A more detailed discussion of this approach is provided in the next section.

In conclusion transdermal iontophoresis has great potential as novel delivery strategy for symptomatic treatment of Pd. Firstly, the results presented in this section show that this non-invasive delivery technique can provide continuous delivery that can be controlled mainly by donor concentration and current density. This makes iontophoresis a flexible delivery technique, enabling rapid titration of drug delivery. Secondly, several dopamine agonists are successfully administered with transdermal iontophoresis *in vitro*, in animals and even in patients. Thirdly, monitoring biomarkers with reverse iontophoresis opens the door to design a feedback system to control drug delivery. Despite these promising results there is still a need for improvement in delivery efficiency. In addition a better understanding of the different transport mechanisms involved in iontophoretic delivery will also contribute to improve drug delivery. This demands for further optimization of the iontophoretic delivery of previously investigated DA and for further exploration of

novel potent dopaminergic drugs with the desired physicochemical properties for transdermal iontophoresis.

4 Modeling transdermal iontophoretic delivery *in vitro* and *in vivo*

Describing the profile of a drug in different parts of the body (e.g. plasma, urine, brain, skin,…) during and after administration with various delivery techniques has been a challenge in drug development for many years. The complexity of the skin as biological membrane makes mathematical modeling of transdermal (iontophoretic) delivery difficult. Most of the models found in literature focus on the transport mechanisms during transport of the molecules [93, 130-141]. In some of these reports a correlation was suggested between the physicochemical properties (pKa, electrophoretic mobility, lipophilicity, Mw,…) of the solutes and the corresponding transport efficiency [93, 130, 132, 134-135, 139-141]. One of the limitations of these physicochemical property-transport relationships is that they are based on a single parameter to describe the transdermal iontophoretic transport. With this approach the information on the shape of the iontophoretic flux curve is neglected, which makes extrapolation from *in vitro* experiments towards the *in vivo* situation more difficult. However, very little research has been performed on development of models describing the whole transport profile during iontophoresis *in vitro* and *in vivo*. Most of the models used to describe the plasma concentration following transdermal iontophoresis were based on a zero order mass input from the donor solution into the systemic circulation in analogy to intravenous infusion [142-144]. However this assumes that immediate steady state conditions would apply after turning on the current. But the development of a steady state takes time, because of the barrier function of this biological membrane. This is clearly demonstrated by the profiles that have been published [112-113, 116, 129, 145-148].

To account for the change of input rate during iontophoresis before reaching steady state more complex kinetic models have been developed by Nugroho et al. [147-148]. In these models the rate of mass transfer (I_0) from the patch into the skin during iontophoresis is assumed to be constant due to the iontophoretic driving force. Furthermore it is believed that the release from the skin into the acceptor solution (*in vitro*) and in the systemic circulation (*in vivo*) is according to a first order process with a release constant K_R. This approach was successfully applied to describe the iontophoretic transport *in vitro* [147] and *in vivo* [148] during and also after current application. The proposed *in vivo* pharmacokinetic (PK) models were combined with a pharmacological model (indirect response type I) to analyze the pharmacokinetics

and pharmacodynamics (PD) of 5-OH-DPAT following transdermal iontophoresis. Besides adequately describing the plasma concentration and the pharmacodynamic effect in rats, it was shown that based on results from *in vitro* transport studies across rat stratum corneum and dermatomed rat skin it was possible to predict the plasma profile as well as the dopaminergic effect [129].

These results illustrate several strong benefits of compartmental modeling. Firstly an integrated approach makes it possible to combine data from several experiments, facilitating analysis of different experiments. Secondly compartmental modeling can be helpful in understanding the different mechanisms involved in iontophoretic transport. In addition the establishment of a PK-PD relationship gives more insight in the causal path from blood to the pharmacodynamic effect. Thirdly a robust *in vitro-in vivo* correlation can be very useful for screening newly developed compounds and can be a powerful tool to design new assays at various stages of drug development. To improve screening a next step would be the identification of the relationships between the molecular and physicochemical properties and the different transport parameters, which can offer a base for selecting potential candidates.

In conclusion the compartmental modeling approach can reduce, refine, and maybe even replace *in vivo* studies, which are often very costly and time consuming certainly at later stages of drug development.

References

1. Tugwell, C., *Parkinson's disease in focus*. 1st ed. In focus. 2008, London: Pharmaceutical Press. 237.
2. Gershanik, O.S., *Early onset parkinsonism.* Front Biosci, 2003. **8**: p. s568-78.
3. Lees, A.J., *The Parkinson chimera.* Neurology, 2009. **72**(7 Suppl): p. S2-11.
4. Olanow, C.W., *The scientific basis for the current treatment of Parkinson's disease.* Annu Rev Med, 2004. **55**: p. 41-60.
5. Prausnitz, M.R., S. Mitragotri, and R. Langer, *Current status and future potential of transdermal drug delivery.* Nat Rev Drug Discov, 2004. **3**(2): p. 115-24.
6. von Campenhausen, S., et al., *Prevalence and incidence of Parkinson's disease in Europe.* Eur Neuropsychopharmacol, 2005. **15**(4): p. 473-90.
7. Huang, Y., et al., *Genetic contributions to Parkinson's disease.* Brain Res Brain Res Rev, 2004. **46**(1): p. 44-70.
8. Harris, M.K., et al., *Movement disorders.* Med Clin North Am, 2009. **93**(2): p. 371-88, viii.
9. McInerney-Leo, A., et al., *Genetic testing in Parkinson's disease.* Mov Disord, 2005. **20**(1): p. 1-10.
10. Lesage, S. and A. Brice, *Parkinson's disease: from monogenic forms to genetic susceptibility factors.* Hum Mol Genet, 2009. **18**(R1): p. R48-59.
11. Lai, B.C., et al., *Occupational and environmental risk factors for Parkinson's disease.* Parkinsonism Relat Disord, 2002. **8**(5): p. 297-309.
12. Shastry, B.S., *Parkinson disease: etiology, pathogenesis and future of gene therapy.* Neurosci Res, 2001. **41**(1): p. 5-12.
13. Olanow, C.W., et al., *Lewy-body formation is an aggresome-related process: a hypothesis.* Lancet Neurol, 2004. **3**(8): p. 496-503.
14. Levy, O.A., C. Malagelada, and L.A. Greene, *Cell death pathways in Parkinson's disease: proximal triggers, distal effectors, and final steps.* Apoptosis, 2009. **14**(4): p. 478-500.
15. Rochet, J.C., K.A. Conway, and P.T. Lansbury, Jr., *Inhibition of fibrillization and accumulation of prefibrillar oligomers in mixtures of human and mouse alpha-synuclein.* Biochemistry, 2000. **39**(35): p. 10619-26.
16. Nutt, J.G. and G.F. Wooten, *Clinical practice. Diagnosis and initial management of Parkinson's disease.* N Engl J Med, 2005. **353**(10): p. 1021-7.
17. Hughes, A.J., S.E. Daniel, and A.J. Lees, *Improved accuracy of clinical diagnosis of Lewy body Parkinson's disease.* Neurology, 2001. **57**(8): p. 1497-9.
18. Tolosa, E., G. Wenning, and W. Poewe, *The diagnosis of Parkinson's disease.* Lancet Neurol, 2006. **5**(1): p. 75-86.
19. Walter, B.L. and J.L. Vitek, *Surgical treatment for Parkinson's disease.* Lancet Neurol, 2004. **3**(12): p. 719-28.
20. Breit, S., J.B. Schulz, and A.L. Benabid, *Deep brain stimulation.* Cell Tissue Res, 2004. **318**(1): p. 275-88.
21. Barker, R.A. and T. Foltynie, *The future challenges in Parkinson's disease.* J Neurol, 2004. **251**(3): p. 361-5.
22. Olanow, C.W., J.H. Kordower, and T.B. Freeman, *Fetal nigral transplantation as a therapy for Parkinson's disease.* Trends Neurosci, 1996. **19**(3): p. 102-9.
23. Olanow, C.W., M.B. Stern, and K. Sethi, *The scientific and clinical basis for the treatment of Parkinson disease (2009).* Neurology, 2009. **72**(21 Suppl 4): p. S1-136.
24. Fahn, S. and C.W. Olanow, *Fetal Nigral Transplantation for Parkinson's Disease: Current Status and Future Directions*. Restorative Therapies in Parkinson's Disease, ed. O.C. Brundin P. 2006, New York: Springer Publishers.
25. Snyder, B.J. and C.W. Olanow, *Stem cell treatment for Parkinson's disease: an update for 2005.* Curr Opin Neurol, 2005. **18**(4): p. 376-85.

26. Sonntag, K.C., R. Simantov, and O. Isacson, *Stem cells may reshape the prospect of Parkinson's disease therapy.* Brain Res Mol Brain Res, 2005. **134**(1): p. 34-51.
27. Svendsen, C., *The first steps towards gene therapy for Parkinson's disease.* Lancet Neurol, 2007. **6**(9): p. 754-6.
28. Freeman, T.B., et al., *Use of placebo surgery in controlled trials of a cellular-based therapy for Parkinson's disease.* N Engl J Med, 1999. **341**(13): p. 988-92.
29. Olanow, C.W., *Double-blind, placebo-controlled trials for surgical interventions in Parkinson disease.* Arch Neurol, 2005. **62**(9): p. 1343-4.
30. Rajput, A.H., et al., *Clinical-pathological study of levodopa complications.* Mov Disord, 2002. **17**(2): p. 289-96.
31. Syed, N., et al., *Ten years' experience with enteral levodopa infusions for motor fluctuations in Parkinson's disease.* Mov Disord, 1998. **13**(2): p. 336-8.
32. Fernandez, H.H. and J.J. Chen, *Monoamine oxidase-B inhibition in the treatment of Parkinson's disease.* Pharmacotherapy, 2007. **27**(12 Pt 2): p. 174S-185S.
33. Elmer, L.W. and J.M. Bertoni, *The increasing role of monoamine oxidase type B inhibitors in Parkinson's disease therapy.* Expert Opin Pharmacother, 2008. **9**(16): p. 2759-72.
34. Lewitt, P.A., *MAO-B inhibitor know-how: back to the pharm.* Neurology, 2009. **72**(15): p. 1352-7.
35. Tatton, W., R. Chalmers-Redman, and N. Tatton, *Neuroprotection by deprenyl and other propargylamines: glyceraldehyde-3-phosphate dehydrogenase rather than monoamine oxidase B.* J Neural Transm, 2003. **110**(5): p. 509-15.
36. Youdim, M.B., W. Maruyama, and M. Naoi, *Neuropharmacological, neuroprotective and amyloid precursor processing properties of selective MAO-B inhibitor antiparkinsonian drug, rasagiline.* Drugs Today (Barc), 2005. **41**(6): p. 369-91.
37. Hornykiewicz, O., *L-DOPA: from a biologically inactive amino acid to a successful therapeutic agent.* Amino Acids, 2002. **23**(1-3): p. 65-70.
38. Lang, A.E. and A.M. Lozano, *Parkinson's disease. First of two parts.* N Engl J Med, 1998. **339**(15): p. 1044-53.
39. Mytilineou, C., et al., *Levodopa is toxic to dopamine neurons in an in vitro but not an in vivo model of oxidative stress.* J Pharmacol Exp Ther, 2003. **304**(2): p. 792-800.
40. Schapira, A.H., *The clinical relevance of levodopa toxicity in the treatment of Parkinson's disease.* Mov Disord, 2008. **23 Suppl 3**: p. S515-20.
41. Fahn, S., et al., *Levodopa and the progression of Parkinson's disease.* N Engl J Med, 2004. **351**(24): p. 2498-508.
42. Muller, T. and H. Russ, *Levodopa, motor fluctuations and dyskinesia in Parkinson's disease.* Expert Opin Pharmacother, 2006. **7**(13): p. 1715-30.
43. Guridi, J., et al., *L-dopa-induced dyskinesia and stereotactic surgery for Parkinson's disease.* Neurosurgery, 2008. **62**(2): p. 311-23; discussion 323-5.
44. Yamamoto, M. and A.H. Schapira, *Dopamine agonists in Parkinson's disease.* Expert Rev Neurother, 2008. **8**(4): p. 671-7.
45. Antonini, A. and P. Barone, *Dopamine agonist-based strategies in the treatment of Parkinson's disease.* Neurol Sci, 2008. **29 Suppl 5**: p. S371-4.
46. Grace, A.A., *Phasic versus tonic dopamine release and the modulation of dopamine system responsivity: a hypothesis for the etiology of schizophrenia.* Neuroscience, 1991. **41**(1): p. 1-24.
47. Steiger, M., *Constant dopaminergic stimulation by transdermal delivery of dopaminergic drugs: a new treatment paradigm in Parkinson's disease.* Eur J Neurol, 2008. **15**(1): p. 6-15.
48. Jenner, P., *Preventing and controlling dyskinesia in Parkinson's disease--a view of current knowledge and future opportunities.* Mov Disord, 2008. **23 Suppl 3**: p. S585-98.
49. Jenner, P., *Molecular mechanisms of L-DOPA-induced dyskinesia.* Nat Rev Neurosci, 2008. **9**(9): p. 665-77.
50. Di Stefano, A., et al., *New drug delivery strategies for improved Parkinson's disease therapy.* Expert Opin Drug Deliv, 2009. **6**(4): p. 389-404.

51. Nyholm, D., *Pharmacokinetic optimisation in the treatment of Parkinson's disease : an update.* Clin Pharmacokinet, 2006. **45**(2): p. 109-36.
52. Pappert, E.J., et al., *Liquid levodopa/carbidopa produces significant improvement in motor function without dyskinesia exacerbation.* Neurology, 1996. **47**(6): p. 1493-5.
53. Nutt, J.G., et al., *Motor fluctuations during continuous levodopa infusions in patients with Parkinson's disease.* Mov Disord, 1997. **12**(3): p. 285-92.
54. Macleod, A., et al., *Monoamine oxidase B inhibitors for early Parkinson's disease.* Cochrane Database Syst Rev, 2005(3): p. CD004898.
55. Stocchi, F., et al., *Intermittent vs continuous levodopa administration in patients with advanced Parkinson disease: a clinical and pharmacokinetic study.* Arch Neurol, 2005. **62**(6): p. 905-10.
56. Nyholm, D. and S.M. Aquilonius, *Levodopa infusion therapy in Parkinson disease: state of the art in 2004.* Clin Neuropharmacol, 2004. **27**(5): p. 245-56.
57. Olanow, W., A.H. Schapira, and O. Rascol, *Continuous dopamine-receptor stimulation in early Parkinson's disease.* Trends Neurosci, 2000. **23**(10 Suppl): p. S117-26.
58. Olanow, C.W., *Can we achieve neuroprotection with currently available anti-parkinsonian interventions?* Neurology, 2009. **72**(7 Suppl): p. S59-64.
59. Schapira, A.H., *Dopamine agonists and neuroprotection in Parkinson's disease.* Eur J Neurol, 2002. **9 Suppl 3**: p. 7-14.
60. Weber, J. and G.M. Keating, *Ropinirole prolonged release: in advanced Parkinson's disease.* CNS Drugs, 2009. **23**(1): p. 81-90.
61. Haq, I.U., P.A. Lewitt, and H.H. Fernandez, *Apomorphine therapy in Parkinson's disease: a review.* Expert Opin Pharmacother, 2007. **8**(16): p. 2799-809.
62. Stocchi, F., et al., *Prospective randomized trial of lisuride infusion versus oral levodopa in patients with Parkinson's disease.* Brain, 2002. **125**(Pt 9): p. 2058-66.
63. Stocchi, F., et al., *Apomorphine and lisuride infusion. A comparative chronic study.* Adv Neurol, 1993. **60**: p. 653-5.
64. Moore, L. and Y.W. Chien, *Transdermal drug delivery: a review of pharmaceutics, pharmacokinetics, and pharmacodynamics.* Crit Rev Ther Drug Carrier Syst, 1988. **4**(4): p. 285-349.
65. Barry, W., ed. *Dermatological formulations. Percutaneous Absorption.* . 1983: New York: Marcel Dekker.
66. Bouwstra, J.A., et al., *Structure of the skin barrier and its modulation by vesicular formulations.* Prog Lipid Res, 2003. **42**(1): p. 1-36.
67. Barry, B.W., *Action of skin penetration enhancers-the Lipid Protein Partitioning theory.* Int J Cosmet Sci, 1988. **10**(6): p. 281-93.
68. Barry, B.W., *Drug delivery routes in skin: a novel approach.* Adv Drug Deliv Rev, 2002. **54 Suppl 1**: p. S31-40.
69. Ahlskog, J.E., et al., *Parkinson's disease monotherapy with controlled-release MK-458 (PHNO): double-blind study and comparison to carbidopa/levodopa.* Clin Neuropharmacol, 1991. **14**(3): p. 214-27.
70. Muenter, M.D., et al., *PHNO [(+)-4-propyl-9-hydroxynaphthoxazine]: a new and effective anti-Parkinson's disease agent.* Neurology, 1988. **38**(10): p. 1541-5.
71. Pfeiffer, R.F., *Potential of transdermal drug delivery in Parkinson's disease.* Drugs Aging, 2002. **19**(8): p. 561-70.
72. Degim, I.T., et al., *Transdermal administration of bromocriptine.* Biol Pharm Bull, 2003. **26**(4): p. 501-5.
73. Honeywell-Nguyen, P.L., et al., *Transdermal delivery of pergolide from surfactant-based elastic and rigid vesicles: characterization and in vitro transport studies.* Pharm Res, 2002. **19**(7): p. 991-7.
74. Woitalla, D., et al., *Transdermal lisuride delivery in the treatment of Parkinson's disease.* J Neural Transm Suppl, 2004(68): p. 89-95.
75. Montastruc, J.L., et al., *A randomized, double-blind study of a skin patch of a dopaminergic agonist, piribedil, in Parkinson's disease.* Mov Disord, 1999. **14**(2): p. 336-41.

76. Smith, L.A., et al., *Transdermal administration of piribedil reverses MPTP-induced motor deficits in the common marmoset.* Clin Neuropharmacol, 2000. **23**(3): p. 133-42.
77. Durif, F., et al., *Comparison between percutaneous and subcutaneous routes of administration of apomorphine in rabbit.* Clin Neuropharmacol, 1994. **17**(5): p. 445-53.
78. Peira, E., P. Scolari, and M.R. Gasco, *Transdermal permeation of apomorphine through hairless mouse skin from microemulsions.* Int J Pharm, 2001. **226**(1-2): p. 47-51.
79. Priano, L., et al., *Transdermal apomorphine permeation from microemulsions: a new treatment in Parkinson's disease.* Mov Disord, 2004. **19**(8): p. 937-42.
80. Rascol, O. and S. Perez-Lloret, *Rotigotine transdermal delivery for the treatment of Parkinson's disease.* Expert Opin Pharmacother, 2009. **10**(4): p. 677-91.
81. *UCB brings Neupro® back to all patients in Europe. UCB press release* 2009 29-06-2009; Available from: http://www.ucb.com/media-room/newsdetail/?det=1325571&select-year=&select-archive=.
82. *EMEA. European Public Assessment Report (EPAR), annex I: summary of product characteristics for Neupro*. 2009; Available from: http://www.emea.europa.eu/humandocs/PDFs/EPAR/neupro/H-626-PI-en.pdf
83. Braun, M., et al., *Steady-state pharmacokinetics of rotigotine in patients with early-stage Parkinson's disease.* Eur J Neurol, 2005. **12(suppl. 2)**: p. 37.
84. Kehr, J. and D. Scheller, *Continuous delivery of rotigotine leads to continuous dopamine receptor stimulation in a rat model.* Eur J Neurol, 2005. **12(suppl. 2)**: p. 37.
85. Watts, R.L., et al., *Randomized, blind, controlled trial of transdermal rotigotine in early Parkinson disease.* Neurology, 2007. **68**(4): p. 272-6.
86. *A controlled trial of rotigotine monotherapy in early Parkinson's disease.* Arch Neurol, 2003. **60**(12): p. 1721-8.
87. Giladi, N., et al., *Rotigotine transdermal patch in early Parkinson's disease: a randomized, double-blind, controlled study versus placebo and ropinirole.* Mov Disord, 2007. **22**(16): p. 2398-404.
88. LeWitt, P.A., K.E. Lyons, and R. Pahwa, *Advanced Parkinson disease treated with rotigotine transdermal system: PREFER Study.* Neurology, 2007. **68**(16): p. 1262-7.
89. Poewe, W.H., et al., *Efficacy of pramipexole and transdermal rotigotine in advanced Parkinson's disease: a double-blind, double-dummy, randomised controlled trial.* Lancet Neurol, 2007. **6**(6): p. 513-20.
90. Batheja, P., R. Thakur, and B. Michniak, *Transdermal iontophoresis.* Expert Opin Drug Deliv, 2006. **3**(1): p. 127-38.
91. Prausnitz, M.R. and R. Langer, *Transdermal drug delivery.* Nat Biotechnol, 2008. **26**(11): p. 1261-8.
92. Pikal, M.J., *The role of electroosmotic flow in transdermal iontophoresis.* Adv Drug Deliv Rev, 2001. **46**(1-3): p. 281-305.
93. Abla, N., et al., *Capillary zone electrophoresis for the estimation of transdermal iontophoretic mobility.* J Pharm Sci, 2005. **94**(12): p. 2667-75.
94. Abla, N., et al., *Contributions of electromigration and electroosmosis to peptide iontophoresis across intact and impaired skin.* J Control Release, 2005. **108**(2-3): p. 319-30.
95. Marro, D., R.H. Guy, and M.B. Delgado-Charro, *Characterization of the iontophoretic permselectivity properties of human and pig skin.* J Control Release, 2001. **70**(1-2): p. 213-7.
96. Marro, D., et al., *Contributions of electromigration and electroosmosis to iontophoretic drug delivery.* Pharm Res, 2001. **18**(12): p. 1701-8.
97. Sebastiani, P., S. Nicoli, and P. Santi, *Effect of lactic acid and iontophoresis on drug permeation across rabbit ear skin.* Int J Pharm, 2005. **292**(1-2): p. 119-26.
98. Burnette, R., ed. *Iontophoresis.* . Transdermal delivery, ed. J. Hadgraft and R.H. Guy. 1988: New York: Marcel Dekker. 247-288.
99. Wallace, S.M. and G. Barnett, *Pharmacokinetic analysis of percutaneous absorption: evidence of parallel penetration pathways for methotrexate.* J Pharmacokinet Biopharm, 1978. **6**(4): p. 315-25.

100. Jadoul, A., et al., *Quantification and localization of fentanyl and trh delivered by iontophoresis in the skin* Int J Pharm, 1995. **120**(2): p. 221-228.
101. Alvarez-Roman, R., et al., *Visualization of skin penetration using confocal laser scanning microscopy.* Eur J Pharm Biopharm, 2004. **58**(2): p. 301-316.
102. *EMEA. European Public Assessment Report (EPAR) for ionsys*. 2007; Available from: http://www.emea.europa.eu/humandocs/PDFs/EPAR/ionsys/061206en1.pdf.
103. *Opschorting registratie IONSYS®. Janssen-cilag.* 2008 26-11-2008; Available from: http://www.janssen-cilag.nl/news/detail.jhtml?itemname=opschorting_registratie_van_ionsys_26-11-2008.
104. *General product information*. Available from: http://www.vyteris.com/home/legal/LidositePI_PN20137Rev1.pdf.
105. Leboulanger, B., et al., *Lithium monitoring by reverse iontophoresis in vivo.* Clin Chem, 2004. **50**(11): p. 2091-100.
106. Leboulanger, B., R.H. Guy, and M.B. Delgado-Charro, *Non-invasive monitoring of phenytoin by reverse iontophoresis.* Eur J Pharm Sci, 2004. **22**(5): p. 427-33.
107. Delgado-Charro, M.B. and R.H. Guy, *Transdermal reverse iontophoresis of valproate: a noninvasive method for therapeutic drug monitoring.* Pharm Res, 2003. **20**(9): p. 1508-13.
108. Nixon, S., et al., *Reverse iontophoresis of L-lactate: in vitro and in vivo studies.* J Pharm Sci, 2007. **96**(12): p. 3457-65.
109. Wascotte, V., et al., *Non-invasive diagnosis and monitoring of chronic kidney disease by reverse iontophoresis of urea in vivo.* Eur J Pharm Biopharm, 2008. **69**(3): p. 1077-82.
110. Sieg, A., et al., *Extraction of amino acids by reverse iontophoresis in vivo.* Eur J Pharm Biopharm, 2009. **72**(1): p. 226-31.
111. Tierney, M.J., et al., *Clinical evaluation of the GlucoWatch biographer: a continual, non-invasive glucose monitor for patients with diabetes.* Biosens Bioelectron, 2001. **16**(9-12): p. 621-9.
112. van der Geest, R., M. Danhof, and H.E. Bodde, *Iontophoretic delivery of apomorphine. I: In vitro optimization and validation.* Pharm Res, 1997. **14**(12): p. 1798-803.
113. van der Geest, R., et al., *Iontophoretic delivery of apomorphine. II: An in vivo study in patients with Parkinson's disease.* Pharm Res, 1997. **14**(12): p. 1804-10.
114. Li, G.L., et al., *Pretreatment with a water-based surfactant formulation affects transdermal iontophoretic delivery of R-apomorphine in vitro.* Pharm Res, 2003. **20**(4): p. 653-9.
115. Li, G.L., et al., *Iontophoretic R-apomorphine delivery in combination with surfactant pretreatment: in vitro validation studies.* Int J Pharm, 2003. **266**(1-2): p. 61-8.
116. Li, G.L., et al., *Transdermal iontophoretic delivery of apomorphine in patients improved by surfactant formulation pretreatment.* J Control Release, 2005. **101**(1-3): p. 199-208.
117. Luzardo-Alvarez, A., M.B. Delgado-Charro, and J. Blanco-Mendez, *In vivo iontophoretic administration of ropinirole hydrochloride.* J Pharm Sci, 2003. **92**(12): p. 2441-8.
118. Luzardo-Alvarez, A., M.B. Delgado-Charro, and J. Blanco-Mendez, *Iontophoretic delivery of ropinirole hydrochloride: effect of current density and vehicle formulation.* Pharm Res, 2001. **18**(12): p. 1714-20.
119. Beart, P.M., et al., *Radioreceptor binding reveals the potencies of N,N-disubstituted 2-aminotetralins as D2 dopamine agonists.* Naunyn Schmiedebergs Arch Pharmacol, 1987. **336**(5): p. 487-93.
120. Beaulieu, M., et al., *N,N-disubstituted 2-aminotetralins are potent D-2 dopamine receptor agonists.* Eur J Pharmacol, 1984. **105**(1-2): p. 15-21.
121. Hacksell, U., et al., *N-Alkylated 2-aminotetralins: central dopamine-receptor stimulating activity.* J Med Chem, 1979. **22**(12): p. 1469-75.
122. Horn, A.S., et al., *Synthesis and dopaminergic activity of a new oxygen isostere of the 2-aminotetralins: N,N-dipropyl-8-hydroxy-3-chromanamine.* Eur J Med Chem, 1988. **22**(4): p. 325-328.
123. Thorberg, S.O., et al., *Aminochromans: potent agonists at central dopamine and serotonin receptors.* Acta Pharm Suec, 1987. **24**(4): p. 169-82.

124. van Vliet, L.A., et al., *Affinity for dopamine D2, D3, and D4 receptors of 2-aminotetralins. Relevance of D2 agonist binding for determination of receptor subtype selectivity.* J Med Chem, 1996. **39**(21): p. 4233-7.
125. Vermue, N.A., et al., *Pharmacological profile of N,N dipropyl-8-hydroxy-3-chromanamine, an oxygen isostere of the dopamine agonist N,N dipropyl-5-hydroxy-2-aminotetralin with enhanced presynaptic selectivity.* Arch Int Pharmacodyn Ther, 1988. **293**: p. 37-56.
126. Nugroho, A.K., et al., *Transdermal iontophoresis of rotigotine: influence of concentration, temperature and current density in human skin in vitro.* J Control Release, 2004. **96**(1): p. 159-67.
127. Nugroho, A.K., et al., *Transdermal iontophoresis of the dopamine agonist 5-OH-DPAT in human skin in vitro.* J Control Release, 2005. **103**(2): p. 393-403.
128. Nugroho, A.K., et al., *Transdermal iontophoresis of rotigotine across human stratum corneum in vitro: influence of pH and NaCl concentration.* Pharm Res, 2004. **21**(5): p. 844-50.
129. Nugroho, A.K., et al., *Pharmacokinetics and pharmacodynamics analysis of transdermal iontophoresis of 5-OH-DPAT in rats: in vitro-in vivo correlation.* J Pharm Sci, 2006. **95**(7): p. 1570-85.
130. Abla, N., et al., *Effect of charge and molecular weight on transdermal peptide delivery by iontophoresis.* Pharm Res, 2005. **22**(12): p. 2069-78.
131. Del Terzo, S., C.R. Behl, and R.A. Nash, *Iontophoretic transport of a homologous series of ionized and nonionized model compounds: influence of hydrophobicity and mechanistic interpretation.* Pharm Res, 1989. **6**(1): p. 85-90.
132. Henchoz, Y., et al., *A fast screening strategy for characterizing peptide delivery by transdermal iontophoresis.* J Control Release, 2009.
133. Lai, P.M. and M.S. Roberts, *An analysis of solute structure-human epidermal transport relationships in epidermal iontophoresis using the ionic mobility: pore model.* J Control Release, 1999. **58**(3): p. 323-33.
134. Mudry, B., et al., *Quantitative structure-permeation relationship for iontophoretic transport across the skin.* J Control Release, 2007. **122**(2): p. 165-72.
135. Peck, K.D., et al., *Quantitative description of the effect of molecular size upon electroosmotic flux enhancement during iontophoresis for a synthetic membrane and human epidermal membrane.* J Pharm Sci, 1996. **85**(7): p. 781-8.
136. Pikal, M.J., *Transport mechanisms in iontophoresis. I. A theoretical model for the effect of electroosmotic flow on flux enhancement in transdermal iontophoresis.* Pharm Res, 1990. **7**(2): p. 118-26.
137. Pikal, M.J. and S. Shah, *Transport mechanisms in iontophoresis. III. An experimental study of the contributions of electroosmotic flow and permeability change in transport of low and high molecular weight solutes.* Pharm Res, 1990. **7**(3): p. 222-9.
138. Pikal, M.J. and S. Shah, *Transport mechanisms in iontophoresis. II. Electroosmotic flow and transference number measurements for hairless mouse skin.* Pharm Res, 1990. **7**(3): p. 213-21.
139. Schuetz, Y.B., et al., *Structure-permeation relationships for the non-invasive transdermal delivery of cationic peptides by iontophoresis.* Eur J Pharm Sci, 2006. **29**(1): p. 53-9.
140. Yoshida, N.H. and M.S. Roberts, *Solute molecular size and transdermal iontophoresis across excised human skin* J control release, 1993. **25**(3): p. 177-195.
141. Yoshida, N.H. and M.S. Roberts, *Prediction of cathodal iontophoretic transport of various anions across excised skin from different vehicles using conductivity measurements.* J Pharm Pharmacol, 1995. **47**(11): p. 883-90.
142. Singh, P., M.S. Roberts, and H.I. Maibach, *Modelling of plasma levels of drugs following transdermal iontophresis.* J control release, 1995. **33**: p. 293-298.
143. Chaturvedula, A., et al., *Dermal, subdermal, and systemic concentrations of granisetron by iontophoretic delivery.* Pharm Res, 2005. **22**(8): p. 1313-9.
144. Chaturvedula, A., et al., *In vivo iontophoretic delivery and pharmacokinetics of salmon calcitonin.* Int J Pharm, 2005. **297**(1-2): p. 190-6.

145. Lopez, R.F., et al., *Optimization of aminolevulinic acid delivery by iontophoresis.* J Control Release, 2003. **88**(1): p. 65-70.
146. Singh, P., et al., *Transdermal iontophoresis and solute penetration across excised human skin.* J Pharm Sci, 1995. **84**(11): p. 1342-6.
147. Nugroho, A.K., et al., *Compartmental modeling of transdermal iontophoretic transport: I. In vitro model derivation and application.* Pharm Res, 2004. **21**(11): p. 1974-84.
148. Nugroho, A.K., et al., *Compartmental modeling of transdermal iontophoretic transport II: in vivo model derivation and application.* Pharm Res, 2005. **22**(3): p. 335-46.

2

Objective and outline of the thesis

1 Objective of the thesis

In the previous chapter the transdermal iontophoretic delivery of several dopamine agonists was reviewed. Despite the promising results further optimization of the transdermal iontophoretic delivery of dopamine agonists is required. The general objective of the presented research is the optimization of the transdermal iontophoretic delivery of dopamine agonists and its prodrugs for the symptomatic treatment of Parkinson's disease (Pd). To achieve this goal, the following specific items are considered:

1. Optimizing the transdermal iontophoretic delivery *in vitro* of a series of potent dopamine agonists, including rotigotine, 5-OH-DPAT and other potent structural analogs. In addition the mechanisms driving the iontophoretic transport are addressed.
2. Synthesis of novel dopaminergic prodrugs of 5-OH-DPAT with an extra chargeable group for transdermal iontophoretic delivery. Subsequently the chemical and enzymatic stability are examined. This part of the investigations was performed by Jeroen De Graan and will result in a dissertation at the Rijks Universiteit Groningen, Groningen, The Netherlands
3. *In vitro* iontophoresis of selected prodrugs of 5-OH-DPAT to investigate the feasibility for transdermal iontophoretic delivery
4. Pharmacokinetic-pharmacodynamic (PK-PD) studies in an animal model with the most promising candidates with a special focus on controlling the plasma concentration and the pharmacodynamic effect with transdermal iontophoresis
5. Evaluation and optimization of the kinetic models, developed by Nugroho et al. for the characterization of transdermal iontophoretic transport *in vitro* and *in vivo* [1-3]

2 Outline of the thesis

Part I-Optimizing the *in vitro* transdermal iontophoretic delivery of dopaminergic drugs

Although the potential of transdermal iontophoretic delivery of 5-OH-DPAT has already been demonstrated [3-4], a comprehensive characterization of iontophoresis of this potent dopamine agonist is necessary. Specifically, understanding of the mechanisms during iontophoresis driving 5-OH-DPAT across the skin barrier is essential to further improve the delivery *in vivo* in patients. In **CHAPTER 3** the optimization of the iontophoretic delivery of 5-OH-DPAT is approached from a mechanistic perspective. The influence of the following parameters is investigated: drug donor concentration, electro-osmotic contribution, influence of co-ions, current density and composition of the acceptor phase. In addition the feasibility of acetaminophen as a marker for the electro-osmotic flux is examined.

Rotigotine, another more lipophilic dopamine agonist from the 2-aminotetraline group (like 5-OH-DPAT), showed promising results when administered with transdermal iontophoresis [5-6]. However in these studies the solubility of the compound was the limiting factor for further increasing its delivery. Besides changing the donor formulation, the solubility and consequently the iontophoretic delivery can be improved by changing the salt form of the compound. In **CHAPTER 4** the influence of different salt forms of rotigotine (H_3PO_4 *vs* HCl) on the solubility and on the passive and iontophoretic transport efficiency is investigated. In addition the *in vitro* transport parameters are analyzed using compartmental modeling. The estimated parameters are combined with pharmacokinetic parameters from literature to evaluate the iontophoretic delivery *in vivo* in a series of simulations.

Next to 5-OH-DPAT and rotigotine, also other members of the 2-aminotetralins are very potent at the D_1- and/or D_2-receptor in the striatum and are potential candidates for transdermal iontophoresis. In **CHAPTER 5** the transdermal iontophoretic delivery of a series of novel dopamine agonists across human stratum corneum (HSC) and dermatomed human skin (DHS) is investigated. The molecules from the 2-aminotetraline group were selected based on their potency and molecular structure: 5-OH-MPAT, 5-OH-EPAT, 5,6-di-OH-MPAT and 5,6-di-OH-DPAT. In addition a potent chromanamine (8-OH-DPAC), which is structurally closely related to the above mentioned group, is added to the investigations. In these investigations the applicability of the kinetic models for the characterization of transdermal iontophoresis, developed by Nugroho et al., are also evaluated. The small structural

changes between the compounds tested allowed us to investigate the influence of the molecular structure and physicochemical properties on the iontophoretic delivery.

Part II-*In vivo* assessment of controlling the iontophoretic delivery of (S)-5-OH-DPAT

In **CHAPTER 6** the pharmacokinetics (PK) and pharmacodynamics (PD) following transdermal iontophoretic delivery of the active enantiomer of 5-OH-DPAT, (S)-5-OH-DPAT is investigated in male Wistar rats. The first aim of this study is to examine the relationship between the current density, the *in vivo* iontophoretic transport and the (S)-5-OH-DPAT plasma profile. To conduct transdermal iontophoresis studies, it is necessary to anesthetize the animals. Therefore the second aim of the present study is to examine the effect of the anesthetic mixture, together with the effect of transdermal iontophoresis, and blood sampling on the striatal dopamine release. This is important since the striatal dopamine release is the pharmacodynamic end-point chosen to monitor the pharmacological response following transdermal iontophoresis. The third aim is to address the PK-PD relationship following transdermal iontophoresis of (S)-5-OH-DPAT under non-saturated conditions. This implies the establishment of a controlled and reversible effect. The effect is monitored in the striatum with on-line microdialysis, while simultaneously blood samples are taken. In this chapter extensive analysis is performed with non-linear mixed effects modeling, using an integrated compartmental PK-PD model.

Part III-Transdermal iontophoretic delivery of ester prodrugs of 5-OH-DPAT: from synthesis to *in vivo* studies

In **CHAPTER 7** the transdermal delivery of 4 new ester prodrugs of 5-OH-DPAT is studied: glycine-, proline, valine- and β-alanine-5-OH-DPAT. Since ester prodrugs are susceptible to hydrolysis, stability assays are performed to select the optimal candidate(s) for further investigations. Furthermore the solubility of the prodrugs is investigated and compared to the parent drug 5-OH-DPAT. In a series of transport studies the iontophoretic delivery across HSC and DHS is examined. The main focus of the *in vitro* transport studies is to identify a prodrug that is efficiently transported with iontophoresis and which is hydrolyzed during transport through the skin. These results lead to the selection of the optimal prodrug for follow-up studies *in vivo*.

The pharmacokinetics and pharmacodynamic effect of the prodrug of (S)-5-OH-DPAT are examined in the newly developed animal model, described in **CHAPTER 6**. The resulting PK-PD parameters of the prodrug, obtained with compartmental modeling, are discussed and compared to the parameters of the parent drug (S)-5-OH-DPAT.

In **CHAPTER 8** a summary of all the results of the presented research is provided. Furthermore these results are discussed and put in perspective to the general applicability of transdermal iontophoresis of dopamine agonist for the treatment of Parkinson's disease. Finally future perspectives of transdermal iontophoresis of dopamine agonists are addressed from a mechanistic, mathematical and clinical point of view.

References

1. Nugroho, A.K., et al., *Compartmental modeling of transdermal iontophoretic transport: I. In vitro model derivation and application.* Pharm Res, 2004. **21**(11): p. 1974-84.
2. Nugroho, A.K., et al., *Compartmental modeling of transdermal iontophoretic transport II: in vivo model derivation and application.* Pharm Res, 2005. **22**(3): p. 335-46.
3. Nugroho, A.K., et al., *Pharmacokinetics and pharmacodynamics analysis of transdermal iontophoresis of 5-OH-DPAT in rats: in vitro-in vivo correlation.* J Pharm Sci, 2006. **95**(7): p. 1570-85.
4. Nugroho, A.K., et al., *Transdermal iontophoresis of the dopamine agonist 5-OH-DPAT in human skin in vitro.* J Control Release, 2005. **103**(2): p. 393-403.
5. Nugroho, A.K., et al., *Transdermal iontophoresis of rotigotine: influence of concentration, temperature and current density in human skin in vitro.* J Control Release, 2004. **96**(1): p. 159-67.
6. Nugroho, A.K., et al., *Transdermal iontophoresis of rotigotine across human stratum corneum in vitro: influence of pH and NaCl concentration.* Pharm Res, 2004. **21**(5): p. 844-50.

Part I

Optimizing the *in vitro* transdermal iontophoretic delivery of dopaminergic drugs

3

Mechanistic studies of the transdermal iontophoretic delivery of 5-OH-DPAT *in vitro*

Oliver W. Ackaert[a], Jeroen Van Smeden[a], Jeroen De Graan[c], Durk Dijkstra[c], Meindert Danhof[b] and Joke A. Bouwstra[a]

[a]Division of Drug Delivery Technology, Leiden/Amsterdam Center for Drug Research, Leiden, The Netherlands

[b]Division of Pharmacology, Leiden/Amsterdam Center for Drug Research, Leiden, The Netherlands

[c]Department of Medicinal Chemistry, University Center of Pharmacy, University of Groningen, Groningen, The Netherlands

adapted from *Journal of Pharmaceutical Sciences.* 2010 Jan;99(1):275-85

Abstract

A characterization and optimization of the *in vitro* transdermal iontophoretic transport of 5-hydroxy-2-(N,N,-di-n-propylamino)tetralin (5-OH-DPAT) is presented. The utility of acetaminophen as a marker of electroosmotic flow was studied as well. The following parameters of iontophoretic transport of 5-OH-DPAT were examined: drug donor concentration, electroosmotic contribution, influence of co-ions, current density and composition of the acceptor phase. The steady-state flux ($Flux_{ss}$) of acetaminophen was linearly correlated with the donor concentration and co-iontophoresis of acetaminophen did not influence the iontophoretic flux of 5-OH-DPAT, indicating that acetaminophen is an excellent marker of electroosmotic flow. Lowering the Na^+ concentration from 78 mM to 10 mM in the donor phase, resulted in a 2.5 fold enhancement of the $Flux_{ss}$. The $Flux_{ss}$ showed a non-linear relation with the drug donor concentration and an excellent linear correlation with the current density. Reducing the pH of the acceptor phase from 7.4 to 6.2 resulted in a dramatic decrease of the $Flux_{ss}$ of 5-OH-DPAT, explained by a reduced electroosmotic flow and an increased counter-ion flow. Optimization of the conditions resulted in a maximum $Flux_{ss}$ of 5-OH-DPAT of 1.0 $\mu mol.cm^{-2}.h^{-1}$ demonstrating the potential of the iontophoretic delivery of this dopamine agonist for the symptomatic treatment of Parkinson's disease.

Key words: Controlled release; Skin; Transdermal drug delivery; Iontophoresis; Percutaneous; Electroosmosis; Acceptor phase; Dopamine agonist; Parkinson's disease

1 Introduction

Parkinson's disease is an age-related progressive neurological disorder with a prevalence of 1-2 % in people over the age of 50. Pharmacotherapy is the first line symptomatic treatment of this disease [1]. Currently orally administered levodopa is still considered the golden standard, but its possible neurotoxicity and the induction of movement disorders after chronic use demands for the development of alternative therapies [2]. One of the most important alternatives is the use of dopamine agonists, such as apomorphine, carbergoline, ropinirole and rotigotine which directly activate the postsynaptic dopamine receptor [3]. However when these dopamine agonists are administered orally, often fluctuations in plasma concentrations occur resulting in pulsatile dopaminergic stimulation. Therefore, the continuous dopamine stimulation may be the optimal symptomatic treatment of Parkinson's disease, reducing *off* periods and dyskenisias [2, 4].

Transdermal iontophoresis is one of the promising techniques for non-invasive continuous delivery of dopamine agonists. By applying an electric current across the skin it is possible to enhance the transdermal delivery of small charged molecules. In addition by modulation of the current and donor concentration it will be possible to adjust the rate of administration to the requirements of the individual patient, which will be an important advantage. In the last ten years several dopamine agonists have been studied for their ability to be administered by iontophoresis [5-10]. The potent dopamine agonist 5-hydroxy-2-(N,N,-di-n-propylamino)tetralin (5-OH-DPAT) [11-12], has already been proven to be suitable for iontophoretic delivery *in vitro* as well as *in vivo* [5, 13]. However characterization of the transport mechanisms driving the iontophoretic delivery *in vitro* is crucial to understand and optimize the iontophoretic delivery *in vivo* to patients.

Transdermal migration of chemicals during iontophoresis is influenced by several factors such as pH, the presence of ions having the same charge (co-ions) and ions having the opposite charge [14]. This implies that the iontophoretic transport of chemicals is influenced by the composition of the donor phase as well as the acceptor phase. In contrast to the donor phase, the effect of the composition in the acceptor phase has not been widely studied [14-16].

The aim of the present study was to fully characterize the transdermal iontophoretic transport of the dopamine agonist 5-OH-DPAT across the skin. Especially the electroosmotic contribution, the influence of ion composition in the donor and acceptor phase on the iontophoretic delivery of 5-OH-DPAT were studied.

Several marker molecules, like ^{14}C-mannitol and acetaminophen, are available to estimate the electroosmotic contribution during iontophoretic transport [17-21]. In the last few years acetaminophen has gained more interest over ^{14}C-mannitol, because of its practical advantages. Although acetaminophen has been widely used as a marker for electroosmosis, until now its transport has not been fully characterized. Therefore in the current study acetaminophen as a marker molecule for electroosmosis is evaluated as well.

2 Materials and methods

2.1 Materials

5-OH-DPAT (HBr salt, purity>98%) was synthesized at the Department of Medicinal Chemistry of the University of Groningen, Groningen, the Netherlands. Silver, silver chloride (purity>99.99%), Trypsin (Type III from bovine pancreas) and trypsin inhibitor (Type II-S from soybean) were obtained from Sigma-Aldrich (Zwijndrecht, The Netherlands). Acetaminophen was purchased from Brocacef BV (Maarssen, the Netherlands) and D(-)Mannitol was obtained from BDH Laboratory supplies (Poole, UK). Bacteriological agar was purchased from Life Technologies (Paisley, Scotland). Spectra/Por® RC dialysis membrane disks (cut off value of 6000-8000 Da) were purchased from Spectrum laboratories, Inc (Rancho Dominquez, Ca, USA). Tetrahydrofuran (THF, stabilized, purity>99.8%) was obtained from Biosolve (Valkenswaard, the Netherlands). Triethylamine (TEA, purity>99%) was obtained from Acros Organics (Geel, Belgium). All other chemicals and solvents were of analytical grade. All solutions were prepared in Millipore water with a restitivity of more than 18 MΩ.cm.

2.2 Preparation of Human Stratum Corneum (HSC)

The preparation of human stratum corneum was performed according to the method described previously [13]. Briefly, within 24h after surgical removal of the human skin residual subcutaneous fat was removed. Dermatomed human skin (DHS) was obtained by dermatoming the skin to a thickness of about 300 μm. In order to obtain HSC, DHS was incubated with the dermal side on Whatman paper soaked in a solution of 0.1% trypsin in 150 mM phosphate buffered saline (PBS) pH 7.4 (NaCl: 8 g.L-1 , Na_2HPO_4: 2.86 g.L-1 , KH_2PO_4: 0.2 g.L-1 , KCl: 0.19 g.L-1) overnight at 4 °C and subsequently for 1h at 37 °C after which HSC was peeled off from the underlying viable epidermis and dermis. HSC was subsequently washed in a 0.1%

trypsin inhibitor solution in Millipore water and several times in water and stored in a desiccator in a N_2 environment.

2.3 Preparation of salt bridge

The use of salt bridges enables to reduce the amount of competing cations in the donor phase, while the salt bridge still contains enough Cl^--ions, added as NaCl, to feed the anodal electrochemistry. An agar suspension was prepared as follows: 100 mL of PBS pH 7.4 was heated in an Erlenmeyer flask to boiling. Then 3.0 g agar was added, stirring was commenced and the solution was continuously heated until a uniform suspension was formed. The mixture was transferred to a silicon tube of appropriate length (total volume 1.0 mL). The tube was then left at room temperature until the mixture had gelled. Thereafter the anode was placed carefully in the salt bridge.

2.4 Solubility of 5-OH-DPAT

The solubility was determined according to the method described previously [6]. Briefly, 5-OH-DPAT was solubilized in 5 mM citrate buffer pH 5.0 and 6.0, containing 68 mM NaCl. After adjusting the pH of the solution with 0.05 M NaOH or HCl, each solution was shaken for 48h at 700 rpm (IKA-VIBRAX-VXR, Omnilabo International BV, Breda, The Netherlands) at room temperature. All saturated solutions were centrifuged at 3600 rpm (Allegra™ 6R centrifuge, Beckman Coulter, Fullerton, CA, USA) for 30 minutes. Each supernatant was then filtered by using a 0.2 μm porous membrane (PTFE Acrodisc®, Pall, East Hills, NY, USA), after which the concentration was determined by HPLC.

2.5 *In vitro* transport studies

A 9-channel computer controlled power supply was used to provide a constant direct current (Electronics Department, Gorlaeus Laboratories, Leiden University, The Netherlands) during iontophoresis. The system was equipped with differential input channels per current source enabling on-line measurement of the electric resistance across HSC in each diffusion cell. Ag/AgCl was used as driver electrode pair. All transport studies were carried out, using a three chamber continuous flow through cell as described elsewhere [13]. In all experiments HSC of at least 2 different donors was used. The donor formulation was buffered with 5 mM citric acid and D-mannitol was added to the donor phase to obtain iso-osmolar conditions. Unless stated otherwise the cathodal chamber was filled with PBS pH 7.4 and the acceptor chamber was continuously perfused with PBS pH 7.4 at a flow rate of ± 6.5 $ml.min^{-1}$.

During the experiment the temperature of the acceptor phase was maintained at 32 °C, the skin temperature *in vivo*. Unless stated otherwise, the following protocol was used for *in vitro* iontophoretic transport studies: 6h passive diffusion, followed by 9h of iontophoresis at a current density of 500 $\mu A.cm^{-2}$ and finishing with 5h passive diffusion. During the experiment the anodal and cathodal chamber were continuously stirred at 365 rpm. Samples were collected every hour with an automatic fraction collector (ISCO Retriever IV, Beun De Ronde BV, Abcoude, The Netherlands). The specific conditions for each individual series of experiments are described below.

2.5.1 Acetaminophen as marker molecule for the electroosmotic flow

To determine whether there is a linear correlation between the donor concentration acetaminophen and its iontophoretic transport, studies were performed with 3 different donor concentrations acetaminophen (7.5 mM, 15 mM and 30 mM) in a citric buffer pH 5.0, containing 68 mM NaCl.

The influence of co-iontophoresis of acetaminophen on the 5-OH-DPAT flux was also investigated. The donor formulation was at pH 5.0 in the presence of 68 mM NaCl and 3.9 mM 5-OH-DPAT. The iontophoretic transport of 5-OH-DPAT in presence (15 mM) and absence of acetaminophen was measured.

2.5.2 Electromigrative and Electroosmotic contribution to the transport of 5-OH-DPAT

The concentration of 5-OH-DPAT in the donor concentration was 1.5 or 3.9 mM. Acetaminophen (15 mM) was added to the donor solution as a marker molecule for the electroosmosis. The donor solution was buffered with citric buffer at a pH of either 5.0 or 6.0. All experiments were performed in the presence of 68 mM NaCl in the donor solution.

2.5.3 Influence of competing ions in the donor phase

The influence of competing co-ions in the donor phase was investigated, using different concentrations of 5-OH-DPAT varying from 0.15 to 35.1 mM. The concentration of NaCl in the donor phase was either 0 or 68 mM. In the absence of NaCl the only source of Na^+ was Na_3citrate.$2H_2O$, used to buffer the solution and the amount of Na^+ was calculated at 10 mM. Therefore the total Na^+-concentration was either 10 mM or 78 mM. In the case of 10 mM Na^+ the Ag-electrode (anode) was placed in a salt bridge. The donor solution was buffered at pH 6.0.

2.5.4 Influence of the pH of the acceptor phase

The iontophoretic delivery of 5-OH-DPAT was investigated using PBS with a different pH as acceptor phase. The acceptor solution was either PBS pH 7.4 or PBS pH 6.2. (8 $g.L^{-1}$ NaCl, 0.19 $g.L^{-1}$ KCl, 0.43 $g.L^{-1}$ $Na_2HPO_4.2H_2O$, 0.97 $g.L^{-1}$ KH_2PO_4), both at iso-osmolar conditions. The concentration of 5-OH-DPAT was 1.5, 3.9 or 7.0 mM. All experiments were conducted in the presence of 68 mM NaCl in the donor solution, buffered at pH 5.0.

The electroosmotic or water flow across HSC was investigated using PBS as acceptor phase. The pH of the acceptor solution was either 7.4 or 6.2. The concentration of acetaminophen, used as a marker molecule for the electroosmotic flow, was 15 mM. The donor solution was buffered at pH 6.0 using 5 mM citrate buffer. All experiments were conducted in the presence of 68 mM NaCl in the donor phase.

The ion transport across HSC was investigated using PBS with different pH as acceptor phase. The pH of the acceptor solution was either 7.4 or 6.2. The pH of the donor solution was 6.0. A current of 500 $\mu A.cm^{-2}$ was applied during 19h. This experiment was performed in the absence of NaCl and the Ag-electrode (anode) was placed in a salt bridge. At regular time intervals (0, 2, 4, 6 and 19h) an aliquot of 100 µL of the donor solution was sampled to measure the osmolarity with an osmometer (Micro-osmometer type 13, Roebling, Berlin, Germany).

2.5.5 Influence of current density

The iontophoretic transport of 5-OH-DPAT (3.9 mM), buffered at pH 6.0, across HSC was investigated at different current densities. The protocol used for these experiments is: 2h passive diffusion + 6h 125 $\mu A.cm^{-2}$ + 6h 250 $\mu A.cm^{-2}$ + 4h 500 $\mu A.cm^{-2}$ + 6h passive diffusion. The Na^+-concentration in the donor phase was 10 mM and the Ag-electrode (anode) was placed in a salt bridge.

2.6 Analytical methods

Prior to and at the end of a transport study pH and osmolarity of donor and acceptor compartment were measured. All samples of the iontophoretic transport studies were analyzed by RP-HPLC using a Superspher® 60 RP-select B, 75 mm-4 mm column (Merck KGaA, Darmstadt, Germany). 5-OH-DPAT was detected using a scanning fluorescence detector (Waters™ 474, Millipore, Milford, MA, USA) at excitation and emission wavelengths of 275 and 302 nm. Acetaminophen was detected using a UV detector (Dual λ Absorbance Detector 2487, Waters, Milford, USA) at a

wavelength of 254 nm. Filtered and degassed mobile phase contained 100 mM acetate buffer (pH 3.6)/THF (95/5 v/v) with the addition of 30 mM TEA to prevent peak tailing. The injection volume was 50 µL and the flow rate was set to 1.5 $mL.min^{-1}$. Calibration curves showed a linear response when using concentrations of compounds between 0.1 and 40 $\mu g.mL^{-1}$ (R^2>0.9999). The limit of detection (LOD) and limit of quantification (LOQ) were experimentally determined for all compounds of interest: 5-OH-DPAT has a LOD and LOQ of 3.5 and 5.8 $ng.mL^{-1}$ respectively. Acetaminophen has a LOD and LOQ of 5.8 and 9.6 $ng.mL^{-1}$, respectively.

2.7 Determination of electromigrative and electroosmotic contribution

The total iontophoretic flux consists of the passive flux (J_{pass}), the electroosmotic flux (J_{EO}) and the electromigrative flux (J_{EM}). The passive flux is calculated during 6h prior to the iontophoretic phase. The electroosmotic flow is calculated as described below. The electromigrative flux is calculated by subtracting the passive and electroosmotic flux from the total flux.

The water flow during iontophoresis can be derived from the flux of the neutral permeant acetaminophen by the following Equation [22]:

$$Vw = \frac{J_{ace}}{C_{ace}} \quad (1)$$

where V_w is the water flow, J_{ace} is the steady state flux ($Flux_{ss}$) and C_{ace} the donor concentration of acetaminophen. When plotting the J_{ace} as function of the donor concentration of acetaminophen C_{ace}, the water flow can be calculated from the slope of the regression line. The electroosmotic flow of 5-OH-DPAT (J_{EO}) is proportional to the volume flow (V_w) and the molar concentration of the solute, 5-OH-DPAT ($C_{5\text{-}OH\text{-}DPAT}$) [22] and can be calculated as follows:

$$J_{EO} = V_w \times C_{5-OH-DPAT} \quad (2)$$

2.8 Data analysis

The cumulative flux of 5-OH-DPAT and acetaminophen during iontophoretic transport was plotted as a function of time. The $Flux_{ss}$ was estimated from the linear part of the slope of this plot according to the permeation lag-time method [13]. All data are presented as mean ± standard deviations (SD). When the effect of two factors was investigated simultaneously two-way ANOVA was used for statistical analysis. When a statistical analysis was performed for only 2 groups, a Students t-test was used. For all statistical analysis a significance level of $p<0.05$ was used.

3 Results

3.1 Acetaminophen as marker molecule for the electroosmotic flow

First the proportionality of the flux with the donor concentration was investigated, As depicted in Figure 1A a variation in donor concentration of acetaminophen of 7.5, 15.0 and 30.0 mM resulted in steady state fluxes ($Flux_{ss}$) of 30.6 ± 7.3, 48.6 ± 7.8 and 103.5 ± 26.5 nmol.cm^{-2}.h^{-1}, respectively. The acetaminophen concentration and $Flux_{ss}$ are linearly related. The linear regression line was forced through zero (R^2=0.995). According to Equation 1 the slope of the regression line represents the water flow during iontophoretic transport and is estimated at 3.39 ± 0.17 ml.cm^{-2}.h^{-1}. Furthermore as depicted in Figure 1B a change from pH 5.0 to 6.0 in the donor phase results in a significant increase in acetaminophen flux from 50.0 ± 11.0 nmol.cm^{-2}.h^{-1} to 68.0 ± 5.9 nmol.cm^{-2}.h^{-1} (t-test; $p<0.05$). Secondly the influence of co-iontophoresis of acetaminophen on the $Flux_{ss}$ of 5-OH-DPAT is presented in Table 1. The steady state flux of 5-OH-DPAT (3.9 mM), buffered at pH 5.0, remained

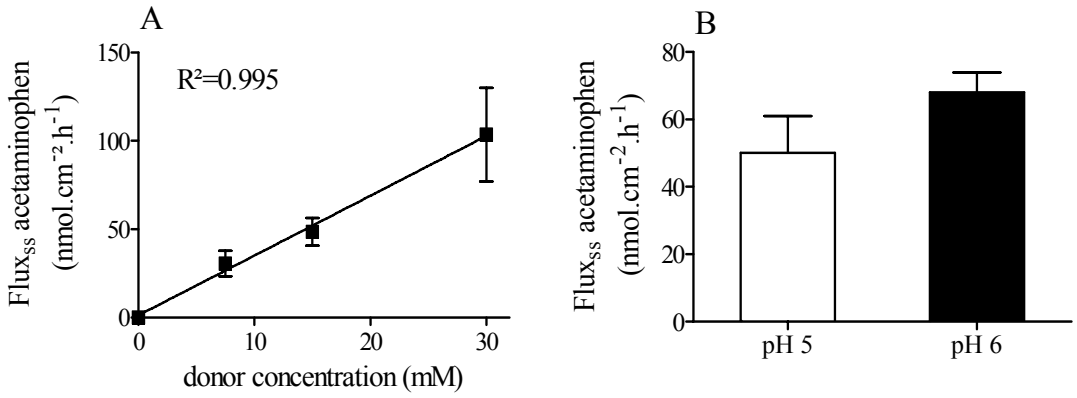

Figure 1 A: The linear correlation between the steady state flux ($Flux_{ss}$) *vs* the donor concentration during iontophoresis (500 µA.cm^{-2}) of acetaminophen at donor pH 5.0. Data are presented as mean ± SD (n=5-7). The acceptor phase consisted of PBS pH 7.4.
B: bar plot of the $Flux_{ss}$ of acetaminophen (15 mM) at donor pH 5.0 (white bar) and pH 6 (black bar). Data are presented as mean + SD (n≥4). A current density of 500 µA.cm^{-2} was applied and PBS pH 7.4 was used as acceptor phase. A significant difference is observed between the $Flux_{ss}$ at pH 5.0 and 6.0 (t-test; $p<0.05$).

unaffected when acetaminophen (15mM) was added to the donor phase (t-test; $p>0.05$). Moreover the iontophoretic flux profile of 5-OH-DPAT remained also unchanged (data not shown).

3.2 Solubility of 5-OH-DPAT

The solubility of 5-OH-DPAT was determined in a citric buffer (5 mM), containing 68 mM NaCl at pH 5.0 and 6.0. The maximum solubility decreases with increasing pH from 56.7 ± 1.4 mM at pH 5.0 to 47.4 ± 1.4 mM at pH 6.0.

3.3 Iontophoretic delivery of 5-OH-DPAT

3.3.1 Electromigrative and electroosmotic contribution

The passive flux appeared to be negligible, contributing only a maximum of 0.02% to the total flux. The results of the determination of the electromigrative and electroosmotic contribution are provided in Table 1. The electroosmosis flux has a minor but significant contribution to the 5-OH-DPAT iontophoretic flux. No

Table 1: The steady state flux of 5-OH-DPAT after iontophoresis (500 $\mu A.cm^{-2}$) by the difference in pH, acetaminophen concentration and Na^+ concentration. The acceptor phase consisted of PBS pH 7.4. Results are presented as mean ± SD (n≥3).

Donor phase				**Results**			
5-OH-DPAT conc. (mM)	Ace conc. (mM)	Na^+ conc. (mM)	pH	$Flux_{ss}$ of 5-OH-DPAT ($nmol.cm^{-2}.h^{-1}$)	J_{EO} ($nmol.cm^{-2}.h^{-1}$)	Relative contribution (% J_{EO})	J_{EM} ($nmol.cm^{-2}.h^{-1}$)
3.9	0	78	5	188.9 ± 25.5	n.a.	n.a.	n.a.
3.9	15	78	5	210.4 ± 13.0	13.7 ± 3.4	6.5 ± 1.7	196.7 ± 13.4
3.9	15	78	6	214.3 ± 6.0	14.5 ± 1.0	6.8 ± 0.5	199.8 ± 6.0
3.9	15	10	6	482.0 ± 36.8	14.7 ± 4.4	3.0 ± 0.9	467.3 ± 37.0

n.a.: not applicable
Ace: acetaminophen

significant change in the contribution of J_{EO} and J_{EM} to the total flux of 5-OH-DPAT is observed when changing the pH of the donor solution from pH 5.0 to 6.0 ($p>0.05$).

Also depicted in Table 1, at a donor concentration of 3.9 mM 5-OH-DPAT a pH change from 5.0 to 6.0 does not significantly change the 5-OH-DPAT $Flux_{ss}$ ($p>0.05$). When focusing on the influence of 5-OH-DPAT on the acetaminophen flux, 3.9 mM 5-OH-DPAT buffered at either pH 5.0 or 6.0 does not change the acetaminophen flux demonstrating that 5-OH-DPAT does not change the negative charge of the HSC and thus does not change the permselectivity of the HSC (data not shown).

3.3.2 Influence of competing ions in the donor phase on the iontophoretic flux of 5-OH-DPAT

The effect of NaCl in the donor compartment was studied. The total concentration of Na^+ in the donor phase was either 10 mM (absence of NaCl) or 78 mM (addition of 68 mM NaCl). The transport studies were conducted with 5 different donor concentrations of 5-OH-DPAT varying between 0.15 and 35.1 mM 5-OH-DPAT. Figure 2A shows the flux profile of 5-OH-DPAT (1.5 mM) when 10 mM or 78 mM

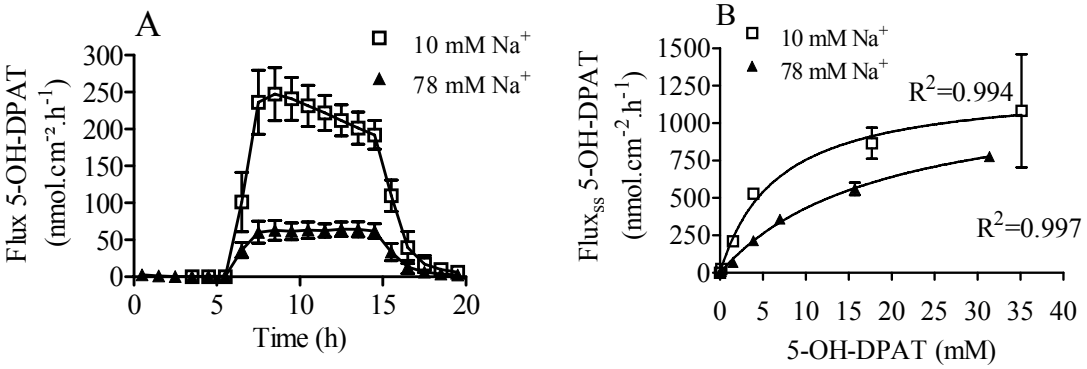

Figure 2 A: Iontophoretic flux (500 $\mu A.cm^{-2}$) *vs* time profile of 5-OH-DPAT solution (1.5 mM) buffered at pH 6.0 in the presence of 10 mM (open square) and 78 mM Na^+ (closed triangle). PBS pH 7.4 was used as acceptor phase. Data are presented as mean ± SD (n=3). **B:** The non-linear correlation of the $Flux_{ss}$ *vs* the donor concentration in the presence of 10 mM (open square) and 78 mM Na^+ (closed triangle) in the donor phase, buffered at pH 6.0. A current density of 500 $\mu A.cm^{-2}$ was applied and PBS pH 7.4 was used as acceptor phase. Data are presented as mean ± SD (n=3-6).

Na^+ was present in the donor phase. Reduction of the amount Na^+ in the donor phase augments the flux of 5-OH-DPAT dramatically. These results show a clear steady state flux when 78 mM Na^+ is present in the donor phase. However when the amount Na^+ present in the donor phase is 10 mM the flux is reduced gradually during the iontophoretic period.

As shown in Figure 2B non-linear regression analysis showed a hyperbolic correlation between the $Flux_{ss}$ *vs* donor concentration when the Na^+ content in the donor phase was 10 mM (R^2=0.997) and 78 mM (R^2=0.994). In the presence of NaCl the $Flux_{ss}$ of 5-OH-DPAT gradually increased from 9.4 ± 0.3 (0.15 mM 5-OH-DPAT) to 775.0 ± 28.4 $nmol.cm^{-2}.h^{-1}$ (31.4 mM 5-OH-DPAT). In the absence of NaCl there was an increase in $Flux_{ss}$ of 5-OH-DPAT from 25.7 ± 2.8 (0.15 mM 5-OH-DPAT) to 1081.9 ± 377.8 $nmol.cm^{-2}.h^{-1}$ (35.1 mM 5-OH-DPAT). Comparing the 5-OH-DPAT $Flux_{ss}$ at equal donor concentrations, an enhancement factor varying between 2.5 and 3.0 is observed when the amount of competing co-ions in the donor phase was reduced. As presented in Table 1 the addition of 68 mM NaCl to the donor solution has no influence on the absolute value of the electroosmotic flux of 3.9 mM 5-OH-DPAT in a donor solution, buffered at pH 6.0 ($p>0.05$).

Table 2: Comparison of the steady state flux of 5-OH-DPAT when using PBS pH 7.4 or PBS pH 6.2 as acceptor phase at different donor concentrations. The donor phase consisted of 5-OH-DPAT buffered at pH 5.0, containing 78 mM Na^+ and a current density of 500 $\mu A.cm^{-2}$ was applied. Results are presented as mean ± SD (n=4-9).

	PBS pH 7.4	**PBS pH 6.2**
Donor concentration (mM)	$Flux_{ss}$ ($nmol.cm^{-2}.h^{-1}$)	$Flux_{ss}$ ($nmol.cm^{-2}.h^{-1}$)
1.5	69.8 ± 7.2	68.2 ± 8.2
3.9	211.9 ± 11.1[a]	137.7 ± 8.6[a]
7.0	358.9 ± 28.5[b]	208.9 ± 10.2[b]

a,b: t-test: $p<0.05$

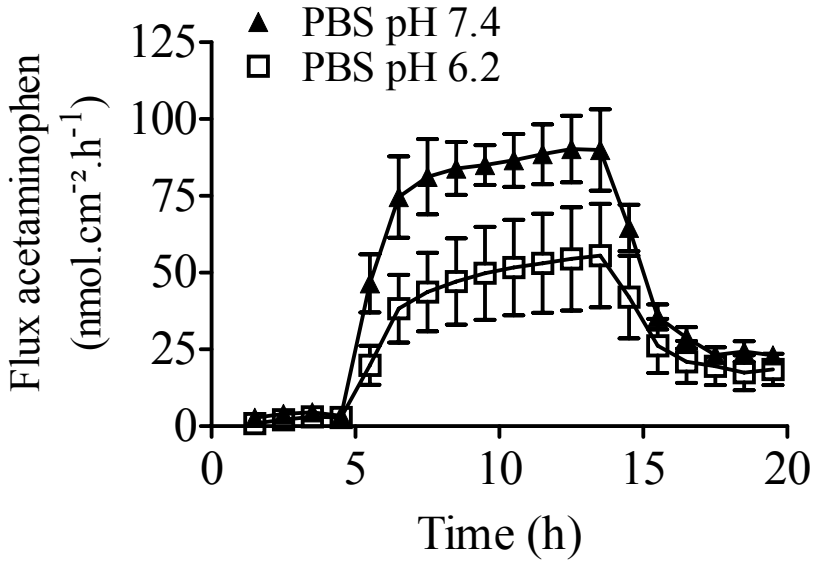

Figure 3: The acetaminophen flux *vs* time profiles, during iontophoresis using PBS pH 7.4 (closed triangle) and PBS pH 6.2 (open square) as acceptor phase. A buffered donor solution (pH 6.0) containing 15 mM acetaminophen was used, applying a current density of 500 $\mu A.cm^{-2}$. Data are presented as mean ± SD (n=3-4).

3.3.3 Influence of the pH of the acceptor phase on the 5-OH DPAT iontophoretic flux

All 5-OH-DPAT steady state fluxes ($Flux_{ss}$) during iontophoresis with different acceptor phase are summarized in Table 2. At a concentration of 1.5 mM 5-OH-DPAT no difference in steady state flux was observed ($p>0.05$), however at increased 5-OH-DPAT concentrations of 3.9 mM and 7.0 mM an acceptor phase at pH 6.2 resulted in a dramatically lower steady state flux ($p<0.001$) compared to the 5-OH-DPAT iontophoretic $Flux_{ss}$ using an acceptor phase at pH 7.4.

As the pH value of the acceptor phase had a strong affect on the 5-OH-DPAT iontophoretic flux, several studies were performed to unravel the underlying mechanism. A reduction in the pH in the acceptor phase may reduce the charge density of the HSC and therefore reduce its permselectivity. The permselectivity with an acceptor phase of either pH 7.4 or pH 6.2 was studied by iontophoretic transport of acetaminophen. A reduction in pH of the acceptor phase from pH 7.4 to pH 6.2

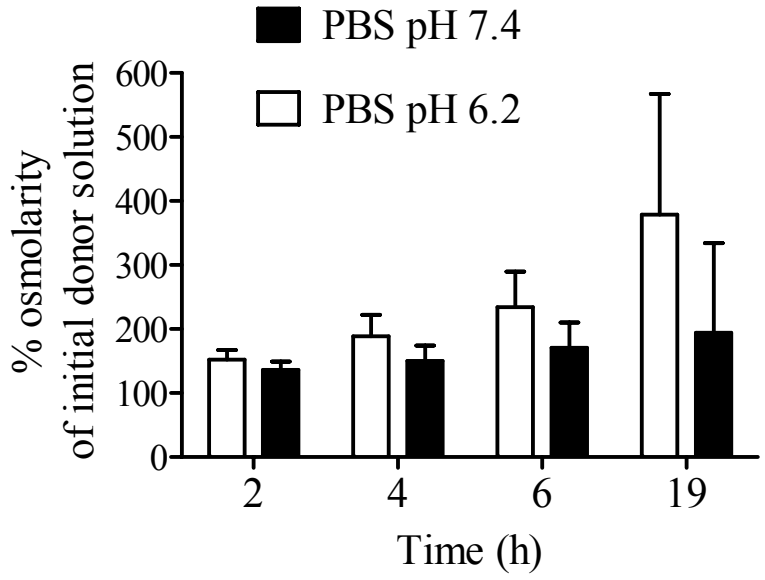

Figure 4: Bar plot of the osmolarity of the donor phase at different time points when using PBS pH 6.2 (white bar) or PBS pH 7.4 (black bar) as acceptor phase. The donor solution, buffered at pH 6, contained 10 mM Na^+, a salt bridge was used and a current density of 500 $\mu A.cm^{-2}$ was applied. Data are presented as mean ± SD (n=4-5).

resulted in a decrease in the $Flux_{ss}$ of acetaminophen from 86.4 ± 5.5 $nmol.cm^{-2}.h^{-1}$ to 51.2 ± 16.1 $nmol.cm^{-2}.h^{-1}$ ($p<0.05$) (Figure 3), demonstrating that the permselectivity of the stratum corneum is indeed reduced at the acceptor phase of 6.2. The flux pattern remained unaffected.

A change in the permselective properties may influence the flux of ions during iontophoresis across the stratum corneum from donor to acceptor phase and from acceptor to donor phase and therefore affect the osmolarity in the donor phase when changing the pH in the acceptor phase from 7.4 to 6.2. The osmolarity of the donor phase was measured using the same iontophoretic conditions as in the studies described in the previous section. The osmolarity expressed as % osmolarity of the original donor solution, at different time points during current application, is depicted in Figure 4. Simultaneous linear regression of osmolarity *vs* time shows a good correlation for both conditions (R^2=0.8642 for pH 7.4 and R^2=0.9835 for pH 6.2) and shows a significant difference between the slopes of both regression lines (t-test; $p<0.05$). Decreasing the pH of the acceptor phase from 7.4 to 6.2 causes a higher increase in osmolarity in the donor phase.

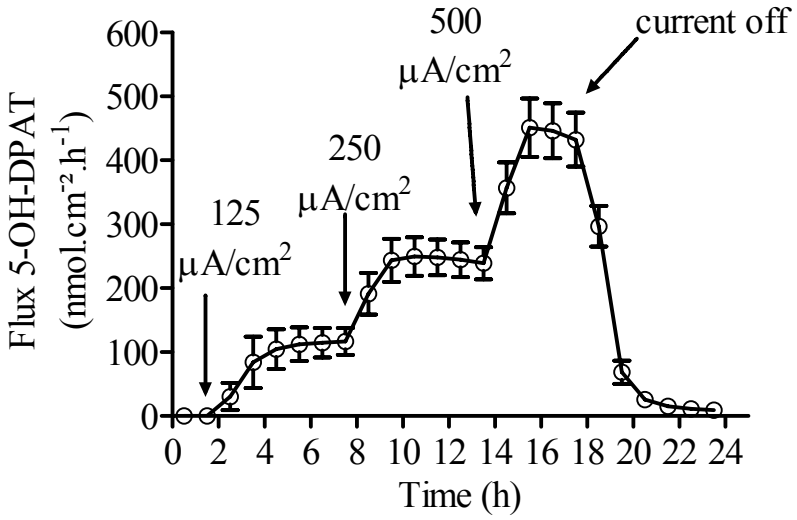

Figure 5: Iontophoretic flux *vs* time profile of 5-OH-DPAT, using a salt bridge. The following protocol was used: 2h passive+ 6h 125 $\mu A.cm^{-2}$ + 6h 250 $\mu A.cm^{-2}$ + 4h 500 $\mu A.cm^{-2}$ + 6h passive. The anodal compartment consisted of 3.9 mM 5-OH-DPAT in citric buffer at pH 6, containing 10 mM Na^+ and the acceptor compartment consisted of PBS pH 7.4. Data are presented as mean ± SD (n=6).

3.3.4 Effect of current density on iontophoretic transport of 5-OH-DPAT

The relationship between the $Flux_{ss}$ and the current density was studied when 3.9 mM 5-OH-DPAT and 10 mM Na^+ were present in the donor compartment (pH=6.0). During iontophoretic transport studies the current density was increased using 6h time intervals from 125 $\mu A.cm^{-2}$ to 250 $\mu A.cm^{-2}$ and finally to a current density of 500 $\mu A.cm^{-2}$. As shown in Figure 5, in which the flux *vs* time profile is plotted, an increase in the current density every 6h resulted in a significant increase in flux, which reaches steady state within the 6h of iontophoresis. A current density of 125, 250 and 500 $\mu A.cm^{-2}$ resulted in a $Flux_{ss}$ of 116.9 ± 20.9 $nmol.cm^{-2}.h^{-1}$, 239.2 ± 25.2 $nmol.cm^{-2}.h^{-1}$ and 432.3 ± 42.2 $nmol.cm^{-2}.h^{-1}$, respectively. Linear regression analysis of the steady state flux *vs* the current density, showed an excellent linear correlation ($R^2 = 0.996$).

4 Discussion

The principal transport mechanisms during iontophoresis of small charged medium hydrophilic compounds, like 5-OH-DPAT, are electroosmosis and electromigration. To calculate the relative contribution of electroosmosis, neutral hydrophilic marker molecules are used. The first aim of this study is to evaluate acetaminophen as marker molecule for the electroosmotic flow. The second aim is to investigate the transport mechanisms of iontophoretic delivery of 5-OH-DPAT and to optimize the iontophoretic delivery of this potent dopamine agonist.

4.1 Acetaminophen as marker molecule for electroosmosis

The hydrophilic neutral permeant, acetaminophen, is a generally accepted marker for quantification of the electroosmotic contribution to the iontophoretic delivery of different compounds [17-18, 23-25]. When a marker molecule is used to quantify the electroosmotic flow 3 assumptions are made: (i) the compound of interest and the marker molecule are transported by the convective flow in the same manner, (ii) the flux of the marker molecule is proportional to its concentration in the donor compartment and (iii) the marker molecule does not influence the flux of the drug of interest [20, 24]. If the molecular weight of the compound of interest is in the same range as the marker molecule (< 2x Mw of acetaminophen), it is reasonable to assume that both molecules are transported similarly by the current induced solvent flow.

First with respect to the proportionality of the steady state flux of acetaminophen to the donor concentration our data show that the $Flux_{ss}$ of acetaminophen is linearly proportional to its donor concentration (R^2=0.995). According to Equation 1, these results show that the water flow, V_w, quantified by the $Flux_{ss}$ of acetaminophen divided by the donor concentration, remains constant in the selected concentration range.

Secondly with respect to the effect of acetaminophen on the 5-OH-DPAT iontophoretic transport, acetaminophen did not affect the iontophoretic 5-OH-DPAT transport. Our results show that acetaminophen is an excellent marker molecule to determine the electroosmotic flow contribution to the iontophoretic transport of 5 OH-DPAT.

4.2 Electromigrative and electroosmotic contribution

In subsequent studies acetaminophen was used as a marker molecule to determine the contribution of the osmotic flow to the total iontophoretic 5-OH-DPAT transport.

At a pH of 6.0 the relative contributions of the J_{EO} and J_{EM} were estimated between 6.5-13.5% and between 86.5-93.2%, respectively. Reducing the pH of the donor phase from 6.0 to 5.0 gave a slight but not statistically significant decrease in the electroosmotic transport of 5-OH-DPAT. Furthermore, 5-OH-DPAT did not inhibit the electroosmotic flow across the skin during iontophoresis. Even when a salt bridge is used and a high amount of 5-OH-DPAT is transported across the skin, no change in electroosmotic flux was observed, which can be explained by the relative high hydrophilicity of 5-OH-DPAT [6, 26-27].

4.3 Effect of competing ions in the donor phase

Addition of NaCl to the donor solution is required for feeding the electrochemical reaction. However, Na^+ competes with 5-OH-DPAT as a carrier of charge transfer for iontophoretic transport through the skin. The steady-state flux of 5-OH-DPAT reduced dramatically when the NaCl concentration was doubled from 70 to 140 mM [13]. The reduction of Na^+ level in the donor phase from 78 mM to 10 mM resulted in a 2.5 to 3 fold increase in 5-OH-DPAT $Flux_{ss}$. This increase in transport can be attributed to an increase in the electromigration, since the electroosmosis was unaffected by the amount of Na^+ present in the donor solution.

The steady state flux of 5-OH-DPAT reaches a plateau towards the maximum solubility of 5-OH-DPAT in the donor phase (Figure 2B). When using low concentrations 5-OH-DPAT a dependency of the transport number on the donor concentration can still be observed. The plateau towards the maximum $Flux_{ss}$, depending on the physicochemical properties of 5-OH-DPAT is reached at lower donor concentrations when competition of co-ions was reduced [28]. Thereby focusing on the flux pattern during iontophoresis, as shown in Figure 2A, a concentration of 1.5 mM 5-OH-DPAT shows a steady state flux when 78 mM Na^+ is present in the donor phase. However when Na^+ concentration is reduced to 10 mM, the steady state 5-OH-DPAT flux is reduced gradually during the 6h iontophoresis period, which can be explained by a depletion of 5-OH-DPAT in the donor phase due to the high 5-OH-DPAT transport after the iontophoretic phase: almost 40.2 % has been transported through HSC.

The good correlation between the $Flux_{ss}$ and the current density (Figure 5) and between the $Flux_{ss}$ and donor concentration in presence and absence of NaCl in the donor phase are very important for the therapeutic treatment of Parkinson's disease. By modulation of these two parameters it will be possible to titrate the administered dose of this dopamine agonist, adjusted to the demand of the patient and to account for the inter- and intra-individual variability.

In the assumption that the same flux can be achieved *in vivo* and *in vitro*, it is possible to deliver approximately 1.00 μmol.cm^{-2}.h^{-1}. Previous studies showed that 5-OH-DPAT is more potent compared to rotigotine [12, 29]. Therefore it is reasonable to assume that the required dose of 5-OH-DPAT equal or lower than that of Rotigotine. The rotigotine patch Neupro® (UCB, Schwarz Pharma, Monheim, Germany) delivers 8 mg rotigotine in 24h, which corresponds with approximately 25 μmol rotigotine base (Mw=315.45 g/mol) [7, 30-31]. This means that for 5-OH-DPAT (35 mM in the patch) in the presence of 68 mM NaCl and applying a current density of 500 μA.cm^{-2} a patch size of approximately 2.0 cm² (anode and cathode patch) would be sufficient to provide the required amount of 5-OH-DPAT in combination with iontophoresis. When the patch size is increased, the donor concentration and the current density can be reduced. In addition, the use of a salt bridge results in even higher fluxes and therefore it will be possible to administer the same dose with a reduced amount of 5-OH-DPAT or a reduced current density.

4.4 Influence of the composition of the acceptor compartment

Conducting iontophoresis experiments with a different acceptor phase can provide more detailed insight in the transport mechanism during iontophoresis, important for selecting those conditions that result in the most efficient iontophoretic drug transport. Therefore a series of transport studies were conducted to compare the iontophoretic delivery of 5-OH-DPAT with a pH of 6.2 or 7.4 in the acceptor phase. In the present study the acceptor phase pH was varied in order to provide more insight in the mechanisms involved in the transport of 5-OH-DPAT. Our studies show that at a pH of 7.4 in the acceptor phase, 5-OH-DPAT is transported more efficiently than at a pH of 6.2. Similar results were found by Lai *et al.*, who observed that a decrease in acceptor pH from 7.4 to 4.5 resulted in a decrease in the iontophoretic transport of a series of local anaesthetics [32]. Whether this is due to an increase in the negative charge density in the stratum corneum and a subsequent reduction in Cl^-- transport, can be studied by measuring the acetaminophen transport and osmolarity in the donor compartment. As demonstrated in Figure 3, the pH of the acceptor phase influences the permselective properties of the stratum corneum, as the flux of acetaminophen, when using an acceptor pH of 6.2 is significantly lower compared to an acceptor pH of 7.4. Whether this also increases the ion transport from acceptor to donor compartment is indirectly monitored by measuring the osmolarity in the donor compartment (Figure 4). During the iontophoretic period a higher increase in osmolarity is observed with the acceptor phase at pH 6.2 compared to that at pH 7.4, most probably due to a higher ion transport (Cl^--ion) from acceptor to donor compartment. This results in an increased competition for charge transfer

and thus in a reduction in 5-OH-DPAT transport at pH of 6.2 compared to the transport at pH of 7.4 in the acceptor phase. As clearly shown the transport of 5-OH-DPAT is strongly affected by the composition of the acceptor phase, which is in agreement with the high sensitivity of 5-OH-DPAT iontophoretic transport for competitive ions such as Na^+ in the donor phase.

In conclusion, the research described in this paper demonstrates the high transport efficiency of 5-OH-DPAT and elucidates different mechanisms involved in its iontophoretic transport. Optimization of the composition of the donor phase resulted in high fluxes, making the drug an excellent candidate for treatment of Parkinson's disease using transdermal iontophoresis. Acetaminophen, identified as a good marker molecule for the quantification of the electroosmotic flux can be used in future transport studies to characterize the iontophoretic delivery of other molecules.

Acknowledgments

This research was financially supported by a grant (LKG 6507) of the Dutch Technology Foundation STW, Utrecht, The Netherlands.

References

1. Olanow, C.W., *The scientific basis for the current treatment of Parkinson's disease.* Annu Rev Med, 2004. **55**: p. 41-60.
2. Olanow, C.W., J.A. Obeso, and F. Stocchi, *Continuous dopamine-receptor treatment of Parkinson's disease: scientific rationale and clinical implications.* Lancet Neurol, 2006. **5**(8): p. 677-87.
3. Lim, E., *A walk through the management of Parkinson s disease.* Ann Acad Med Singapore, 2005. **34**(2): p. 188-95.
4. Nutt, J.G., *Continous Dopaminergic Stimulation: Is It the Answer to the Motor Complicaions of Levodopa?* Mov Disord, 2007. **22**(1): p. 1-9.
5. Nugroho, A.K., et al., *Pharmacokinetics and pharmacodynamics analysis of transdermal iontophoresis of 5-OH-DPAT in rats: in vitro-in vivo correlation.* J Pharm Sci, 2006. **95**(7): p. 1570-85.
6. Nugroho, A.K., et al., *Transdermal iontophoresis of rotigotine across human stratum corneum in vitro: influence of pH and NaCl concentration.* Pharm Res, 2004. **21**(5): p. 844-50.
7. Nugroho, A.K., et al., *Transdermal iontophoresis of rotigotine: influence of concentration, temperature and current density in human skin in vitro.* J Control Release, 2004. **96**(1): p. 159-67.
8. Luzardo-Alvarez, A., M.B. Delgado-Charro, and J. Blanco-Mendez, *In vivo iontophoretic administration of ropinirole hydrochloride.* J Pharm Sci, 2003. **92**(12): p. 2441-8.
9. Luzardo-Alvarez, A., M.B. Delgado-Charro, and J. Blanco-Mendez, *Iontophoretic delivery of ropinirole hydrochloride: effect of current density and vehicle formulation.* Pharm Res, 2001. **18**(12): p. 1714-20.
10. van der Geest, R., M. Danhof, and H.E. Bodde, *Iontophoretic delivery of apomorphine. I: In vitro optimization and validation.* Pharm Res, 1997. **14**(12): p. 1798-803.
11. Hacksell, U., et al., *N-Alkylated 2-aminotetralins: central dopamine-receptor stimulating activity.* J Med Chem, 1979. **22**(12): p. 1469-75.
12. van Vliet, L.A., et al., *Affinity for dopamine D2, D3, and D4 receptors of 2-aminotetralins. Relevance of D2 agonist binding for determination of receptor subtype selectivity.* J Med Chem, 1996. **39**(21): p. 4233-7.
13. Nugroho, A.K., et al., *Transdermal iontophoresis of the dopamine agonist 5-OH-DPAT in human skin in vitro.* J Control Release, 2005. **103**(2): p. 393-403.
14. Phipps, J.B., Gyory, J.R., *Transdermal ion migration.* Adv Drug Deliv Rev, 1992. **9**: p. 137-176.
15. Sanderson, J.E., S. de Riel, and R. Dixon, *Iontophoretic delivery of nonpeptide drugs: formulation optimization for maximum skin permeability.* J Pharm Sci, 1989. **78**(5): p. 361-4.
16. Del Terzo, S., C.R. Behl, and R.A. Nash, *Iontophoretic transport of a homologous series of ionized and nonionized model compounds: influence of hydrophobicity and mechanistic interpretation.* Pharm Res, 1989. **6**(1): p. 85-90.
17. Sebastiani, P., S. Nicoli, and P. Santi, *Effect of lactic acid and iontophoresis on drug permeation across rabbit ear skin.* Int J Pharm, 2005. **292**(1-2): p. 119-26.
18. Abla, N., et al., *Capillary zone electrophoresis for the estimation of transdermal iontophoretic mobility.* J Pharm Sci, 2005. **94**(12): p. 2667-75.
19. Abla, N., et al., *Contributions of electromigration and electroosmosis to peptide iontophoresis across intact and impaired skin.* J Control Release, 2005. **108**(2-3): p. 319-30.
20. Marro, D., et al., *Contributions of electromigration and electroosmosis to iontophoretic drug delivery.* Pharm Res, 2001. **18**(12): p. 1701-8.

21. Marro, D., R.H. Guy, and M.B. Delgado-Charro, *Characterization of the iontophoretic permselectivity properties of human and pig skin.* J Control Release, 2001. **70**(1-2): p. 213-7.
22. Pikal, M.J. and S. Shah, *Transport mechanisms in iontophoresis. II. Electroosmotic flow and transference number measurements for hairless mouse skin.* Pharm Res, 1990. **7**(3): p. 213-21.
23. Cazares-Delgadillo, J., et al., *Transdermal delivery of cytochrome C--A 12.4 kDa protein--across intact skin by constant-current iontophoresis.* Pharm Res, 2007. **24**(7): p. 1360-8.
24. Schuetz, Y.B., et al., *Effect of amino acid sequence on transdermal iontophoretic peptide delivery.* Eur J Pharm Sci, 2005. **26**(5): p. 429-37.
25. Bath, B.D., et al., *Scanning electrochemical microscopy of iontophoretic transport in hairless mouse skin. Analysis of the relative contributions of diffusion, migration, and electroosmosis to transport in hair follicles.* J Pharm Sci, 2000. **89**(12): p. 1537-49.
26. Denet, A.R., B. Ucakar, and V. Preat, *Transdermal delivery of timolol and atenolol using electroporation and iontophoresis in combination: a mechanistic approach.* Pharm Res, 2003. **20**(12): p. 1946-51.
27. Delgado-Charro, M.B. and R.H. Guy, *Characterization of convective solvent flow during iontophoresis.* Pharm Res, 1994. **11**(7): p. 929-35.
28. Mudry, B., et al., *Quantitative structure-permeation relationship for iontophoretic transport across the skin.* J Control Release, 2007. **122**(2): p. 165-72.
29. Van Oene, J.C., et al., *In vivo dopamine autoreceptor selectivity appears to be critically dependent upon the aromatic hydroxyl position in a series of N,N-disubstituted 2-aminotetralins.* Eur J Pharmacol, 1984. **102**(1): p. 101-15.
30. Giladi, N., et al., *Rotigotine transdermal patch in early Parkinson's disease: A randomized, double-blind, controlled study versus placebo and ropinirole.* Mov Disord, 2007. **22**(16): p. 2398-2404.
31. *UCB announces The U.S. Launch of Neupro® (Rotigotine Transdermal System) for the Treatment of Early-Stage Parkinson's Disease*. 2007, UCB Milwaukee (USA).
32. Lai, P.M. and M.S. Roberts, *Epidermal iontophoresis: II. Application of the ionic mobility-pore model to the transport of local anesthetics.* Pharm Res, 1998. **15**(10): p. 1579-88.

4

Comparing different salt forms of rotigotine to improve transdermal iontophoretic delivery

Oliver W. Ackaert[a], Jacob Eikelenboom[a], H-Michael Wolff[b], and Joke A. Bouwstra[a]

[a]Division of Drug Delivery Technology, Leiden/Amsterdam Center for Drug Research, Leiden, The Netherlands

[b]UCB Schwarz Biosciences GmbH, Monheim, Germany

adapted from *European Journal of pharmaceutics and biopharmaceutics.* 2010 Feb;742:304-10

Abstract

The transdermal delivery of a new salt form of the dopamine agonist rotigotine, rotigotine.H_3PO_4 is presented and compared with rotigotine.HCl. A comparison was made on the level of solubility, passive and iontophoretic delivery. Different aspects of the delivery were investigated: delivery efficiency, maximum flux, donor pH, electroosmotic contribution and transport number. Changing the salt form from rotigotine.HCl to rotigotine.H_3PO_4 increases significantly the solubility and rules out the influence of NaCl on the solubility by the absence of the common ion effect. At low donor concentration no difference in transdermal delivery was observed between the salt forms. Due to an increase in the maximum solubility of rotigotine.H_3PO_4, a 170% increase in maximum flux, compared to rotigotine.HCl, was achieved. A balance between solubility and delivery efficiency can be obtained by choosing the correct donor pH between 5 and 6. A slight increase in electroosmotic contribution and transport number was observed. Using the parameters, determined by modeling the *in vitro* transport, *in vivo* simulations revealed that with iontophoresis therapeutic levels can be achieved with a rapid onset time and be maintained in a controlled manner by adjusting the current density.

Keywords: solubility, transdermal, iontophoresis, rotigotine, salt form, modeling

1 Introduction

Transdermal drug delivery is an attractive alternative for oral drug delivery and hypodermic injections. Different delivery methods have been investigated over the years to increase the drug delivery through the skin. One of the possibilities is iontophoresis. By applying a small current across the skin it is possible to enhance the transdermal delivery of small charged ionic molecules. One of the interesting properties of this technique is the possibility to modulate the transport rate into and through the skin. This is an important advantage for drugs with a narrow therapeutic window, such as dopamine agonists. Rotigotine is a dopamine agonist used for the symptomatic treatment of Parkinson's disease. Studies, investigating the transdermal iontophoretic delivery of rotigotine.HCl revealed that by applying an electrical current across the skin higher steady state fluxes can be achieved with a shorter lag time compared to passive delivery. However in these studies the maximum solubility of rotigotine.HCl in the donor phase appeared to be the limiting factor for its iontophoretic transport through the skin [1-3]. Increasing the solubility of rotigotine can be achieved by changing the donor solution, e.g. by adding surfactants or co-solvents or changing the source of Cl^--ions. Another possibility to improve the solubility is altering the salt form of the drug of interest. In transdermal iontophoretic delivery the chloride anion is often added to the donor phase at the anodal side to feed the electrochemical reaction. To increase the solubility of rotigotine, another counterion may be chosen to destabilize the crystal structure and therefore to increase the solubility of rotigotine in the buffer solution. In the current study, H_3PO_4 was chosen as an alternative salt form for rotigotine. H_3PO_4 accounts for 2% of the FDA approved NCE's in the period from 1995 to 2006, is biocompatible, has a low molecular weight and circumvents the common ion effect in the donor phase, making it a very interesting candidate as salt form for iontophoresis [4]. Moreover in literature very few reports, investigating different salt forms for transdermal delivery were described. Fang *et al.* studied the passive and iontophoretic delivery of three different salts of the anion diclofenac, showing that the counter ion can affect the transdermal delivery [5-6].

In the current study the solubility and transdermal delivery of rotigotine.H_3PO_4 were evaluated in comparison to rotigotine.HCl to illustrate the influence of the choice of a salt form on the passive and iontophoretic transport through the skin. In addition the *in vitro* transport of rotigotine.H_3PO_4 was analyzed with compartmental modeling and the parameters were used to evaluate the iontophoretic delivery *in vivo* in a series of simulations.

2 Materials and methods

2.1 Materials

Rotigotine.H_3PO_4 and rotigotine.HCl were kindly supplied by UCB Schwarz Biosciences GmbH (Monheim, Germany). Silver, silver chloride (purity>99.99%), Trypsin (Type III from bovine pancreas), trypsin inhibitor (Type II-S from soybean) and methanesulfonic acid were obtained from Sigma-Aldrich (Zwijndrecht, The Netherlands). Acetaminophen was purchased from Brocacef (Maarsen, The Netherlands) and D-Mannitol was obtained from Scharlau Chemie S.A. (Barcelona, Spain). Spectra/Por® RC dialysis membrane sheets (cut off value of 6000-8000 Da) were purchased from Spectrum laboratories, Inc (Rancho Dominquez, Ca, USA). Acetonitrile was purchased from Biosolve (Valkenswaard, the Netherlands). All other chemicals and solvents were of analytical grade. All solutions were prepared in Millipore water with a resistance of more than 18 MΩ.cm.

2.2 Solubility of rotigotine.H_3PO_4

In order to compare the maximum solubility of rotigotine.H_3PO_4 with rotigotine.HCl, the solubility studies of rotigotine.H_3PO_4 were carried out as described by Nugroho *et al.* [3], who determined the solubility of rotigotine.HCl. Briefly, rotigotine.H_3PO_4 was solubilized in 10 mM citric buffer at pH 4.0, 5.0 and 6.0 with and without the presence of NaCl. Subsequent adjustment of pH in each test tube was performed by alternatingly adding small quantities of 1M NaOH under continuous shaking and subsequent pH measurements, until the pH of each solution had stabilized at the original buffer value. Each solution was shaken for an additional 48h, after which each solution was centrifuged and filtered. The concentration in each solution was determined by HPLC.

2.3 Capillary electrophoresis

The electrophoretic mobility of rotigotine.HCl and rotigotine.H_3PO_4 was investigated with capillary electrophoresis (CE). These experiments were performed according to a method, described elsewhere [7]. Briefly, the electrophoretic mobility of the samples (0.5 mM) was determined in triplicate using a phosphate buffer pH 7.4 (Na_2HPO_4: 5.82 $g.l^{-1}$; NaH_2PO_4: 5.1 $g.l^{-1}$) as electrolyte solution (mobile phase).

2.4 Preparation of human stratum corneum

The preparation of human stratum corneum (HSC) was performed according to the method described previously [8]. Briefly, within 24h after surgical removal of the

human skin residual subcutaneous fat was removed. Dermatomed human skin (DHS) was obtained by dermatoming the skin to a thickness of about 300 µm. In order to obtain HSC, DHS was incubated with the dermal side on Whatman paper soaked in a solution of 0.1% trypsin in 150 mM phosphate buffered saline (PBS) pH 7.4 (NaCl: 8 $g.L^{-1}$, Na_2HPO_4: 2.86 $g.L^{-1}$, KH_2PO4: 0.2 $g.L^{-1}$, KCl: 0.19 $g.L^{-1}$) overnight at 4 °C and subsequently for 1h at 37 °C after which HSC was peeled off from the underlying viable epidermis and dermis. HSC was subsequently washed in a 0.1% trypsin inhibitor solution in Millipore water and several times in water and stored in a desiccator in a N_2 environment.

2.5 *in vitro* transport studies

A 9-channel computer controlled power supply was used to provide a constant direct current (Electronics Department, Gorlaeus Laboratories, Leiden University, The Netherlands) during iontophoresis. The system was equipped with differential input channels per current source enabling on-line measurement of the electric resistance across HSC in each diffusion cell. Ag/AgCl was used as driver electrode pair. All transport experiments were carried out, using a three chamber continuous flow through cell as described elsewhere [8]. The donor formulation, buffered with a 10 mM citric buffer, was applied at the anodal side. The cathodal chamber was filled with PBS pH 7.4. The acceptor phase, maintained at 32°C, was continuously perfused with PBS pH 6.2 (NaCl: 8 $g.L^{-1}$, KCl: 0.19 $g.L^{-1}$, $Na_2HPO_4.2H_2O$: 0.43 $g.L^{-1}$, KH_2PO_4: 0.97 $g.L^{-1}$) at a flow rate of 7.0 $ml.h^{-1}$. Unless described elsewhere, the following protocol for the iontophoresis experiments was used: 6h of passive diffusion, followed by 9h of iontophoresis with a current density of 500 $\mu A.cm^{-2}$ and 5h of passive diffusion. Samples were collected every hour with an automatic fraction collector (ISCO Retriever IV, Beun De Ronde BV, Abcoude, The Netherlands). The specific conditions of the individual transport studies are described below.

2.5.1 Flux of rotigotine.H_3PO_4 *vs* rotigotine.HCl

The donor concentration of rotigotine.H_3PO_4 and rotigotine.HCl was kept constant (3.7 mM). The donor phase was buffered at pH 5.0 and contained 68 mM NaCl.

2.5.2 $Flux_{ss}$ *vs* donor concentration rotigotine.H_3PO_4 and influence of pH

In these transport studies 4 different concentrations rotigotine.H_3PO_4 (4.4 mM, 9.5 mM, 22.2 mM and 47.5 mM), buffered at pH 5.0, were used. Thereby the transport of rotigotine.H_3PO_4 (4.4 and 13.0 mM), buffered at pH 6.0 was investigated as well.

All transport experiments were performed in the presence of 68 mM NaCl in the donor phase.

2.5.3 Electroosmotic flow

The donor concentration of rotigotine.H_3PO_4 was 3.9 mM and 11.6 mM. Acetaminophen (15 mM) was added to the donor phase as a marker for the electroosmotic flow. The donor phase was buffered at pH 5.0 and contained 68 mM NaCl.

2.5.4 Current density flux-relationship

The relationship between the current density was studied with a rotigotine.H_3PO_4 concentration of 31.3 mM, buffered with a citric buffer at pH 5.5, containing 68 mM NaCl. The following protocol was used: 6h passive+ 6h 166 $\mu A.cm^{-2}$+ 6h 333 $\mu A.cm^{-2}$ + 6h 500 $\mu A.cm^{-2}$ + 6h passive.

2.6 Analytical method

Prior to and at the end of a transport study the pH of donor and acceptor compartment was measured. All samples of the iontophoretic transport studies were analyzed by RP-HPLC using a Superspher® 60 RP-select B, 75 mm-4 mm column (Merck KGaA, Darmstadt, Germany). Rotigotine was detected using a scanning fluorescence detector (Waters™ 474, Millipore, Milford, MA, USA) at excitation and emission wavelengths of 276 and 302 nm. Acetaminophen was detected using a UV detector (Dual λ Absorbance Detector 2487, Waters, Milford, USA) at a wavelength of 254 nm. Filtered and degassed mobile phase contained 60% H_2O (v/v), 40% ACN (v/v) and 0.05% methanesulfonic acid (v/v). The injection volume was 50 µL and the flow rate was set to 1.0 $mL.min^{-1}$.

The concentration of rotigotine was quantified according to 3 standards with a concentration of 0.005, 2 and 5 $\mu g.mL^{-1}$. The intra-assay variation of the retention time and of the area was less then 2.0%. For acetaminophen, calibration curves showed a linear response when using concentrations of compounds between 0.1 and 40 $\mu g.mL^{-1}$ (R^2>0.9999). The limit of detection (LOD) and limit of quantification (LOQ) of acetaminophen were experimentally determined at 5.8 and 9.6 $ng.mL^{-1}$ respectively. According to literature the limit of detection of rotigotine (base) was 11 $ng.mL^{-1}$ [2].

2.7 Determination of the passive, electroosmotic and electromigrative flux

The total iontophoretic flux consists of the passive flux (J_{pass}), the electroosmotic flux (J_{EO}) and the electromigrative flux (J_{EM}). The passive flux is calculated during 6h prior to the iontophoretic phase. The neutral permeant acetaminophen was added to the donor solution as a marker molecule for quantification of the electroosmotic flow during iontophoretic transport. The electromigrative flux is calculated by subtracting the passive and electroosmotic flux from the total flux.

2.8 Data analysis

To calculate the steady state flux during passive and iontophoretic transport, the cumulative flux of the transport was plotted as a function of time. The steady state flux was estimated from the linear part of the slope of this plot according to the permeation lag-time method [8]. All data are presented as mean ± standard deviation (SD). When a statistical analysis was performed comparing only 2 groups, a Student's t-test was used. When 3 or more groups were compared, a 1-way ANOVA statistical analysis was executed. If the overall p-value was less than 0.05, a bonferonni post-test was applied to compare different groups. For all statistical analysis a significance level of $p<0.05$ was used.

2.9 *in vitro* modeling and *in vivo* simulation

Next to the permeation lag-time method the data of the *in vitro* transport of rotigotine.H_3PO_4 at the selected condition (donor pH 5.0, donor conc 47 mM) was analyzed using non-linear mixed effects modeling with the compartmental models described elsewhere [9]. Briefly, in these models the starting point was a zero order mass transport from the donor solution into the skin during and after iontophoresis. The equations, to describe *in vitro* iontophoretic transport during current application:

$$J(t) = \frac{I_0}{S}(1 - e^{-K_R.(t-t_L)}) \tag{1}$$

$$J_{ss} = \frac{I_0}{S} \tag{2}$$

$$J(t) = \frac{P_{PI}}{S}(1 - e^{-K_R.(t-t_L)}) + \frac{I_0}{S}(1 - e^{-K_R.(T-t_L)}).e^{-K_R(t-T)} \tag{3}$$

Where $J(t)$ is the flux at time t and S is the diffusion area, K_R is a first order skin release rate constant, I_0 the zero-order iontophoretic mass transfer from the donor compartment into the skin compartment during current application, t_L is the kinetic lag time parameter, introduced to address the time required for drug molecules to enter the skin compartment, T is time of current application and P_{PI} is the zero order drug input due to the passive driving force in the post iontophoretic period. Fitting the data was performed using the subroutines ADVANCE6 TRANS1 TOL=5 from PREDPP in NONMEM (NONMEM version VI). Interindividual variability was modeled using an exponential error model and the residual error was characterized by an exponential and additive error model. The estimates of the population parameters were performed using a conventional first order method. The model was evaluated graphically by plotting the population predicted *vs* the observed flux and the individual predicted *vs* the observed flux. Finally, from the final parameter estimates a number of 100 samples were simulated. Post processing of NONMEM simulations creating plots of visual predictive check (VPC) was done using xpose 4, implemented in the software R (R version 2.7.0, R-foundation) [10].

The pharmacokinetic model used to simulate the iontophoretic delivery of rotigotine was based on a model, described elsewhere [9]. Assuming a 1-compartment model, different protocols were investigated for simulating the pharmacokinetic profile of iontophoretic delivery of rotigotine.H_3PO_4 during 24h using a patch size of 10 cm^2:

Protocol 1: 24h 350 $\mu A.cm^{-2}$

Protocol 2: 5h 350 $\mu A.cm^{-2}$ + 19 h 150 $\mu A.cm^{-2}$

At time=24h the patch was removed. In this case the simulations were performed with the $SIMULATION function provided in NONMEM. A population of 5 subjects was simulated and the simulated population prediction was displayed graphically.

3 Results

3.1 Solubility and electrophoretic mobility of rotigotine.H_3PO_4

The results of the solubility assay of rotigotine.H_3PO_4 are presented in Table 1. At the selected pH values the addition of NaCl did not affect significantly the solubility of rotigotine.H_3PO_4 (2-way ANOVA; $p>0.05$). This is in contrast with the results obtained with rotigotine.HCl by Nugroho *et al.* [3]. For rotigotine.HCl the solubility

Table 1: The solubility of Rotigotine.H_3PO_4 and Rotigotine.HCl in different medium at pH 4.0, 5.0 and 6.0 in the presence and absence of 68 mM NaCl (n=2-3).

	Rotigotine.H_3PO_4		**Rotigotine.HCl***	
pH	No NaCl mM (mean)	68 mM NaCl mM (mean)	No NaCl mM (mean ± SD)	68 mM NaCl mM (mean ± SD)
4.00	83.48[a]	80.08[c]	24.39 ± 4.66 [a,b]	6.75 ± 0.31 [b,c]
5.00	41.89[a]	42.95[c]	22.45 ± 0.63 [a,b]	6.35 ± 0.34 [b,c]
6.00	15.67	14.44[d]	15.87 ± 1.25 [b]	6.52 ± 0.17 [b,d]

*values obtained from literature: [3]
a-c: $p<0.001$; d: $p<0.01$

reduced tremendously after adding 68 mM NaCl. Furthermore decreasing the pH of the donor phase from 6.0 to 5.0 and again to pH 4.0 resulted in a significant increase in the solubility of rotigotine.H_3PO_4 (2-way ANOVA; $p<0.05$). The electrophoretic mobility of rotigotine.H_3PO_4 (1.53 ± 0.02 x10^{-4} $cm^2.s^{-1}.V^{-1}$) showed no significant difference with the electrophoretic mobility of rotigotine.HCl (1.49 ± 0.04 x10^{-4} $cm^2.s^{-1}.V^{-1}$) (t-test; $p=0.134$).

3.2 Passive diffusion of rotigotine.H_3PO_4

A series of iontophoretic transport studies under various conditions were performed. During 6h prior to iontophoresis no current was applied and passive transport reached steady state conditions within this period. From the slope of the linear part of the cumulative flux *vs* time profile the passive steady state flux ($Flux_{pss}$) was calculated. Firstly, rotigotine.H_3PO_4 and rotigotine.HCl both at a concentration of 3.7 mM, buffered at pH 5.0, showed no significant difference in $Flux_{pss}$ (t-test; $p>0.05$) (Table 2). Secondly, the results of transport studies of rotigotine.H_3PO_4 at various donor concentrations, comparing a donor pH of 5.0 and 6.0 are depicted in Figure 1. A non-linear hyperbolic fit showed a correlation between the $Flux_{pss}$ and the donor concentration at pH 5.0 ($R^2=0.889$). Increasing the pH of the donor phase from 5.0 to

Table 2: Comparison of the steady state passive flux ($Flux_{pss}$) and the steady state iontophoretic flux ($Flux_{ss}$) of Rotigotine.H_3PO_4 with Rotigotine.HCl at pH 5.0 in the presence of 68 mM NaCl. Results are presented as mean ± SD (n=3-4).

		$Flux_{pss}$	**$Flux_{ss}$**
	mM	nmol.cm^{-2}.h^{-1} (mean ± SD)	nmol.cm^{-2}.h^{-1} (mean ± SD)
Rotigotine.HCl	3.77	1.7 ± 0.8	69.4 ± 6.4
Rotigotine.H_3PO_4	3.74	1.6 ± 0.4	73.8 ± 12.6

6.0 increased the passive flux of rotigotine.H_3PO_4 quite drastically: Close to saturation of rotogotine.H_3PO_4 in the donor phase the maximum flux that could be achieved was 10.8 ± 1.9 nmol.cm^{-2}.h^{-1} at pH 5 and 24.9 ± 2.5 nmol.cm^{-2}.h^{-1} at pH 6.0.

3.3 Iontophoresis of rotigotine.H_3PO_4

A series of iontophoretic transport studies was conducted to investigate the iontophoretic transport of rotigotine.H_3PO_4 specially focusing on: (i) comparison with the iontophoretic flux of rotigotine.HCl, (ii) the relationship between the flux and donor concentration, (iii) the influence of the pH, (iv) the contribution of the electroosmotic flow and (v) the determination of the transport number.

3.3.1 Flux of rotigotine.H_3PO_4 *vs* rotigotine.HCl

During the transport studies after 6h of passive diffusion a current density was applied of 500 µA.cm^{-2} during 9h. The steady state flux ($Flux_{ss}$) of rotigotine.H_3PO_4 during iontophoresis showed no significant difference to the $Flux_{ss}$ of rotigotine.HCl ($p>0.05$) (Table 2).

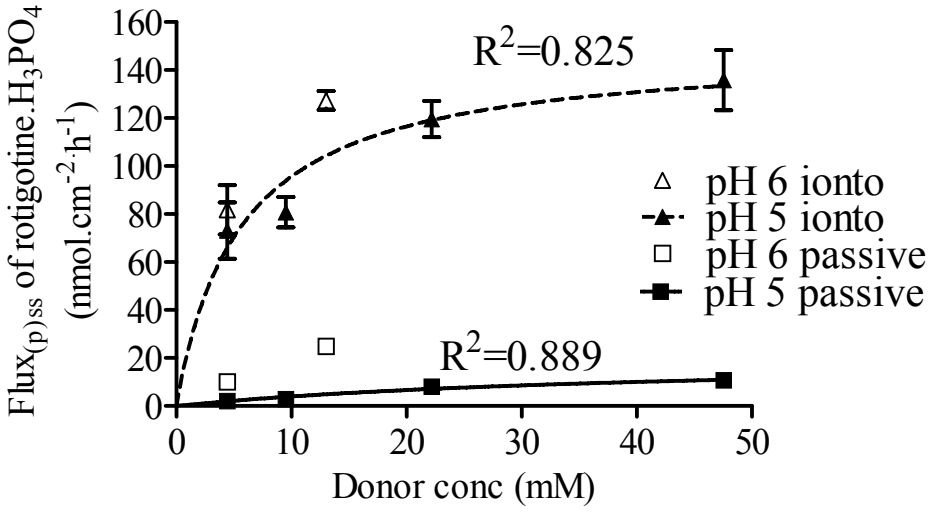

Figure 1: The $Flux_{(p)ss}$ of rotigotine.H_3PO_4 during the passive phase (square) (no current) and the iontophoretic phase (triangle) (current density=500 $\mu A.cm^{-2}$) at various donor concentrations at donor pH 5.0 (closed) and pH 6.0 (open). The correlation of the $Flux_{(p)ss}$ *vs* donor concentration was determined at pH 5.0. The line of correlation of passive $Flux_{pss}$ *vs* donor concentration is full and the line of correlation of the iontophoretic $Flux_{ss}$ *vs* donor concentration is intermittent. Data are presented as mean ± SD (n=3)

3.3.2 $Flux_{ss}$ as function of donor concentration rotigotine.H_3PO_4 and influence of pH in donor formulation

As shown in Figure 2, current application resulted in an immediate increase in the flux of rotigotine.H_3PO_4, which reached steady state within 4h. The results of a series of iontophoretic transport studies of rotigotine.H_3PO_4 at pH 5.0 and pH 6.0 are depicted in Figure 1. A non-linear relationship could be described between the $Flux_{ss}$ and the donor concentration at pH 5.0 (R^2=0.825). Thereby the $Flux_{ss}$ at equal rotigotine.H_3PO_4 concentration increased with increasing pH of the donor solution. However, close to saturation in the donor phase, the $Flux_{ss}$ at pH 5.0 (135.8 ± 12.5 $nmol.cm^{-2}.h^{-1}$) was not significantly different from the Flux at pH 6.0 (127.3 ± 4.0 $nmol.cm^{-2}.h^{-1}$) (t-test; $p>0.05$).

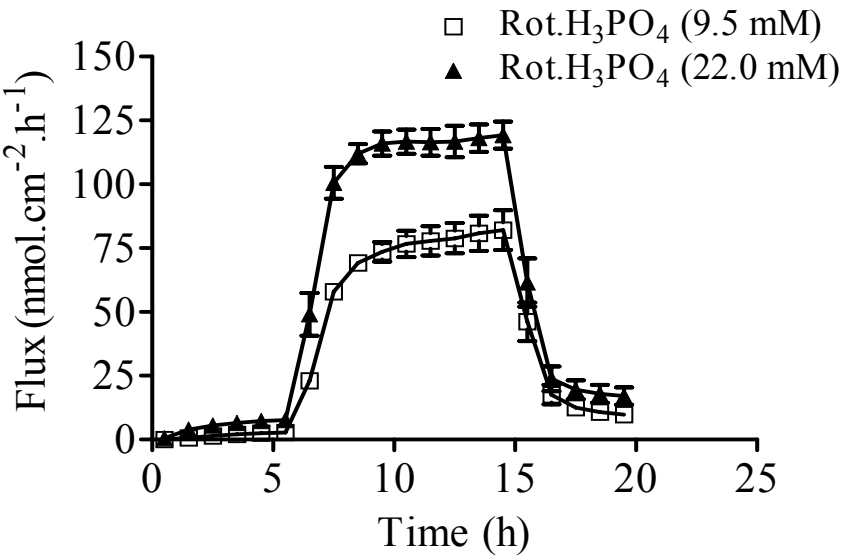

Figure 2: The iontophoretic flux *vs* time profile of rotigotine.H_3PO_4 dissolved in citric buffer pH 5 at 2 different concentrations, 9.5 mM (open square) and 22.0 mM (closed triangle). Data are presented as mean ± SD (n=3)

3.3.3 Electroosmotic contribution

To quantify the electroosmotic contribution acetaminophen was co-transported with rotigotine. The electroosmotic flux was investigated at two different concentrations rotigotine.H_3PO_4 (3.9 and 11.6 mM) at pH 5.0 in the donor phase. The relative contributions of J_{pass}, J_{EO} and J_{EM} are depicted in Figure 3. With increasing donor concentrations the relative contribution of the passive flux significantly increased from 13.1 ± 0.1% for 3.9 mM to 17.6 ± 0.1% for 11.6 mM (t-test; $p<0.05$). An increase in rotigotine.H_3PO_4 concentration from 3.9 mM to 11.6 mM resulted in a significant decrease in the relative contribution of the electroosmotic flow from 5.1 ± 0.1 % to 2.8 ± 0.3 % (t-test; $p<0.05$). Electromigration was the main driving force and accounted for 81.8 ± 0.03 and 79.5 ± 0.1 % of the total flux of 3.9 mM and 11.6 mM rotigotine.H_3PO_4, respectively.

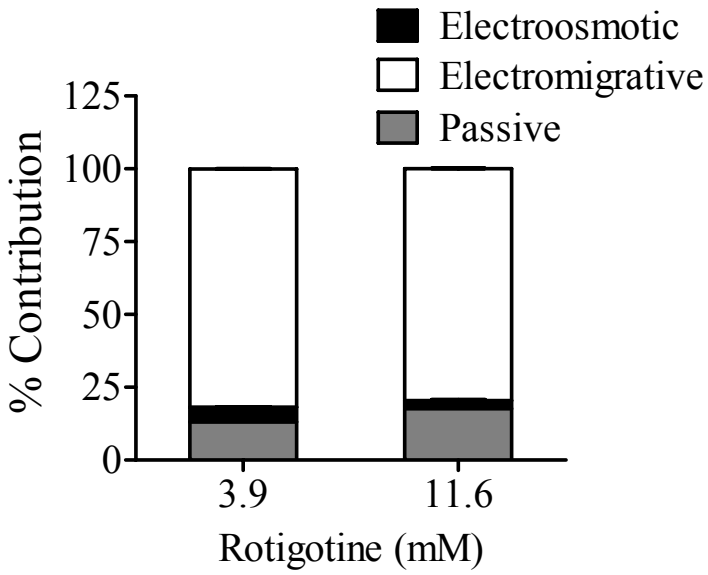

Figure 3: The relative contribution of the passive (grey), electroosmotic (black) and electromigrative (white) flux to the total (100%) flux of rotigotine.H_3PO_4 at 2 different concentrations (3.9 and 11.6 mM). The donor phase was buffered at pH 5 and the applied current density was 500 µA.cm^{-2}. Data are presented as mean ± SD (n=3)

3.3.4 Determination of transport number

With increasing pH from 5.0 to 6.0 a decrease in solubility, but an increase in delivery efficiency was observed. At pH 5.5 a balance is expected between maximum solubility and delivery efficiency. At this selected pH under near to saturated conditions the transport number was determined. Therefore in a single experiment the relationship between the $Flux_{ss}$ and the current density was studied with a donor phase containing 31.3 mM rotigotine.H_3PO_4, which was 90% of the maximum solubility of rotigotine.H_3PO_4.

An increase in the current density resulted in a significant increase in flux, which reached steady state within 6h of current application. A current density of 0 µA.cm^{-2} (passive phase), 166 µA.cm^{-2}, 333 µA.cm^{-2} and 500 µA.cm^{-2} resulted in a $Flux_{ss}$ of 24.4 ± 1.9 nmol.cm^{-2}.h^{-1}, 65.8 ± 9.3 nmol.cm^{-2}.h^{-1}, 109.7 ± 15.7 nmol.cm^{-2}.h^{-1} and 154.5 ± 27.0 nmol.cm^{-2}.h^{-1}, respectively. An excellent linear correlation could be observed between the $Flux_{ss}$ and the current density (R^2=0.999). The transport number was calculated from the slope of the correlation at 0.7%.

Table 3: Best fit-results of the estimated parameters, steady state flux ($Flux_{ss}$) release constant (K_R), the lag time (t_L) and the passive flux post iontophoresis (pass) and comparison to the value obtained with the permeation lag time method. The data are presented as mean and standard error of the mean (SEM). Furthermore values of the elimination constant (k_e), clearance (Cl) and apparent volume of distribution, considering the bioavailability (Vd/F) of rotigotine as found in literature, are depicted.

		Model prediction		**Permeation- lag time method**		**Literature values***
	Unit	Best fit value	SEM	Best fit value	SEM	
$Flux_{ss}$	$nmol.cm^{-2}.h^{-1}$	135	3.56	135.8	4.18	
K_R	h^{-1}	1.08	0.04	n.d.	n.d.	
t_L	h^{-1}	negligible		n.d.	n.d.	
pass	h	12.3	0.4	n.d.	n.d.	
k_e	h^{-1}					0.125
Cl	$L.h^{-1}$					450
Vd/F	L					3600

*values obtained from ref. [11-17]
n.d. not determined

3.4 Modeling *in vitro* iontophoretic transport of rotigotine.H_3PO_4

The *in vitro* iontophoretic transport across HSC was analyzed using compartment modeling. The kinetic model to describe the flux was based on zero-order mass transport from donor to skin and a first order release from skin to acceptor. The best-fit results and the standard error of the mean (SEM) of $Flux_{ss}$, the first order release constant (K_R), the lag time (t_L) and the passive flux post iontophoresis (pass) can be found in Table 3. No significant difference could be observed between the best fit of $Flux_{ss}$, estimated by the compartmental model and by the permeation lag-time method (t-test; $p>0.05$). The quality of fitting and model parameter estimation was evaluated graphically. The diagnostic plots of the model can be found in Figure 4. The population predicted (PRED) *vs* the observed flux (Figure 4A) and the

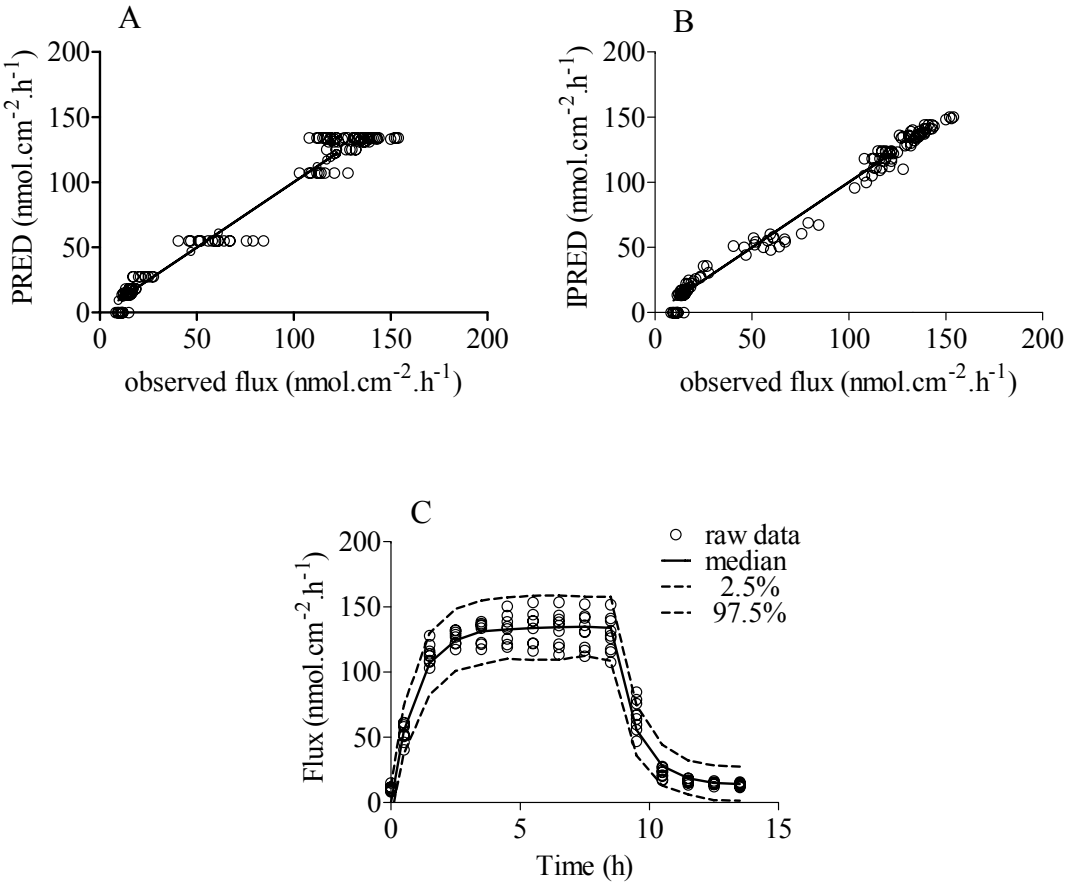

Figure 4: Diagnostic plots of the compartemental modeling of the *in vitro* iontophoretic transport of rotigotine (47 mM), buffered at pH 5. **A**: plot of the population predicted flux (PRED) *vs* the observed flux. **B**: plot of the individual predicted flux (IPRED) *vs* the observed flux. **C**:Visual predictive check of the *in vitro* model: raw data superimposed on median, 2.5th and 97.5th percentiles of data simulated from model. Median (full line); 2.5th and 97.5th percentile (dashed line; raw data (open circle)

individual predicted (IPRED) *vs* the observed flux (Figure 4B) show that the model can describe adequately the *in vitro* iontophoretic transport. Moreover the visual predictive check, displayed in Figure 4C demonstrates that the observed data are well distributed in the 95% confidence interval of the simulated data. This suggests that the variability, predicted by the model, represents the variability of the actual observed data.

4 Discussion

4.1 Solubility

In a previous study one of the major limitations in the iontophoretic transport of rotigotine.HCl was its low solubility. The maximum solubility of rotigotine.HCl was only 7.1 ± 0.4 mM at pH 5.0. In that study the iontophoretic transport at varying rotigotine.HCl concentrations between 1.4 and 3.9 mM showed a linear relationship between the $Flux_{ss}$ and the donor concentration [2]. This demonstrated that the maximum iontophoretic flux of rotigotine was not yet achieved, but the low solubility of rotigotine.HCl was the limiting factor for further increasing the iontophoretic flux. Higher donor concentrations could be achieved by replacing HCl by another salt [20-21]. As shown in Table 1, in the presence of 68 mM NaCl, the solubility of rotigotine increased substantially when HCl was replaced by H_3PO_4. Compared to rotigotine.HCl the solubility of rotigotine.H_3PO_4 is 2, 6, 10 fold higher at pH 6.0, 5.0 and 4.0, respectively. Furthermore in contrast to the solubility of the HCl-salt the presence of NaCl did not affect the solubility of rotigotine.H_3PO_4. This can be explained by an absence of the common ion effect. The next step was to investigate the transdermal delivery of rotigotine as H_3PO_4 salt.

4.2 *in vitro* transdermal delivery

The transdermal passive delivery of rotigotine.H_3PO_4 (3.77 mM) was investigated in comparison with rotigotine.HCl at the same donor concentration (3.74 mM). At pH 5.0 no difference in passive delivery could be observed. The solubility of rotigotine.HCl at pH 5.0 was lower compared to the solubility of rotigotine.H_3PO_4. The higher thermodynamic activity of rotigotine.HCl under these conditions was expected to result in a higher passive flux for rotigotine.HCl [22]. It seems that replacement of HCl by H_3PO_4 in the rotigotine salt not only increases the solubility of rotigotine, but also increases the efficiency in passive transport of rotigotine across HSC. In analogy to the passive flux, no difference in total iontophoretic flux could be observed between rotigotine.H_3PO_4 (3.77 mM) and rotigotine.HCl (3.74

mM). This observation is strengthened by the observed equal electrophoretic mobility of both salt forms, determined with capillary electrophoresis. This indicates that under these conditions an equal part of the current is carried by rotigotine, regardless it salt form, resulting in the same total iontophoretic flux.

The use of rotigotine.H_3PO_4 compared to that of rotigotine.HCl has two major advantages. (i) Increasing the donor pH from 5.0 to 6.0 significantly increases the passive flux of rotigotine.H_3PO_4. The maximum solubility of rotigotine.H_3PO_4 at pH 6.0 is much lower than at pH 5.0. Consecutively the thermodynamic activity at equal concentration of this compound is higher at pH 6.0, which results in an increased passive diffusion [23]. Due to this increase in passive flux, an increase in total flux during the iontophoresis period was also observed with increasing pH. In contrast, the total iontophoretic flux of rotigotine.HCl did not change when the pH was increased from 5.0 to 6.0 [3]. (ii) The second advantage is the increase in maximum solubility of rotigotine.H_3PO_4 compared to that of rotigotine.HCl. Due to a higher maximum solubility of the phosphate salt, higher donor concentrations of rotigotine can be obtained. Iontophoretic delivery of higher donor concentrations results in an increase in the maximum iontophoretic transport. At pH 5.0 the maximum iontophoretic flux of rotigotine.HCl was 80.2 ± 14.4 nmol.cm^{-2}.h^{-1}, while with rotigotine.H_3PO_4 a maximum flux of 135.8 ± 12.5 nmol.cm^{-2}.h^{-1} was achieved [2]. This means that the maximum flux can be increased with 170% by replacing the HCl salt with a H_3PO_4 salt. Besides a higher flux another practical advantage can be established when using a high donor concentration at pH 5.0. Calculations revealed that after 24h, maintaining a maximum flux of 135.8 nmol.cm^{-2}.h^{-1}, the amount rotigotine.H_3PO_4 in the donor phase decreased with 35%. This decrease in donor concentration would result only in a decrease of 10% in steady state flux. This shows that with a high donor concentration a high flux can be maintained for a long time. Taking these results together, one must seek a balance between transport efficiency and donor concentration by choosing the pH of the donor solution. On one hand by increasing the pH it is possible to increase the transport efficiency, however the limited solubility of the compound at pH 6.0 prevents the use of a high concentration. On the other hand at pH 5.0 the transport efficiency is lower, nonetheless a high flux can be established for a long time due to the higher solubility of rotigotine.H_3PO_4.

The total flux is driven by the passive, the electromigrative and the electroosmotic flux. The electroosmotic contribution of rotigotine.H_3PO_4, estimated at 5%, is higher than the electroosmotic contribution of rotigotine.HCl, calculated at 2.3% [2]. This is mainly due to the higher concentration of rotigotine.H_3PO_4 in the donor formulation.

Nonetheless the main driving force of the iontophoretic delivery of both salt forms remains electromigration, and in case of rotigotine.H_3PO_4 accounts for approximately 80% of the total flux at two different concentrations (Figure 3). The transport number of rotigotine.H_3PO_4 at pH 5.5 was estimated from the slope of relationship between the $Flux_{ss}$ and the current density at 0.7%. This is higher than the transport number of rotigotine.HCl (0.4%) at pH 5.0, which can be explained by a higher donor concentration of rotigotine.H_3PO_4 [2].

4.3 From *in vitro* modeling to *in vivo* simulation

After characterizing and optimizing the transdermal delivery of this promising compound *in vitro*, the potential of the iontophoretic delivery of rotigotine *in vivo* was evaluated. A series of simulations was performed, using pharmacokinetic modeling. The first step was to determine the parameters driving the iontophoretic delivery *in vitro* across human stratum corneum of rotigotine.H_3PO_4 (47 mM), buffered at pH 5.0. The value of the $Flux_{ss}$ corresponds well with the value estimated by the permeation lag time method (Table 3). In addition, diagnostic plots of the data modeling (Figure 4) confirm that this model successfully describes the *in vitro*

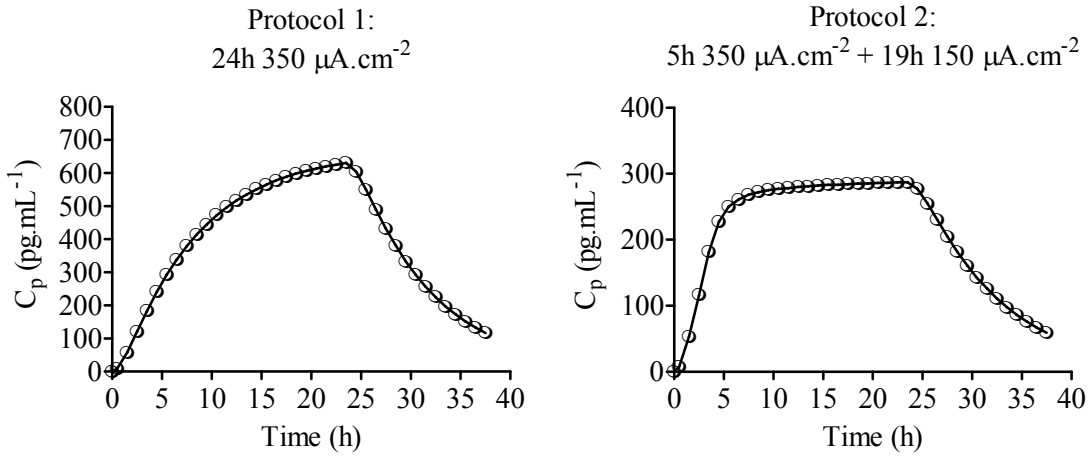

Figure 5: Population prediction of the simulations of iontophoretic delivery of rotigotine.H_3PO_4 (47 mM) using different protocols: Protocol 1: 24h 350 μA.cm^{-2}; Protocol 2: 5h 350 μA.cm^{-2} + 19h 150 μA.cm^{-2}. The open circles are the population prediction of the simulated plasma concentration (C_p).

iontophoretic transport of rotigotine.H_3PO_4. In the next step the apparent pharmacokinetic parameters of rotigotine, reported in literature, are combined with the best-fit values of $Flux_{ss}$, K_R and t_L to predict the plasma levels *in vivo* [11-17]. A comparison was made with the passive delivery of rotigotine. Neupro®, a passive transdermal delivery system of rotigotine, is approved by the EMEA for symptomatic treatment of Parkinson's disease [24]. The patch delivers 1 to 8 mg rotigotine in 24h, depending on the patch size. As reported in literature, passive delivery of rotigotine with a patch size of 10 cm^2, estimated to deliver 2 mg in 24h, resulted in a maximum plasma concentration (C_{max}) of 215 $pg.ml^{-1}$ at 16 h [16]. Two different protocols were used to evaluate the iontophoretic delivery of rotigotine (47 mM, pH 5.0) during 24h. As shown in Figure 5 applying a current density of 350 $\mu A.cm^{-2}$ during 24h (protocol 1) is expected to result in C_{max} of 630 $pg.ml^{-1}$. Not only can a higher flux be established with iontophoresis, but more interestingly already at time=5h a plasma concentration of 240 $pg.ml^{-1}$ can be reached. Therefore the *in vivo* iontophoretic delivery of rotigotine was simulated using protocol 2, applying initially a current density of 350 $\mu A.cm^{-2}$ for 5h, after which the current density was decreased to 150 $\mu A.cm^{-2}$. These simulations demonstrate two very important advantages of iontophoretic delivery of rotigotine in combination with iontophoresis over transdermal passive diffusion. Firstly, because of active transdermal delivery the onset time to achieve the desired level can be significantly decreased. Secondly, by adjusting the current density a titration of the plasma concentration is possible, making it feasible to individually modulate the delivery according to the desired dosing regimen. Both advantages can be of great benefit for symptomatic treatment of Parkinson's disease.

In conclusion despite the lipophilicity of rotigotine, high levels can be achieved with transdermal iontophoretic delivery with a rapid onset time, making it a very promising compound for symptomatic treatment of Parkinson's disease. Thereby changing the salt form of a drug can improve the physicochemical properties and consequently the maximal transdermal transport of a therapeutic drug, without changing its major transport mechanisms.

Acknowledgments

This work was supported by UCB Schwarz Biosciences GmBH, Monheim, Germany. The authors thank Willi Cawello (UCB Schwarz Biosciences GmbH, Monheim, Germany) for providing the correct pharmacokinetic data concerning the transdermal delivery of rotigotine.

References

1. Honeywell-Nguyen, P.L., S. Arenja, and J.A. Bouwstra, *Skin penetration and mechanisms of action in the delivery of the D2-agonist rotigotine from surfactant-based elastic vesicle formulations.* Pharm Res, 2003. **20**(10): p. 1619-25.
2. Nugroho, A.K., et al., *Transdermal iontophoresis of rotigotine: influence of concentration, temperature and current density in human skin in vitro.* J Control Release, 2004. **96**(1): p. 159-67.
3. Nugroho, A.K., et al., *Transdermal iontophoresis of rotigotine across human stratum corneum in vitro: influence of pH and NaCl concentration.* Pharm Res, 2004. **21**(5): p. 844-50.
4. Serajuddin, A.T., *Salt formation to improve drug solubility.* Adv Drug Deliv Rev, 2007. **59**(7): p. 603-16.
5. Fang, J., et al., *Passive and iontophoretic delivery of three diclofenac salts across various skin types.* Biol Pharm Bull, 2000. **23**(11): p. 1357-62.
6. Fang, J.Y., et al., *Influence of electrical and chemical factors on transdermal iontophoretic delivery of three diclofenac salts.* Biol Pharm Bull, 2001. **24**(4): p. 390-4.
7. Ackaert, O., et al., *Transdermal iontophoretic delivery of a novel series of dopamine agonists in vitro: physicochemical considerations* J Pharm Pharmacol, 2010. **accepted for publication**.
8. Nugroho, A.K., et al., *Transdermal iontophoresis of the dopamine agonist 5-OH-DPAT in human skin in vitro.* J Control Release, 2005. **103**(2): p. 393-403.
9. Nugroho, A.K., et al., *Pharmacokinetics and pharmacodynamics analysis of transdermal iontophoresis of 5-OH-DPAT in rats: in vitro-in vivo correlation.* J Pharm Sci, 2006. **95**(7): p. 1570-85.
10. Holford, N., *The Visual Predictive Check-Superiority to Standard Diagnostic (Rorschach) Plots.* PAGE 14, Abstr 738 [www.page-meeting.org/?abstract=738], 2005.
11. Cawello, W., M. Braun, and H. Boekens, *Absorption, disposition, metabolic fate, and elimination of the dopamine agonist rotigotine in man: administration by intravenous infusion or transdermal delivery.* Drug Metab Dispos, 2009. **37**(10): p. 2055-60.
12. Cawello, W., M. Braun, and R. Horstmann, *Pharmacokinetics of transdermal rotigotine in subjects with impaired renal function* in *ACCP 34th Annual Meeting*. 2005: Rockville, MD.
13. Cawello, W., et al., *Pharmacokinetics, safety and tolerability of rotigotine after transdermal patch administration in Japanes and Caucasian healthy subjects.* Mov Disord, 2006. **21(S15)**: p. S547.
14. Cawello, W., et al., *Characteristics of Rotigotine Elimination after patch removal.* Eur J Neurol, 2006. **13(suppl2)**: p. 85.
15. Cawello, W., et al., *Transdermal administration of radiolabelled [14C]rotigotine by a patch formulation: a mass balance trial.* Clin Pharmacokinet, 2007. **46**(10): p. 851-7.
16. Cawello W, B.M., Horstmann R., *Pharmacokinetics of transdermal rotigotine in subjects with impaired renal function* in *ACCP 34th Annual Meeting*. 2005: Rockville, MD.
17. Schwarz pharma, L. *Neupro®.* 2007.
18. Braun, M., et al., *Lack of Pharmacokinetic Interactions between Transdermal Rotigotine and Oral Levodopa/Carbidopa.* ClinPharmacol, 2009. **accepted for publication**.
19. Cawello, W., M. Braun, and H. Boekens, *(A)DME of the Dopamine Agonist Rotigotine in Man.* Drug Metabolism and Disposition, 2009. **submitted**.
20. Berge, S.M., L.D. Bighley, and D.C. Monkhouse, *Pharmaceutical salts.* J Pharm Sci, 1977. **66**(1): p. 1-19.

21. Li, S., et al., *Investigation of solubility and dissolution of a free base and two different salt forms as a function of pH.* Pharm Res, 2005. **22**(4): p. 628-35.
22. Higuchi, T., *Physical chemical analysis of percutaneous absorption process from creams and ointments.* J. Soc. Cosmet. Chem, 1960. **11**: p. 85-97.
23. Jeans, C.W. and C.M. Heard, *A therapeutic dose of primaquine can be delivered across excised human skin from simple transdermal patches.* Int J Pharm, 1999. **189**(1): p. 1-6.
24. *EMEA. European Public Assessment Report (EPAR), annex I: summary of product characteristics for Neupro. Available from http://www.emea.europa.eu/humandocs/PDFs/EPAR/neupro/H-626-PI-en.pdf* 2009.

5

Transdermal iontophoretic delivery of a novel series of dopamine agonists *in vitro*: physicochemical considerations

Oliver W. Ackaert[a], Jeroen De Graan[c], Romano Capancioni[a], Durk Dijkstra[c], Meindert Danhof[b] and Joke A. Bouwstra[a]

[a]Division of Drug Delivery Technology, Leiden/Amsterdam Center for Drug Research, Leiden, The Netherlands

[b]Division of Pharmacology, Leiden/Amsterdam Center for Drug Research, Leiden, The Netherlands

[c]Department of Medicinal Chemistry, University Center of Pharmacy, University of Groningen, Groningen, The Netherlands

adapted from *Journal of pharmacy and pharmacology*. 2010. *in press*

Abstract

The transdermal iontophoretic delivery of a novel series of 2-aminotetraline and chromanamine based dopamine agonists was investigated *in vitro*. Systematic structural modifications allowed us to investigate their effect on solubility in the donor phase and iontophoretic delivery across human skin. Transport profiles were analyzed with nonlinear mixed effect modeling, utilizing an extension to an existing compartmental model. Furthermore relationships between physicochemical properties and transport parameters were addressed. A solubility increase was observed: 5,6-di-OH-DPAT < 5-OH-MPAT < 5-OH-EPAT < 8-OH-DPAC. The structure significantly affected the iontophoretic delivery across human stratum corneum and dermatomed human skin with the highest flux for 5-OH-EPAT and 5-OH-MPAT. The extended model with two skin release constants (K_{R1}, K_{R2}) describes more adequately iontophoretic transport profiles than the existing model with one release constant. The extended model suggests 2 parallel transport pathways during current application. Across human stratum corneum the electrophoretic mobility, measured with capillary electrophoresis, showed a linear relationship with the electromigrative flux and the zero order iontophoretic mass input into the skin (I_0). Combining transport parameters (I_0, K_{R1} and K_{R2}), predicted from physicochemical properties, with compartmental modeling provides a powerful tool to simulate iontophoretic transport profiles for screening potential candidates and designing experiments.

Keywords: transdermal, iontophoresis, dopamine agonists, modeling, transport pathway

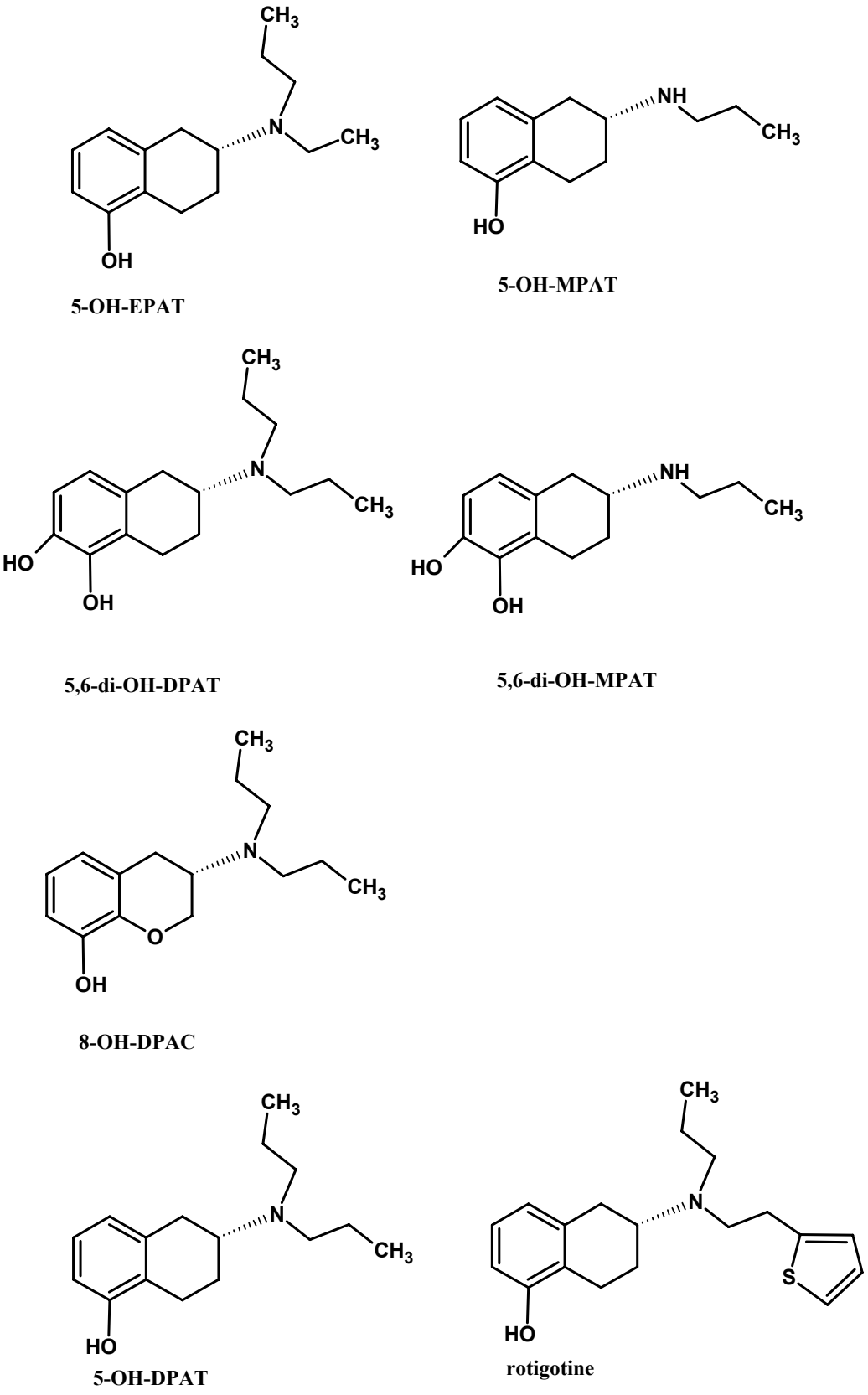

Figure 1: The chemical structures of different dopamine agonists

1 Introduction

Transdermal iontophoresis enhances the delivery of small charged solutes across the skin by application of a small current (≤0.5 $mA.cm^{-2}$) across this membrane. Important advantages of transdermal delivery are circumvention of the hepatic first-pass effect and a continuous administration of the drug. A particular advantage of iontophoresis is the possibility to adjust the rate of delivery by changing the current density [1]. For the symptomatic treatment of Parkinson's disease (Pd) the current strategy is to administer therapeutic agents in a continuous manner to reduce the induction of motor fluctuations after long term use [2-4]. Most of the dopamine agonists have a very narrow therapeutic window, which demands for an accurate individualized titration, adjusted to the needs of the therapy [5-6]. For these reasons, the *in vitro* and *in vivo* iontophoretic delivery of dopamine agonists, such as apomorphine, ropinorole, 5-OH-DPAT and rotigotine, have been intensively investigated [7-16].

To improve the transport efficiency and consequently the therapeutic treatment of Pd, a good understanding is required about the structure-transport relationship. However, with respect to this class of drugs little is known about the structure-transport relationship. In the present study the *in vitro* iontophoretic delivery is investigated of a new series of dopamine agonists, which were selected based on their potency and their molecular structure [17-23]. The small structural differences allow us to investigate in detail the influence of molecular structure and related physicochemical properties of the dopamine agonists on the iontophoretic transport efficiency.

During the years several studies have focused on selecting the key physicochemical properties that determine the transdermal iontophoretic delivery efficiency. It has been reported that the size of the solute, expressed as molecular weight (Mw) or molecular volume (MV), is an important descriptor with a higher transport for smaller molecules [24-26]. Furthermore, an increase in charge/Mw ratio results in an increase in transdermal electromigrative flux, as was observed for a series of peptides [27]. In a follow up study by Abla *et al*. the electrophoretic mobility, measured by capillary zone electrophoresis (CZE), provided an estimation of the electromigrative flux [28]. Finally, the lipophilicity of the transported molecules also affects the transdermal iontophoretic transport, however the relationship with the corresponding transport efficiency is not so straightforward as with passive diffusion [29-30].

Most of these physicochemical property-transport relationships use a single parameter to describe the transdermal iontophoretic flux. As a single end-point the flux at the end of the iontophoresis period or the steady state flux and lag time are often selected. However in these approaches, the information on the shape of the iontophoresis transport curve is neglected, which makes extrapolation towards the *in vivo* situation more difficult. The mathematical models, introduced by Nugroho *et al*., were designed to overcome the aforementioned disadvantages and to make the extrapolation from the *in vitro* to *in vivo* transport studies more reliable [16, 31-32]. The proposed models were based on a commonly used assumption for iontophoresis, namely a constant mass input into the skin during iontophoresis due to the constant iontophoretic driving force resulting from the application of a constant current. An adapted model, based on the compartmental models introduced by Nugroho *et al*. [16, 31], is presented and applied to describe the iontophoretic flux profile of this series of dopamine agonists. In this study the relationship between the physicochemical properties and the transport is addressed, using the electromigrative flux as single end-point and using the adapted model describing the total iontophoretic flux profile.

The objectives of the present work are: (i) to investigate the transdermal iontophoretic delivery *in vitro* of a new series of dopamine agonists, (ii) to evaluate the adapted mathematical compartmental model to describe the *in vitro* iontophoretic delivery of these dopamine agonists and (iii) to study the relationship(s) between the physicochemical properties (clogP, electrophoretic mobility and molecular weight) of the molecules and the J_{EM} and the parameter estimates (zero order mass input from donor to skin and skin release constants), using the adapted model.

2 Materials and methods

The 2-aminotetralines 5-Hydroxy-2-(N-ethyl,N-n-propylamino)tetralin (5-OH-EPAT.HBr), 5-Hydroxy-2-(N-n-propylamino)tetralin (5-OH-MPAT.HBr), 5,6-di-hydroxy-2-(N-n-propylamino)tetralin (5,6-di-OH-MPAT.HBr), 5,6-di-hydroxy-2-(N,N-di-n-propylamino)tetralin (5,6-di-OH-DPAT.HBr), 5-hydroxy-2-(N,N,-di-n-propylamino)tetralin (5-OH-DPAT.HBr) and the chromanamine 8-hydroxy-3-(N,N,-di-n-propylamino)chroman (8-OH-DPAC.HBr) (Figure 1; purity > 95%, determined with HPLC and NMR) were synthesized at the Department of Medicinal Chemistry of the University of Groningen, Groningen, the Netherlands. Silver, silver chloride (purity >99.99%), Trypsin (Type III from bovine pancreas) and trypsin inhibitor (Type II-S from soybean) were obtained from Sigma-Aldrich (Zwijndrecht, The

Netherlands). Acetaminophen was purchased from Brocacef BV (Maarssen, the Netherlands) and D-Mannitol was obtained from BDH Laboratory supplies (Poole, UK). Spectra/Por® RC dialysis membrane disks (cut off value of 6000-8000 Da) were purchased from Spectrum laboratories, Inc (Rancho Dominquez, Ca, USA). Tetrahydrofuran (THF, stabilized, purity > 99.8%) was obtained from Biosolve (Valkenswaard, the Netherlands). Triethylamine (TEA, purity > 99%) was obtained from Acros Organics (Geel, Belgium). All other chemicals and solvents were of analytical grade. All solutions were prepared in Millipore water with a resistance of more than 18 MΩ.cm.

2.1 Maximum solubility

The solubility studies of the different compounds were carried out as described elsewhere [14]. Briefly, each compound was solubilized in citric buffer 5 mM, pH 5.0 + 4 $g.l^{-1}$ NaCl + 23.1 $g.l^{-1}$ D-mannitol. Subsequently the pH in each test tube was adjusted to pH 5.0 with 1M NaOH or 1M HCl under continuous shaking. Each solution was shaken for 48h, after which the solution was centrifuged and filtered. The concentration in each solution was determined with HPLC.

2.2 Stability of 5,6-di-OH-MPAT and 5,6-di-OH-DPAT

The oxidation of 5,6-di-OH-MPAT and 5,6-di-OH-DPAT was investigated under various conditions. At the starting point 0.1 $mg.ml^{-1}$ of 5,6-di-OH-DPAT and 5,6-di-OH-MPAT were dissolved in the buffer solution. The solutions were continuously stirred and kept constant at the desired temperature, using a thermostat controlled water bath. If required a circular sheet of HSC (ø=18 mm) was added to the solution and a current of 320 μA was applied. At regular time intervals samples were taken from the solution and diluted in Millipore water, containing 2.86% v/v anti-oxidant solution (0.5% w/v ascorbic acid 0.05% w/v EDTA and 25% v/v H_3PO_4) to prevent the molecule to further oxidize. The amount of remaining drug was quantified by RP-HPLC (section 2.6).

2.3 Capillary electrophoresis

Previous studies have shown that the electrophoretic mobility at pH 7.4 is related to the iontophoretic mobility during transdermal transport [28, 33]. The electrophoretic mobility of various compounds in the current study was investigated with capillary electrophoresis (CE). These experiments were performed using a HPCE system (modelnumber: G1600OAX, Agilent Technologies, Amstelveen, The Netherlands) equipped with an on-column diode-array detector, an autosampler, and a 30 kV

power supply. CE Chemstation (Agilent Technologies) was used for CE control, data acquisition, and handling. The separation was performed in a 50 µm fused-silica capillary 48.5 cm in total length, and 40 cm to the UV detector. All experiments were carried out in cationic mode (the anode at the inlet and cathode at the outlet). The concentration of the samples was 0.5 mM in water and DMSO in water (0.5% v/v) was added to the solution as a marker for the electroosmotic flow. The electrophoretic mobility was determined using a phosphate buffer pH 7.4 (Na_2HPO_4: 5.82 $g.l^{-1}$; NaH_2PO_4: 5.1 $g.l^{-1}$) as electrolyte solution (mobile phase). UV detection was applied at 220 and 278 nm for the detection of DMSO and the molecule, respectively. The capillary was preconditioned as follows: 5 min 0.1 M NaOH + 10 min electrolyte solution. The sample was injected during 5 sec under a pressure of 50 mbar. Every sample was measured 3 times and every analysis a fresh electrolyte solution was used. The effective electrophoretic mobility (μ_{eff}) was calculated as follows:

$$\mu_{eff} = \mu_{obs} - \mu_{EOF} = \frac{L_{tot} L_{eff}}{V} \left[\left(\frac{1}{t_{obs}}\right) - \left(\frac{1}{t_{EOF}}\right) \right] \quad (1)$$

with μ_{obs} and μ_{EOF} as the electrophoretic mobility of the compound and the electroosmotic marker DMSO, respectively. Furthermore L_{tot} and L_{eff} are the total distance of the capillary and the distance from the inlet to the detection point, respectively. t_{obs} and t_{EOF} are the time required to reach the detection point for the analyte and the electroosmotic marker DMSO, respectively and V is the applied voltage [34-35].

2.4 *In vitro* transport studies

The preparation of dermatomed human skin (DHS) and human stratum corneum (HSC) was performed according to the method described previously [15]. All transport experiments were carried out as described elsewhere [15]. The donor formulation (citric buffer 5 mM, pH 5.0, NaCl: 4 $g.l^{-1}$, D-mannitol: 23.1 $g.l^{-1}$), containing the solute, was added to the anodal chamber. The cathodal chamber was filled with PBS pH 7.4 (NaCl: 8 $g.l^{-1}$, Na_2HPO_4: 2.86 $g.l^{-1}$, KH_2PO_4: 0.2 $g.l^{-1}$, KCl: 0.19 $g.l^{-1}$). The acceptor phase, maintained at 32°C, was continuously perfused with PBS pH 7.4 at a flow rate of 7.0 $ml.h^{-1}$. The following protocol was used: 6h passive diffusion + 9h iontophoresis (500 $\mu A.cm^{-2}$) + 5h passive diffusion. Samples were collected every hour with an automatic fraction collector (ISCO Retriever IV, Beun De Ronde BV, Abcoude, The Netherlands). The specific conditions of the individual transport studies are described below. To prevent oxidation of 5,6-di-OH-DPAT and 5,6-di-OH-MPAT after transdermal transport and prior to analysis, 200 µl of the anti-

oxidant solution (EDTA (Titriplex III): 0.5 $g.l^{-1}$, $Na_2S_2O_5$: 5 $g.l^{-1}$, H_3PO_4 (85 wt. % in H_2O): 294 $ml.l^{-1}$) was added to every collecting tube in the fraction collector.

2.4.1 Total iontophoretic flux

The iontophoretic delivery of 5-OH-EPAT, 5-OH-MPAT, 5,6-di-OH-MPAT and 5,6-di-OH-DPAT and 8-OH-DPAC across HSC was studied at 3.9 mM. Two additional concentrations (1.5 and 7.0 mM) of 5-OH-EPAT and 5-OH-MPAT were studied. Of 5-OH-EPAT, 5-OH-MPAT, 5,6-di-OH-DPAT, 5-OH-DPAT and 8-OH-DPAC, transport studies across DHS were performed using a donor concentration of 3.9 mM.

2.4.2 Electroosmotic flux

According to the Nernst-planck Equation the total flux (J_{tot}) consists of three transport mechanisms:

$$J_{tot} = J_{EM} + J_{EO} + J_P \qquad (2)$$

with the electromigrative flux (J_{EM}) and the electroosmotic flux (J_{EO}) as the principal driving mechanisms for iontophoresis of charged species. The passive flux (J_P) is often negligible. The electroosmotic flux across HSC was investigated during iontophoretic transport of 5-OH-EPAT, 5-OH-MPAT, 5,6-di-OH-DPAT and 8-OH-DPAC (3.9 mM). Acetaminophen (15 mM) was added to the donor phase as a marker for the electroosmotic flux. The electroosmotic flux was calculated, using the following Equation, assuming a similar electroosmotic transport for the analogs and acetaminophen:

$$J_{EO} = \frac{J_{ace}}{C_{ace}} x C_m \qquad (3)$$

with J_{ace} as the flux of acetaminophen and C_m and C_{ace} as the donor concentration of the molecule and acetaminophen, respectively.

2.5 Compartmental modelling

The iontophoretic transport *in vitro* of different molecules was analyzed using non-linear mixed effects modelling. The starting point of the models is a zero order mass transport form the donor solution into the skin during and after iontophoresis. In this paper an extension to the basic model is presented.

2.5.1 Basic model *in vitro*

An extensive explanation and description of the basic model is presented elsewhere [31]. Briefly, the basic model assumes a constant rate of mass input from the donor into the skin during iontophoresis due to a constant iontophoretic driving force. Based on this assumption the equations, to describe *in vitro* iontophoretic transport during (Equation 4) and after current application (Equation 6) are:

$$J(t) = \frac{I_0}{S}(1 - e^{-K_R.(t-t_L)}) \tag{4}$$

$$J_{ss} = \frac{I_0}{S} \tag{5}$$

$$J(t) = \frac{P_{PI}}{S}(1 - e^{-K_R.(t-T)}) + \frac{I_0}{S}(1 - e^{-K_R.(T-t_L)}).e^{-K_R(t-T)} \tag{6}$$

where $J(t)$ is the flux at time t and S is the diffusion area, K_R is a first order skin release rate constant, I_0 the zero-order iontophoretic mass transfer from the donor compartment into the skin compartment during current application, t_L is the kinetic lag time parameter, introduced to address the time required for drug molecules to enter the skin compartment, T is time of current application, J_{ss} is the flux at steady state and P_{PI} is the zero order drug input due to the passive driving force post-iontophoresis.

2.5.2 Extended model *in vitro*

As observed from the iontophoretic flux profile of the compounds presented in this paper, the flux increases in time during the current application. This suggests that two transport routes are involved in the iontophoretic delivery, linked in parallel. The observed flux is the total amount of drug released in the acceptor compartment. In analogy to the basic model the zero order mass transfer from the donor into the skin remains constant, but the first order release constant from the skin to the acceptor will be different for both transport mechanisms. Therefore the iontophoretic flux *in vitro* during iontophoresis ($t \leq T$) can be described by the equation:

$$J(t) = \frac{I_0}{S}(1 - e^{-K_{R1}.(t-t_L)}) + \frac{I_0}{S}(1 - e^{-K_{R2}.(t-t_L)}) \tag{7}$$

$$J_{ss} = 2 * \frac{I_0}{S} \tag{8}$$

With K_{R1} and K_{R2} as the release constants to describe both transport routes. During the post iontophoresis period (t>T) only one release constant appeared to be sufficient to describe the passive flux, resulting in the following Equation:

$$J(t) = \frac{P_{PI}}{S}(1 - e^{-K_{R2}.(t-T)}) + \left(\frac{I_0}{S}(1 - e^{-K_{R1}.(T-t_L)}) + \frac{I_0}{S}(1 - e^{-K_{R2}.(T-t_L)}) \right).e^{-K_{R2}(t-T)} \quad (9)$$

2.5.3 Curve fitting and model evaluation

Fitting the data was performed using the subroutines ADVANCE6 TRANS1 TOL=5 from PREDPP in NONMEM (NONMEM version VI). Interindividual variability was modeled using an exponential model and the residual error was characterized by an exponential and/or additive error model. The estimation of the population parameters was performed using a conventional first order method [36].
The extended model was evaluated in comparison to the basic model. The statistical analysis was based on the objective function, which is defined as -2 times the logarithm of the likelihood. If the objective function of the extended model with 2 release constants during the current application, decreases with a value of 3.84 (and/or more) compared to the objective function of the basic model, the extended model is significantly better ($p<0.05$; χ^2-test).

2.6 Analytical method

Different HPLC methods were developed to analyze the respective molecule and acetaminophen by RP-HPLC. The aminotetralins and the chromanamine were detected using a scanning fluorescence detector (Waters™ 474, Millipore, Milford, MA, USA) and acetaminophen was detected using a UV detector (Dual λ Absorbance Detector 2487, Waters, Milford, USA). The column, the composition of the mobile phase, the volume of injection and the respective excitation and emission wavelengths to analyze the different compounds are depicted in Table 1. The flow rate was set to 1.0 $ml.min^{-1}$. Calibration curves showed a linear response between 100 and 40000 $ng.ml^{-1}$ ($R^2>0.99$). The limit of detection (LOD) and limit of quantification (LOQ) for these HPLC methods can also be found in Table 1.

2.7 Data analysis

All data are presented as mean ± standard deviation (SD) or as mean ± standard error of the mean (SEM). When a statistical analysis was performed comparing only 2 groups, a Students t-test was used. When 3 or more groups were compared, a 1-way ANOVA statistical analysis was executed. Comparing the effect of two factors

Table 1: The HPLC method of the different compounds investigated in the current paper including column, mobile phase composition, volume of injection, excitation wavelength (λ_{ex}), emission wavelength (λ_{em}), limit of detection (LOD) and limit of quantification (LOQ)

Compound	**Column**	**Mobile phase**			**Fluorescence**			
		Composition	TEA	injection volume	λ_{ex}	λ_{em}	LOD	LOQ
		(% v/v)	(mM)	(µl)	(nm)	(nm)	($ng.ml^{-1}$)	($ng.ml^{-1}$)
5-OH-EPAT	Superspher RP-select B C8	Ace 50 mM/THF 95/5	30	20	275	302	21.0	35.0
5-OH-MPAT	Inertsil 5ODS-2	Ace 100 mM/ACN 90/10	15	50	280	310	8.2	12.3
5,6-di-OH-DPAT	Superspher RP-select B C8	Ace 50 mM/THF 97/3	15	200	276	305	61.4	115.9
5,6-di-OH-MPAT	Inertsil 5ODS-2	Ace 50 mM/THF 96/4	15	50	280	310	90.7	150.5
8-OH-DPAC	Superspher RP-select B C8	Ace 50 mM/THF 95/5	30	50	277	306	29.9	44.9

Acetaminophen: mobile phase, column, limit of detection and quantification are dependent on the compound co-analyzed;
UV-detection: λ=243 nm;
Ace: acetatebuffer pH 3.6

simultaneously was performed using 2-way ANOVA. If the overall p-value was less than 0.05, a Bonferonni post-test was applied to compare different groups. Statistical tests were performed by using GraphPad Prism version 5.00 for Windows (GraphPad Software, San Diego, CA, USA). For all statistical analysis a significance level of $p<0.05$ was used.

3 Results

3.1 Maximum solubility

The maximum solubility of the different compounds was determined in citric buffer 5 mM at pH 5.0 in the presence of 68 mM NaCl and D-mannitol as this is the composition of the donor solution, used for transport studies. The results of the solubility assay can be found in Table 2. The solubility data of rotigotine.HCl and 5-OH-DPAT, adapted from literature, were added to the table for comparison. An increase in solubility was observed ranking the molecules in the following order:

Table 2: The physicochemical properties of the various compounds investigated. The molecular weight (Mw) and the calculated logP (clogP) are presented together with the solubility in a citric buffer 5mM pH 5.0, containing 4 $g.l^{-1}$ NaCl and 23.1 $g.l^{-1}$ D-mannitol, and the electophoretic mobility, determined with capillary electrophoresis. The solubility of 5-OH-DPAT and rotigotine, obtained from literature, are added to the table for comparison.

Compound	**Mw** ($g.mol^{-1}$)	**clogP[c]**	**Solubility** (mM)	**Electrophoretic mobility (μ_{em})** 10^{-4} ($cm^2.s^{-1}.V^{-1}$) mean ± SD
5-OH-EPAT	233.36	3.71	111.7	1.84 ± 0.01
5-OH-MPAT	205.30	2.93	93.1	1.88 ± 0.00
5,6-di-OH-DPAT	263.38	3.74	44.2	1.56 ± 0.01
5,6-di-OH-MPAT	221.30	2.5	n.d	1.61 ± 0.01
8-OH-DPAC	249.36	3.4	282.5	1.64 ± 0.01
5-OH-DPAT	247.38	4.15	56.7[a]	1.76 ± 0.01
rotigotine	315.48	4.82	7.1[b]	1.49 ± 0.04

[a,b]: value adapted from literature [14, 40]
[c]: cLogP was calculated using alogsP [37-39]
n.d.: not determined

rotigotine < 5,6-di-OH-DPAT < 5-OH-DPAT < 5-OH-MPAT < 5-OH-EPAT < 8-OH-DPAC. Furthermore the relative hydrophilicity of the different analogs, expressed with the octanol-water partition coefficient, clogP, was calculated/computed using the ALOGPS 2.1 webservice [37-39]. The results are also provided in Table 2.

3.2 Stability of 5,6-di-OH-MPAT and 5,6-di-OH-DPAT

The catecholgroup of 5,6-di-OH-MPAT and 5,6-di-OH-DPAT is expected to be susceptible to photo-, auto- and chemical oxidation to ortho-semiquinone and subsequently to ortho-quinone, similar as apomorphine, another catecholamine [41]. Therefore the stability of these 2 molecules was investigated under various conditions, mimicking the different compartments during *in vitro* iontophoretic transport. Figure 2, evaluating the % remaining catechol after 24h and 48h, shows that 5,6-di-OH-MPAT remains stable at pH 5.0 at room temperature. Increasing only

the temperature had little influence on the stability: after 48h the remaining 5,6-di-OH-MPAT was 95.9 % and 87.7 ± 5.6 % at room temperature and 32 °C, respectively. Addition of HSC and application of a current decreased the remaining drug from 96.2 ± 3.1% to 90.2% after 24h. In analogy to other catecholamines, the pH of the solution had a strong influence on the stability of the 2 compounds [41-42]. At pH 5.0 5,6-di-OH-MPAT and 5,6-di-OH-DPAT were more stable than at pH 6.0. Increasing the pH to 7.4 resulted even in a more pronounced degradation of 5,6-di-OH-MPAT.

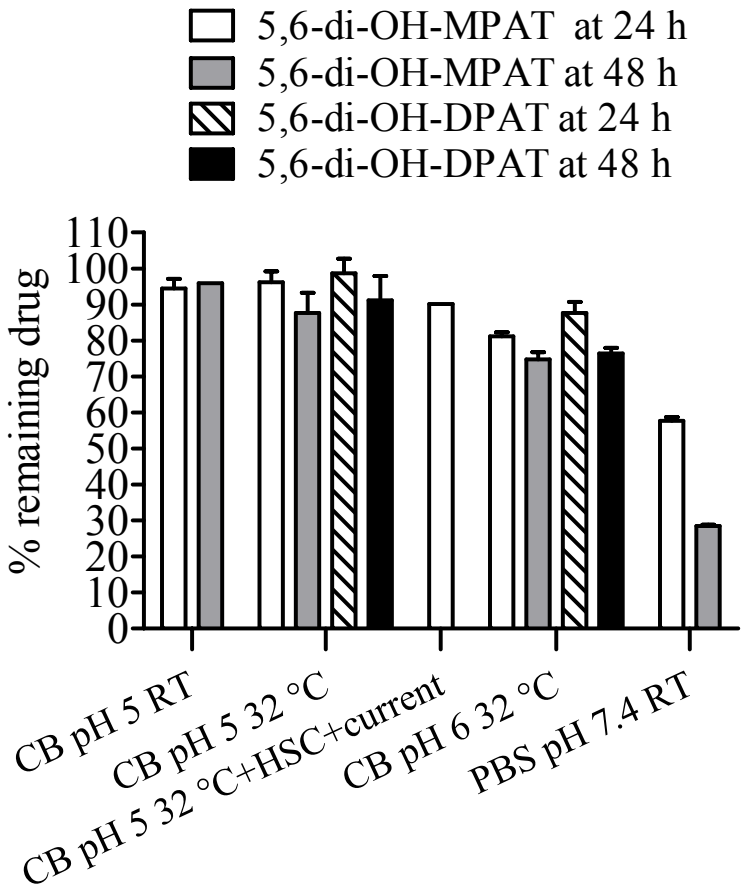

Figure 2: Bar plot of the % remaining 5,6-di-OH-MPAT after 24h (white) and 48h (grey) and of the % remaining 5,6-di-OH-DPAT after 24h (striped) and 48h (black) at various conditions. The data are presented as mean ± SD (n=2-3).
CB=citric buffer, Current=320µA, HSC=circular sheet of human stratum corneum (ø=18 mm), RT=room temperature.

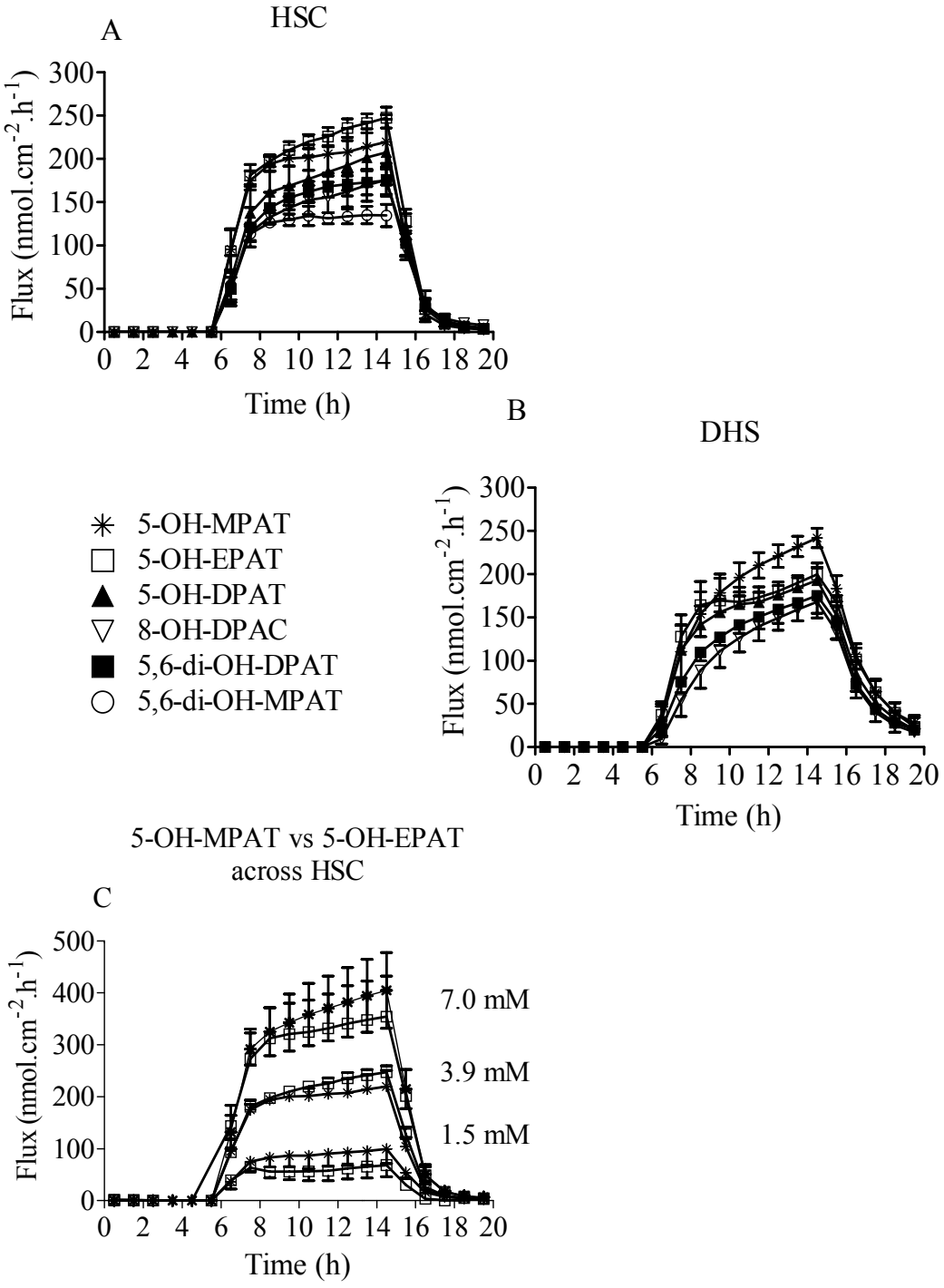

Figure 3: The iontophoretic flux profile of the different aminotetralines, 5-OH-MPAT (star), 5-OH-EPAT (open square), 5-OH-DPAT (closed triangle), 5,6-di-OH-DPAT (closed square), 5,6-di-OH-MPAT (open circle) and the chromanamine 8-OH-DPAC (open triangle) across two different skin types HSC (**A**) and across DHS (**B**). The donor concentration of all the compounds was 3.9 mM. Panel **C** shows the comparison of the iontophoretic flux vs time profile of 5-OH-MPAT (star) and 5-OH-EPAT (open square) across HCS at 3 different concentrations (1.5, 3.9, 7.0 mM). The data are presented as mean ± SD (n=4-7).

3.3 Capillary electrophoresis

To assess the electrophoretic mobility of the various compounds, capillary electrophoresis was performed. The results of the capillary electrophoresis are summarized in Table 2. The electrophoretic mobility of the various compounds increased in the following order: rotigotine 5,6-di-OH-DPAT < 5,6-di-OH-MPAT < 8-OH-DPAC < 5-OH-DPAT < 5-OH-EPAT < 5-OH-MPAT.

3.4 Iontophoretic transport

3.4.1 Total transport across HSC and DHS

Transport studies with the dopamine agonists at 3.9 mM were performed to compare the iontophoretic delivery of the various compounds. The different flux profiles of the analogs across HSC and DHS are depicted in Figure 3A and 3B, respectively. The flux of the different compounds was evaluated statistically after 9h of iontophoresis (current density is 500 $\mu A.cm^{-2}$). Across HSC 1-way ANOVA analysis showed an overall significant difference in the flux of the different compounds ($p<0.0001$). The observed flux after 9h increased in the following order: 5,6-di-OH-MPAT (134.5 ± 12.9 $nmol.cm^{-2}.h^{-1}$) < 5,6-di-OH-DPAT (175.0 ± 15.9 $nmol.cm^{-2}.h^{-1}$) < 8-OH-DPAC (175.9 ± 18.9 $nmol.cm^{-2}.h^{-1}$) < 5-OH-DPAT (207.7 ± 38.0 $nmol.cm^{-2}.h^{-1}$) < 5-OH-MPAT (219.7 ± 31.4 $nmol.cm^{-2}.h^{-1}$) < 5-OH-EPAT (247.7 ± 12.1 $nmol.cm^{-2}.h^{-1}$). In a follow up study 2 additional concentrations (1.5 and 7.0 mM) of 5-OH-MPAT and 5-OH-EPAT were investigated. Comparing the flux of 5-OH-MPAT and 5-OH-EPAT after 9h of iontophoresis at 1.5 (99.6 ± 15.9 vs 68.7 ± 22.0 $nmol.cm^{-2}.h^{-1}$), 3.9 mM (see above) and 7.0 mM (404.9 ± 72.9 vs 354.2 ± 78.1 $nmol.cm^{-2}.h^{-1}$) showed no significant difference (2-way ANOVA; $p>0.05$) (Figure 3C). A similar trend was seen for iontophoretic transport studies across DHS: 8-OH-DPAC (168.2 ± 13.2 $nmol.cm^{-2}.h^{-1}$) < 5,6-di-OH-DPAT (175.2 ± 25.9 $nmol.cm^{-2}.h^{-1}$) < 5-OH-DPAT (193.0 ± 19.9 $nmol.cm^{-2}.h^{-1}$) < 5-OH-EPAT (199.8 ± 8.0 $nmol.cm^{-2}.h^{-1}$) < 5-OH-MPAT (241.8 ± 11.2 $nmol.cm^{-2}.h^{-1}$). A significant difference could be observed between the fluxes of the different compounds (1-way ANOVA; $p<0.05$).

3.4.2 Electroosmotic contribution across human stratum corneum

Acetaminophen (15 mM) was added to the donor solution to investigate the electroosmotic flow across HSC during iontophoretic transport. The resulting electroosmotic contribution, calculated using Equation 3, expressed as % of the total flux, is depicted in Figure 4. A significantly higher electro-osmotic contribution was observed when 5,6-di-OH-DPAT (12.1 ± 3.4 %) was transported through HSC,

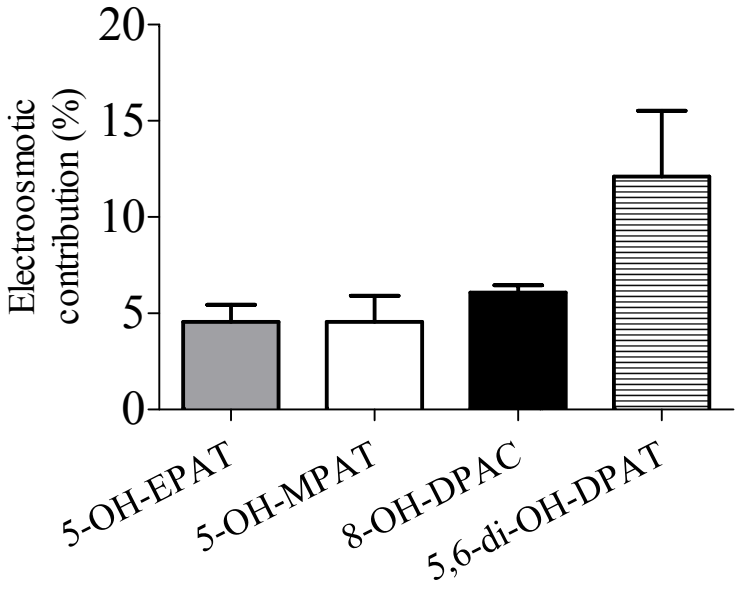

Figure 4: bar plot of the electroosmotic contribution during iontophoretic transport across human stratum corneum of different compounds. The donor concentration was 3.9 mM. Acetaminophen (15 mM) was co-transported to determine the electroosmotic flow during iontophoretic transport. The data are presented as mean ± SD (n=5-6).

compared to the other compounds 5-OH-EPAT (4.5 ± 0.9 %), 5-OH-MPAT (4.6 ± 1.4 %) and 8-OH-DPAC (6.1 ± 0.4 %) (1-way ANOVA, Bonferroni post test; $p<0.01$).

3.5 Model evaluation

The iontophoretic transport of the different compounds was fitted using the basic and extended model. The basic model assumes a constant input during iontophoresis with one skin release constant K_R. As an example the iontophoretic flux of 8-OH-DPAC (3.9 mM) across HSC is shown in Figure 5. The iontophoretic transport of 3.9 mM 8-OH-DPAC (open circle), together with the model predictions of the basic model (dashed line) clearly shows that the basic model does not fit to the experimental data. For this reason we employed the extended model with two release constants, K_{R1} and

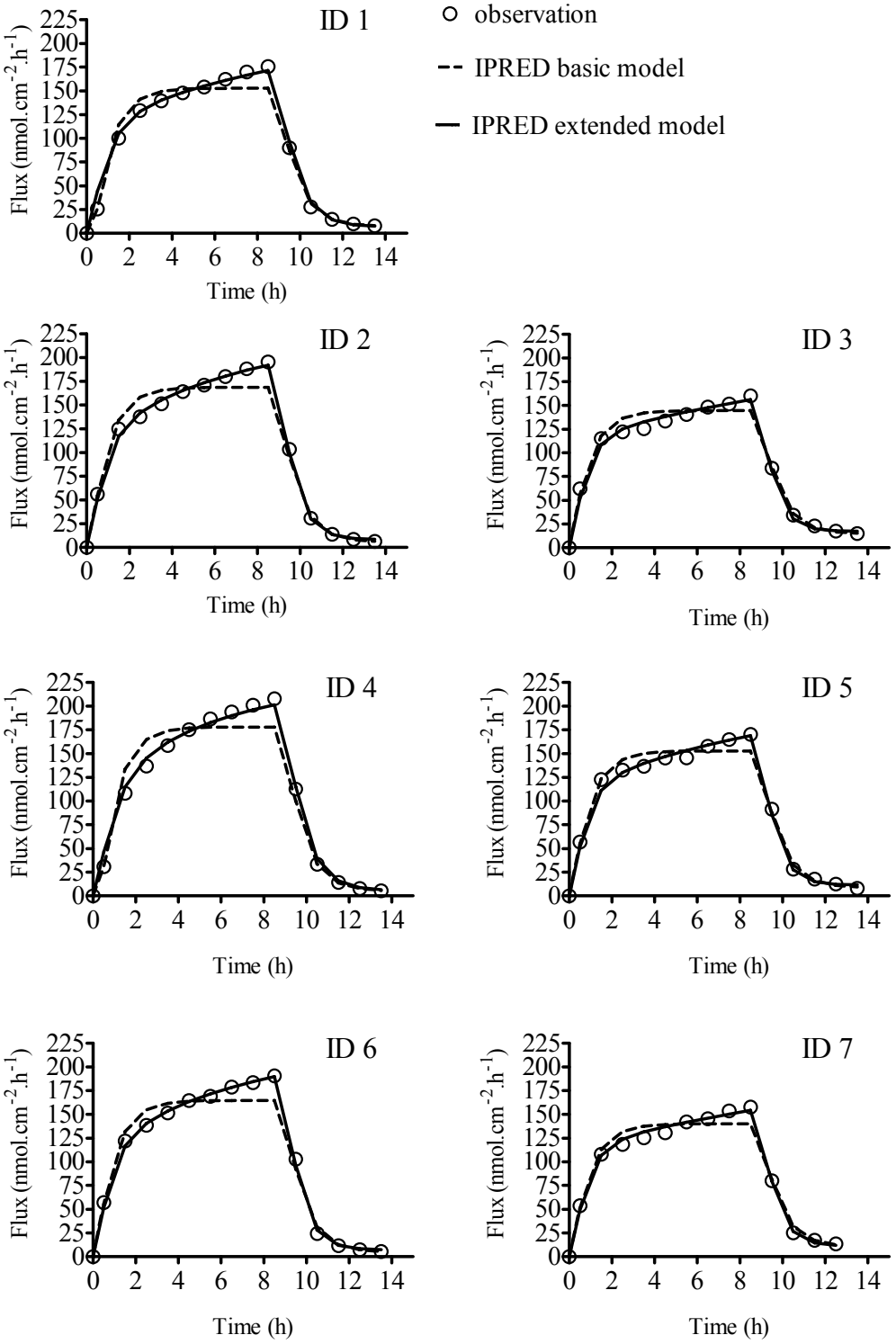

Figure 5: The individual iontophoretic flux (500 μA.cm^{-2}) vs time profiles of 8-OH-DPAC (3.9 mM) across human stratum corneum. The data are plotted as individual observations (open circle), together with the individual prediction (IPRED) based on the basic *in vitro* model (intermittent line) and on the extended *in vitro* model with two different release constants (solid line)

Table 3: The parameter estimates of data fitting the *in vitro* iontophoretic delivery (500 $\mu A.cm^{-2}$) across human stratum corneum (HSC) and dermatomed human skin (DHS) of the various 2-aminotetralins and chromanamine. The intrinsic driving force corrected for the surface area (I_0/S), the skin release constants (K_{R1} and K_{R2}), the passive driving force post iontophoresis corrected for the surface area (P_{PI}/S;Pass) and the lag time (t_L) are depicted. The donor concentration was 3.9 mM. Results are presented as population mean ± standard error of the estimate (n=4-7).

skin type	**Compound**		**I_0/S**		**K_{R1} (slow)**		**K_{R2} (fast)**		**Pass**		**t_L**	
			$nmol.cm^{-2}.h^{-1}$		h^{-1}		h^{-1}		$nmol.cm^{-2}.h^{-1}$		h	
		n	Mean	SE	Mean	SE	Mean	SE	Mean	SE	Mean	SE
HSC	5-OH-EPAT	6	176.56	9.33	0.06	0.02	1.43	0.13	3.17	0.58	n.d.	n.d
	5-OH-MPAT	5	178.13	6.36	0.02	0.02	1.63	0.09	3.33	0.23	n.d.	n.d
	5,6-di-OH-MPAT	5	133.28	5.11	n.d	n.d	1.38	0.23	n.d	n.d	0.08	0.13
	5,6-di-OH-DPAT	5	91.25	1.86	0.43	0.12	1.19	0.07	2.77	1.28	0.06	0.05
	8-OH-DPAC	7	113.91	2.55	0.09	0.01	1.41	0.04	8.82	1.72	0.14	0.05
	5-OH-DPAT[a]	6	119.69	8.67	0.25	0.15	1.39	0.14	4.47	0.74	0.06	0.07
	rotigotine.HCl[b]	6	45.31	0.42	0.32	0.10	0.96	0.06	20.30	0.39	n.d	n.d
DHS	5-OH-EPAT	6	99.22	2.25	1.27	0.69	0.46	0.04	0.02	n.d	0.27	0.01
	5-OH-MPAT	7	118.91	1.49	0.47	0.11	0.54	0.04	4.64	1.32	0.26	0.08
	5,6-di-OH-DPAT	6	116.25	2.66	0.08	0.02	0.63	0.02	10.10	1.12	0.21	0.05
	8-OH-DPAC	7	101.88	1.12	0.08	0.04	0.53	0.04	n.d	n.d	0.47	0.08
	5-OH-DPAT	4	95.16	1.43	0.73	0.33	0.56	0.06	5.15	2.99	0.22	0.03
	rotigotine.HCl[b]	6	35.31	3.33	0.03	0.02	0.28	0.04	22.70	1.62	n.d	n.d

[a,b]: data was adapted from literature[14, 40]
n.d: not determined because the parameter was constrained to 0

K_{R2}. The extended model describes more adequately the flux of the drug than the basic model (Figure 5, solid line). This graphical analysis was performed for all compounds across DHS and HSC. The majority of the individual fits showed an improvement when using the extended model. The two models were also evaluated statistically by comparison of the objective function of the models. Except for rotigotine.HCl across DHS and 5,6-di-OH-MPAT across HSC, in all cases the objective function decreased with a value larger than 3.84. This indicates that although an extra parameter (K_{R2}) was added to the model, a clear improvement in fitting the iontophoretic transport across HSC and DHS was obtained ($p<0.05$; Chi-square test). A model using two zero order mass input rates (I_0) or an additional release constant (K_{R3}) did not further improve data fitting. The estimated transport parameters, using the extended model with one zero order mass input rate and 2 release constants, can be found in Table 3.

4 Discussion

In this study the transdermal iontophoretic delivery of a series of 2-aminotetralins and 1 chromanamine (8-OH-DPAC) is presented. The systematic structural differences of these compounds allowed us to investigate the effect of molecular structure on the solubility and on iontophoretic delivery efficiency.

4.1 Solubility

The differences in structure highly affected the solubility of the various compounds. Compared to 5-OH-DPAT, approximately a 2-fold higher solubility was observed for 5-OH-EPAT and 5-OH-MPAT, indicating that decreasing the length of the alkyl side chain on the nitrogen group improves the solubility of the compound, most probably due to reduction in lipophilicity and an increase in chargeability of the nitrogen group. Furthermore for 8-OH-DPAC almost a 5-fold higher solubility was observed compared to 5-OH-DPAT. This demonstrates that replacement of the tetrahydronaphtalene moiety, present in the structure of 5-OH-DPAT, by a chroman moiety (as in 8-OH-DPAC), increases the solubility. In contrast, 5,6-di-OH-DPAT showed a reduced solubility, which can be explained by the formation of intermolecular hydrogen bridges, decreasing its water solubility.

4.2 Efficiency of iontophoretic transport

Small structural changes influence the transport efficiency of the different analogs significantly across HSC and DHS. Although steady state had not been reached yet after 9h of current application, already a clear difference can be observed at this time point. Despite the increase in hydrophilicity of 5,6-di-OH-MPAT and 5,6-di-OH-DPAT by introducing an extra oxygen on the phenylring, the iontophoretic flux reduced, compared to 5-OH-MPAT and 5-OH-DPAT. It has been reported that an increase in molecular volume results in a decrease in total iontophoretic flux, but in an increase in electroosmotic contribution [24, 43]. The significantly higher electroosmotic contribution for 5,6-di-OH-DPAT might be due to an increased molecular volume, caused by intermolecular hydrogen bonds, which would also account for the reduced iontophoretic flux. Decreasing the alkyl length of one side chain on the nitrogengroup from propyl (5-OH-DPAT) to ethyl (5-OH-EPAT) or further to a hydrogen (5-OH-MPAT) resulted in an increased efficiency of iontophoretic transport. This is in agreement with the observations by Del Terzo *et al.*, who obtained a similar result with ionized n-alkalanoic acids [29].

4.3 Transport pathways

In literature different iontophoretic transport routes are proposed: (i) the transport route across the appendageal structures, such as hair follicles and sweat glands, and (ii) the transport route via the intercellular route in the skin [44-47]. In agreement, fitting the iontophoretic flux using a model with two release constants also suggests the presence of at least 2 different transport routes across human skin during current application. In the initial time period of iontophoresis transport across the more permeable pores, possibly the appendages, with a faster release to the acceptor phase (described by K_{R2}) is the major contributor to the total iontophoretic flux. However, when the iontophoresis proceeds, the contribution of the second penetration route, suggested as the intercellular pathway, with a slower release (described by K_{R1}) increases. This results in an increase in the total iontophoretic flux (Figure 5). Modeling transport across HSC and DHS post iontophoresis revealed that the release from the skin was best described by K_{R2}. This suggests that the appendageal route post iontophoresis is still the predominant route. Similar observations by Turner and co-workers reported that the predominant transport route for the ionized calcein after iontophoresis pre-treatment was via the pores [47].

Comparing the skin release constant K_{R2} for HSC and DHS transport, it was observed that K_{R2} was smaller during transport across DHS. This can at least partly be attributed by the presence of hydrophilic regions and negative charged cell

membranes at pH 7.4 in both the epidermis and the upper part of the dermis, slowing down the partitioning of the compounds from the skin to the acceptor phase.

4.4 Physicochemical considerations for iontophoretic delivery

In literature several *in vitro* methods have been proposed as first screening methods for transdermal iontophoretic delivery. The molecular descriptors for iontophoresis in these methods were charge, molecular weight/volume and ionic/electrophoretic mobility [28, 33, 48-49].

As the electrophoretic mobility was reported as a good descriptor for the electromigrative flux (J_{EM}) [28, 33], in the present study, J_{EM} after 9h of iontophoresis was calculated using Equation 2. The passive flux was considered to be negligible. For the transport studies across HSC J_{EM} correlated linearly with the electrophoretic mobility (R^2=0.85) (Figure 6C).

Although capillary electrophoresis to estimate the J_{EM} at 9h is a good screening method for transdermal iontophoresis, this single end-point approach has some limitations. Firstly, this approach assumes that the end-point is representative for the entire iontophoretic flux, also before and after this point. However it does not account for the shape of the curve. Secondly, it is also important to understand the influence of the physicochemical properties on the different transport parameters, such as the zero order mass input and the release constants (Table 3). This information is important to make a realistic extrapolation towards *in vivo*. The iontophoretic mass transfer is driven by a potential gradient. This implies that besides the current density and the donor composition, which are kept constant in the transport studies, the zero order mass transfer is dependent on the electrophoretic properties of the molecule. It is observed that the zero order mass input, corrected for the surface area (I_0/S), is linearly correlated to the electrophoretic mobility (R^2=0.93) (Figure 6A). This also means that the steady state flux, calculated using Equation (8), can be predicted by the electrophoretic mobility. Previous studies demonstrated that the transport efficiency decreased with increasing molecular weight (Mw) [24-26]. For instance Lai and co-worker considered in the ionic mobility-pore model, that the logarithm of the permeability coefficient decreases linearly with increasing Mw [24]. If our interpretations are correct and K_{R2} describes the release during appendageal transport, it can be expected that the release from these pores into the acceptor phase is size dependent. Plotting the fast release constant K_{R2} against the Mw confirms this size dependency. The fast release constant K_{R2} is reduced linearly with increased Mw (Figure 6B; R^2=0.90).

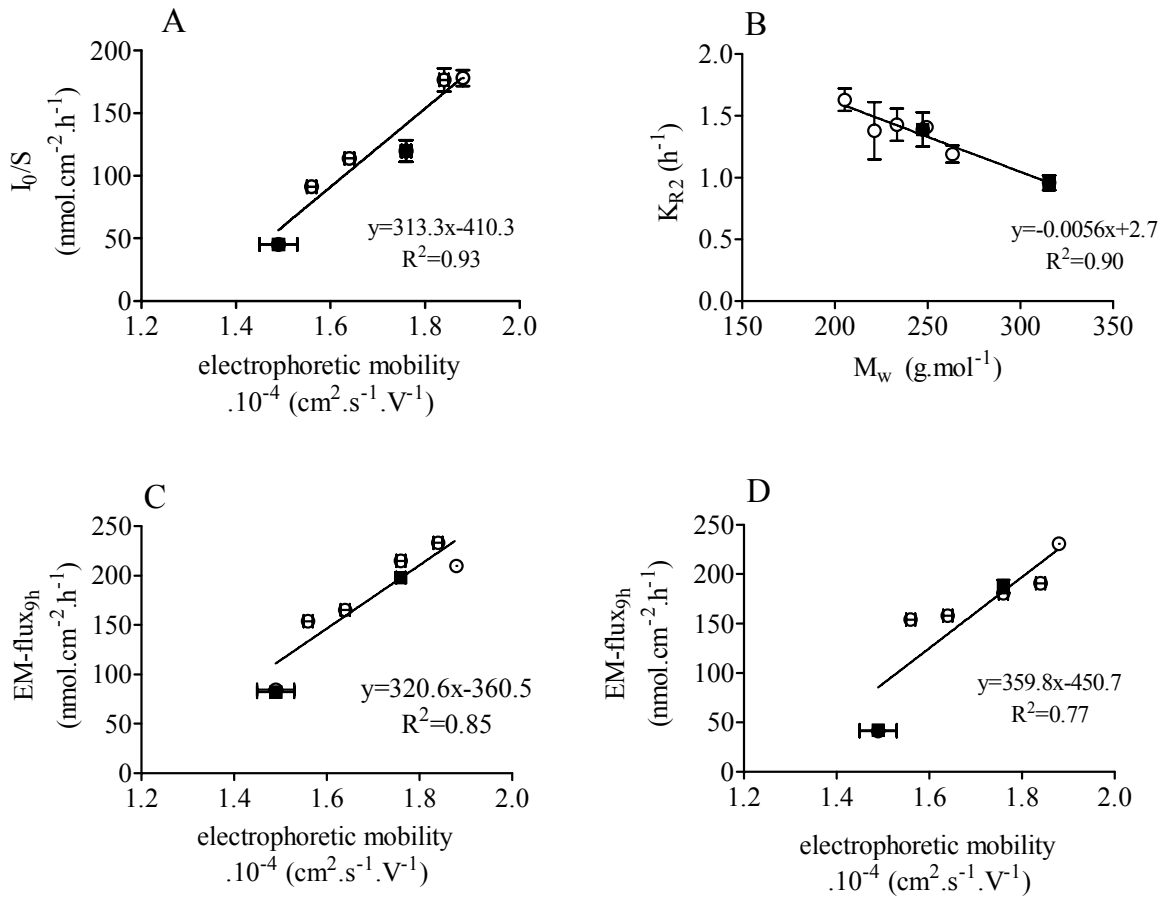

Figure 6: The relationships between the physicochemical properties of the compounds (open circle) and the transport parameters. The data of 5-OH-DPAT and rotigotine (closed square) were added to the graphs and included in the correlations. In all cases the donor concentration of the dopamine agonist was 3.9 mM. Data are presented as mean ± SD for the EM-flux and electrophoretic mobilty (n≥3). The parameter estimates (I_0 and K_{R2}) are presented as mean ± standard error of the estimate (n≥4). The regression analysis was performed with the mean point estimates. **A**: The linear correlation between the intrinsic driving force corrected for the surface area (I_0/S) vs the mean electrophoretic mobility. **B**: The linear correlation between the K_{R2} and the molecular weight. **C**: The electromigrative flux (EM-flux) at 9h across human stratum corneum is plotted against the mean electrophoretic mobility. **D**: The correlation between the flux at 9h across dermatomed human skin versus the mean electrophoretic mobility.

Although not fully understood yet, the lipophilicity of the molecules can be of importance for the transport efficiency and transport pathway. For instance Jadoul *et al*. showed that fentanyl, a relatively lipophilic molecule, was distributed across the whole HSC, while the more hydrophilic thyrotropin releasing hormone was mainly localized in the pores after iontophoresis [50]. In analogy, our observations show that the relative contribution of the two different transport pathways is dependent on the lipophilicity of the solute. For the more lipophilic compounds, rotigotine and 5-OH-DPAT, a relatively high K_{R1} value was observed, while for the more hydrophilic compounds K_{R1} remained small. For the most hydrophilic compound 5,6-di-OH-MPAT even a negligible value for K_{R1} was observed. An exception was made for 5,6-di-OH-DPAT, since other mechanisms play a role in its iontophoretic transport.

Due to the increased membrane complexity of DHS, the aforementioned relationships between the physicochemical properties (electrophoretic mobility, Mw, clogP) and the transport parameters (J_{EM}, I_0/S, K_{R2}, K_{R1}) were not so evident, contrasting the observations for transport across HSC. For instance across DHS, assuming that the relative electromigrative contribution is similar to that across HSC, the linear correlation between the J_{EM} and the electrophoretic mobility was not so clear (Figure 6D) (R^2=0.78). DHS includes HSC, the viable epidermis, and a part of the dermis, and therefore the complexity of the transport membrane augments. Further research is necessary to fully understand the underlying transport mechanism(s) involved in epidermal transport. A larger set of molecules, covering a broader range of electrophoretic mobilities presumably will increase the predictive value of capillary electrophoresis for the J_{EM} across DHS, as was observed for a series of dipeptides [28, 33]. These dipeptides were grouped in 3 clusters, where the correlation within the groups was far less than the overall correlation, including all 11 peptides. Nonetheless the electrophoretic mobility and the corresponding J_{EM} across DHS, observed for the dopamine agonists in the current paper were similar to the values obtained for the dipeptides at pH 7.4 [28, 33].

Next to identifying the physicochemical-transport parameter relationships, compartmental modeling can be very useful for extrapolation towards the *in vivo* situation. Assuming transport across HSC *in vitro* is representative for transport *in vivo* in humans, combining these transport parameters with pharmacokinetic parameters, applying non-linear mixed effect modeling, simulations can be made of the iontophoretic flux *in vivo*. Nugroho *et al*. demonstrated that for transdermal iontophoresis such an extrapolation from *in vitro* to *in vivo* is possible in rats, predicting the plasma concentration and even the pharmacodynamic effect [16].

In conclusion, this study shows that small structural changes affect the solubility, electrophoretic mobility, the iontophoretic delivery efficiency and the contribution of the transport route during iontophoresis. Increasing the hydrophilicity by addition of an extra OH-group on the phenyl ring (5,6-di-OH-MPAT and 5,6-di-OH-DPAT) did not result in an increase in solubility nor transport efficiency. On the other hand solubility and iontophoretic transport can benefit from reduction in the alkyl groups at the nitrogen. In addition the electrophoretic mobility and the Mw can be applied to estimate the zero order mass input I_0/S and K_{R2}, respectively. The clogP might be helpful in determination of the relative contribution of the different transport pathways by estimation of K_{R1}, although further research is required to define a clear relationship. With the estimated parameters, using the proposed compartmental model, it will be possible to simulate the iontophoretic flux profile across HSC *in vitro*. Simulations can be a helpful tool in designing future experiments, giving the opportunity to explore different flux profiles and different study designs.

Acknowledgements

This research was financially supported by a grant (LKG 6507) of the Dutch Technology Foundation STW, Utrecht, The Netherlands.

References

1. Sage, B.H., *Iontophoresis*, in *Percutaneous Penetration Enhancers*, E.W. Smith and H.I. Maibach, Editors. 1995, CRC Press Inc.: Boca Raton. p. 351-365.
2. Nutt, J.G., *Continuous dopaminergic stimulation: Is it the answer to the motor complications of Levodopa?* Mov Disord, 2007. **22**(1): p. 1-9.
3. Olanow, C.W., *The scientific basis for the current treatment of Parkinson's disease.* Annu Rev Med, 2004. **55**: p. 41-60.
4. Olanow, C.W., M.B. Stern, and K. Sethi, *The scientific and clinical basis for the treatment of Parkinson disease (2009).* Neurology, 2009. **72**(21 Suppl 4): p. S1-136.
5. van Laar, T., et al., *Stepwise intravenous infusion of apomorphine to determine the therapeutic window in patients with Parkinson's disease.* Clin Neuropharmacol, 1998. **21**(3): p. 152-8.
6. Tugwell, C., *Parkinson's disease in focus*. 1st ed. In focus. 2008, London: Pharmaceutical Press. 237.
7. van der Geest, R., M. Danhof, and H.E. Bodde, *Iontophoretic delivery of apomorphine. I: In vitro optimization and validation.* Pharm Res, 1997. **14**(12): p. 1798-803.
8. van der Geest, R., et al., *Iontophoretic delivery of apomorphine. II: An in vivo study in patients with Parkinson's disease.* Pharm Res, 1997. **14**(12): p. 1804-10.
9. Li, G.L., et al., *Transdermal iontophoretic delivery of apomorphine in patients improved by surfactant formulation pretreatment.* J Control Release, 2005. **101**(1-3): p. 199-208.
10. Li, G.L., et al., *Iontophoretic R-apomorphine delivery in combination with surfactant pretreatment: in vitro validation studies.* Int J Pharm, 2003. **266**(1-2): p. 61-8.
11. Luzardo-Alvarez, A., M.B. Delgado-Charro, and J. Blanco-Mendez, *Iontophoretic delivery of ropinirole hydrochloride: effect of current density and vehicle formulation.* Pharm Res, 2001. **18**(12): p. 1714-20.
12. Luzardo-Alvarez, A., M.B. Delgado-Charro, and J. Blanco-Mendez, *In vivo iontophoretic administration of ropinirole hydrochloride.* J Pharm Sci, 2003. **92**(12): p. 2441-8.
13. Nugroho, A.K., et al., *Transdermal iontophoresis of rotigotine: influence of concentration, temperature and current density in human skin in vitro.* J Control Release, 2004. **96**(1): p. 159-67.
14. Nugroho, A.K., et al., *Transdermal iontophoresis of rotigotine across human stratum corneum in vitro: influence of pH and NaCl concentration.* Pharm Res, 2004. **21**(5): p. 844-50.
15. Nugroho, A.K., et al., *Transdermal iontophoresis of the dopamine agonist 5-OH-DPAT in human skin in vitro.* J Control Release, 2005. **103**(2): p. 393-403.
16. Nugroho, A.K., et al., *Pharmacokinetics and pharmacodynamics analysis of transdermal iontophoresis of 5-OH-DPAT in rats: in vitro-in vivo correlation.* J Pharm Sci, 2006. **95**(7): p. 1570-85.
17. Beart, P.M., et al., *Radioreceptor binding reveals the potencies of N,N-disubstituted 2-aminotetralins as D2 dopamine agonists.* Naunyn Schmiedebergs Arch Pharmacol, 1987. **336**(5): p. 487-93.
18. Beaulieu, M., et al., *N,N-disubstituted 2-aminotetralins are potent D-2 dopamine receptor agonists.* Eur J Pharmacol, 1984. **105**(1-2): p. 15-21.
19. Hacksell, U., et al., *N-Alkylated 2-aminotetralins: central dopamine-receptor stimulating activity.* J Med Chem, 1979. **22**(12): p. 1469-75.
20. Horn, A.S., et al., *Synthesis and dopaminergic activity of a new oxygen isostere of the 2-aminotetralins: N,N-dipropyl-8-hydroxy-3-chromanamine.* Eur J Med Chem, 1988. **22**(4): p. 325-328.

21. Thorberg, S.O., et al., *Aminochromans: potent agonists at central dopamine and serotonin receptors.* Acta Pharm Suec, 1987. **24**(4): p. 169-82.
22. van Vliet, L.A., et al., *Affinity for dopamine D2, D3, and D4 receptors of 2-aminotetralins. Relevance of D2 agonist binding for determination of receptor subtype selectivity.* J Med Chem, 1996. **39**(21): p. 4233-7.
23. Vermue, N.A., et al., *Pharmacological profile of N,N dipropyl-8-hydroxy-3-chromanamine, an oxygen isostere of the dopamine agonist N,N dipropyl-5-hydroxy-2-aminotetralin with enhanced presynaptic selectivity.* Arch Int Pharmacodyn Ther, 1988. **293**: p. 37-56.
24. Lai, P.M. and M.S. Roberts, *An analysis of solute structure-human epidermal transport relationships in epidermal iontophoresis using the ionic mobility: pore model.* J Control Release, 1999. **58**(3): p. 323-33.
25. Roberts, M.S., P.M. Lai, and Y.G. Anissimov, *Epidermal iontophoresis: I. Development of the ionic-mobility pore model.* Pharm Res, 1998. **15**(10): p. 1569-1578.
26. Yoshida, N.H. and M.S. Roberts, *Solute molecular size and transdermal iontophoresis across excised human skin* Journal of controlled release, 1993. **25**(3): p. 177-195.
27. Abla, N., et al., *Effect of charge and molecular weight on transdermal peptide delivery by iontophoresis.* Pharm Res, 2005. **22**(12): p. 2069-78.
28. Abla, N., et al., *Capillary zone electrophoresis for the estimation of transdermal iontophoretic mobility.* J Pharm Sci, 2005. **94**(12): p. 2667-75.
29. Del Terzo, S., C.R. Behl, and R.A. Nash, *Iontophoretic transport of a homologous series of ionized and nonionized model compounds: influence of hydrophobicity and mechanistic interpretation.* Pharm Res, 1989. **6**(1): p. 85-90.
30. Schuetz, Y.B., et al., *Structure-permeation relationships for the non-invasive transdermal delivery of cationic peptides by iontophoresis.* Eur J Pharm Sci, 2006. **29**(1): p. 53-9.
31. Nugroho, A.K., et al., *Compartmental modeling of transdermal iontophoretic transport: I. In vitro model derivation and application.* Pharm Res, 2004. **21**(11): p. 1974-84.
32. Nugroho, A.K., et al., *Compartmental modeling of transdermal iontophoretic transport II: in vivo model derivation and application.* Pharm Res, 2005. **22**(3): p. 335-46.
33. Henchoz, Y., et al., *A fast screening strategy for characterizing peptide delivery by transdermal iontophoresis.* J Control Release, 2009.
34. Poole, S.K., et al., *Determination of acid dissociation constants by capillary electrophoresis.* J Chromatogr A, 2004. **1037**(1-2): p. 445-54.
35. Wan, H., et al., *Rapid screening of pKa values of pharmaceuticals by pressure-assisted capillary electrophoresis combined with short-end injection.* J Chromatogr A, 2002. **979**(1-2): p. 369-77.
36. Holford, N., *The Visual Predictive Check-Superiority to Standard Diagnostic (Rorschach) Plots.* PAGE 14, Abstr 738 [www.page-meeting.org/?abstract=738], 2005.
37. Tetko, I.V. and P. Bruneau, *Application of ALOGPS to predict 1-octanol/water distribution coefficients, logP, and logD, of AstraZeneca in-house database.* J Pharm Sci, 2004. **93**(12): p. 3103-10.
38. Tetko, I.V., et al., *Virtual computational chemistry laboratory--design and description.* J Comput Aided Mol Des, 2005. **19**(6): p. 453-63.
39. VCCLAB. *Virtual Computational Chemistry Laboratory,* http://www.vcclab.org. 2005.
40. Ackaert, O.W., et al., *Mechanistic studies of the transdermal iontophoretic delivery of 5-OH-DPAT in vitro.* J Pharm Sci, 2010. **99**(1): p. 275-85.
41. Cheng, H.Y., Strope, E., Adams, R.N. , *Electrochemical studies of the oxidation pathways of apomorphine.* Anal Chem, 1979. **51**(13): p. 2243-2246.
42. Afkhami, A., Nematollahi, D. ,Khalafi, L. , Rafiee, M., *Kinetic study of the oxidation of some catecholamines by digital simulation of cyclic voltammograms.* Int J Chem Kinet, 2005. **37**(1): p. 17-24.

43. Peck, K.D., et al., *Quantitative description of the effect of molecular size upon electroosmotic flux enhancement during iontophoresis for a synthetic membrane and human epidermal membrane.* J Pharm Sci, 1996. **85**(7): p. 781-8.
44. Alvarez-Roman, R., et al., *Visualization of skin penetration using confocal laser scanning microscopy.* Eur J Pharm Biopharm, 2004. **58**(2): p. 301-316.
45. Barry, W., ed. *Dermatological formulations. Percutaneous Absorption.* . 1983: New York: Marcel Dekker.
46. Cullander, C., *What are the pathways of iontophoretic current flow through mammalian skin?* Advanced Drug Delivey Reviews, 1992. **9**: p. 119-135.
47. Turner, N. and R.H. Guy, *Iontophoretic transport pathways: dependence on penetration physcicochemical properties.* J Pharm Sci, 1997. **86**(12): p. 1385-1389.
48. Mudry, B., et al., *Quantitative structure-permeation relationship for iontophoretic transport across the skin.* J Control Release, 2007. **122**(2): p. 165-72.
49. Yoshida, N.H. and M.S. Roberts, *Prediction of cathodal iontophoretic transport of various anions across excised skin from different vehicles using conductivity measurements.* J Pharm Pharmacol, 1995. **47**(11): p. 883-90.
50. Jadoul, A., et al., *Quantification and localization of fentanyl and trh delivered by iontophoresis in the skin* International Journal of Pharmaceutics, 1995. **120**(2): p. 221-228.

Part II

In vivo assessment of controlling the iontophoretic delivery of (S)-5-OH-DPAT

6

Controlling the pharmacokinetics and the pharmacodynamic effect of (S)-5-OH-DPAT with transdermal iontophoresis

Oliver W. Ackaert[a*], Jeroen De Graan[b*], Shanna Shi[d], Rob Vreeken[d], Oscar E. Della Pasqua[c,f] , Durk Dijkstra[b], Ben H. Westerink[b,e] , Meindert Danhof[c] and Joke A. Bouwstra[a]

[a]Division of Drug Delivery Technology, Leiden/Amsterdam Center for Drug Research, Leiden, The Netherlands
[b]Department of Medicinal Chemistry, University Center of Pharmacy, University of Groningen, The Netherlands
[c]Division of Pharmacology, Leiden/Amsterdam Center for Drug Research, Leiden, The Netherlands
[d]Division of Analytical biosciences, Leiden/Amsterdam Center for Drug Research, Leiden, The Netherlands
[e]Department of biomonitoring and sensoring, University Center of Pharmacy, University of Groningen, The Netherlands
[f]Clinical Pharmacology and Discovery Medicine, GlaxoSimthKline, Greenford, United Kingdom

[*]Contributed equally as first author
2010. *submitted for publication*

Abstract

The pharmacokinetic (PK) and pharmacodynamic (PD) properties of the active (S)-enantiomer of the potent dopamine agonist 5-OH-DPAT were investigated in a novel anesthetized animal model. Firstly, the relationship between current density, *in vivo* transport and plasma profile was characterized. Secondly, the effect of the anesthetic mixture, transdermal iontophoresis and blood sampling on the striatal dopamine release (PD endpoint) was investigated. Thirdly, the PK-PD relationship following transdermal iontophoresis was investigated during a controlled and reversible pharmacological response. As pharmacodynamic effect the dopamine release in striatum was selected. Given that the striatal dopamine levels are unaltered during experimental procedures, this rat model can be used to investigate the PK-PD relationship. The *in vivo* flux was found to be linearly correlated with the current density, which indicates that drug delivery can carefully be titrated by the current density. Following both transdermal iontophoresis and IV infusion, a strong and reversible PD effect was observed. Compartmental modeling showed that the relationship between drug plasma concentration and biomarker response can be best characterized by an effect compartment, rather than an indirect response model. In addition, covariate analysis suggested that the delivery rate can affect the pharmacodynamic efficiency. Finally, simultaneous PK-PD analysis revealed that steady delivery rates are translated into continuous dopaminergic stimulation. This can be of great benefit for reducing side effects in the symptomatic treatment of Parkinson's disease with 5-OH-DPAT.

Keywords: PK-PD, compartmental modeling, iontophoresis, (S)-5-OH-DPAT, microdialysis

1 Introduction

Transdermal iontophoresis is a well established physical method to facilitate the percutaneous penetration of molecules [1]. By application of a small electrical current across the skin iontophoresis enhances the transdermal delivery of therapeutic agents. An important advantage of transdermal delivery is the circumvention of the hepatic first-pass metabolism, making it an interesting non-invasive alternative for oral drug delivery. A particular advantage of iontophoresis is the possibility to tailor the delivery to the patient's needs by adjusting the current density. This may allow for better therapeutic efficacy and reduction in overdosing and subsequent side effects. These properties make iontophoresis an excellent method for the transdermal delivery of drug molecules for the symptomatic treatment of Parkinson's disease.

Parkinson's disease is a neurodegenerative disorder, which is characterized by tremor, akinesia, rigidity and postural instability [2]. Up to today orally dosed levodopa is still the most effective symptomatic treatment, but chronic use eventually leads to severe long-term side-effects, i.e. dyskinesia and the *on-off* phenomenon [3-4]. Current strategy to prevent or delay the onset of these side-effects is to administer therapeutics in a constant and controlled manner [5]. Therefore, the transdermal iontophoretic delivery of the dopaminergic agonists R-apomorphine, ropinirole and 5-OH-DPAT were investigated *in vivo* for their application in symptomatic treatment of Parkinson's disease [6-9].

Besides a constant and controlled delivery, another attractive property of iontophoresis is the possibility to develop a feedback system. In this approach, the concentration of a relevant biomarker, extracted for instance with reverse iontophoresis, can be used to titrate the transdermal iontophoretic delivery of the drug molecule. Preferably, a pharmacodynamic endpoint instead of the drug plasma concentration should be chosen to monitor the drug effect. Under experimental conditions, striatal dopamine concentration, measured by microdialysis, has been shown to be a biomarker for dopaminergic activity [10-11].

In the current investigation, we have therefore characterized pharmacokinetic-pharmacodynamic (PK-PD) relationships of the dopamine agonist following transdermal iontophoresis using dopamine as a measure of the pharmacological effect. In order to optimize the feedback system, we have also performed an integrated evaluation of relationship between the pharmacodynamics,

pharmacokinetics and the delivery rates of the compound. In a previous study, the PK-PD of 5-OH-DPAT was assessed, however a ceiling effect was observed, with dopaminergic levels not altering throughout the time frame of the experiments [7]. Modelling of the data was therefore difficult and demanded for a follow-up study to investigate the PK-PD relationship under a wider exposure range, in which maximum effect (ceiling) is short lasting. In addition, during the previous study 5-OH-DPAT was administered as racemic mixture, while (S)-5-OH-DPAT is the only enantiomer with dopaminergic activity. In contrast to previous studies, in the present investigation, experiments are conducted with the active enantiomer (S)-5-OH-DPAT [7].

The aims of this study were three-fold. First, to examine the relationship between the current density, the *in vivo* iontophoretic transport and the (S)-5-OH-DPAT plasma profile. Given the requirement for the use of anaesthesia to conduct transdermal iontophoresis, second, to examine the effect of the anesthetic mixture, transdermal iontophoresis and blood sampling on the striatal dopamine release. Third, to assess the PK-PD relationship following transdermal iontophoresis of (S)-5-OH-DPAT,

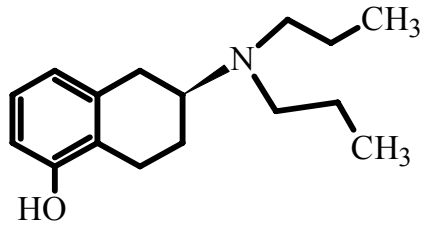

(S)-5-OH-DPAT

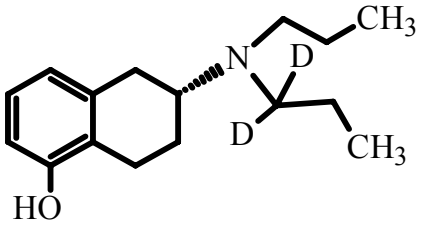

(R)-d_2-5-OH-DPAT

Figure 1: The molecular structures of (S)-5-hydroxy-2-(N,N,-di-n-propylamino)tetralin ((S)-5-OH-DPAT) and (R)-5-hydroxy-2-(N-*n*-propyl-N-α,α-dideutero-propylamino)-tetralin ((R)-d_2-5-OH-DPAT)

ensuring the induction of a controlled and reversible effect [7]. A comprehensive approach based on non-linear mixed effects modeling was used that allows us to characterize and predict the time course of drug action. Furthermore this approach enables to combine data from different experiments to obtain individual and population PK-PD parameter estimates [12]. Extensive PK-PD modeling is further applied to characterize the pharmacokinetics of (S)-5-OH-DPAT in plasma and the corresponding pharmacodynamic effect. The PK model to describe the plasma concentration was adapted from literature [7]. Given that a delay is observed between plasma concentrations and the onset of the pharmacological response, two PD models are compared to describe the DA release: the effect compartment model [13] *vs* the indirect response type I model [14]. The results of this comparison add value to the efforts in the optimization of drug delivery. We ultimately illustrate how PK-PD relationships can be used to design a delivery system for symptomatic treatment of Parkinson's disease.

2 Materials and Methods

2.1 Chemistry

5-hydroxy-2-(N,N,-di-n-propylamino)tetralin ((S)-5-OH-DPAT) and (R)-5-hydroxy-2-(N-*n*-propyl-N-α,α-dideutero-propylamino)-tetralin ((R)-d_2-5-OH-DPAT) (HBr salts, purity > 98%) were synthesized at the Department of Medicinal Chemistry of the University of Groningen, Groningen, the Netherlands (Figure 1). To synthesize d_2-5-OH-DPAT the following deuteration strategy was employed: (+)-5-Methoxy-2-(N-*n*-propylamino)tetralin was converted to the propionamide. Subsequently, the propionamide was reduced with lithium aluminium deuteride and after demethylation with 48% hydrobromic acid, the final compound d_2-5-OH-DPAT hydrobromide was obtained with an overall yield of 13%.

2.2 Materials

Silver, silver chloride (puritiy >99.99%) and octanesulfonic acid were obtained from Sigma-Aldrich (Zwijndrecht, the Netherlands). Acetonitrile (LC-MS grade), ammonium acetate (LC-MS grade), acetic acid (LC-MS grade) and methanol (LC-MS grade) were purchased from Biosolve (Valkenswaard, the Netherlands). Ammonium hydroxide (25% w/v; analytical grade) was obtained from Baker (Deventer, the Netherlands). NaCl 0.9% was purchased from the hospital pharmacy of LUMC (Leiden, the Netherlands). EDTA was obtained from Merck (Merck

KGaA, Darmstadt, Germany). All solutions were prepared in Millipore water with a resistivity of more than 18 MΩ.cm.

2.3 Iontophoresis patches

A detailed description of the iontophoresis patches, used for the transdermal iontophoresis studies can be found elsewhere [7]. Briefly, the iontophoresis patches were prepared by the Fine Mechanical Department of Leiden University from elastic silicon materials (silicon: Smooth-Sil 920; Smooth-on Inc., Easton, PA, USA). The volume of the patches was 2.3 ml and the active area was 2.5 cm². The patch was fixed on wound dressing film (Opsite Flexigrid, Smith&Nephew, Hoofdorp, the Netherlands), which can be attached to the skin during the experiment. Ag/AgCl was used as driver electrode pair.

2.4 Animals

Animal procedures were conducted in accordance with guidelines published in the NIH guide for the care and use of laboratory animals and all protocols were approved by the Institutional Animal Care and Use Committee of the University of Groningen and Leiden University. The pharmacokinetic (PK) and the pharmacokinetic-pharmacodynamic (PK-PD) studies were performed in albino male Wistar rats (280-340 g) obtained from Charles River (Maastricht, the Netherlands) and Harlan (Horst, the Netherlands), respectively. Prior to surgery the animals were housed at least 1 week in Plexiglas cages, maximum 6 animals per cage with free access to water and standard laboratory chow. The cages were placed in a room with a controlled temperature at 21 °C and controlled humidity between 60-65% and a light-dark cycle of 12h.

2.5 Pharmacokinetic (PK) studies

In these experiments the relationship between the current density and the plasma concentration profile of (S)-5-OH-DPAT following transdermal iontophoresis was investigated. (S)-5-OH-DPAT was administered by transdermal iontophoresis and intravenous (IV) infusion to the same animals with a one week interval between treatments. The use of both routes of administration allowed improved pharmacokinetic parameter estimation. A detailed description of the experiments is given below.

2.5.1 Surgical procedures

Prior to surgery the animals were anaesthetized with a combination of Dormicum® (midazolam, 5 $mg.ml^{-1}$, Roche Nederland, Mijdrecht, the Netherlands) and Hypnorm® (fentanyl citrate 0.315 $mg.ml^{-1}$ + fluanizone 10 $mg.ml^{-1}$, Janssen Pharmaceutica, Beerse, Belgium) at a dose of 0.5 $mL.kg^{-1}$ rat weight. The permanent cannulation was performed using Polethene tubings (Rubler BV, Hilversum, the Netherlands) with the diameter of 0.58 mm (I.D.) – 0.96 mm (O.D.) and 0.28 mm (I.D.) – 0.61 mm (O.D.), respectively for femoral vein and artery cannulation. After surgery the animals were housed individually and were allowed to recover during one week.

2.5.2 Experimental procedures

In the first part of the study (S)-5-OH-DPAT was administered by transdermal iontophoresis. Firstly the animals were anesthetized with Hypnorm® and Dormicum® (0.5 $mL.kg^{-1}$) and the hair of the back was removed using an electrical clipper and a scalpel. A pair of patches was attached to the skin surface. After 15 min the patches were filled with (S)-5-OH-DPAT (3.9 mM) at pH 5.0 (citric buffer, 5 mM) and with PBS pH 7.4 (NaCl: 8 $g.L^{-1}$, Na_2HPO_4: 2.86 $g.L^{-1}$, KH_2PO_4: 0.2 $g.L^{-1}$, KCl: 0.19 $g.L^{-1}$) at the anodal and the cathodal side, respectively. The following protocol was used for the iontophoresis studies: 15 min passive diffusion + 120 min 75 $\mu A.cm^{-2}$ + 120 min 150 $\mu A.cm^{-2}$. At time=255 min, the patches were removed and the skin was wiped using a tissue paper. Blood samples were taken at regular time intervals during the current application and after removal of the patch: 0, 15, 45, 75, 105, 135, 165, 195, 225, 255, 270, 285, 315, 345, 390, 435 min. Blood samples (0.2 ml) were collected using lithium-heparin containing tubes (Microvette® 200 Plasma/Lithium Heparin, Sarsted BV, Etten-Leur, the Netherlands). Plasma was then separated by centrifugation at a speed of 6000 rpm during 10 min. The samples were kept at -20 °C prior to analysis with LC-MS-MS (section 2.7).

After 1 week of recovery in individualized housing, animals received a total dose of 29 nmol (S)-5-OH-DPAT, dissolved in 0.9% NaCl, during a 15-min IV infusion. At regular time intervals blood samples were taken from the femoral artery cannula: 0, 15, 20, 30, 45, 60, 75, 90, 105, 120, 150, 180 min. The samples were prepared in the same way as described above following iontophoretic delivery (see above). In all experiments the animals were kept in an anaesthetized condition during the experiment using Hypnorm® and Dormicum®.

2.6 On-line microdialysis studies (PK-PD studies)

This series of experiments consisted of three parts. Firstly, the influence of anesthesia and iontophoresis on the striatal dopamine release (PD end point) was determined with on-line microdialysis. Secondly, the pharmacokinetic (PK) and pharmacodynamic (PD) properties following transdermal iontophoretic delivery were examined. Thirdly, to explore the implications of differences in delivery rate on the PK and PD parameters, (S)-5-OH-DPAT was administered with IV infusion. In all experiments the striatal dopamine level and the striatal 5-OH-DPAT concentration were monitored by microdialysis with simultaneous blood sampling for the analysis of (S)-5-OH-DPAT plasma concentrations. A detailed description of the experiments is given below.

2.6.1 Surgical procedures

Prior to surgery the rats were anaesthetized with Isofluran 2% in N_2O/O_2 (2/1). The permanent cannulations were performed using silicone catheters (inner diameter (I.D.): 0.5 mm; outer diameter (O.D.): 0.9 mm) (UNO BV, Zevenaar, The Netherlands). The catheters were inserted approximately 2 cm inside the vessels. The catheters were tunneled subcutaneously, externalized at the back of the head. After the cannulation the rats were kept under anaesthetized condition and mounted into a stereotaxic frame for the implementation of microdialysis probes in left and right striatum according to a method described previously [10-11]. After exposing and anesthetizing the skull with 0.5% marcaine-adrenaline, the holes for probe insertion were drilled. A Y-shaped dialysis probe was used for the experiments, with an exposed tip length of 3 mm. The dialysis cannula (I.D.: 0.24 mm; O.D.: 0.34 mm) was prepared from polyacrylonitrile/sodium methallyl sulfonate copolymer (AN 69, Hospal, Bologna, Italy). The microdialysis cannula was implanted in the striatum. The following coordinates were used according to the atlas of Paxinos and Watson [15]: AP +0.9, LM ± 3.0 relative to bregma, and Vd – 6.0 below dura. Before insertion into the brain, the dialysis probe was perfused successively with 70% ethanol, ultrapure water and Ringer solution (140 mM NaCl, 3.0 mM KCl, 1.2 mM $CaCl_2$, 1.0 mM $MgCl_2$). The dialysis probe was positioned in the burr hole under stereotaxic guidance. The probe was cemented in this position with dental cement. Thereafter the rats were housed solitary.

2.6.2 Experimental procedures

The PK-PD experiments were performed 15-20 h after cannulation and implantation of the probes. The rats were anaesthetized prior to and kept under anesthetized

condition during the experiment with Hypnorm® and Dormicum® at a starting dose of 0.5 mL.kg^{-1} and subsequently with hourly doses of 0.17 mL.kg^{-1}.
Firstly, to dismiss the potential confounding effects of anaesthesia, an iontophoretic control experiment was conducted administering only citric buffer (pH 5.0, 5 mM), as this is the donor phase used for transdermal iontophoresis, without (S)-5-OH-DPAT. Before the start of the experiment, the hair of the back of the anesthetized rat was removed with an electrical clipper and scalpel. 15 min after attaching the patches to the skin surface, the cathodal patch was filled with PBS pH 7.4 and the anodal patch was filled with the donor solution. The protocol for iontophoresis was: 15 min passive diffusion + 90 min current application (250 µA.cm^{-2}). The patch was removed and the skin was wiped using tissue paper. To include the influence of blood sampling on the DA level, blood samples were taken at regular time intervals: 0, 15, 30, 45, 60, 75, 90, 105, 120, 135, 165, 195, 225, 255, and 285. Blood sampling and subsequent preparation of the samples were identical to the procedures used for the PK studies following transdermal iontophoresis (*cf*. supra).

Secondly, a PK-PD microdialysis study following transdermal iontophoretic delivery of (S)-5-OH-DPAT was performed. The donor solution consisted of (S)-5-OH-DPAT (3.9 mM), buffered with a citric buffer (pH 5.0, 5 mM). All the experimental procedures were identical to the control experiment, as described in the previous paragraph. Thirdly, a PK-PD microdialysis study was performed with a total dose of 113 nmol 5-OH-DPAT, dissolved in NaCl 0.9%, administered as a 10-min IV infusion. Blood sampling and subsequent preparation of the samples were identical to the procedures used for the PK studies following IV infusion (*cf*. supra).

In all the PK-PD studies the dopamine level and the 5-OH-DPAT concentration were monitored in the left and right striatum, respectively, with microdialysis. The microdialysis probes in the striata were perfused with Ringer solution at a flow of 2 µL.min^{-1} (CMA/102 Microdialysis Pump, Sweden). Every 15 min a sample was collected for analysis with a total volume of 30 µl. The analysis of the microdialysate samples is described below (section 2.7.2).

2.7 Sample analysis

2.7.1 Blood samples of (S)-5-OH-DPAT

The blood samples of 5-OH-DPAT were analyzed with an on-line solid-phase extraction-liquid-chromatography-mass spectrometry/mass spectrometry (SPE-LC-MS/MS) method. 5 µl of the internal standard (d_2-5-OH-DPAT; 5 ng.ml^{-1}) was added to 35 µl of the collected plasma and 350 µl acetonitrile was added to precipitate the

proteins. The mixture was vortexed and centrifuged at a speed of 8000 rpm during 10 min at 10 °C. The supernatant was dried and redissolved in 50 µl MilliQ and 3 µl was injected on to the SPE cartridge. An external binary HPLC pump (Gynkotek, Munich, Germany) and an external Agilent 1200, 2/6 switch valve (Agilent Technology, Santa Clara. CA, USA) were used for the SPE sample trapping. The samples were trapped on a Hysphere Resin C8, endcapped, 10 x 4 mm, 10 µm SPE cartridge (Spark Holland B.V, Emmen, The Netherlands). Prior to injection, the SPE cartridge was conditioned with 50mM ammonium acetate buffer pH 9.0, after the injection the sample was trapped with 10mM ammonium acetate buffer pH 9.0/ACN (4:1 v/v) during 1 min with a flow of 0.4 $ml.min^{-1}$. Subsequently, the valve was switched placing the SPE cartridge in-line with the LC system for elution onto the analytical column. Elution of 5-OH-DPAT and its internal standard was accomplished by flushing the SPE column with H_2O/ACN (1:9 v/v) during 4 min with a flow of 0.05 $ml.min^{-1}$ and 1 min with 1 $ml.min^{-1}$. Finally, the cartridge was switched off-line again and re-conditioned using a 50mM ammonium acetate buffer at pH 9.0 during 2 min with a flow of 1 $ml.min^{-1}$. To analyze the extracted sample an Agilent 1200 HPLC system with autosampler (Agilent Technology, Santa Clara. CA, USA) was coupled online with an Agilent 6460 Triple Quadrupole mass spectrometer (Agilent Technology, Santa Clara. CA, USA). The samples were analyzed by µPLC-MS/MS using an Altima HP C18 column (150X 1.0 mm; 5 µm) (Grace Davison Discovery Sciences, Lokeren, Belgium). The mobile phase consisted of 10 mM ammonium acetate buffer pH 3.7: Acetonitril (2.3:1 v/v) was used. The total analysis time was 11 min, the flow-rate was 100 $\mu l.min^{-1}$, the temperature of the autosample tray was set to 4 ºC and the column temperature was set to room temperature. The detection was performed with a triple quadrupole mass spectrometer in the positive-ion electrospray mode and all analytes were monitored with Multiple Reaction Monitoring (MRM). 5-OH-DPAT and the internal standard d_2-5-OH-DPAT were ionized to produce the protonated molecules at m/z 248 and m/z 250, respectively. Upon collision (collision energy 15 eV; fragmentor enenergy 120 V) the pre-cursor ions of both of 5-OH-DPAT and d_2-5-OH-DPAT produced the same product-ion at m/z 147, corresponding to 5-hydroxy-aminotetraline. System operation and handling the acquired data was performed using Agilent MassHunter data acquisition software (version, B.02.00; Agilent). Calibration curves showed a linear response when using concentrations of compounds between 0.2 and 50 $ng.ml^{-1}$ (R^2>0.999). The recovery, limit of detection (LOD) and limit of quantification (LOQ) were experimentally determined at 93.9 ± 2.9 %, 0.07 and 0.2 $ng.ml^{-1}$, respectively.

2.7.2 Microdialysate samples of (S)-5-OH-DPAT

To analyze the striatal 5-OH-DPAT concentration the dialysate from the probe in the right striatum was collected every 15 min, resulting in a total volume of 30 µL per sample. Subsequently, 70 µL of a 7.15 nM solution of (R)-d_2-5-OH-DPAT as internal standard was added to yield final concentrations of 5 nM internal standard in a 100 µL mixture of water + 0.1% formic acid and Ringer (1:1). The solution was analyzed using LC-MS/MS. The HPLC system consisted of a Shimadzu LC 20 AD binary system with a Shimadzu SIL 20AC autosampler. The samples were injected on a Grace Alltech Alltima HP C18 EPS reverse-phased column (3 µm, length 150 x 2.1 mm I.D.) (Grace Alltech, Lokeren, Belgium). The mobile phase consisted of a mixture of 0.1% formic acid in water (solvent A) and 0.1% formic acid in acetonitrile (solvent B). The gradient was programmed as follows: 1 minute isocratically at 15% B, increase in 7.5 min to 95% B, 2.5 min isocratically at 95% B, decrease in 1 minute to 15% B and isocratically for 5 min at 15% B. The total runtime was 17 min. The flow was set at 0.4 $mL.min^{-1}$ and the analysis was performed at room temperature. The injection volume was 20 µL (partial loop fill) and the compounds were detected on a SCIEX API3000 triple quadrupole mass spectrometer (Applied Biosystems/MDS SCIEX, Foster City, CA, USA) equipped with a Turbo Ion Spray interface. The mass spectrometer was operated in the positive ion mode with MRM, quantifying transition pairs of m/z 248.2/147.1 and 250.2/147.1 for 5-OH-DPAT and d_2-5-OH-DPAT, respectively. Instrument parameters were as follows: Ion spray voltage 5000 V, nebulizer gas 13, curtain gas 13, TIST (Turbo Ion Spray Temperature) 500 °C, collision activated dissociation (CAD) gas 4, declustering potential (DP)=35 V, focusing potential (FP)=130 V, entrance potential (EP)=10 V. The detection limit of 5-OH-DPAT was 1 fmol which is 0.25 pg (5×10^{-11} M, 20 µL injection volume).

2.7.3 Striatal concentration of dopamine (DA) and metabolites

The dialysate contents of dopamine (DA) and its metabolites were quantified from the probe implanted at the left striatum by an on-line HPLC with electrochemical detection with the detection limit of 1 fmol/sample. A HPLC pump (LC-10AD vp, Shimadzu, Kyoto, Japan) was used in conjunction with an analytical cell (5011A, ESA, Chelmsford, MA, USA) and a electrochemical detector (Coulochem II, ESA, Chelmsford, MA, USA) working at +300 mV for DOPAC and HIAA and -300 mV for DA. The analytical column was a Supelco Supelcosil™ LC-18-DB column (150 mm x 4.6 mm, 3 µm) (Sigma-Aldrich Chemie B.V., Zwijndrecht, The Netherlands). The mobile phase consisted of a mixture of 4.1 g.L-1 sodium acetate (Merck), 215

mg.L^{-1} octane sulphonic acid, 186 mg.L^{-1} EDTA, 7% methanol and ultrapure water (pH=4.2 with glacial acetic acid). Data were converted into percentage of basal levels. The basal levels were determined from four consecutive samples (less than 20% variation), and set to 100%. After the experiments the rats were sacrificed and the brains were removed. The brains were kept in 4% paraformaldehyde solution until they were sectioned to control the location of the dialysis probes.

2.8 Data analysis

A non-linear mixed effects modeling approach was used to describe the pharmacokinetics of (S)-5-OH-DPAT in plasma and the dopamine levels (PD endpoint) in the striatum. The *in vivo* data following transdermal and IV infusion were combined for analysis.

2.8.1 PK model

A detailed description of the pharmacokinetic model for (S)-5-OH-DPAT has been reported elsewhere [7]. Briefly, the PK model is based on compartmental mass transfer to describe the iontophoretic transport *in vivo*. Data fitting was performed according to the ordinary differential equations 1, 2 and 3 for transdermal iontophoretic delivery:

$$\frac{dX_1(t)}{dt} = I_0.N - K_R.X_1(t) \quad (1)$$

$$\frac{dX_2(t)}{dt} = K_R.X_1(t) - k.X_2(t) - k_{23}.X_2(t) + k_{32}.X_3(t) \quad (2)$$

$$\frac{dX_3(t)}{dt} = k_{23}.X_2(t) - k_{32}.X_3(t) \quad (3)$$

With $\frac{dX_i(t)}{dt}$ as the rate of change in the amount of the drug in compartment *i*, X_i as the amount of the drug in compartment *i*, which refers to the skin compartment (*i*=1), the plasma compartment (*i*=2) and the peripheral compartment (*i*=3). I_0 is defined as the zero order mass input during iontophoresis, K_R as the first order release rate constant from skin to plasma, *k* as the first order elimination rate constant, k_{23} and k_{32} as the first order distribution rate constants from plasma to tissue and tissue to plasma, respectively. N is a flag in the model to indicate that the input rate I_0 is only valid during the iontophoresis period.

Following intravenous administration, data was modeled using Equation 4, which describes the rate of change in amount of the drug in the plasma compartment:

$$\frac{dX_2(t)}{dt} = Rate.M - k.X_2(t) - k_{23}.X_2(t) + k_{32}.X_3(t) \tag{4}$$

With *Rate* as the zero order intravenous infusion rate and *M* as a flag to indicate that the *Rate* only applies during the duration of the infusion. Equation 3 was used to describe the rate of change in the peripheral compartment.

2.8.2 PD model

Two PD models were compared to fit the data of the dopamine release in the striatum during and after transdermal iontophoresis and intravenous infusion. The first model was the indirect response (IDR) type I model in analogy to the model proposed by Nugroho *et al.* [7]. The levels of 5-OH-DPAT in the plasma (C_p) were directly linked to the dopaminergic effect. The equations of the model to describe the rate of change in the dopamine concentration $\frac{dC_{DA}(t)}{dt}$ in the striatum:

$$\frac{dC_{DA}(t)}{dt} = k_{in}^0.\left(1 - \frac{I_{\max}.C_p(t)^H}{IC_{50} + C_p(t)^H}\right) - k_{out}.C_{DA}(t) \tag{5}$$

$$k_{in}^0 = k_{out}.C_{DA}(0) \tag{6}$$

With I_{max} as the maximum inhibition of the dopamine production, IC_{50} is the plasma concentration of 5-OH-DPAT at which 50% of maximum inhibition is observed, *H* is the slope of the curve (Hill coefficient), k^0_{in} is the zero order rate constant for the production of response, k_{out} is the first order rate constant for the loss of response, $C_{DA}(0)$ is the baseline values of dopamine (i.e., dopamine concentration prior to the inhibiting effect of 5-OH-DPAT).

In the second model, an extra hypothetic compartment was introduced to account for the delay between plasma concentration and the response, i.e., the effect compartment. The rate of change of drug concentration $\frac{dC_e(t)}{dt}$ in the effect compartment can be described as follows:

$$\frac{dC_e(t)}{dt} = k_{e0}.\left(C_2(t) - C_e(t)\right) \tag{7}$$

With k_{e0} as the first order distribution rate constant from plasma to effect compartment and the elimination rate constant from the effect compartment. The effect is described by the sigmoid I_{max} model using the following equation:

$$C_{DA} = C_{DA}(0).\left(1 - \frac{I_{\max}.C_e(t)^H}{IC_{50}{}^H + C_e(t)^H}\right) \quad (8)$$

With C_e as the drug concentration in the effect compartment.

2.8.3 Model parameters

A detailed description of the PK and PD modeling steps is presented elsewhere [7]. In short, the data analysis was performed using NONMEM version VI (NONMEM project group, University of California, San Francisco, USA), using the ADVAN6 TRANS1 TOL=5 from PREDPP, as subroutines. The fixed effect parameters (θ) included: I_0, K_R, clearance (CL), inter compartmental clearance (Q), volume of the central compartment (V_2), volume of the peripheral compartment (V_3), k_{out}, I_{max}, IC_{50} and k_{e0}. Variability in pharmacokinetic parameters was assumed to be log-normally distributed in the population. Inter-individual variability was modeled by an exponential error model as written in Equation 9:

$$P_i = \theta.\exp(\eta_i) \quad (9)$$

in which θ is the population value for the fixed effect parameter P, P_i is the individual estimate and η_i is the normally distributed interindividual random variable with mean zero and variance ω^2. The coefficient of variation (CV %) of the structural model parameters is expressed as percentage of the root mean square of the interindividual variability term. The residual error was modeled by a proportional error model as written in Equation 10:

$$C_{obs,ij} = C_{pred,ij}.(1 + \varepsilon_{ij,1}) \quad (10)$$

where $C_{obs,ij}$ is the jth observed concentration in the ith individual, $C_{pred,ij}$ is the predicted concentration, and ε_{ij} is the normally distributed residual random variable with mean zero and variance σ^2. The estimation of the final population parameters was performed using the conventional first order estimation method (FOCE). The PK model parameters were estimated independently and subsequently used as input for the PD analysis. During model building, goodness-of-fit was based on statistical and graphical diagnostic criteria. Model selection and identification was based on the

likelihood ratio test, coefficient of variation of parameter estimates, parameter correlations and goodness-of-fit plots. For the likelihood ratio test, the significance level for the inclusion of one parameter was set at $p<0.05$, which corresponds with a decrease of 3.84 points in the minimum value of the objective function (MVOF) under the assumption that the difference in MVOF between two nested models is χ^2 distributed. Non-nested models are evaluated using the Aikaike Information Criterion (AIC), which is the MVOF plus two times the number of parameters. The following goodness-of-fit plots were subjected to visual inspection to detect systemic deviations from the model fits: individual observed versus population and individual predicted values. Finally, the performance of the population PK and PK-PD models were assessed by simulating 100 data sets with the final model parameter estimates. The evaluation of model performance also included visual predictive check (VPC), as implemented in Xpose 4 (R version 2.7.0, R-foundation) [16].

3 Results

Three series of *in vivo* experiments were conducted to investigate the controllability of transdermal iontophoresis and to explore the potential impact of delivery rate on the PK-PD relationship of (S)-5-OH-DPAT. In the first study, the influence of the current density on drug pharmacokinetics in plasma profile was assessed. Two current densities were applied consecutively for 2h (75 and 150 $\mu A.cm^{-2}$). In addition, (S)-5-OH-DPAT was administered as an IV infusion to the same animals to discriminate delivery-related properties from intrinsic pharmacokinetic properties. The crossover design also allowed higher precision of the parameter estimates. In the second study, the influence of the anesthetics, iontophoresis and blood sampling on the striatal dopamine level (PD endpoint) was investigated as a validation procedure for this experimental model. In the third study, the PK-PD relationship was investigated across a range of exposures, with maximum effects being attained for a short period followed by return of DA levels back to baseline conditions. For this reason, transdermal iontophoresis (250 $\mu A.cm^{-2}$) was applied up to 1.5h. In analogy to the first study presented above, (S)-5-OH-DPAT was also administered with IV infusion to enable separation of delivery-related properties from intrinsic pharmacokinetic properties.

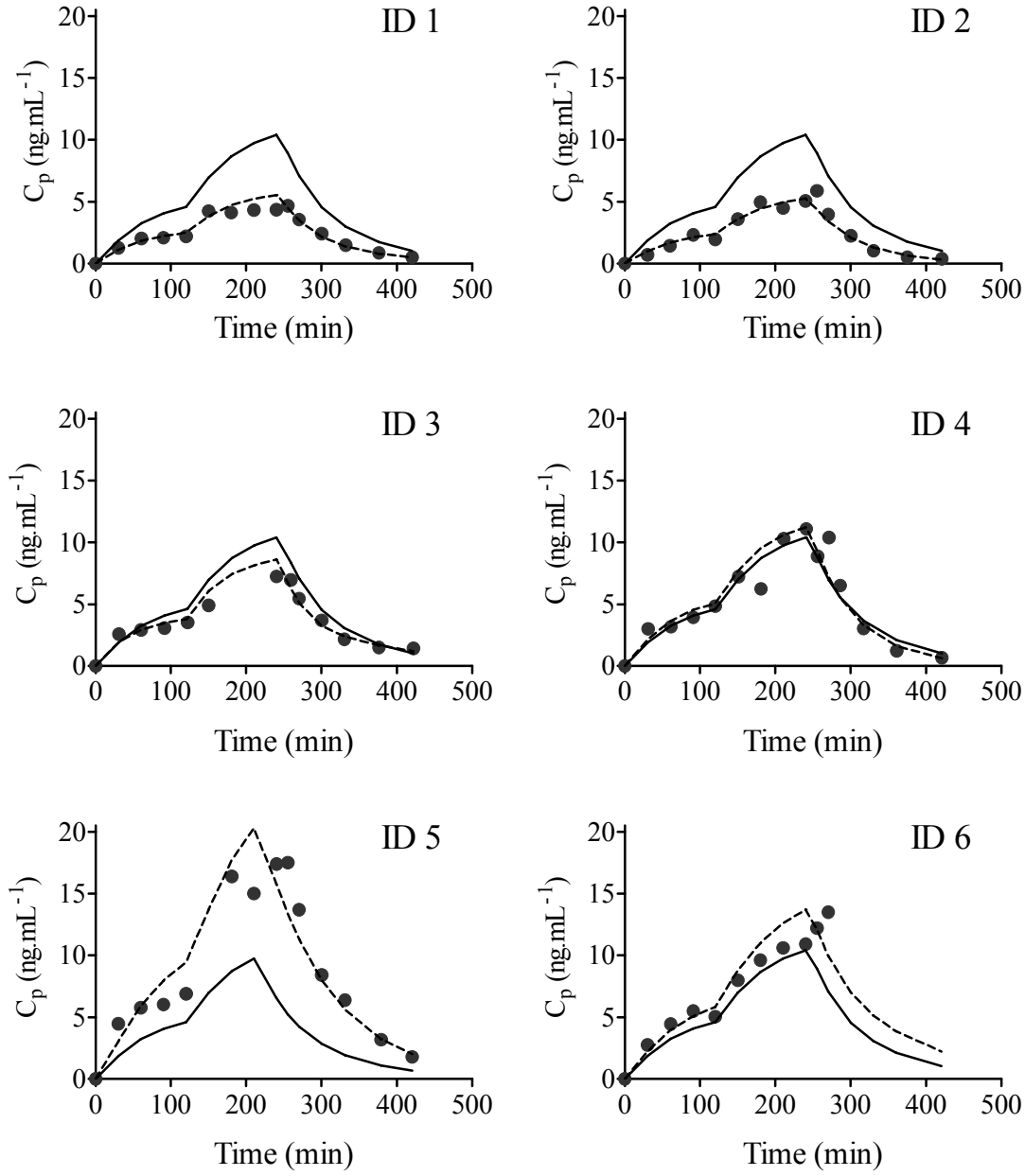

Figure 2: The observed data (filled circles) of the plasma concentration (C_p) of the individual rats during and after transdermal iontophoretic delivery of (S)-5-OH-DPAT (3.9 mM) together with the population model prediction (solid line) and the individual model prediction (dashed line). The following protocol was used: 120 min current density of 75 $\mu A.cm^{-2}$+ 120 min current density of 150 $\mu A.cm^{-2}$. The patch was removed after 240 min

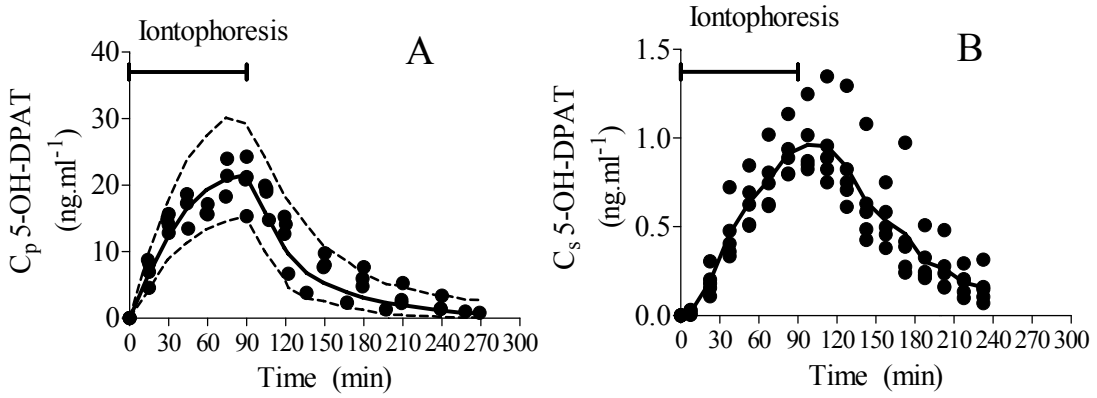

Figure 3: **A**: (S)-5-OH-DPAT concentration-time profiles in blood plasma following transdermal iontophoresis of (S)-5-OH-DPAT (3.9 mM). Depicted are the observed data (filled circles) together with simulated median (50%, solid line) and the upper and lower limit of the model-simulated interquantile concentration range (97.5%-5%, dashed lines).
B: (S)-5-OH-DPAT concentration-time profiles in striatum following transdermal iontophoresis of (S)-5-OH-DPAT (3.9 mM). Depicted are the observed data together with the mean.

3.1 PK properties following iontophoresis and IV infusion

In these studies two different current densities (75 and 150 μA.cm^{-2}) were applied consecutively during 2h to investigate the impact of flux on plasma profiles. Moreover it was of interest to determine the time to reach steady state conditions. The results of the pharmacokinetic studies are depicted in Figure 2. After 15 min of passive diffusion prior to iontophoresis no detectable amount was transported into the plasma (data not shown). In contrast, drug plasma levels increase immediately when switching on the current. In almost all the animals steady state plasma levels were achieved after 2h of 75 μA.cm^{-2} current application, with an average plasma concentration (C_p) of 4.1 ± 1.9 ng.ml^{-1}. By further increasing the current density to 150 μA.cm^{-2}, C_p increased to 9.4 ± 4.8 ng.ml^{-1} after 2h approximately. In parallel, following IV infusion, C_p reached a maximum of 5.3 ± 0.5 ng.ml^{-1} after 15 min (data

not shown). After the discontinuation of infusion or upon termination of the current application, the C_p declined according to a 2-compartment disposition model.

3.2 Validation of the rat model to investigate the PD effect

The potential effects of anaesthesia (fentanyl+fluanisone and midazolam), of blood sampling and of transdermal iontophoresis on the striatal levels of dopamine (PD end-point) were investigated. The results of this control experiment are presented in Figure 4A. Dopamine levels remained stable in the period immediately before attaching the patch (-60 to -15 min) and in the 15 minute period of passive diffusion before iontophoresis (-15 to 0 min). The DA levels, which were set to 100% showed a non-significant small increase from 97 ± 3% to 100 ± 4% during iontophoresis, followed by a stronger increase to 114 ± 6% during 115 min after the end of iontophoresis. These results indicate the suitability of the anesthetized rat model for monitoring of DA levels to evaluate the properties of transdermal iontophoretic delivery or IV infusion of (S)-5-OH-DPAT.

3.3 PK-PD relationships following iontophoresis and IV infusion

The pharmacokinetics and pharmacodynamics of (S)-5-OH-DPAT were assessed following transdermal iontophoresis and IV infusion. With regard to the PK, no detectable plasma concentration could be observed after 15 min passive diffusion (data not shown). When starting the current application (250 $\mu A.cm^{-2}$) the plasma concentration increased immediately and tended towards steady state after 90 min of current application (Figure 3A). The average concentration after 90 min of iontophoresis was 20.4 ± 3.7 $ng.ml^{-1}$. Following IV infusion, C_p reached a maximum of 29.9 ± 2.4 $ng.ml^{-1}$ after 10 min (data not shown). The decline in plasma concentration post (S)-5-OH-DPAT administration was best described by a 2-compartment disposition model. Following transdermal iontophoresis, (S)-5-OH-DPAT concentrations in the striatum were also monitored. As shown in Figure 3B, 5-OH-DPAT concentrations increased to 0.96 ± 0.18 $ng.ml^{-1}$ during current application, but this effect occurred after a small delay (between 7.5 and 22.5 min) in relation to the beginning of iontophoresis. The concentrations decreased again with the same delay upon discontinuation of the iontophoretic current.

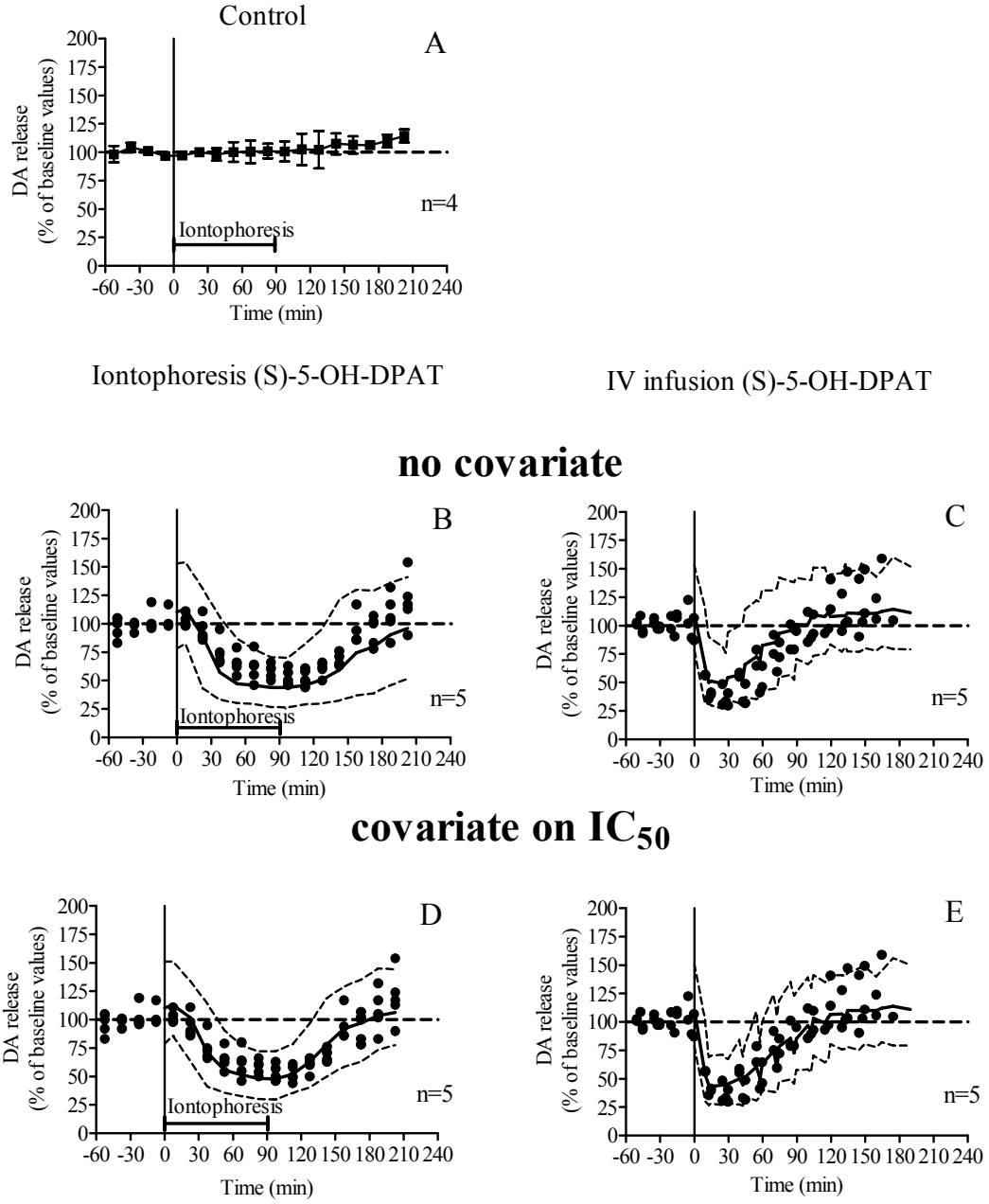

Figure 4: The dopamine release, expressed as % of baseline *vs* time. **A**: transdermal iontophoresis of only buffer (control experiment) **B, D**: transdermal iontophoresis of (S)-5-OH-DPAT (3.9mM).**C, E**: IV infusion of (S)-5-OH-DPAT (113 µM).
A: depicted is the mean ± SD. **B-E**: depicted are the observations (filled circles) together with the model simulated interquantile DA% range (2.5 %-97.5%, dashed lines) and the simulated median (50%, solid line). A number of 100 samples were simulated based on the final parameter estimates.
B, **C**: the visual predictive check without including a covariate of route of administration on IC_{50}. **D**, **E**: the visual predictive check including a covariate of route of administration on IC_{50}. In all panels the average dopamine release of 4 consecutive points prior to administration (time=-60 to -15 min) was set to 100%.

Table 1: The population estimates obtained from fitting the plasma profile and/or the pharmacological response following transdermal iontophoresis. During the PK study, two different current densities (75 and 150 µA.cm^{-2}) were applied consecutively for 2h. During the PK-PD study, a current density of 250 µA.cm^{-2} was applied for 1.5h.

		PK study				**PK-PD study**			
		Estimate		**Between animal variabity**		**Estimate**		**Between animal variabity**	
parameter	unit	mean	RSE %	mean	RSE %	mean	RSE %	mean	RSE %
V_2	L	0.5	6			0.5	18	0.100	71
V_3	L	1.7	16	0.189	46	0.7	16	0.109	42
CL	L.h^{-1}	2.6	13	0.194	45	2.0	6	0.027	29
Q	L.h^{-1}	2.5	9			1.9	23	0.218	44
J_{ss} 75	nmol.cm^{-2}.h^{-1}	24.7	29						
J_{ss} 150	nmol.cm^{-2}.h^{-1}	51.3	30						
J_{ss} 250	nmol.cm^{-2}.h^{-1}					87.3	8	0.000	/
K_R	h^{-1}	2.2	21			5.5	26	0.000	/
k_{e0}	h^{-1}					3.9	10	0.192	77
IC_{50} IONTO	ng.ml^{-1}					4.4	13	0.162	50
IC_{50} IV	ng.ml^{-1}					1.9	11		
N						3.2	10	0.000	/
I_{MAX}	DA%					41.6	8	0.045	36
Sigma PK		0.037	12			0.0246	20		
Sigma PD						0.0120	22		

The striatal dopamine release (PD endpoint) was monitored on-line simultaneously with plasma and striatal concentrations of (S)-5-OH-DPAT. These results are presented in Figure 4. Firstly, the pharmacodynamic effect was monitored following iontophoresis (15 min passive diffusion + 90 min of iontophoresis 250 $\mu A.cm^{-2}$) (Figure 4B). During passive diffusion (-15 to 0 min) no change in DA levels were observed. Subsequently, dopamine levels gradually decreased to a minimum of 48.8 ± 5.1% of basal values within 94.5 ± 16.4 min after the start of the iontophoresis. DA levels returned to baseline values within 79.4 ± 11.3 min after the end of iontophoresis. In contrast, IV infusion of (S)-5-OH-DPAT resulted in an immediate decrease in the DA level. Maximum inhibition of 38.3 ± 8.4 % relative to baseline values was achieved after 42.1 ± 2.5 min (t_{max}) after start of IV infusion (Figure 4C). DA levels returned to baseline values within 120.4 ± 20.5 min after the end of infusion. A slight rebound effect was observed at the end of the experiment. DA level further increased to 119 ± 22 and 120 ± 23% relative to baseline after transdermal delivery and IV infusion, respectively.

3.4 PK-PD analysis following transdermal iontophoretic delivery and IV infusion

The pharmacokinetic data following transdermal iontophoresis was analyzed simultaneously with the PK data following intravenous infusion. The objective of the integrated analysis was to facilitate discrimination between delivery-specific parameters (I_0, K_R) and drug-specific parameters (V_2, V_3, CL, Q). The larger sample size also allowed for more precise estimation of model parameters. The resulting parameters are provided in Table 1. The low relative standard error (RSE) for all the fixed effect parameters (RSE ≤ 30%) indicates high precision of estimates. Moreover, as observed in Figure 2 and in Figure 5A, the model accurately describes the time course of plasma concentration during and after current application.

An integrated approach was also applied to the PK-PD experiments. The analysis of the PK PD data following IV administration and iontophoresis was performed simultaneously. In analogy to the PK study, the plasma concentration profile could be described by the proposed compartmental model. In Figure 3A, the VPC depicts the goodness of fit, with observed data randomly distributed within the 95% confidence interval (C.I.). In addition, the diagnostic plots (Figure 5B) show a good correlation between the observed and predicted C_p.

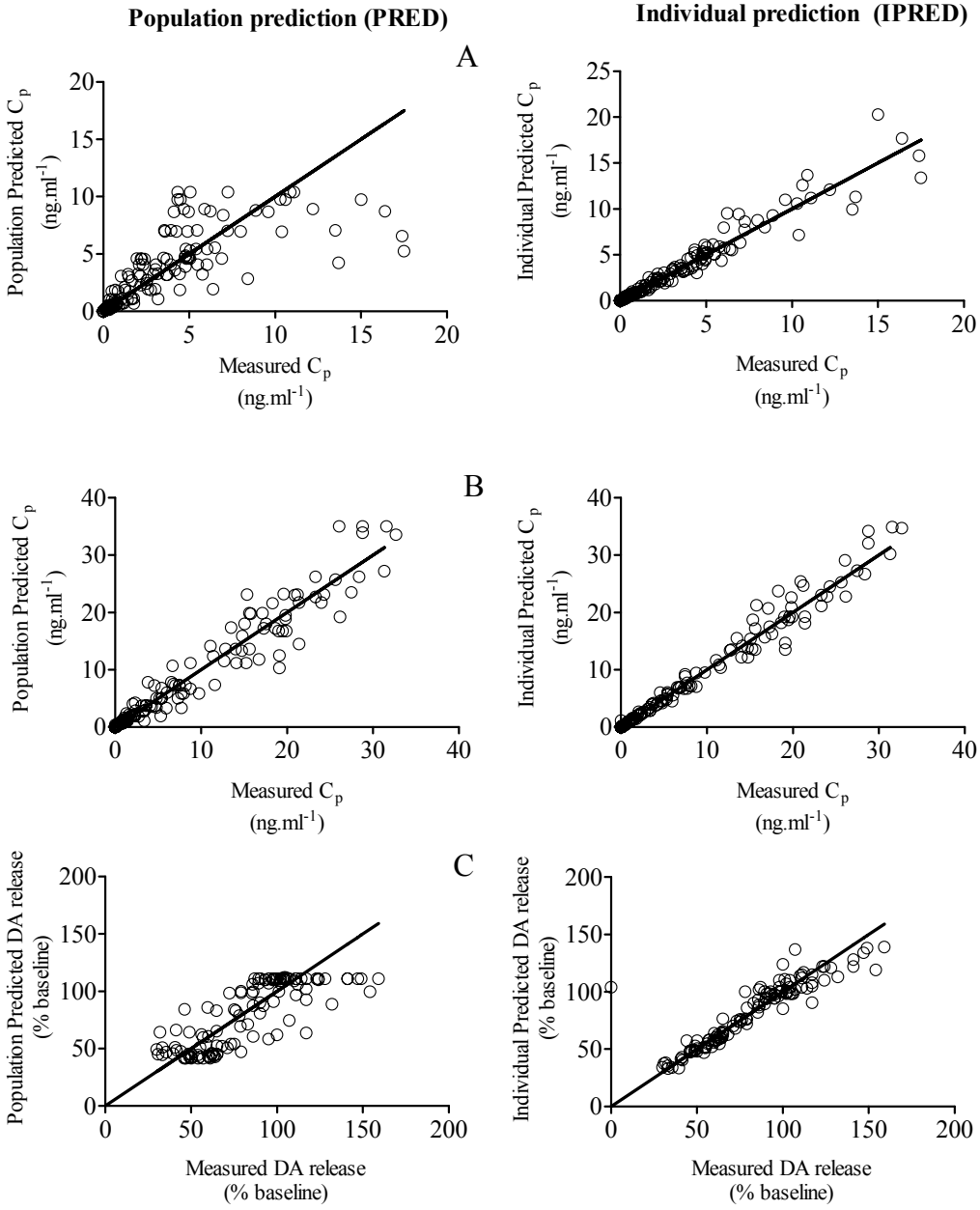

Figure 5: Diagnostic plots of the plasma and striatum analysis using the integrated PK-PD model. **A**: Analysis of plasma concentration (C_p) of (S)-5-OH-DPAT following IV infusion and iontophoresis during the PK study. **B**: Analysis of plasma concentration (C_p) of (S)-5-OH-DPAT following IV infusion and iontophoresis during the microdialysis study. **C**: Analysis of dopamine (DA) release in striatum, expressed as % of baseline values, following IV infusion and iontophoresis. In every panel the population prediction (left graph) and individual prediction (right graph) *vs* the measured value is displayed.

The effect of (S)-5-OH-DPAT (striatal dopamine release) was assessed by two pharmacodynamic models. The first model consisted of a turnover model, i.e., with indirect response type I [14], and the second model consisted of an effect compartment and a sigmoid I_{max} model [13]. The AIC of the effect compartment model was lower than the turnover model. In addition, an improved distribution of the observations in the 95% C.I. of the VPC and a lower residual standard error (RSE) of the parameter estimates were observed when fitting the data with the effect compartment model (comparison not shown). Therefore the effect compartment model was selected for further evaluation of the PK-PD relationship of (S)-5-OH-DPAT. Given the small bias observed in the simulated median profiles of DA (Figure 4B and 4C), a covariate analysis was performed, which revealed differences in IC_{50} depending upon the administration route. Incorporation of the route of administration as covariate into the model improved the VPC (Figure 4D and 4E) and the objective function decreased significantly (χ^2-test; $p<0.05$). The resulting parameters are summarized in Table 1. PK and PD parameters were estimated with good precision, as indicated by a relatively low RSE of the parameters (≤26 %).

Figure 4D and 4E depict the 95 C.I. together with the simulated median response when including route of administration as covariate in the model. It can be observed that the model slightly under- and overpredicts the median of the DA release following transdermal iontophoresis and IV infusion, respectively. Nonetheless, 95% of the observations can be found within the boundaries of the confidence interval. Finally, goodness-of-fit plots for the dopamine release (Figure 5C) show that the model accurately predicts the observed DA release for both administration routes.

4 Discussion

The present study provides novel information on the pharmacokinetic and pharmacodynamic properties of the active enantiomer of the potent dopamine agonist (S)-5-OH-DPAT. Specifically, the present investigation focused on the controllability of the transdermal iontophoretic delivery of this compound with regard to the plasma concentration and the dopaminergic activity in the striatum.

4.1 Relationship between current density and plasma profile

With regard to the controllability of the plasma concentration, the relationship between the applied current density and the corresponding plasma profile was investigated. Three different current densities (75, 150 and 250 $\mu A.cm^{-2}$) were applied in 2 different studies. A comparison of the pharmacokinetic parameters of

the PK-study (using two current densities 75, 150 μA.cm^{-2}) and the PK-PD study (applying 250 μA.cm^{-2}) revealed a difference in peripheral volume of distribution (V_3), central (CL) and peripheral clearance (Q). The difference in these pharmacokinetic parameters can be attributed to the difference in recovery period after surgery of the animals in the two studies, rather than due to differences in transport/delivery. For the PK-studies, the animals were allowed to recover for at least 1 week, whereas the PK-PD studies were executed 15-20h post surgery. Similar results were found by Torres-Molina and co-workers, who demonstrated that the placement of a permanent cannula in the jugular vein influences the PK parameters of amoxycilin and antipyrin in rats. The PK parameters depended on the time of execution of the experiment after placement of the cannula [17]. This should be taken into account when designing new experiments, especially with a cross-over design.

Despite the difference in PK parameters between the two studies, a clear linear dependency (R^2=0.999) was observed (Figure 6) between the applied current density and the *in vivo* steady state flux, calculated from the zero order mass input using the following equation [18]:

$$Flux_{ss} = \frac{I_0}{S} \tag{11}$$

In literature, similar results were reported for the iontophoretic delivery *in vivo* of hydromorphone and ropinirole [6, 19]. Moreover, Patel *et al.* recently demonstrated the controllability of the plasma concentration profiles by the current density for zolmitriptan [20]. These results show that, despite differences in PK properties, the drug input into the skin can be controlled very carefully by adjusting the current density. This can be very useful in initiating therapeutic treatment with dopamine agonist, adjusting the dose to the demand of the individual patient.

Based on this relationship between the *in vivo* flux and the current density, the *in vivo* flux, applying a current density of 500 μA.cm^{-2}, was estimated at 174.9 nmol.cm^{-2}.h^{-1}. Despite the interspecies differences, this value differs only 21% from the *in vitro* flux across human stratum corneum (211.9 ± 11.1 nmol.cm^{-2}.h^{-1}), when applying a current density of 500 μA.cm^{-2} [21]. This indicates that *in vitro* transport parameters can be used to predict drug delivery properties *in vivo*, even across species. Regarding the rat skin, iontophoretic transport is frequently comparable with human skin, in which iontophoresis may diminish interspecies variations in *in vitro* skin permeation studies [22-23].

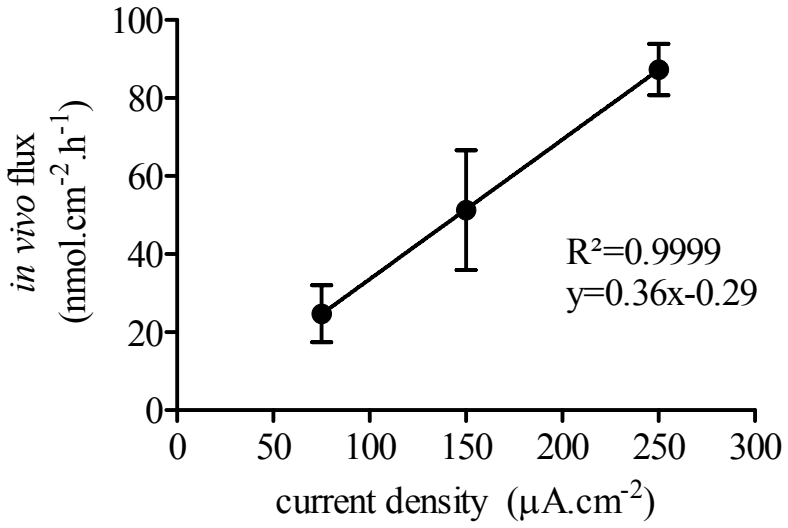

Figure 6: *In vivo* flux *vs* current density. Each data point represents the parameter estimate, determined with compartmental modeling, with the standard error of the parameter estimate. In each experiment 4-6 rats were used.

Our findings suggest the possibility of further refinement of future experiments for the evaluation of drug delivery by iontophoresis. In fact, a model-based approach can be used to to provide guidance for optimal sampling and dose selection as well as by allowing a more quantitative assessment of safety margins. This is one of the reasons why PK-PD modeling is gaining a more prominent place in the different stages of drug development [24].

4.2 PK-PD relationship

Next to a controlled plasma concentration the second aim of our investigation was to characterize the PK-PD relationship of (S)-5-OH-DPAT. A previous study showed that 5-OH-DPAT, administered with transdermal iontophoresis can cause a very strong pharmacodynamic effect. However it was observed that even after 3h post-iontophoresis the dopamine level (PD end-point) did not recover to its initial state [7]. In addition, during these studies choral hydrate was used as anesthetic [7]. Chloral hydrate is not considered the optimal choice for anesthesia of small animals,

like rodents. Moreover several studies showed that choral hydrate influences the striatal DA turnover [25-27] and enhances the suppressive effects of several DA agonists [28]. Therefore our studies were performed following IV infusion and iontophoresis to explore the implications and validate the use of new anesthetic procedures in conjunction with on-line brain microdialysis [10-11]. In addition, we assessed the PK-PD relationship under a wider range of exposures, ensuring reversibility of the PD effect.

A mixture of fentanyl, fluanisone and midazolam was chosen to anesthetize the animals. However, it has been reported in literature that these anesthetics individually also can affect the striatal DA metabolism. Fentanyl and fluanisone can increase the DA turnover in the striatum [29-31], while midazolam has been reported to decrease the DA levels in a dose dependent manner [32]. Besides the effect of the combination of anesthetics, the effect of iontophoresis and blood sampling on the dopamine level was also investigated. As shown in Figure 4A, the stimulating effect of fentanyl and fluanisone and the inhibiting effect of midazolam on the dopamine release were balanced during iontophoresis. After iontophoresis the dopamine release increased slightly, which could indicate a dominating effect of fentanyl. Nonetheless a rat model was established with stable dopamine release levels during anesthesia, which enabled us to investigate the dopaminergic effect of (S)-5-OH-DPAT following intravenous infusion and transdermal iontophoresis.

For both administration routes a decrease in striatal DA level can be observed which returns to baseline within 2h after ending the administration. This demonstrates that a controlled reversible effect can be obtained. Moreover, DA levels seem to reach steady state following transdermal iontophoresis, in parallel to time course of concentrations in plasma. These results suggest that steady state concentrations of (S)-5-OH-DPAT translate into a steady state decrease of the dopamine level. Given that dopamine synthesis is indirectly controlled by presynaptic dopamine receptors, these findings suggest a continuous stimulation of the dopamine receptors [33-34]. Likewise, it has been shown that stable plasma levels of rotigotine, another potent 2-aminotetralin, also result into continuous dopaminergic stimulation [35]. This could be of great benefit for symptomatic treatment of Parkinson's disease. It is generally believed that continuous dopaminergic stimulation is currently the best strategy to reduce motor complications after long-term use of dopaminergic agents [5]. However, further investigations are required applying current for a longer time period with different doses to confirm the applicability of transdermal iontophoresis of dopamine agonists like (S)-5-OH-DPAT.

4.3 PK-PD modeling

The plasma profile and the DA release following IV infusion and transdermal iontophoresis were analyzed using compartmental modeling. Plotting the DA release *vs* the plasma concentration showed a counter clock-wise hysteresis (data not shown). This indicates a time delay between the plasma concentration and the pharmacological response. To account for this delay an effect compartment model [13] was compared with an indirect response model type I [14]. In the present study, it is shown that the DA release is best described by an effect compartment in conjunction with the sigmoidal I_{max} model. This suggests that the delay between plasma concentration and pharmacological response is attributed to the distribution from plasma to site of action, rather than because of a slow onset of the effect. This is further supported by the delayed increase in striatal 5-OH-DPAT concentration following transdermal iontophoresis in Figure 3B. These findings shed light into the mechanisms underlying delay reported by Nugroho *et al.*, who described the DA release, following transdermal iontophoresis of 5-OH-DPAT with an indirect response model type I [7].

As observed in Table 1, the IC_{50} is approximately 2.3 times lower when administering (S)-5-OH-DAT with IV infusion compared to the IC_{50} with transdermal administration. This raises an important question regarding the role of the delivery rate: Do differences in delivery rate alter the response profiles of (S)-5-OH-DPAT? This question can be addressed by estimating the pharmacodynamic efficiency (EFF), defined as the pharmacological response per unit of concentration, as shown in the following equation:

$$EFF = \frac{AAEC}{AUC} \tag{12}$$

Where AUC ($ng.ml^{-1}.min$) is the area under the plasma 5-OH-DPAT concentration curve and AAEC (DA%.min) is the area above the effect curve (normalized for baseline dopamine levels). For the IV infusion EFF was 9.2 ± 2.3 $ml.ng^{-1}$, which is approximately 1.9 ± 0.8 times higher than the EFF following transdermal iontophoresis, estimated at 4.8 ± 1.7 $ml.ng^{-1}$. Given that the delivery rate during IV infusion was approximately 3.5 times higher than during transdermal iontophoresis, these observations suggest that a high delivery rate may improve the pharmacodynamic efficiency. In this respect. transdermal iontophoresis can be a suitable delivery technique, since the delivery rate can easily be adjusted using different current densities (Figure 6). For instance a loading dose, by applying a higher current density at the start of the iontophoretic delivery, can be combined with

a maintenance dose, by gradually decreasing the current density to a certain level. Follow-up studies based on drug administration with different delivery rates should be performed to confirm these findings.

The use of an integrated PK-PD approach, simultaneously monitoring drug concentrations in plasma and pharmacodynamic effects, has several benefits over experimental designs in which C_p or the PD effect are evaluated independently. Firstly, it was shown that a steady state plasma concentration may result in a continuous stimulation of the dopamine receptor. Secondly, PK-PD modeling contributes to further understanding of the mechanisms and time course of drug action. Thirdly, PK-PD model parameters can be used to support the design of future experiments. Furthermore, the assessment of PK-PD relationships enables discrimination between delivery-specific and drug-specific parameters. This distinction is critical in drug delivery research, in that it warrants the identification of the factors which may ultimately determine treatment response *in vivo*.

In conclusion, these studies demonstrate that transdermal iontophoresis can be an excellent delivery route for continuous controlled administration of (S)-5-OH-DPAT and other potent dopamine agonists for the symptomatic treatment of Parkinson's disease. PK-PD modeling suggests that target distribution causes the delay between plasma concentration and drug effect. In addition, modulation of the delivery rate seems to have a direct impact on the pharmacodynamics. These results are very important for understanding of the mechanisms underlying drug transport and disposition following transdermal iontophoresis. This information will be crucial for designing a self-controlled delivery device, guided by a feedback system.

Acknowledgements

This research was financially supported by a grant (LKG 6507) of the Dutch Technology Foundation STW, Utrecht, The Netherlands. The authors thank D.J. Vandenberg from the Division of Pharmacology (Leiden/Amsterdam Center for Drug Research, The Netherlands) for the set-up and execution of the analysis of the plasma samples. The authors also acknowledge J.B. De Vries from the Department of biomonitoring and sensoring (University Center of Pharmacy, University of Groningen, The Netherlands) and S.G. Romeijn from the department of Drug Delivery Technology (Leiden/Amsterdam Center for Drug Research, The Netherlands) for their support with the animal studies.

References

1. Dixit, N., et al., *Iontophoresis - an approach for controlled drug delivery: a review.* Curr Drug Deliv, 2007. **4**(1): p. 1-10.
2. Tugwell, C., *Parkinson's disease in focus*. 1st ed. In focus. 2008, London: Pharmaceutical Press. 237.
3. Rajput, A.H., et al., *Clinical-pathological study of levodopa complications.* Mov Disord, 2002. **17**(2): p. 289-96.
4. Syed, N., et al., *Ten years' experience with enteral levodopa infusions for motor fluctuations in Parkinson's disease.* Mov Disord, 1998. **13**(2): p. 336-8.
5. Steiger, M., *Constant dopaminergic stimulation by transdermal delivery of dopaminergic drugs: a new treatment paradigm in Parkinson's disease.* Eur J Neurol, 2008. **15**(1): p. 6-15.
6. Luzardo-Alvarez, A., M.B. Delgado-Charro, and J. Blanco-Mendez, *In vivo iontophoretic administration of ropinirole hydrochloride.* J Pharm Sci, 2003. **92**(12): p. 2441-8.
7. Nugroho, A.K., et al., *Pharmacokinetics and pharmacodynamics analysis of transdermal iontophoresis of 5-OH-DPAT in rats: in vitro-in vivo correlation.* J Pharm Sci, 2006. **95**(7): p. 1570-85.
8. van der Geest, R., M. Danhof, and H.E. Bodde, *Iontophoretic delivery of apomorphine. I: In vitro optimization and validation.* Pharm Res, 1997. **14**(12): p. 1798-1803.
9. van der Geest, R., et al., *Iontophoretic delivery of apomorphine II: An in vivo study in patients with Parkinson's disease.* Pharm Res, 1997. **14**(12): p. 1804-1810.
10. Imperato, A. and G. Di Chiara, *Trans-striatal dialysis coupled to reverse phase high performance liquid chromatography with electrochemical detection: a new method for the study of the in vivo release of endogenous dopamine and metabolites.* J Neurosci, 1984. **4**(4): p. 966-77.
11. Westerink, B.H.C., *Monitoring molecules in the consious brain by microdialysis.* Trac-Trends Anal Chem, 1992. **11**: p. 176-182.
12. Wright, P.M., *Population based pharmacokinetic analysis: why do we need it; what is it; and what has it told us about anaesthetics?* Br J Anaesth, 1998. **80**(4): p. 488-501.
13. Holford, N.H. and L.B. Sheiner, *Understanding the dose-effect relationship: clinical application of pharmacokinetic-pharmacodynamic models.* Clin Pharmacokinet, 1981. **6**(6): p. 429-53.
14. Sharma, A. and W.J. Jusko, *Characterization of four basic models of indirect pharmacodynamic responses.* J Pharmacokinet Biopharm, 1996. **24**(6): p. 611-35.
15. Paxinos, G. and C. Watson, *The rat brain in sterotaxic coordinated. Academic Press: Sydney.* 1982.
16. Holford, N., *The Visual Predictive Check-Superiority to Standard Diagnostic (Rorschach) Plots.* PAGE 14, Abstr 738 [www.page-meeting.org/?abstract=738], 2005.
17. Torres-Molina, F., et al., *Influence of permanent cannulation of the jugular vein on pharmacokinetics of amoxycillin and antipyrine in the rat.* Pharm Res, 1992. **9**(12): p. 1587-91.
18. Nugroho, A.K., et al., *Compartmental modeling of transdermal iontophoretic transport II: in vivo model derivation and application.* Pharm Res, 2005. **22**(3): p. 335-46.
19. Padmanabhan, R., et al., *In vitro and in vivo evaluation of transdermal iontophoretic delivery of hydromorphone* J Control Release, 1990. **11**(1-3): p. 123-135.
20. Patel, S.R., et al., *Controlled non-invasive transdermal iontophoretic delivery of zolmitriptan hydrochloride in vitro and in vivo.* Eur J Pharm Biopharm, 2009. **72**(2): p. 304-9.

21. Ackaert, O.W., et al., *Mechanistic studies of the transdermal iontophoretic delivery of 5-OH-DPAT in vitro.* J Pharm Sci, 2010. **99**(1): p. 275-85.
22. Godin, B. and E. Touitou, *Transdermal skin delivery: predictions for humans from in vivo, ex vivo and animal models.* Adv Drug Deliv Rev, 2007. **59**(11): p. 1152-61.
23. Kanikkannan, N., J. Singh, and P. Ramarao, *In vitro transdermal iontophoretic transport of timolol maleate: effect of age and species.* J Control Release, 2001. **71**(1): p. 99-105.
24. Rajman, I., *PK/PD modelling and simulations: utility in drug development.* Drug Discov Today, 2008. **13**(7-8): p. 341-6.
25. Ford, A.P. and C.A. Marsden, *Influence of anaesthetics on rat striatal dopamine metabolism in vivo.* Brain Res, 1986. **379**(1): p. 162-6.
26. Westerink, B.H. and J. Korf, *Comparison of effects of drugs on dopamine metabolism in the substantia nigra and the corpus striatum of rat brain.* Eur J Pharmacol, 1976. **40**(1): p. 131-6.
27. Zhang, W., et al., *Repeated haloperidol administration changes basal release of striatal dopamine and subsequent response to haloperidol challenge.* Brain Res, 1989. **484**(1-2): p. 389-92.
28. Kelland, M.D., A.S. Freeman, and L.A. Chiodo, *Chloral hydrate anesthesia alters the responsiveness of identified midbrain dopamine neurons to dopamine agonist administration.* Synapse, 1989. **3**(1): p. 30-7.
29. Fregnan, G.B. and R. Porta, *A comparison between some biochemical and behavioural effects produced by neuroleptics.* Arzneimittelforschung, 1981. **31**(1): p. 70-4.
30. Freye, E. and K. Kuschinsky, *Effects of fentanyl and droperidol on the dopamine metabolism of the rat striatum.* Pharmacology, 1976. **14**(1): p. 1-7.
31. Milne, B., L. Quintin, and J.F. Pujol, *Fentanyl increases catecholamine oxidation current measured by in vivo voltammetry in the rat striatum.* Can J Anaesth, 1989. **36**(2): p. 155-9.
32. Takada, K., et al., *Effects of midazolam and flunitrazepam on the release of dopamine from rat striatum measured by in vivo microdialysis.* Br J Anaesth, 1993. **70**(2): p. 181-5.
33. Roth, R.H. and M.C. Nowycky, *Nonstriatal dopaminergic neurons: role of presynaptic receptors in the modulation of transmitter synthesis.* Adv Biochem Psychopharmacol, 1977. **16**: p. 465-70.
34. Westfall, T.C., et al., *The role of presynaptic receptors in the release and synthesis of 3H-dopamine by slices of rat striatum.* Naunyn Schmiedebergs Arch Pharmacol, 1976. **292**(3): p. 279-87.
35. Kehr, J., et al., *Continuous delivery of rotigotine decreases extracellular dopamine suggesting continuous receptor stimulation.* J Neural Transm, 2007. **114**(8): p. 1027-31.

Part III

Transdermal iontophoretic delivery of ester prodrugs of 5-OH-DPAT:

From synthesis to *in vivo* studies

7

The *in vitro* and *in vivo* evaluation of new synthesized prodrugs of 5-OH-DPAT for iontophoretic delivery

Oliver W. Ackaert[a*], Jeroen De Graan[c*], Romano Capancioni[a], Oscar E. Della Pasqua[b,e], Durk Dijkstra[c], Ben H. Westerink[d], Meindert Danhof[b] and Joke A. Bouwstra[a]

[a]Division of Drug Delivery Technology, Leiden/Amsterdam Center for Drug Research, Leiden, The Netherlands
[b]Division of Pharmacology, Leiden/Amsterdam Center for Drug Research, Leiden, The Netherlands
[c]Department of Medicinal Chemistry, University Center of Pharmacy, University of Groningen, Groningen, the Netherlands
[d]Department of biomonitoring and sensoring, University Center of Pharmacy, University of Groningen, Groningen, The Netherlands
[e]Clinical Pharmacology and Discovery Medicine, GlaxoSimthKline, Greenford, United Kingdom
[*]Contributed equally as first author

adapted from *Journal of controlled release.* 2010. *in press.*

Abstract

The feasibility of transdermal iontophoretic transport of 4 novel ester prodrugs of 5-OH-DPAT (glycine-, proline-, valine- and β-alanine-5-OH-DPAT) was investigated *in vitro* and *in viv*o. Based on the chemical stability of the prodrugs, the best candidates were selected for *in vitro* transport studies across human skin. The pharmacokinetics and pharmacodynamic effect of the prodrug with highest transport efficiency, was investigated in a rat model. The *in vitro* transport, plasma profile and pharmacological response were analyzed with compartmental modeling. Valine- and β-alanine-5-OH-DPAT were acceptably stable in the donor phase and showed a 4-fold and 14-fold increase in solubility compared to 5-OH-DPAT. Compared to 5-OH-DPAT, valine- and β-alanine-5-OH-DPAT were transported less and more efficiently across human skin, respectively. Despite a higher *in vitro* transport, lower plasma concentrations were observed following 1.5 h current application (250 $\mu A.cm^{-2}$) of β-alanine-(S)-5-OH-DPAT in comparison to (S)-5-OH-DPAT. However the prodrug showed higher plasma concentrations post-iontophoresis, explained by a delayed release due to hydrolysis and skin depot formation. This resulted in a pharmacological effect with the same maximum as 5-OH-DPAT, but the effect lasted for a longer time. The current findings suggest that β-alanine-5-OH-DPAT is a promising prodrug, with a good balance between stability, transport efficiency and enzymatic conversion.

Keywords: prodrugs, stability, iontophoresis, PK-PD

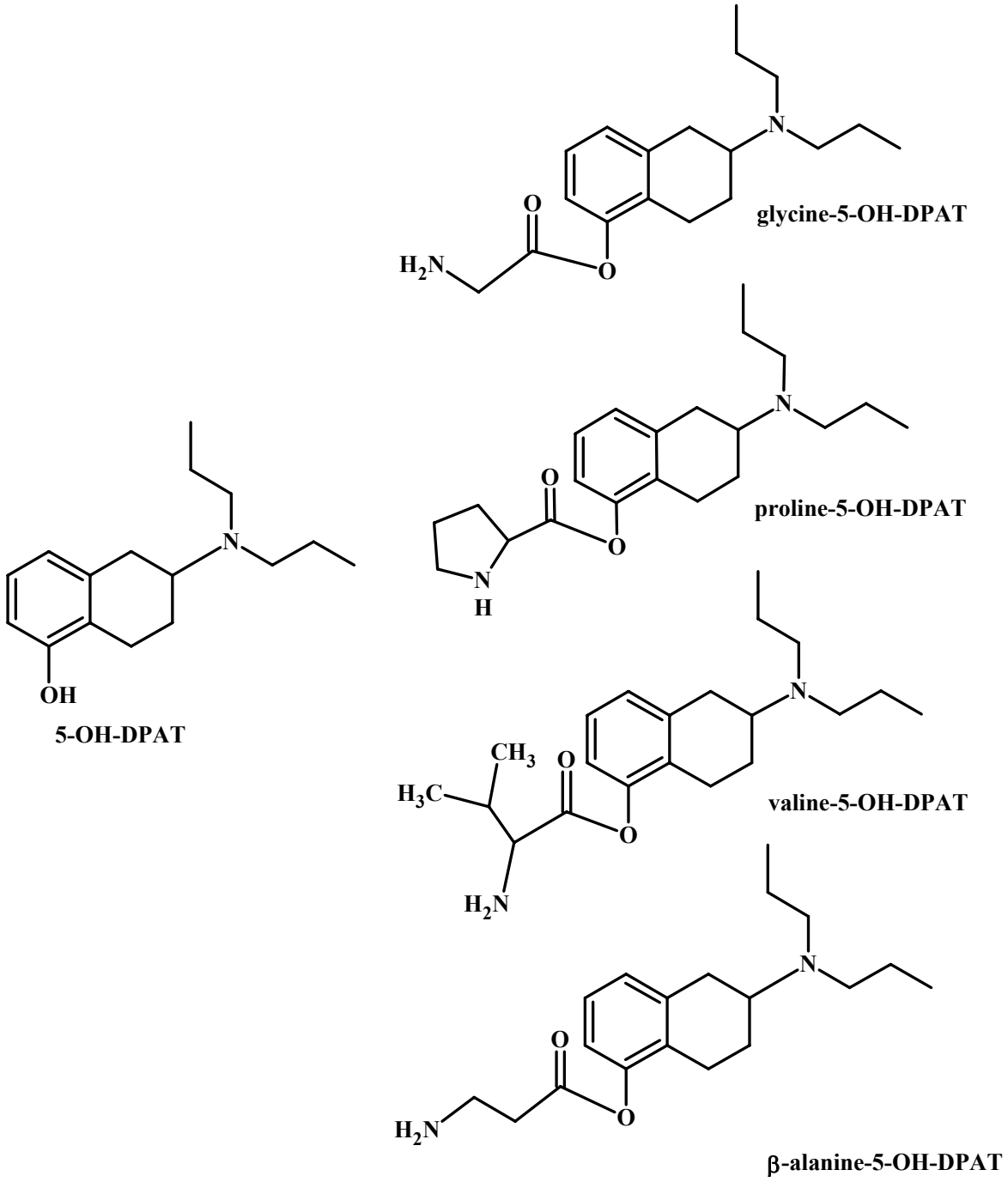

Figure 1: Molecular structure of 5-OH-DPAT and the 4 synthesized prodrugs, glycine-5-OH-DPAT, proline-5-OH-DPAT, valine-5-OH-DPAT and β-alanine-5-OHDPAT

1 Introduction

Transdermal delivery has been explored thoroughly as an alternative for oral delivery and injections. However, the main hurdle for transdermal delivery is the barrier function of the skin located in the outermost layer of the skin, the stratum corneum. An attractive approach to overcome this main barrier for drug delivery is iontophoresis. By applying a small current across the skin it is possible to enhance the transport of low molecular weight molecules across the skin. One of the interesting properties of this technique is the possibility to modulate the transport rate into and through the skin. This is an important advantage for drugs with a narrow therapeutic window, such as dopamine agonists (e.g. rotigotine, apomorphine, pergolide, 5-OH-DPAT). Most of the dopamine agonists are considered moderate lipophillic and have a relative low solubility in aqueous solutions [2-4]. For this reason, besides a low efficiency in iontophoretic transport, the low solubility of dopamine agonists can be a limitation for application with transdermal iontophoresis. Increasing the maximum solubility in the donor phase can be achieved by adjusting the donor phase (co-solvent, surfactant, source of Cl^--ions) or by changing the salt form. Another approach is the use of prodrugs with the desired physicochemical properties to overcome the problem of solubility and increase the efficiency in iontophoretic transport [5]. The principle goal of synthesizing prodrugs is to chemically modify an existing pharmacologically active drug in a form that can be reversed to the parent drug *in vivo*, with the aim to change the physicochemical and/or pharmacokinetic properties. Moreover for transdermal delivery a prodrug should be enzymatically metabolized in a controllable and predictable manner once it has penetrated the main barrier, the stratum corneum [6-8].

The main focus of the present study is to identify a prodrug that is transported efficiently with transdermal iontophoresis and is hydrolyzed during transport through the skin. This implies a good balance between the transport rate and the rate of enzymatic conversion of the prodrug. Previous studies showed that transdermal iontophoretic delivery of 5-OH-DPAT resulted in a strong pharmacological response, which is believed to meet the requirements for symptomatic therapy with a reasonable patch size and acceptable current density [1, 9]. However further improving the iontophoretic delivery could merely enhance the clinical applicability of this potent dopamine agonist by reduction of the patch size and more importantly minimization of the current density. Therefore 5-OH-DPAT, a dopamine agonist with limited aqueous solubility, was esterified with 4 different natural occurring amino acids (Figure 1). These amino acids contain an extra chargeable aminogroup, providing the possibility to investigate the influence of an additional charge on the

iontophoretic delivery of 5-OH-DPAT. The stability of these 4 prodrugs is investigated and the most stable compounds are selected for transdermal iontophoretic transport. Depending on the iontophoretic transport efficiency of the selected prodrugs *in vitro* across human stratum corneum and dermatomed human skin, the *in vivo* transport of the most promising candidate is further investigated. The plasma profile and the pharmacodynamic effect are monitored simultaneously in an animal model under anaesthetized conditions. Both *in vitro* and *in vivo* transport profiles are analyzed using compartmental modeling. Taking the hydrolysis of the prodrug into account, an adaptation to existing kinetic models is made to describe the transdermal iontophoretic delivery *in vivo* [1, 9].

2 Materials and Methods

2.1 General synthesis of the glycine, L-proline, β-alanine and L-valine esters of 5-OH-DPAT

The full description of the synthesis of the 4 prodrugs of 5-OH-DPAT is described elsewhere [10]. Briefly, 5-OH-DPAT was esterified to the N-protected amino acid with the carbodiimide coupling reagent N-(3-dimethylaminopropyl)-N'-ethylcarbodiimide (EDC). 1-Hydroxybenzotriazole (HOBt) was added to suppress racemisation. The deprotection of the Boc-protected compound was carried out in 4N HCl in dioxane. After removal of the solvent and evaporation *in vacuo*, the solid hygroscopic foams were reprecipitated from dry methanol with dry ether to remove excess dioxane. The prodrugs were obtained as white hygroscopic dihydrochloride salts with a purity of >95% (HPLC).

2.2 Materials

5-OH-DPAT and 5-hydroxy-2-(N-n-propyl-N-α,α-dideutero-propylamino)-tetralin (d_2-5-OH-DPAT) (HBr salts, purity >98%) were synthesized at the Department of Medicinal Chemistry of the University of Groningen, Groningen, the Netherlands. Silver, silver chloride (purity >99.99%), trypsin (Type III from bovine pancreas) and trypsin inhibitor (Type II-S from soybean) were obtained from Sigma-Aldrich (Zwijndrecht, The Netherlands). Acetaminophen was purchased from Brocacef BV (Maarssen, the Netherlands) and D-Mannitol was obtained from BDH Laboratory supplies (Poole, UK). Spectra/Por® RC dialysis membrane disks (cut off value of 6000-8000 Da) were purchased from Spectrum laboratories, Inc (Rancho Dominquez, Ca, USA). Tetrahydrofuran (THF, stabilized, purity >99.8%) was obtained from Biosolve (Valkenswaard, the Netherlands). Triethylamine (TEA,

purity >99%) was obtained from Acros Organics (Geel, Belgium). All other chemicals and solvents were of analytical grade. All solutions were prepared in Millipore water with a resistance of more than 18 MΩ.cm.

2.3 Stability of glycine-, proline-, valine- and β-alanine-5-OH-DPAT

The stability of the prodrugs was investigated under various conditions. At the starting point 1 $mg.ml^{-1}$ of proline- and glycine-5-OH-DPAT and 0.02 $mg.ml^{-1}$ of valine- and β-alanine-5-OH-DPAT were dissolved in the buffer solution. The buffer solution was citric buffer (5 mM, pH 5.0 + 4 $g.L^{-1}$ NaCl + 23.1 $g.L^{-1}$ D-mannitol), PBS pH 6.2 (NaCl: 8 $g.l^{-1}$, KCl: 0.19 $g.l^{-1}$, $Na_2HPO_4.2H_2O$: 0.43 $g.l^{-1}$, KH_2PO_4: 0.97 $g.l^{-1}$) or PBS pH 7.4 (NaCl: 8 $g.l^{-1}$, Na_2HPO_4: 2.86 $g.l^{-1}$, KH_2PO_4: 0.2 $g.l^{-1}$, KCl: 0.19 $g.l^{-1}$). The solutions were continuously stirred and kept constant at the desired temperature, using a thermostat controlled water bath. If required a circular sheet of human stratum corneum (HSC) (ø=18 mm) was added to the solution and a current of 320 µA was applied. At regular time intervals samples were taken from the solution and diluted in Millipore water, containing 0.1% trifluoroacetic acid [11] to stop degradation. Both the amount of remaining prodrug and the parent drug 5-OH-DPAT were quantified by RP-HPLC. The amount of remaining prodrug was plotted as a function of time to calculate the first order rate constant of hydrolysis and the corresponding half life.

2.4 Maximum solubility of valine-5-OH-DPAT and β-alanine-5-OH-DPAT

The solubility studies of the different compounds were carried out as described elsewhere [3]. Briefly, each compound was solubilized in citric buffer 5 mM, pH 5.0 + 4 $g.L^{-1}$ NaCl + 23.1 $g.L^{-1}$ D-mannitol. Subsequently the pH in each test tube was adjusted to pH 5.0 with 1M NaOH or 1M HCl under continuous shaking. Each solution was shaken for 48h, after which the solution was centrifuged and filtered. The concentration in each solution was determined with HPLC. Due to the limited availability of the compound and the relative high solubility, this assay was performed in monoplicate (n=1).

2.5 *In vitro* transport studies

The preparation of dermatomed human skin (DHS) and human stratum corneum was performed according to the method described previously [12]. All transport experiments were carried out as described elsewhere [12]. The donor formulation (citric buffer 5 mM, pH 5.0, NaCl: 4 $g.L^{-1}$, D-mannitol: 23.1 $g.L^{-1}$), containing the solute, was added to the anodal chamber. The cathodal chamber was filled with PBS

pH 7.4. Unless described differently, the acceptor phase, maintained at 32°C, was continuously perfused with PBS 7.4 at a flow rate of 7.0 $ml.h^{-1}$. The following protocol was used: 6h passive diffusion + 9h iontophoresis (500 $\mu A.cm^{-2}$) + 5h passive diffusion. Samples were collected every hour with an automatic fraction collector (ISCO Retriever IV, Beun De Ronde BV, Abcoude, The Netherlands). To stop the hydrolysis after transport through the skin and before analysis TFA (0.1% v/v) was added to each sample. The specific conditions of the individual transport studies are described below.

2.5.1 Iontophoretic delivery of valine-OH-DPAT and β-alanine-5-OH-DPAT

The iontophoretic delivery of valine-5-OH-DPAT across HSC and DHS was studied at a concentration of 3.9 mM.

Iontophoretic delivery of β-alanine-5-OH-DPAT across HSC was studied at 3 different concentrations (1.5 mM, 3.9 mM or 7.0 mM). For the transport study with 1.5 mM as donor phase the current was only applied for 7h, after which the experiment was stopped. Transport studies across DHS were performed with a donor concentration of 3.9 mM. For all experiments PBS pH 7.4 was used as acceptor phase.

2.5.2 Electroosmotic flux across HSC

The electroosmotic flux across HSC was investigated during iontophoretic transport of valine- and β-alanine-5-OH-DPAT (3.9 mM), buffered at pH 5.0. Acetaminophen (15 mM) was added to the donor phase as a marker for the electroosmosis. PBS pH 7.4 was used as acceptor phase.

2.6 Hydrolysis during transport across HSC and DHS

The prodrugs valine-5-OH-DPAT and β-alanine-5-OH-DPAT are expected to hydrolyze during transdermal transport. Although stratum corneum is considered as the main barrier of the skin, the majority of the enzymes, such as esterases can be found in the epidermis [13]. Therefore the hydrolysis of the prodrugs (donor conc: 3.9 mM) was determined during iontophoresis across HSC and DHS. In case of valine-5-OH-DPAT, PBS pH 6.2 was used as acceptor phase and for β-alanine-5-OH-DPAT PBS pH 7.4 was used. The remaining prodrug was determined in the acceptor phase every hour after transport, taking the degradation in the donor phase and acceptor phase into account.

2.7 PK-PD studies

In the following studies the pharmacokinetic (PK) and pharmacodynamic (PD) properties of β-ala-(S)-5-OH-DPAT following transdermal iontophoretic delivery were determined simultaneously by taking blood samples (PK) and using on-line microdialysis (PD). For these studies, the active enantiomer (S)-5-OH-DPAT, was esterified with β-alanine. Animal procedures were conducted in accordance with guidelines published in the NIH guide for the care and use of laboratory animals and all protocols were approved by the Institutional Animal Care and Use Committee of the University of Groningen. The surgical, experimental and analytical procedures were identical to the methods used for PK-PD studies performed with the parent drug (S)-5-OH-DPAT [1]. A brief description is outlined below.

2.7.1 Animals

The pharmacokinetic-pharmacodynamic (PK-PD) studies were performed in albino male wistar rats (280-340 g) obtained from Harlan (Horst, the Netherlands). Prior to surgery the animals were housed at least 1 week in plexiglas cages, maximum 6 animals per cage with free access to water and standard laboratory chow. The cages were placed in a room with a controlled temperature at 21 °C and controlled humidity between 60-65% and a light-dark cycle of 12h.

2.7.2 Surgical procedures

Prior to surgery the rats were anaesthetized with Isofluran 2% in N_2O/O_2 (2/1). The permanent cannulations in the femoral vein and femoral artery were performed using silicone catheters (inner diameter (I.D.): 0.5 mm; outer diameter (O.D.): 0.9 mm) (UNO BV, Zevenaar, The Netherlands). After the cannulation the rats were kept under anaesthetized condition and mounted into a sterotaxic frame for the implementation of the microdialysis probes. A Y-shaped dialysis probe was used for the experiments, with an exposed tip length of 3 mm. The dialysis canulla (I.D.: 0.24 mm; O.D.: 0.34 mm) was prepared from polyacrylonitrile/sodium methallyl sulfonate copolymer (AN 69, Hospal, Bologna, Italy). The microdialysis canulla was implanted in the striatum. The following coordinates were used according to the atlas of Paxinos and Watson [14]: AP +0.9, LM ± 3.0 relative to bregma, and Vd – 6.0 below dura. The dialysis probe, filled with Ringer solution (140 mM NaCl, 3.0 mM KCl, 1.2 mM $CaCl_2$, 1.0 mM $MgCl_2$), was positioned and fixed in the burr hole under stereotaxic guidance. Thereafter the rats were housed solitary.

2.7.3 Experimental procedures

The PK-PD studies were performed 15-20 h after permanent cannulation and implementation of the probes. The rats were anaesthetized prior to and kept under anesthetized condition during the experiment with Hypnorm® and Dormicum® at a starting dose of 0.5 mL.kg^{-1} and subsequent 1h doses of 0.17 mL.kg^{-1}.

The donor solution consisted of β-ala- (S)-5-OH-DPAT (3.9 mM), buffered in citric buffer 5 mM at pH 5.0. Before the start of the experiment, the hair of the back of the anesthetized rat was removed with an electrical clipper and scalpel. 15 min after attaching the patches to the skin surface, the cathodal patch was filled with PBS pH 7.4 and the anodal patch was filled with donor solution. The volume of the patches was 2.3 ml and the active area was 2.5 cm². The protocol for the transdermal iontophoretic PK-PD studies was: 15 min passive diffusion + 90 min current application (250 μA.cm^{-2}). The patch was removed and the skin was wiped using tissue paper. Blood samples were taken at regular time intervals: 0, 15, 30, 45, 60, 75, 90, 105, 120, 135, 165, 195, 225, 255, 285 min. The blood samples (0.2 ml) were collected using lithium-heparin containing tubes (Microvette® 200 Plasma/Lithium Heparin, Sarsted BV, Etten-Leur, the Netherlands) and subsequently the plasma samples were separated from the blood cells by centrifugation. The samples were kept at -20 °C prior to analysis with LC-MS/MS. The microdialysis probes in the striata were perfused with Ringer solution at a flow of 2 μL.min^{-1} (CMA/102 Microdialysis Pump, Sweden). The analysis of the microdialysate samples are described below.

2.8 Analytical method

2.8.1 *in vitro* samples

Different HPLC methods were developed, in order to analyze simultaneously the respective prodrug, the parent drug 5-OH-DPAT and, if required, acetaminophen by RP-HPLC using a Superspher® 60 RP-select B, 75 mm-4 mm column (Merck KGaA, Darmstadt, Germany). The prodrugs of 5-OH-DPAT and acetaminophen were detected using a UV detector (Dual λ Absorbance Detector 2487, Waters, Milford, USA). The absorption wavelengths for the prodrugs and acetaminophen were 220 nm and 243 nm respectively. 5-OH-DPAT was detected using a scanning fluorescence detector (Waters™ 474, Millipore, Milford, MA, USA) with excitation wavelength and emission wavelength of 276 nm and 302 nm, respectively. The composition of the mobile phase for analyzing the respective prodrug together with 5-OH-DPAT is presented in Table 1. The flow rate was set to 1.5 ml.min^{-1} and the

volume of injection was 200 µl. Calibration curves showed a linear response when using concentrations of compounds between 0.1 and 40 µg.ml^{-1} (R^2>0.999). The limit of detection (LOD) and limit of quantification (LOQ) for these HPLC methods can also be found in Table 1.

2.8.2 Blood samples of (S)-5-OH-DPAT

Since the hydrolysis of β-ala-(S)-5-OH-DPAT to (S)-5-OH-DPAT is occuring very rapidly in human blood plasma ($t_{1/2}$=0.24 min in 80% human blood plasma), only (S)-5-OH-DPAT was analyzed in plasma [10]. Blood samples of 5-OH-DPAT were analyzed with an on-line solid-phase-extraction-liquid-chromatography-mass spectrometry/mass spectrometry (SPE-LC-MS/MS) method, described elsewhere [1]. Briefly, after addition of the internal standard (d_2-5-OH-DPAT; 5 ng.ml^{-1}) to the collected plasma, acetonitrile was added to precipitate the proteins. The mixture was vortexed, centrifuged, after which the supernatant was dried and redissolved in MilliQ and injected on the SPE cartridge (Hysphere Resin C8, endcapped, 10 x 4 mm (ID), 10µm SPE cartridge (Spark Holland B.V, The Netherlands). An external

Table 1: Physicochemical properties of the different molecules investigated (Mw, charge/Mw ratio and cLogP) and the composition of the mobile phase with the corresponding limit of detection (LOD) and limit of quantification (LOQ)

Compound	**Mw** (g.mol^{-1})	**Charge/ Mw** (x10^3) (mol.g^{-1})	**clogP**[a]	**Mobile phase** Composition (v/v)	TEA (mM)	**LOD** (µg.ml^{-1})	**LOQ** (µg.ml^{-1})
gly-5-OH-DPAT	304.4	6.6	3.6	Ace 50 mM/ACN 85/15	0	n.d	n.d
pro-5-OH-DPAT	344.5	5.8	4.1	Ace 50 mM /ACN 74/26	0	n.d	n.d
val-5-OH-DPAT	346.5	5.8	4.8	Ace 100 mM /THF 95/5	30	0.25	0.41
β-ala-5-OHDPAT	318.4	6.3	3.8	Ace 100 mM/THF 97.5/2.5	30	1.6	2.7
5-OH-DPAT	247.4	4.0	4.3	*		$1.4.10^{-3}$	$2.4.10^{-3}$
acetaminophen	151.2	0.0	n.d	*		$0.9.10^{-3}$	$1.4.10^{-3}$

Ace: acetatebuffer pH 3.6; nd: not determined; * :mobile phase is dependent on the prodrug investigated
[a]cLogP was calculated using ACD/Chemsketch [15-17]; n.d.: not determined

binary HPLC pump (Gynkotek, Germany) and an external Agilent 1200, 2/6 switch valve (Agilent Technology, USA) were used for the SPE sample trapping. First the SPE cartridge was conditioned, then the injected sample was trapped, consequently the valve was switched placing the SPE cartridge in-line with the LC system for elution on to the analytical column, after which the SPE cartridge was cleaned. Finally the cartridge was conditioned again. To analyze the extracted sample an Agilent 1200 HPLC system with autosampler (Agilent Technology, USA) was coupled online with an Agilent 6460 Triple Quadrupole mass spectrometer (Agilent Technology, USA). The samples were analyzed by μPLC-MS/MS using an Altima HP C18 column (150X 1.0 mm; 5 μm) (Grace Davison Discovery Sciences, Belgium). The detection was performed with a triple quadrupole mass spectrometer in the positive-ion electrospray mode and all analytes were monitored with Multiple Reaction Monitoring (MRM). System operation and handling the acquired data was performed using Agilent MassHunter data acquisition software (version, B.02.00; Agilent). Calibration curves showed a linear response when using concentrations of compounds between 0.2 and 50 ng.ml^{-1} (r^2>0.999). The recovery, limit of detection (LOD) and limit of quantification (LOQ) were experimentally determined at 93.9 ± 2.9 %, 0.07 and 0.2 ng.ml^{-1}, respectively.

2.8.3 Microdialysate samples

To analyze the striatal 5-OH-DPAT concentration the dialysate from the probe in the left striatum was collected every 15 min resulting a total volume of 30 μL per sample. The solution was analyzed using LC-MS/MS method, described elsewhere [1]. Briefly, d_2-5-OH-DPAT.HBr was added as internal standard to a 100 μL mixture of water + 0.1% formic acid and Ringer (1:1). The HPLC system consisted of a Shimadzu LC 20 AD binary system with a Shimadzu SIL 20AC autosampler. The samples were injected on a Grace Alltech Alltima HP C18 EPS reverse-phased column (150 x 2.1 mm (ID), 3 μm). The compounds were detected on a SCIEX API3000 triple quadrupole mass spectrometer (Applied Biosystems/MDS SCIEX) equipped with a Turbo Ion Spray interface. The mass spectrometer was operated in the positive ion mode with MRM. The detection limit of 5-OH-DPAT was 12.5 pg.ml^{-1}.

The dialysate contents of dopamine (DA) and its metabolites were quantified from the probe implanted at the right striatum by an on-line HPLC with electrochemical detection with the detection limit of 1 fMol per sample. An HPLC pump (LC-10AD vp, Shimadzu, Japan) was used in conjunction with an analytical cell (5011A, ESA, Chelmsford, MA, USA) and an electrochemical detector (Coulochem II, ESA)

working at +300 mV for DOPAC and HIAA and -300 mV for DA. The analytical column was a Supelco Supelcosil™ LC-18-DB column (150 mm x 4.6 mm (I.D.), 3µm). Data were converted into percentage of basal levels. The basal levels were determined from four consecutive samples (less than 20% variation), and set at 100%. After the experiments the rats were sacrificed and the brains were removed. After removal, the brains were kept in 4% paraformaldehyde solution until they were sectioned to control the location of the dialysis probes.

2.9 Data modeling

The data of the *in vitro* transport of valine-, β-alanine-5-OH-DPAT and 5-OH-DPAT and the PK-PD data following transdermal iontophoresis of β-alanine-(S)-5-OH-DPAT were analyzed using non-linear mixed effects modeling.

in vitro model

Previous studies suggested that two transport routes are involved in the iontophoretic delivery, linked in parallel [18]. Therefore to describe the iontophoretic transport across the skin, one zero order mass input I_0 from donor compartment into the skin during current application and two first order release constants K_{R1} and K_{R2} from skin to acceptor are used (Figure 2). The iontophoretic flux *in vitro* during iontophoresis can be described with the following equations:

$$J(t) = \frac{I_0}{S}(1 - e^{-K_{R1}.(t-t_L)}) + \frac{I_0}{S}(1 - e^{-K_{R2}.(t-t_L)}) \quad (1)$$

$$J_{ss} = 2.\frac{I_0}{S} \quad (2)$$

where $J(t)$ is the flux at time t and S is the diffusion area and t_L is the kinetic lag time parameter, introduced to address the time required for drug molecules to enter the skin compartment and J_{ss} as the flux at steady state.

During the post iontophoresis period only one release constant is sufficient to describe the passive flux, resulting in the following equation:

$$J(t) = \frac{P_{PI}}{S}(1 - e^{-K_{R2}.(t-T)}) + \left(\frac{I_0}{S}(1 - e^{-K_{R1}.(T-t_L)}) + \frac{I_0}{S}(1 - e^{-K_{R2}.(T-t_L)})\right).e^{-K_{R2}(t-T)} \quad (3)$$

where T is time of current application and P_{PI} is the zero order drug input due to the passive driving force in the post iontophoretic period.

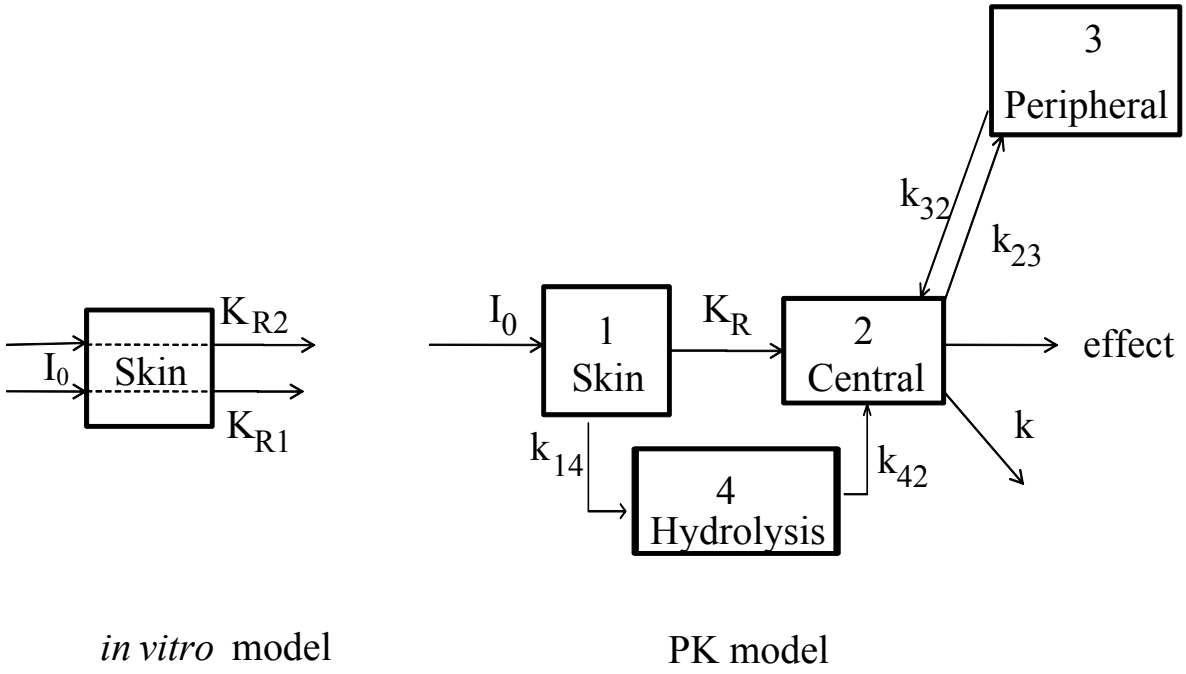

Figure 2: Overview of the compartmental models, used to fit the *in vitro* iontophoretic flux profiles during the iontophoresis period (*in vitro* model) and the model, used to fit the plasma profile during the iontophoretic period (PK model).

I_0: the zero order drug input during time of current application
K_{R1} and K_{R2}: first order release constants from the skin to the acceptor phase (*in vitro*)
K_R: the first order release constants from the skin to the plasma (*in vivo*)
k: the elimination rate constant
k_{14}: the first order skin-hydrolysis compartment distribution rate constant
k_{42}: the first order hydrolysis compartment-plasma distribution rate constant
k_{23}: the first order plasma-peripheral distribution rate constant
k_{32}: the first order peripheral-plasma distribution rate constant

PK model

Since the hydrolysis of β-ala-(S)-5-OH-DPAT to (S)-5-OH-DPAT is occurring very rapidly in the blood, only the plasma concentration of the parent drug S-OH-DPAT was monitored. To account for the hydrolysis of β-ala-(S)-5-OH-DPAT to (S)-5-OH-DPAT during transport, an adaptation was made to the basic PK model, developed by Nugroho *et al.* to describe the plasma concentration following transdermal

iontophoresis [19]. It is believed that during transport of the prodrug into and through the skin 2 effects occur: hydrolysis and depot formation. The resulting effect of both mechanisms is described with the addition of an extra compartment, as illustrated in Figure 2. The differential equations to describe the plasma concentration of (S)-5-OH-DPAT following transdermal iontophoretic delivery of β-ala-(S)-5-OH-DPAT are:

$$\frac{dX_1(t)}{dt} = I_0.N - K_R.X_1(t) - k_{14}.X_1(t) \quad (4)$$

$$\frac{dX_2(t)}{dt} = K_R.X_1(t) + k_{32}.X_3(t) + k_{42}.X_4(t) - k_{23}.X_2(t) - k.X_2(t) \quad (5)$$

$$\frac{dX_3(t)}{dt} = k_{23}.X_2(t) - k_{32}.X_3(t) \quad (6)$$

$$\frac{dX_4(t)}{dt} = k_{14}.X_1(t) - k_{42}.X_4(t) \quad (7)$$

With $\frac{dX_i(t)}{dt}$ as the rate of change in the amount of the drug in compartment *i*, X_i as the amount of the drug in compartment i, which refers to the skin compartment (i=1), the plasma compartment (i=2), the peripheral compartment (i=3) and the hydrolysis compartment (i=4). I_0 is defined as the zero order mass input, K_R as the first order release rate constant from skin to plasma, k as the first order elimination rate constant, k_{23} and k_{32} as the first order distribution rate constants from plasma to tissue and tissue to plasma, respectively. k_{14} and k_{42} are the rate constants for the mass transfer from the skin to hydrolysis compartment and from the hydrolysis compartment to the systemic circulation. N is a flag in the model to indicate that the input rate I_0 is only valid during the iontophoresis period.

PD model

An effect compartment model was used to describe the dopamine release following transdermal iontophoresis of β-ala-(S)-5-OH-DPAT. The rate of change of drug concentration $\frac{dC_e(t)}{dt}$ in the effect compartment can be described as follows:

$$\frac{dC_e(t)}{dt} = k_{eo}.(C_2(t) - C_e(t)) \quad (8)$$

With k_{e0} as the rate constant from plasma to the effect compartment and the elimination rate constant from the effect compartment. The striatal dopamine release C_{DA}, which is the pharmacodynamic end-point, is described by the sigmoid I_{max} model using the following equation:

$$C_{DA} = C_{DA}(0).\left(1 - \frac{I_{\max}.C_e(t)^H}{IC_{50}{}^H + C_e(t)^H}\right) \quad (9)$$

Where I_{max} is the maximum inhibition of the dopamine production, IC_{50} is the plasma concentration of 5-OH-DPAT to produce 50% of I_{max}, H is the Hill-slope coefficient, $C_{DA}(0)$ is the baseline values of dopamine (i.e., dopamine concentration prior to the inhibiting effect of 5-OH-DPAT).

PK-PD data following IV infusion and transdermal delivery of (S)-5-OH-DPAT, obtained from literature, were included in the data set to obtain more reliable parameter estimates [1]. In analogy to the PK-PD model of (S)-5-OH-DPAT a covariate of route of administration for IC_{50} was added [1]. The fixed effect parameters (θ) included: I_0, K_R, clearance (CL), inter compartmental clearance (Q), volume of the central compartment (V_2), volume of the peripheral compartment (V_3), k_{e0}, I_{max}, and IC_{50}. Variability in pharmacokinetic parameters was assumed to be log-normally distributed in the population. Inter-individual variability was modeled by an exponential error model as written in Equation 10:

$$P_i = \theta.\exp(\eta_i) \quad (10)$$

in which θ is the population value for the fixed effect parameter P, P_i is the individual estimate and η_i is the normally distributed interindividual random variable with mean zero and variance ω^2. The coefficient of variation (CV %) of the structural model parameters is expressed as percentage of the root mean square of the interindividual variability term. The residual error was modeled by a proportional error model as written in Equation 11:

$$C_{obs,ij} = C_{pred,ij}.(1 + \varepsilon_{ij,1}) + \varepsilon_{ij,2} \quad (11)$$

where $C_{obs,ij}$ is the jth observed concentration in the ith individual, $C_{pred,ij}$ is the predicted concentration, and ε_{ij} is the normally distributed residual random variable with mean zero and variance σ^2. The estimation of the final population parameters was performed using the conventional first order estimation method (FOCE). The PK model parameters were estimated independently and subsequently used as input for

the PD analysis. During model building, goodness-of-fit was based on statistical and graphical diagnostic criteria. Model selection and identification was based on the likelihood ratio test, coefficient of variation of parameter estimates, parameter correlations and goodness-of-fit plots. For the likelihood ratio test, the significance level for the inclusion of one parameter was set at $p<0.05$, which corresponds with a decrease of 3.84 points, in the minimum value of the objective function (MVOF) under the assumption that the difference in MVOF between two nested models is χ^2 distributed. The following goodness-of-fit plots were subjected to visual inspection to detect systemic deviations from the model fits: individual observed versus population and individual predicted values. Finally, the performance of the population PK and PK-PD models were assessed by simulating 100 data sets with the final model parameter estimates. The evaluation of model performance also included visual predictive check (VPC), as implemented in Xpose 4 (R version 2.7.0, R-foundation) [20].

2.10 Data analysis

All data are presented as mean ± standard deviation (SD). When a statistical analysis was performed comparing only 2 groups, a Students t-test was used. When 3 or more groups were compared, a 1-way ANOVA statistical analysis was executed. Comparing effect of two factors simultaneously was performed using 2-way ANOVA. If the overall p-value was less than 0.05, a bonferonni post-test was applied to compare different groups. For all statistical analysis a significance level of $p<0.05$ was used.

3 Results

3.1 Stability of prodrugs of 5-OH-DPAT in different conditions

A series of prodrugs of 5-OH-DPAT were synthesized by esterification of 5-OH-DPAT with different amino acids [10]. Because ester bounds are known to be susceptible to hydrolysis, the chemical stability of prodrugs was investigated. The various conditions were selected to mimic the conditions in the different compartments during iontophoretic transport. Apparent first order rate constants for hydrolysis were determined from the slopes of various plots of percent remaining prodrug *vs* time. The corresponding half lives are presented in Figure 3. Glycine-5-OH-DPAT and proline-5-OH-DPAT show a limited chemical stability in a citric buffer pH 5.0 at room temperature with a half life of 9.6 and 7.5 h, respectively. Valine-5-OH-DPAT and β-alanine-5-OH-DPAT are stable under this condition with

a half life of 318 and 692h, respectively. However increasing the pH from 5.0 to 6.2 at room temperature (RT) decreases the half life of both valine- and β-alanine-5-OH-DPAT to 7.6 h and to 64.2h, respectively. Further increasing the pH to 7.4 decreases the half life of the prodrugs to 0.7 and 4.5h for valine- and β-alanine-5-OH-DPAT, respectively. Increasing the temperature from RT to 32 °C, the skin temperature, decreased the stability of glycine-, valine- and β-alanine-5-OH-DPAT. For instance the half life of valine-5-OH-DPAT at pH 6.2 decreases from 7.6 to 5.1h when increasing the temperature. Current application and the presence of HSC however do not affect the stability of the prodrugs. Since valine- and β-alanine-5-OH-DPAT are the most stable prodrugs, these 2 compounds were selected for further investigations, concerning solubility and transdermal transport.

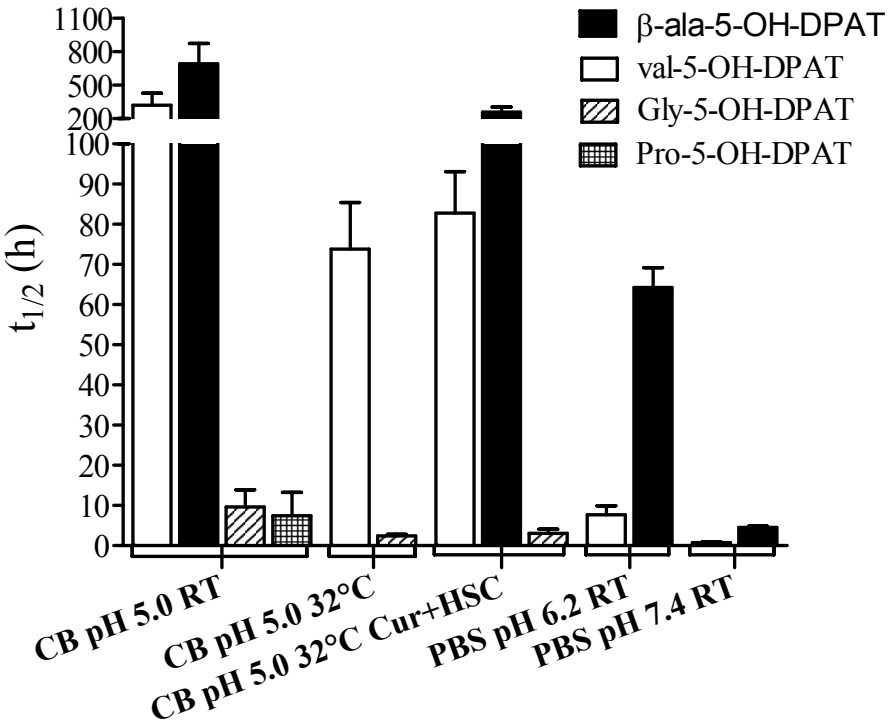

Figure 3: The half life ($t_{1/2}$) of the hydrolysis of the prodrugs glycine-5-OH-DPAT (striped bar), proline-5-OH-DPAT (blocked bar), valine5-OH-DPAT (white bar) and β-alanine-5-OH-DPAT (black bar) under various conditions. The data are presented as estimate + the upper limit of the estimate. CB: citric buffer 5 mM; RT: room temperature; HSC: human stratum corneum; Cur: current 320 μA.

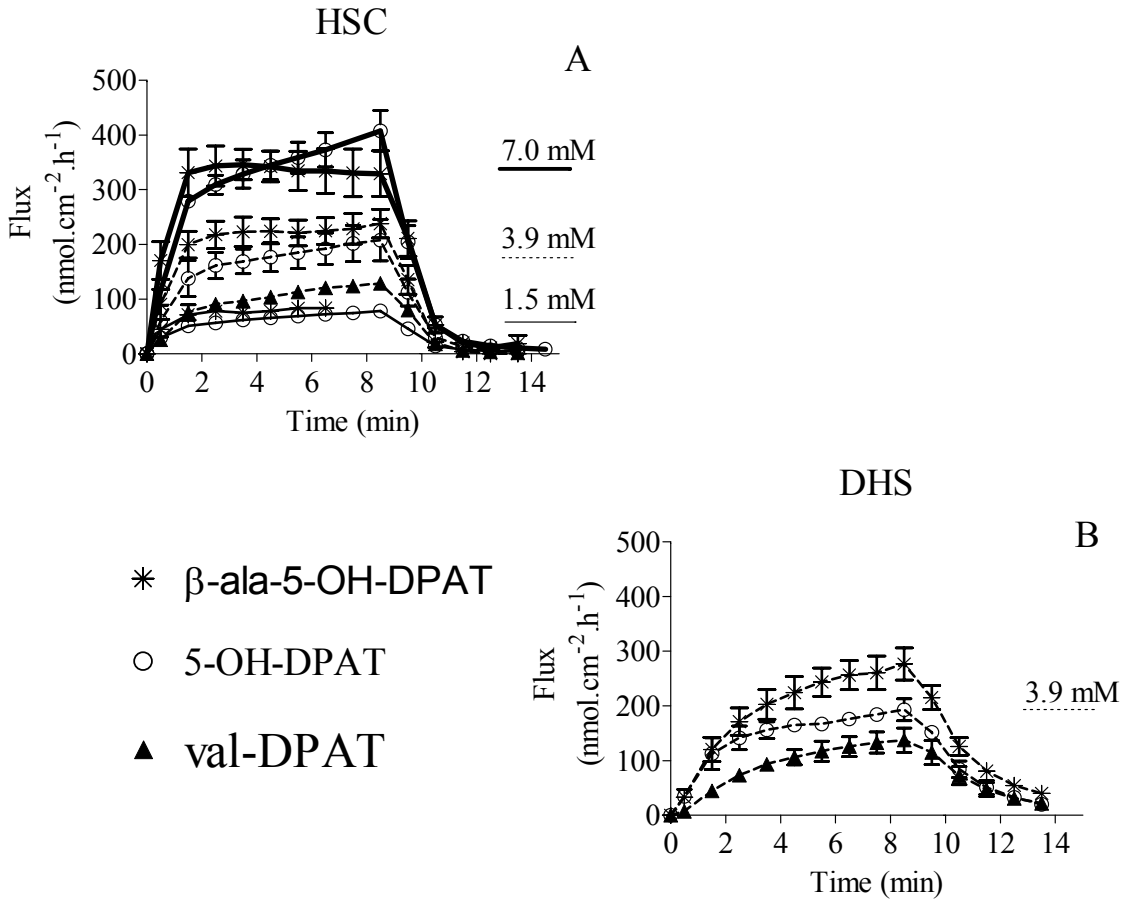

Figure 4: *In vitro* flux profiles of valine-5-OH-DPAT (closed triangle), β-ala-5-OH-DPAT (star) and 5-OH-DPAT (open circle). **A**: Iontophoresis of valine-5-OH-DPAT (only 3.9 mM (intermittent line)) and β-ala-5-OH-DPAT and 5-OH-DPAT at 3 different concentrations (1.5 (solid line), 3.9 (intermittent line), 7.0 mM (thick solid line)) across stratum corneum. **B**: Iontophoresis of 3.9 mM valine-5-OH-DPAT, β-ala-5-OH-DPAT and 5-OH-DPAT across dermatomed human skin. PBS pH 7.4 was used in all experiments as acceptor phase.

3.2 Solubility of valine- and β-alanine-5-OH-DPAT

The maximum solubility was determined in citric buffer 5 mM pH 5.0 as this is the donor solution, used for transport studies. The maximum solubility of valine-5-OH-DPAT is 232.2 mM. With respect to β-alanine-5-OH-DPAT the maximum solubility

is expected to be higher than 832.2 mM. At this concentration the maximum solubility of β-alanine-5-OH-DPAT is not yet reached. However, the study was discontinued due to the limited availability of the compound.

3.3 *In vitro* iontophoresis of the two prodrugs in comparison to 5-OH-DPAT

Figure 4 illustrates the iontophoretic flux profiles of the prodrugs at different concentrations under various conditions. The flux profiles of the parent drug, adapted from literature, were added to the graphs for comparison [21]. In case of the prodrugs the non-hydrolyzed and the hydrolyzed fraction of the prodrug are added and the resulting total flux is displayed in Figure 4. The iontophoretic transport across HSC of the two prodrugs was evaluated in comparison to each other and their parent drug 5-OH-DPAT, using PBS pH 7.4 as acceptor phase (Figure 4B). The flux after 9h current application of β-alanine-5-OH-DPAT (238.0±26.1 and 329.6±41.9 $nmol.cm^{-2}.h^{-1}$) across HSC is not significantly different from the flux of the parent drug 5-OH-DPAT (207.7±38.0 and 407.7±37.0 $nmol.cm^{-2}.h^{-1}$) at 3.9 and 7.0 mM donor concentrations ($p>0.05$; 2-way ANOVA). Since the assay of iontophoretic delivery of 1.5 mM β-alanine-5-OH-DPAT was stopped after 7h of current application this time point was chosen to compare the flux of prodrug and parent drug. A similar flux was observed for β-alanine-5-OH-DPAT (84.1±5.6 $nmol.cm^{-2}.h^{-1}$), compared to 1.5 mM 5-OH-DPAT (78.2±6.2 $nmol.cm^{-2}.h^{-1}$) ($p<0.05$; t-test).

The results of the transport studies across DHS, with PBS pH 7.4 as acceptor phase, are depicted in Figure 4C. 2-way ANOVA was performed to analyze the Flux after 9h of current application ($Flux_{9h}$) across HSC and DHS for all the compounds at 3.9 mM. An overall significant difference could be observed between the $Flux_{9h}$ of the different compounds, which was due to compound variation and not due to the use of the different skin types ($p<0.05$). Bonferonni's post-test demonstrated that the $Flux_{9h}$ of the prodrug β-alanine-5-OH-DPAT is significantly higher compared to the $Flux_{9h}$ of valine-5-OH-DPAT across DHS and HSC. In addition only across DHS the $Flux_{9h}$ of β-alanine-5-OH-DPAT is significantly higher than the $Flux_{9h}$ of the parent drug, 5-OH-DPAT. Furthermore the $Flux_{9h}$ of valine-5-OH-DPAT was significantly lower compared to the $Flux_{9h}$ of the parent drug across HSC and DHS.

Acetaminophen (15 mM) as electroosmotic marker was added to the donor concentration to quantify the electroosmotic flux. 1-way ANOVA, with a bonferonni post test showed that the electroosmotic flux during transport of valine-5-OH-DPAT (7.8±1.9 $nmol.cm^{-2}.h^{-1}$) is significantly lower than the electroosmotic flux of 5-OH-DPAT (13.7±3.4 $nmol.cm^{-2}.h^{-1}$) ($p<0.05$), however not significantly different from

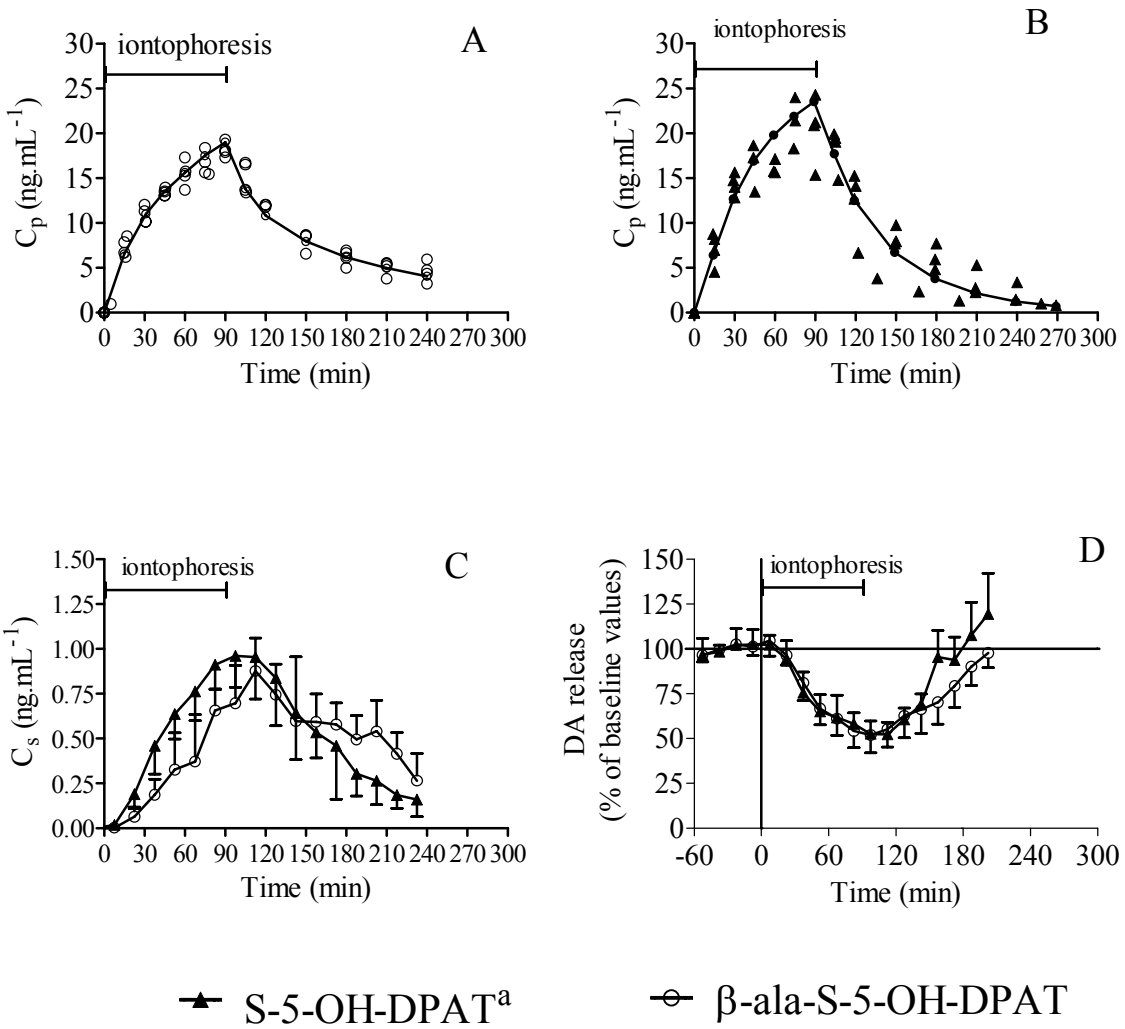

Figure 5: Resulting graphs of the PK-PD study with β-ala-(S)-5-OH-DPAT (open circle) together the results of (S)-5-OH-DPAT (closed triangle), adapted from literature. The observed plasma concentration (C_p) of (S)-5-OH-DPAT, following transdermal iontophoresis of β-ala-(S)-5-OH-DPAT (**A**) and (S)-5-OH-DPAT (**B**) are presented together with the population prediction (PRED) (full line).
C: The striatal concentration of (S)-5-OH-DPAT (C_s), presented as mean ± SD, following iontophoretic delivery of β-ala-(S)-5-OH-DPAT and (S)-5-OH-DPAT.
D: The dopamine (DA) release in the striatum, as % baseline, presented as mean ± SD, following iontophoretic delivery of β-ala-(S)-5-OH-DPAT and (S)-5-OH-DPAT.
[a]adapted from literature [1]

β-alanine-5-OH-DPAT (11.7±4.2 nmol.cm^{-2}.h^{-1}) ($p>0.05$). Also the electroosmotic flux of 5-OH-DPAT and β-alanine-5-OH-DPAT are not significantly different ($p>0.05$).

The iontophoretic transport profile across HSC and DHS of 3.9 mM β-alanine-5-OH-DPAT was modeled using Equations 1 and 3. The resulting parameters are displayed in Table 2. The estimated steady state flux, calculated with Equation 2, is higher for DHS, compared to HSC. The lag time (T_{lag}) and passive driving force post iontophoresis (Pass=P_{PI}/S) are also higher for DHS, whereas the release constants K_{R1} and K_{R2} are lower compared to HSC.

3.4 Hydrolysis during transport through HSC and DHS

Approximately 19.8±2.6% and 55.4±15.1% of β-alanine-5-OH-DPAT is hydrolyzed in 5-OH-DPAT when transported across HSC and DHS, respectively, using PBS pH 7.4 as acceptor phase. A similar observation is found for val-5-OH-DPAT, using PBS pH 6.2 as acceptor phase: 26.8±5.4% and 100% valine-5-OH-DPAT is converted into 5-OH-DPAT when transported through HSC and DHS, respectively.

3.5 *In vivo* iontophoretic delivery of β-ala-(S)-5-OH-DPAT

The PK and PD of the active S-enantiomer of the most promising prodrug β-ala-(S)-5-OH-DPAT following transdermal delivery were investigated simultaneously. For comparison the plasma-, striatum profile and the dopamine release following transdermal iontophoresis of the parent drug (S)-5-OH-DPAT, adapted from literature, are added to the resulting graphs (Figure 5B-D) [1].

3.5.1 Plasma profile

The prodrug is rapidly hydrolyzed to (S)-5-OH-DPAT in blood plasma, since the half life is 0.24 min in 80% human blood plasma [10]. Therefore the plasma concentration of the parent drug (S)-5-OH-DPAT was monitored during the PK-PD study. No detectible amount of (S)-5-OH-DPAT was observed after 15 min of passive diffusion (data not shown). Current application starts at t=0 min, as depicted in Figure 5A. As can be observed current application results in immediate increase in plasma concentration. After 90 min of current application, the plasma profile tends towards a steady state situation. The resulting plasma concentration at time=90 min is 18.2±0.8 ng.ml^{-1}. After current application is discontinued and the patch is removed, the profile shows a decline in plasma concentration, which is best described with a 2-compartmental model.

Table 2: The resulting population estimates of simultaneous modeling the plasma concentration and dopamine release following transdermal iontophoresis of β-ala-(S)-5-OH-DPAT (3.9 mM) in male wistar rats. The resulting parameters of fitting the *in vitro* transdermal iontophoretic transport of β-ala-5-OH-DPAT (3.9 mM) across human stratum corneum (HSC) and dermatomed human skin (DHS) is depicted. PBS pH 7.4 was used as acceptor phase for the *in vitro* experiments

		Estimate		**Between animal variabity**				**Estimate**		**Between subject variabity**	
parameter	**unit**	mean	RSE %	mean	RSE %	**parameter**	**unit**	mean	RSE %	mean	RSE %
PK-PD						**HSC (*in vitro*)**					
V_2	L	0.46	18	0.13	97	J_{ss} 500	*	272.5	4		
V_3	L	0.78	16	0.07	52	K_{R1}	h^{-1}	0.278	28	0.516	82
CL	$L.h^{-1}$	2	6	0.02	38	K_{R2}	h^{-1}	1.69	8	0.035	23
Q	$L.h^{-1}$	1.96	21	0.16	73	T_{lag}	h	0.005			
J_{ss} 250	*	110.6	8			Pass	*	n.d.			
K_R	h^{-1}	0.31	23								
k_{14}	h^{-1}	5.06	23			Sigma 1		0.019	17		
k_{42}	h^{-1}	4.79	21			Sigma 2		1.93	36		
k_{eo}	h^{-1}	3.79	12	0.19	48						
IC_{50}	$ng.ml^{-1}$	4.50	12	0.07	35						
N		3.12	9			**DHS (*in vitro*)**					
I_{max}		40.9	7	0.03	39	J_{ss} 500	*	381.3	7		
						K_{R1}	h^{-1}	0.069	35	0.212	23
						K_{R2}	h^{-1}	0.588	5	0.3	51
						T_{lag}	h	0.22	10		
						Pass	*	29.1	14	0.045	33
Sigma 1	PK	0.02	24			Sigma 1		0.002	67		
Sigma 1	PD	0.01	20			Sigma 2		18.4	59		

*: unit of J_{ss} and Pass is: $nmol.cm^{-2}.h^{-1}$
Sigma 1: proportional error; Sigma 2: additive error
n.d.: not determined because the parameter value was constrained to 0

3.5.2 Striatum profile

The 5-OH-DPAT concentration of the microdialysate samples of the left striatum was analyzed following transdermal iontophoresis of β-ala-(S)-5-OH-DPAT. With a delay of approximately 7.5 min, the striatal 5-OH-DPAT concentration (C_s) increased when starting iontophoresis to a maximum level of 0.88±0.18 ng.ml^{-1}. This maximum was reached 22.5 min after switching off the current (t=112.5 min). After this time point C_s declines again.

3.5.3 Pharmacodynamic effect

With on-line microdialysis the DA concentration (the pharmacodynamic end-point) in the right striatum was monitored. The resulting DA release profile (mean ± SD) is depicted in Figure 5D. Prior to iontophoresis the DA level was monitored and the average DA level from 4 consecutive points was set to 100%. As can be observed, when starting iontophoresis the DA level decreases with a lag time between 7.5 and 22.5 min. The DA level decreases to near steady state level of 48.6±8.2% baseline, 94.5 min after the start of iontophoresis. After removal of the patch, the DA level recovers again to its initial state (DA release=100%) at time=189.2±12.1 min following prodrug iontophoresis.

3.6 Non-linear mixed effects modeling: model evaluation

The *in vitro* transport flux profiles, the plasma profile and the pharmacodynamic effect are modeled with non linear mixed effects modeling, using compartmental models. The resulting parameter estimates are depicted in Table 2. A relatively low Residual Standard Error (RSE%) for the fixed *in vitro* (≤ 35%) and *in vivo* parameters estimates (≤ 23%) indicates a reliable prediction of the estimates. Moreover Figure 6A and B, displaying the visual predictive check (VPC), demonstrates that the *in vivo* observations are well distributed between the 2.5th and the 97.5th percentiles. This indicates that the variability, predicted by the PK-PD model, corresponds with the observed variability. In addition the diagnostic plots of the PK and PD profile, shown in Figure 6C-F, indicate that the proposed PK-PD model adequately describes the plasma profile and pharmacodynamic effect.

4 Discussion

The general aim of the present study is to evaluate different prodrugs and select the best candidate(s) for transdermal iontophoretic delivery. The presence of enzymes in the skin, such as esterases and amidases, makes the use of prodrugs an interesting

approach for transdermal delivery. The prodrugs can be tailored to improve drug delivery and during transport across the skin, the enzymes hydrolyze the prodrugs to their active parent drug [8].

4.1 Chemical stability and solubility

Ester prodrugs, as presented in this paper, are not only susceptible to enzymatic, but also to chemical hydrolysis. The stability of the prodrugs in different aqueous solutions is highly dependent on the side chain, esterified with 5-OH-DPAT (stability: glycine < proline < valine < β-alanine). Based on these results valine- and β-alanine-5-OH-DPAT were selected for further investigating the transdermal iontophoretic transport across human skin. Esterification of 5-OH-DPAT with valine and β-alanine improved its solubility tremendously. The solubility of valine- and β-alanine-5-OH-DPAT was respectively 4 and more than 14 times higher, compared to its parent drug 5-OH-DPAT [21]. A higher solubility enables reduction of the patch volume, while keeping sufficient amount of drug in the patch. Presumably addition of an extra chargeable amine group contributes substantially to the solubility of the prodrugs.

4.2 Transdermal iontophoresis *in vitro*

At pH 5.0 both prodrugs have an additional charge compared to 5-OH-DPAT. When increasing the charge from monovalent to bivalent, this affects in several ways the transport: (i) bivalent ions have a larger hydrated volume, as suggested by Lai and Roberts, which can result in a reduced flux [22], (ii) bivalent ions interact more with charged sites in SC, which according to Phipps *et al.* will result in a reduced flux [23] and (iii) an increase in the charge/molecular weight ratio results in an equivalent higher electromigrative flux [24]. It is suggested that the lipophilicity, indicated by the cLogP (Table 1), of the prodrugs influences the balance between these three factors and therefore affects the transport efficiency [15-17]. Only for the more hydrophilic prodrug β-alanine-5-OH-DPAT with a charge/Mw ratio which is 1.5 times higher compared to 5-OH-DPAT, resulted in almost in an equivalent increase (1.4 times) in the total flux after 9h of current application across DHS. The flux of β-alanine-5-OH-DPAT is less affected by the increased hydrated volume and the skin interaction. In contrast valine-5-OH-DPAT with a hydrophobic prodrug moiety is retained more by the skin and shows a decreased flux compared to 5-OH-DPAT. This hypothesis is strengthened by the decreased electroosmotic flux during transport of valine-5-OH-DPAT. Valine-5-OH-DPAT is retained more strongly and the two positive charges cause a neutralization of the skin negative charges, resulting in a

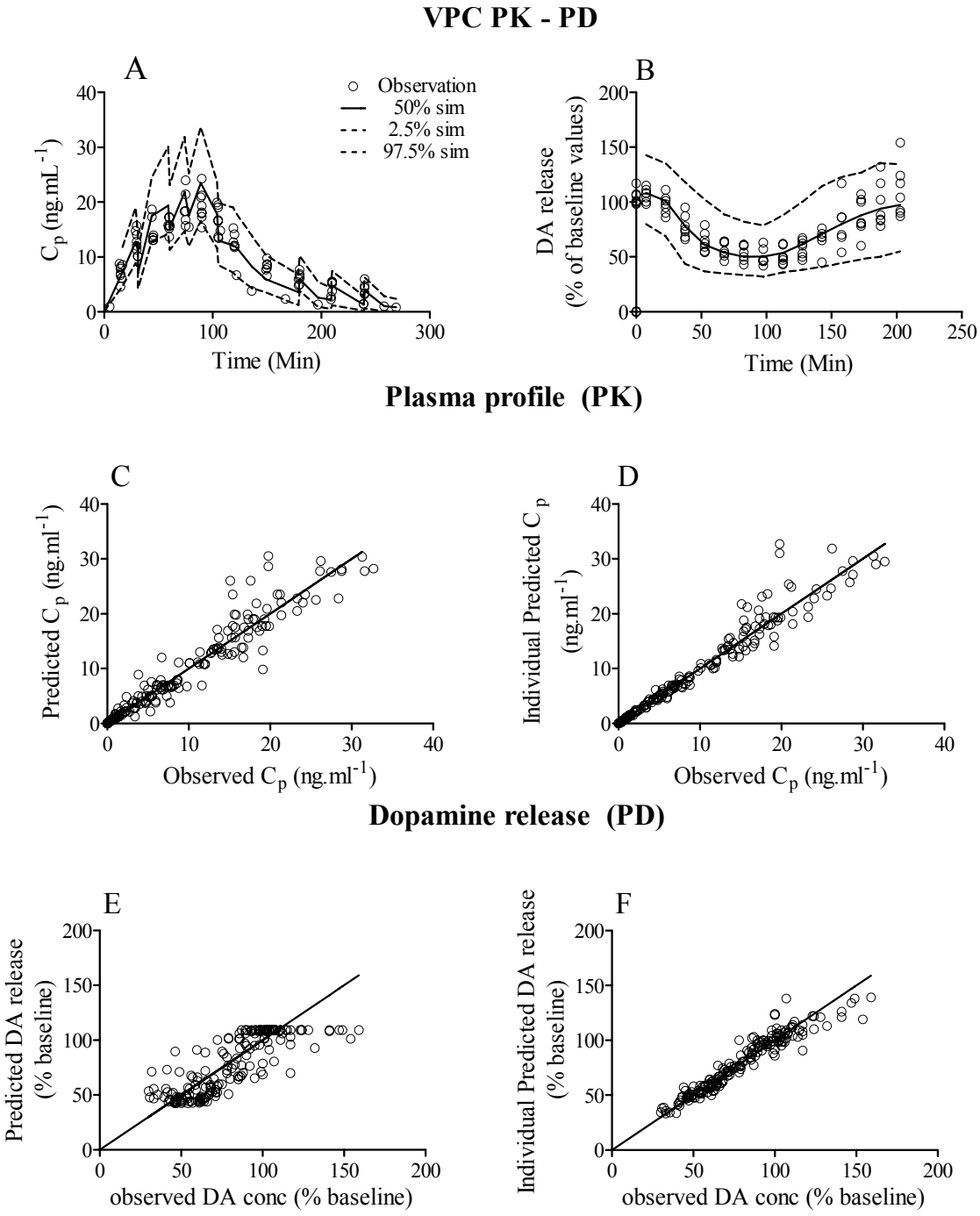

Figure 6: Diagnostic plots of simultaneous fitting the plasma concentration (**A, C, D**) and the dopamine release (**B, E, F**) following the transdermal iontophoresis of β-ala-(S)-5-OH-DPAT. Depicted are the observations (open circles) together with the interquantile concentration range (2.5%-97.5%, intermittent line) and the median (50%, solid line) of the plasma profile (**A**) and the dopamine release profile (**B**). A number of 100 samples were simulated based on the final parameter estimates. **C,E:** population predicted *vs* the observed data. **D,F**: individual prediction *vs* the observed data.

reduced electroosmotic flux. Furthermore, the transport of valine-5-OH-DPAT is less affected by the charge/molecular weight ratio. These results are in agreement with the computational studies performed by Schuetz *et al.*, who predicted with a 3D quantitative structure-permeation relationship that iontophoresis was favored by peptide hydrophilicity and hindered by voluminous localized hydrophobicity [25].

Besides the transport efficiency it is also important to determine the rate of hydrolysis during iontophoretic transport across human skin in order to be able to predict the amount of prodrug and parent drug that will taken up by the blood stream. In analogy to the chemical stability, β-alanine-5-OH-DPAT is the more stable prodrug. For both prodrugs an increased hydrolysis is observed when transported across DHS. This increased hydrolysis rate is the result of 2 mechanisms. Firstly the presence of enzymes, such as esterases, is more abundant in the epidermis [13]. Secondly the increased migration time through DHS and the slower release from the DHS, reflected by K_{R1} and K_{R2} (Table 2), results in a possibly longer interaction of enzymes with the prodrugs augmenting the hydrolysis rate. The remaining prodrug that is not hydrolyzed during transdermal transport is expected to be hydrolyzed rapidly when taken up by the blood stream, since the enzymatic half life of valine- and β-alanine-5-OH-DPAT in 80% human blood plasma was 0.22 and 0.24 min, respectively [10].

4.3 PK-PD properties

The pharmacokinetic and pharmacodynamic properties of β-alanine-(S)-5-OH-DPAT, the more stable and soluble prodrug with improved *in vitro* transport efficiency, were investigated in an animal model. Under anesthetized conditions blood samples were taken and the dopamine level in the striatum (pharmacodynamic end-point) was monitored on-line with microdialysis. This animal model is identical to the animal model used to investigate the PK-PD properties of (S)-5-OH-DPAT, which enables us to compare the prodrug to its parent drug [1]. The plasma concentration profile of (S)-5-OH-DPAT (C_p) following transdermal iontophoresis of the prodrug differs on 3 aspects from the profile following (S)-5-OH-DPAT administration, as can be observed in Figure 5A-B. (i) The increase in plasma concentration during current application is slower for the prodrug than for the parent drug. This is reflected by a decreased skin release constant K_R for the prodrug (Table 2) [1]. (ii) After 90 min of current application the population predicted C_p is lower for β-ala-(S)-5-OH-DPAT (19 $ng.ml^{-1}$) than for (S)-5-OH-DPAT (23.5 $ng.ml^{-1}$). (iii) During the elimination phase the C_p profile is different following administration of prodrug *vs* parent drug. It is hypothesized that these 3 differences can be partially

attributed to the hydrolysis of the prodrug during transdermal transport, assuming the hydrolysis in blood plasma is occurring instantaneously. Furthermore it is believed that after penetration through the stratum corneum depot formation of the prodrug in the viable epidermis also delays the release to the systemic circulation. The resulting effect was included in the PK-model by adding an extra compartment between the skin and the central compartment (Figure 2). This model adequately described the plasma profile following transdermal administration of the prodrug (Figure 6).

In addition the resulting parameter estimates corresponded very well with the parameters of (S)-5-OH-DPAT obtained for the PK-PD study [1]. It can be observed in Figure 5C that in analogy to C_p the increase in C_s during the absorption phase is faster and that the striatal clearance is going more rapidly following iontophoresis of the parent drug (S)-5-OH-DPAT. Finally the difference in C_p and C_s profile following prodrug *vs* parent drug administration resulted also in a different striatal DA release profile (Figure 5D). During the iontophoretic period no difference was observed in DA release with the same maximum. This suggests that despite a lower steady state plasma concentration the same maximum effect can be achieved. Post-iontophoresis however the time for the DA release to recover to baseline values post-iontophoresis was significantly longer for the prodrug (99.2±12.1 min) compared to (S)-5-OH-DPAT (79.4±1.3 min) (t-test; $p<0.05$). This can be attributed to higher C_p values after removal of the patch due to delayed skin release. On the one hand, this prolonged effect can be a drawback to initiate therapy to treat Parkinson's disease, since rapid changes in delivery schemes may be required. On the other hand, the prolonged effect of the prodrug can be beneficial for patients who suffer from nocturnal disturbances. Nocturnal disturbances are one of the most common non-motor complications in patients with Parkinson's disease [26]. It is believed that continuous stimulation of the DA receptor during the night can reduce the occurrence of nocturnal disturbances [27].

4.4 *in vitro-in vivo* correlation

Fitting *in vitro* and *in vivo* transport using compartmental modeling allowed us to compare both iontophoretic transports. Different kinetic models were used to describe the *in vitro* and *in vivo* transport of the prodrug β-alanine-(S)-5-OH-DPAT. This suggests that different transport mechanisms can be involved *in vitro* and *in vivo*. These differences can at least partially be attributed to 3 factors. Firstly, the structure of human skin differs from the structure of rats. Mainly the thickness of the different skin layers, the stratum corneum lipid composition and the density of hair follicles will contribute to the difference [28]. But previous studies showed that

iontophoresis under constant current conditions diminishes the interspecies variations [29] and that rat skin has comparable permeation kinetic parameters with human skin [28]. Secondly the clearance of the penetrant by the acceptor flow may be different from the clearance *in vivo* by the microcirculation in the skin [28]. Thirdly, the activity of the esterase *in vivo* may be different from the esterase activity in freshly excised skin. Despite these differences a good correlation was observed between the steady state flux *in vitro* and *in vivo*. Assuming that there is a linear correlation *in vivo* between the flux and the current density [1], applying a current density of 500 $\mu A.cm^{-2}$ would result in an *in vivo* steady state flux ($J_{ss}=I_0/S$) of 221.2 $nmol.cm^{-2}.h^{-1}$. This flux corresponded best with the *in vitro* J_{ss} across HSC (272.5 $nmol.cm^{-2}.h^{-1}$) compared to the J_{ss} across DHS (381.3 $nmol.cm^{-2}.h^{-1}$). This suggests that transport across HSC can provide valuable information for prediction towards the *in vivo* situation for this particular compound. Whether this is also the case for other drugs, remains to be established.

In conclusion this study demonstrates the potential of improving solubility, iontophoretic transport and changing the plasma profile and the PD effect of the promising dopamine agonist 5-OH-DPAT with the use of prodrugs. A good balance was found between an efficient transport rate and enzymatic conversion to the parent drug during transdermal transport. Of the synthesized prodrugs, presented in this research, β-alanine-5-OH-DPAT is the most promising prodrug and is a potential candidate for further investigation. This sufficiently stable prodrug shows a tremendous increase in solubility, which can be beneficial for manufacturing and practical use. The increased *in vitro* flux of β-alanine-5-OH-DPAT across human skin did not result in higher steady state plasma concentrations, but in a prolonged effect which reached the same maximum level as was observed with the parent drug.

Acknowledgements

This research was financially supported by a grant (LKG 6507) of the Dutch Technology Foundation STW, Utrecht, The Netherlands. The authors thank J.B. De Vries from the Department of biomonitoring and sensoring (University Center of Pharmacy, University of Groningen, the Netherlands) for his support with the animal studies.

References

1. Ackaert, O., et al., *Controlling the pharmacokinetics and the pharmacodynamic effect of (S)-5-OH-DPAT with transdermal iontophoresis.* 2010. **submitted for publication**.
2. Coldwell, M.C., et al., *Comparison of the functional potencies of ropinirole and other dopamine receptor agonists at human D2(long), D3 and D4.4 receptors expressed in Chinese hamster ovary cells.* Br J Pharmacol, 1999. **127**(7): p. 1696-702.
3. Nugroho, A.K., et al., *Transdermal iontophoresis of rotigotine across human stratum corneum in vitro: influence of pH and NaCl concentration.* Pharm Res, 2004. **21**(5): p. 844-50.
4. van der Geest, R., M. Danhof, and H.E. Bodde, *Iontophoretic delivery of apomorphine. I: In vitro optimization and validation.* Pharm Res, 1997. **14**(12): p. 1798-803.
5. Abla, N., et al., *Topical iontophoresis of valaciclovir hydrochloride improves cutaneous aciclovir delivery.* Pharm Res, 2006. **23**(8): p. 1842-9.
6. Laneri, S., et al., *Ionized prodrugs of dehydroepiandrosterone for transdermal iontophoretic delivery.* Pharm Res, 1999. **16**(12): p. 1818-24.
7. Wang, J.J., et al., *Ester prodrugs of morphine improve transdermal drug delivery: a mechanistic study.* J Pharm Pharmacol, 2007. **59**(7): p. 917-25.
8. Guy, R.H., J. Hadgraft, and D.A. Bucks, *Transdermal drug delivery and cutaneous metabolism.* Xenobiotica, 1987. **17**(3): p. 325-43.
9. Nugroho, A.K., et al., *Pharmacokinetics and pharmacodynamics analysis of transdermal iontophoresis of 5-OH-DPAT in rats: in vitro-in vivo correlation.* J Pharm Sci, 2006. **95**(7): p. 1570-85.
10. De Graan, J., et al., *Synthesis and evaluation of the chemical and enzymatic stability of a series of novel amino acid prodrugs of the potent dopamine D2 agonist (S)-5-OH-DPAT developed for transdermal iontophoresis.* 2010. **In preparation**.
11. Westfall, T.C., et al., *The role of presynaptic receptors in the release and synthesis of 3H-dopamine by slices of rat striatum.* Naunyn Schmiedebergs Arch Pharmacol, 1976. **292**(3): p. 279-87.
12. Nugroho, A.K., et al., *Transdermal iontophoresis of the dopamine agonist 5-OH-DPAT in human skin in vitro.* J Control Release, 2005. **103**(2): p. 393-403.
13. Prusakiewicz, J.J., C. Ackermann, and R. Voorman, *Comparison of skin esterase activities from different species.* Pharm Res, 2006. **23**(7): p. 1517-24.
14. Paxinos, G. and C. Watson, *The rat brain in sterotaxic coordinated. Academic Press: Sydney.* 1982.
15. Tetko, I.V. and P. Bruneau, *Application of ALOGPS to predict 1-octanol/water distribution coefficients, logP, and logD, of AstraZeneca in-house database.* J Pharm Sci, 2004. **93**(12): p. 3103-10.
16. Tetko, I.V., et al., *Virtual computational chemistry laboratory--design and description.* J Comput Aided Mol Des, 2005. **19**(6): p. 453-63.
17. VCCLAB. *Virtual Computational Chemistry Laboratory,* http://www.vcclab.org. 2005.
18. Ackaert, O., et al., *Transdermal iontophoretic delivery of a novel series of dopamine agonists in vitro: physicochemical considerations* J Pharm Pharmacol, 2010. **accepted for publication**.
19. Nugroho, A.K., et al., *Compartmental modeling of transdermal iontophoretic transport II: in vivo model derivation and application.* Pharm Res, 2005. **22**(3): p. 335-46.
20. Holford, N., *The Visual Predictive Check-Superiority to Standard Diagnostic (Rorschach) Plots.* PAGE 14, Abstr 738 [www.page-meeting.org/?abstract=738], 2005.
21. Ackaert, O.W., et al., *Mechanistic studies of the transdermal iontophoretic delivery of 5-OH-DPAT in vitro.* J Pharm Sci, 2010. **99**(1): p. 275-85.

22. Lai, P.M. and M.S. Roberts, *An analysis of solute structure-human epidermal transport relationships in epidermal iontophoresis using the ionic mobility: pore model.* J Control Release, 1999. **58**(3): p. 323-33.
23. Phipps, J.B., R.V. Padmanabhan, and G.A. Lattin, *Iontophoretic delivery of model inorganic and drug ions.* J Pharm Sci, 1989. **78**(5): p. 365-9.
24. Abla, N., et al., *Effect of charge and molecular weight on transdermal peptide delivery by iontophoresis.* Pharm Res, 2005. **22**(12): p. 2069-78.
25. Schuetz, Y.B., et al., *Structure-permeation relationships for the non-invasive transdermal delivery of cationic peptides by iontophoresis.* Eur J Pharm Sci, 2006. **29**(1): p. 53-9.
26. Comella, C.L., *Sleep disorders in Parkinson's disease: an overview.* Mov Disord, 2007. **22 Suppl 17**: p. S367-73.
27. Steiger, M., *Constant dopaminergic stimulation by transdermal delivery of dopaminergic drugs: a new treatment paradigm in Parkinson's disease.* Eur J Neurol, 2008. **15**(1): p. 6-15.
28. Godin, B. and E. Touitou, *Transdermal skin delivery: predictions for humans from in vivo, ex vivo and animal models.* Adv Drug Deliv Rev, 2007. **59**(11): p. 1152-61.
29. Kanikkannan, N., J. Singh, and P. Ramarao, *In vitro transdermal iontophoretic transport of timolol maleate: effect of age and species.* J Control Release, 2001. **71**(1): p. 99-105.

8

Summary, conclusions and future perspectives

1 Summary

For more than 45 years orally dosed levodopa (L-DOPA) has been regarded as the gold standard therapy for symptomatic treatment of Parkinson's disease (Pd) [1]. However its possible neurotoxicity and more importantly the induction of movement disorders after chronic use of L-DOPA, demand for alternative therapies [2]. One of the most important alternatives is the use of dopamine agonists, such as apomorphine, ropinorole, rotigotine and 5-OH-DPAT, which directly activate the post synaptic receptor [3]. Dopamine agonists are generally less associated with motor complications after long term use [4-5]. In addition continuous stimulation of the dopamine receptors is believed not only to reduce dyskinesia and motor complications, but also can be beneficial for other non-motor symptoms of Pd [6]. This emphasizes the need for controlled delivery that provides continuous dopaminergic stimulation. An attractive non-invasive delivery technique is transdermal iontophoresis.

By application of a low current across the skin it is possible to enhance the delivery of small charged molecules. At steady state conditions a constant delivery can be provided. In addition by modulation of the current density it is possible to adjust the administration rate and thus the dose to the demand of the therapy [7]. This can be of great benefit in early stage Pd, because initiation of therapy demands rapid dose adjustments. Therefore in the last decade the transdermal iontophoretic delivery of several dopamine agonists has been investigated: apomorphine, ropinirole, 5-OH-DPAT and rotigotine. These non-ergot dopamine agonists showed promising results *in vitro* and *in vivo*, demonstrating the feasibility of transdermal iontophoretic delivery of dopamine agonist for the symptomatic treatment of Parkinson's disease, as discussed in **CHAPTER 1**. But further optimization and improvement of the iontophoretic delivery of dopamine agonist is required to achieve a strong therapeutic effect. Higher transport efficiency can also lead to a reduction of the patch size and minimization of the applied current density. This can merely enhance the clinical applicability of transdermal iontophoresis.

The general objective of the presented research is the optimization of the transdermal iontophoretic delivery of dopamine agonists and its prodrugs for the symptomatic treatment of Parkinson's disease. To achieve this goal, the following specific items are considered:

1. Optimizing the transdermal iontophoretic delivery *in vitro* of a series of potent dopamine agonists, including rotigotine, 5-OH-DPAT and other potent

structural analogs. In addition the mechanisms driving the iontophoretic transport are addressed.

2. Synthesis of novel dopaminergic prodrugs of 5-OH-DPAT with an extra chargeable group for transdermal iontophoretic delivery. Subsequently the chemical and enzymatic stability are examined. This part of the investigations was performed by Jeroen De Graan and will result in a dissertation at the Rijks Universiteit Groningen, Groningen, The Netherlands
3. *In vitro* iontophoresis of selected prodrugs of 5-OH-DPAT to investigate the feasibility for transdermal iontophoretic delivery
4. Pharmacokinetic-pharmacodynamic (PK-PD) studies in an animal model with the most promising candidates with a special focus on controlling the plasma concentration and the pharmacodynamic effect with transdermal iontophoresis
5. Evaluation and optimization of the kinetic models, developed by Nugroho *et al.* for the characterization of transdermal iontophoretic transport *in vitro* and *in vivo* [8-10]

Part I-Optimizing the transdermal iontophoretic delivery of dopaminergic drugs *in vitro*

Previous studies showed the feasibility of transdermal iontophoretic delivery of 5-OH-DPAT *in vitro* [11] and *in vivo* [10]. But a thorough mechanistic characterization is still missing. Elucidating transport mechanisms driving the iontophoretic delivery is crucial to understand and optimize the iontophoretic delivery *in vivo*.

In **CHAPTER 3**, the transdermal iontophoretic delivery *in vitro* of 5-OH-DPAT was investigated from a mechanistic point of view. Especially the electroosmotic flow and the influence of the composition of the donor and acceptor phase were addressed. Acetaminophen as marker for the electroosmotic flow was also evaluated and approved in this chapter. The total flux is the sum of the passive, electroosmotic and electromigrative flux. The contribution of the passive flux was negligible. The main driving force for the iontophoretic delivery of 5-OH-DPAT is electromigration. Electromigration contributes for more than 85% to the total flux. Furthermore decreasing the pH of the donor phase from 6.0 to 5.0 did not affect the total flux at steady state ($Flux_{ss}$) situation. The $Flux_{ss}$ increased 2.5- to 3-fold when the amount of Na^+ in the donor phase decreased from 78 mM to 10 mM. The $Flux_{ss}$ showed a non-linear hyperbolic correlation with the donor concentration of 5-OH-DPAT and

reached a plateau towards the maximum solubility of 5-OH-DPAT in the donor phase. Together with the observed linear correlation between the $Flux_{ss}$ and the current density, this shows that the administered dose can easily be adjusted with transdermal iontophoresis by changing the donor concentration and/or the current density.

The flux of 5-OH-DPAT decreased with decreasing pH of the acceptor phase from 7.4 to 6.2. This phenomenon was explained by an alteration of the permselective properties of the skin. At pH 6.2 the skin is less negatively charged, resulting in a reduced electroosmotic flow and increased competition of the counterions (mainly Cl^- ion) from acceptor to donor phase. This comprehensive study demonstrates the high transport efficiency of 5-OH-DPAT and elucidates different transport mechanisms during iontophoretic delivery.

A structurally related compound, rotigotine, is the first dopamine agonist in a passive patch (Neupro®, UCB pharma) that is on the market in Europe for early and advanced Parkinson's disease [12-13]. *In vitro* investigations of rotigotine.HCl showed that with transdermal iontophoresis a higher transport rate with a shorter lag time can be achieved compared to passive delivery [14]. However in follow up studies, the maximum solubility in the donor phase was a limiting step to further enhance the iontophoretic transport [15].

One of the possibilities to change the physicochemical properties of a compound is the use of a different salt form. Therefore, in **CHAPTER 4**, passive and transdermal iontophoretic studies were conducted with a different salt form of rotigotine, rotigotine.H_3PO_4. The results were compared to those obtained for rotigotine.HCl [14-15]. Prior to the transport studies, solubility studies showed that the solubility of rotigotine.H_3PO_4 was 2, 6 and 10-fold higher than the solubility of the HCl-salt at pH 6.0, 5.0 and 4.0, respectively. Moreover, because of the absence of a common ion effect, the amount of NaCl did not affect the maximum solubility in the donor phase. At low donor concentrations the transdermal passive and iontophoretic flux of rotigotine.H_3PO_4 and rotigotine.HCl were not significantly different. Due to the increase in maximum solubility of rotigotine the maximal iontophoretic transdermal transport of this compound however was almost twice when using rotigotine.H_3PO_4 (135.8±12.5 $nmol.cm^{-2}.h^{-1}$) instead of rotigotine.HCl (80.2±14.4 $nmol.cm^{-2}.h^{-1}$).

Subsequently, the potential of the iontophoretic delivery of rotigotine *in vivo* was evaluated in a series of simulations. In a first step the transport parameters of the iontophoretic delivery *in vitro* across human stratum corneum (HSC) were estimated using the compartmental kinetic models proposed by Nugroho *et al.* [8]. These

models were based on the assumption of a zero-order mass transfer from the patch to the skin and a first order release from the skin to the acceptor phase (*in vitro*) or the systemic circulation (*in vivo*). The transport parameters were the zero-order mass input (I_0), the skin release constant (K_R) and the lag time [16]. The kinetic model described the *in vitro* flux adequately. In the next step the apparent pharmacokinetic parameters, reported in literature [17-21], were combined with the estimated transport parameters to simulate the plasma levels *in vivo*. It was assumed that iontophoretic transport *in vivo* is the same as iontophoretic transport *in vitro* across HSC. The simulations demonstrated two important benefits of iontophoretic over passive transdermal delivery. Firstly, the onset time to achieve the desired level can be significantly reduced. Secondly, the plasma concentration can easily be titrated by modification of the current density to obtain a desired profile.

Next to 5-OH-DPAT and rotigotine, also other members of the 2-aminotetraline group and structural analogs are regarded as potent agonists at the D_1- and/or D_2-receptor in the striatum. 5 candidates were selected based on their potency and molecular structure: 8-OH-DPAC, 5-OH-EPAT, 5-OH-MPAT, 5,6-di-OH-MPAT and 5,6-di-OH-DPAT [22-28]. Except for 8-OH-DPAC, which is a chromanamine, all compounds are 2-aminotetralins. In **CHAPTER 5** the following properties of these 5 therapeutic agents were investigated: solubility, electrophoretic mobility, lipophilicity and *in vitro* transport across HSC and dermatomed human skin (DHS). The results of rotigotine and 5-OH-DPAT, adapted from literature, were added for comparison. Solubility studies ranked these molecules in the following order: rotigotine < 5,6-di-OH-DPAT < 5-OH-DPAT < 5-OH-MPAT < 5-OH-EPAT < 8-OH-DPAC. *In vitro* transport studies demonstrated that small structural changes can affect the iontophoretic transport significantly. Across HSC and DHS 5-OH-EPAT and 5-OH-MPAT showed a significant higher flux, compared to the other compounds investigated.

During current application the observed flux of all compounds did not reach steady state but gradually increased. Therefore to describe the *in vitro* iontophoretic transport a novel kinetic model was introduced. Instead of 1 first order release constant (K_R) to describe the release from the skin to the acceptor phase, as was proposed previously [8], 2 release constants (K_{R1} and K_{R2}) were introduced. This model confirms the presence of at least two transport routes as suggested in literature: (i) transport route across the appendageal structures and (ii) the transport route via the intercellular route in the skin [29-33]. Besides describing the flux profile during and after iontophoresis it is also important to identify the physicochemical properties that are related to the different transport parameters. Our

results demonstrate that the electrophoretic mobility and the molecular weight of the molecules can be used to predict the zero-order mass input into the skin (I_0) and the release constant K_{R2}, respectively. In addition K_{R1} is related to the lipophilicity, although further research is required to establish a clear relationship. With these parameters it will be possible to simulate the flux profile, using the proposed kinetic model, even when no steady state has reached yet. This approach can be of great interest for screening a series of new candidates.

Part II-*In vivo* investigations of the controlled iontophoretic delivery of (S)-5-OH-DPAT

Optimization of the iontophoretic delivery of 5-OH-DPAT *in vitro* (**CHAPTER 3**) showed the great potential of this dopamine agonist and gave rise for investigating the controllability in an *in vivo* setting.

In **CHAPTER 6**, the controlled release following transdermal iontophoresis of (S)-5-OH-DPAT, the active enantiomer of 5-OH-DPAT, was investigated in a rat model under anesthetic conditions. Firstly, in analogy to the *in vitro* flux, the *in vivo* flux was linearly correlated with the applied current density. This confirms that the administered dose can easily be titrated by altering the current density. Next to a controlled plasma profile, the second aim of these studies was to investigate the PK-PD during a controlled and reversible pharmacological response following transdermal iontophoresis. Before conduction these PK-PD studies, an animal model under anesthetic conditions was developed. In a control experiment it was demonstrated that anesthesia (fentanyl, fluanisone and midazolam), current application with transdermal iontophoresis and blood sampling had no influence on the striatal dopamine release (pharmacodynamic end point). Thereafter the plasma profile and the striatal dopamine release were monitored simultaneously in the validated rat model following transdermal iontophoresis and intravenous (IV) infusion of (S)-5-OH-DPAT. For both administration routes a strong decrease in striatal dopamine release was observed, that returns to its initial state within 2h after the end of the administration.

The experimental data were extensively analyzed using non-linear mixed-effect modeling. To facilitate discrimination between delivery-specific parameters (I_0, K_R) and drug specific parameters (Cl, Q, V2, and V3), the data following transdermal

iontophoresis and intravenous (IV) infusion were analyzed simultaneously. The kinetic models to describe the plasma profile following transdermal iontophoresis, adapted from literature, were based on the zero-order mass input from the donor phase into the skin and the first order release from the skin to the systemic circulation [9]. In contrast to *in vitro* iontophoresis, one first order release constant (K_R) was sufficient to adequately describe the plasma profile following iontophoresis. To describe the striatal dopamine release, two models were compared: (i) indirect response model type I with inhibition of the production of response *vs* (ii) effect compartment model with sigmoidal I_{max} model. Based on the Akaike's information criterion (AIC) and the visual predictive check, it can be concluded that the effect compartment model describes more adequately the striatal dopamine release. Furthermore covariate analysis suggested that the delivery rate can be important for establishing a desired effect. The use of an integrated PK-PD model suggested that the steady state plasma concentrations can be translated to continuous dopaminergic stimulation. This can be of great benefit for symptomatic treatment of Parkinson's disease. It is generally believed that continuous stimulation of the dopamine receptor reduces motor fluctuations after chronic use and can be beneficial for non-motor complications, such as nocturnal disturbances [6].

Part III-Transdermal iontophoretic delivery of ester prodrugs of 5-OH-DPAT: from synthesis to *in vivo* studies

The promising results of the iontophoretic delivery *in vitro* and *in vivo* encouraged us to further improve the applicability of 5-OH-DPAT. Therefore 5-OH-DPAT, which has limited aqueous solubility, was esterified with four natural occurring amino acids: glycine-, proline-, valine- and β-alanine. The four resulting prodrugs all contain an extra chargeable amine group, compared to the parent drug.

In **CHAPTER 7** a thorough investigation is presented addressing the following properties of these prodrugs: chemical stability, solubility and transdermal iontophoretic transport. Stability studies investigated the influence of pH, temperature, current application and presence of skin on the stability of the prodrugs. Increasing the pH and temperature decreased the stability of all prodrugs, while current application and the presence of HSC did not affect the stability. Based on these results, valine- and β-alanine-5-OH-DPAT, with acceptable stability, were selected to conduct solubility and iontophoretic transport studies with. Compared to

the parent drug 5-OH-DPAT, valine- and β-alanine-5-OH-DPAT showed a 4- and more than 14-fold increase in maximum solubility in the donor phase (citric buffer, pH 5.0 with 68 mM NaCl), respectively. This enables to reduce significantly the patch size, without reducing the substantial amount of drug present in the patch. Iontophoretic transport studies *in vitro* across HSC and DHS, demonstrated that valine-5-OH-DPAT, a more lipophilic drug, was transported less efficiently than 5-OH-DPAT across both skin types. In contrast, β-alanine-5-OH-DPAT, a more hydrophilic prodrug, was transported with the same efficiency across HSC, but 40% more efficient across DHS compared to 5-OH-DPAT. It was also observed that both prodrugs during iontophoresis are substantially hydrolyzed to the parent drug 5-OH-DPAT, with a higher hydrolysis rate across DHS compared to HSC.

Based on the *in vitro* results, β-alanine-5-OH-DPAT was selected for *in vivo* iontophoretic transport studies in the novel validated animal model, presented in **CHAPTER 6**. The results of the active enantiomer of the prodrug, β-alanine-(S)-5-OH-DPAT, were compared to the results of (S)-5-OH-DPAT, presented in the previous chapter. Despite a higher *in vitro* transport, lower plasma concentrations were observed following 1.5h current application (250 $\mu A.cm^2$) of β-alanine-(S)-5-OH-DPAT in comparison to (S)-5-OH-DPAT. However the prodrug showed higher plasma concentrations post-iontophoresis, explained by a delayed release due to hydrolysis and skin depot formation. This resulted in a pharmacological effect with the same maximum as 5-OH-DPAT, but the effect lasted for a significant longer time. In analogy to (S)-5-OH-DPAT, the plasma profile and dopamine release following transdermal iontophoresis of β-alanine-(S)-5-OH-DPAT were analyzed using an integrated PK-PD model. To account for hydrolysis and depot formation, an extra compartment was integrated in the PK model for transdermal iontophoresis (**CHAPTER 6**) between the skin and the plasma concentration in parallel. Similar to (S)-5-OH-DPAT, an effect compartment model was used to describe the striatal dopamine release. The current findings show the possibility to tailor the physicochemical properties, the pharmacokinetic profile and pharmacological response with the use of prodrugs. The prodrug β-alanine-5-OH-DPAT with a balanced stability and high transport efficiency is a promising candidate for symptomatic treatment of Parkinson's disease.

2 Conclusions and future perspectives

Transdermal iontophoretic delivery of dopamine agonists has great potential for the symptomatic treatment of Parkinson's disease. It can be of benefit for reducing or replacing L-DOPA therapy, certainly in the initial stage of treatment, since continuous administration of dopamine agonists is less associated with motor complications [2]. The results of the studies presented in this thesis, together with previous studies, show that 2-aminotetralins (5-OH-MPAT, 5,6-di-OH-MPAT, 5-OH-EPAT, 5-OH-DPAT, 5,6-di-OH-DPAT, rotigotine) and 8-OH-DPAC can be transported across the skin with high efficiency [10-11, 15]. One of the advantages of transdermal iontophoresis is the possibility to achieve continuous plasma concentrations, leading to constant dopaminergic stimulation, as was demonstrated for (S)-5-OH-DPAT in **CHAPTER 6** and β-alanine-(S)-5-OH-DPAT in **CHAPTER 7**. These observations give rise for further developing an iontophoretic transdermal delivery device, with ultimately the possibility to design a feedback control system. This could result in a self-controlling delivery device, facilitating its therapeutic use. Such a self-controlling iontophoretic delivery device should have the following properties: (i) Drug: the device should contain a potent dopamine agonist which elicits a strong dopaminergic effect with a relatively small dose. Additionally, the dopamine agonist should have a good aqueous solubility, should be transported efficiently across the skin and should have excellent blood-brain barrier permeability. (ii) Delivery: besides an efficient delivery, that enables reducing the applied current density, the transdermal delivery should also be easily adjustable. As demonstrated for (S)-5-OH-DPAT in **CHAPTER 6**, the drug input and plasma concentration can easily be controlled by adjusting the current density. (iii) Biomarker: there should be a valid and sensitive surrogate endpoint available to monitor the drug effect. Preferably a pharmacodynamic biomarker is monitored instead of the drug plasma concentration. This poses quite a challenge for Parkinson's disease, since the biomarkers used up to today to monitor the dopaminergic effect in animals are measured intracranially. For humans, researchers are restricted to pharmacodynamic end-points such as tapping scores, walking time [34] and categorical rating scales [35-36]. All these end-points require active and conscious involvement of the patients. This underscores the need for novel biomarkers to monitor the dopaminergic effect in patients. (iv) monitoring: Such biomarkers are preferably monitored non-invasively, for instance with reverse iontophoresis. The utility of reverse iontophoresis has been demonstrated for the

treatment of diabetes: the Glucowatch® monitors with reverse transdermal iontophoresis the glucose level in plasma [37]. (v) Biosensor, that analyses the biomarker: should be small, preferably on nano or micro scale and therefore be very sensitive.

The development of such a self-controlling delivery device constitutes an enormous challenge, which requires the development and optimization of the chemical structure, the delivery and the detection. This involves an excellent understanding of

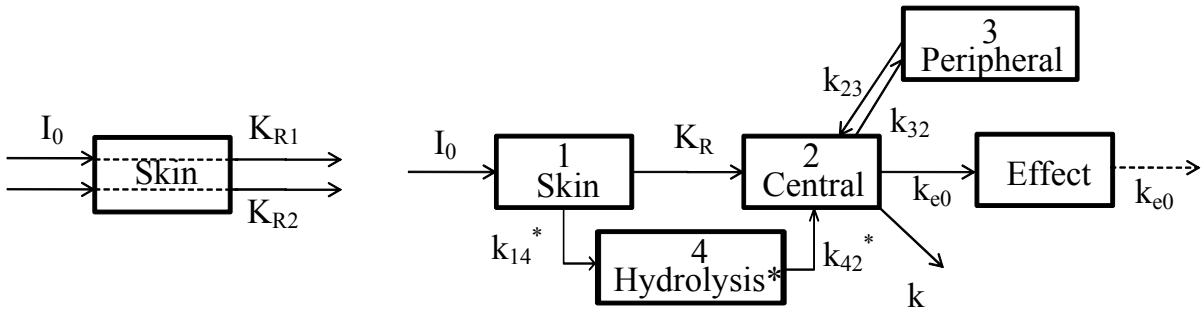

in vitro model PK-PD model

Figure 1: Schematic representation of the compartmental model of the iontophoresis *in vitro*, the pharmacokinetic and pharmacodynamic model following transdermal iontophoresis.

I_0: zero order drug input during time of current application
K_{R1} and K_{R2}: first order release constants from the skin to the acceptor phase (*in vitro*)
K_R: first order release constants from the skin to the plasma (*in vivo*)
k: elimination rate constant
k_{14}: first order skin-hydrolysis compartment distribution rate constant
k_{42}: first order hydrolysis compartment-plasma distribution rate constant
k_{23}: first order plasma-peripheral distribution rate constant
k_{32}: first order peripheral-plasma distribution rate constant
k_{e0}: first order distribution rate constant from plasma to effect compartment and elimination rate constant from effect compartment

*The inclusion of a hydrolysis compartment in the model is only used following transdermal iontophoresis of the prodrug β-ala- (S)-5-OH-DPAT.

the relationships between the molecular properties, the iontophoretic transport, the pharmacokinetics and the pharmacodynamics. To obtain a better understanding of these relationships, a powerful analytical tool or method is required that can describe and predict the time course of the iontophoretic transport, the plasma concentration and the drug effect. The compartmental models, as used in **CHAPTER 5-7**, allow such type of analysis. The models describe in a comprehensive manner the time dependent transport, plasma and drug effect profiles. With regard to the characterization of the iontophoretic transport this offers major advantages over the use of methods based on the estimation of single parameters (e.g. permeation-lag time method). In addition compartmental modeling is able to connect the rate of iontophoretic delivery to the pharmacokinetic and pharmacodynamic properties and ultimately system behavior.

In this thesis the iontophoretic transport of a series of molecules, with small structural differences, were investigated in **CHAPTER 5**. This allowed investigating the influence of the physicochemical properties on the transdermal iontophoretic transport. The transport parameter I_0, which is the zero-order mass input during iontophoresis from donor to skin, could be related not only to the donor concentration and applied current density, but also to the electrophoretic mobility of the compound. Furthermore the two first order release constants from skin to acceptor phase, K_{R1} and K_{R2} are related to the lipophilicity and molecular weight, respectively. Based on these property-transport relationships, simulations were conducted with the kinetic models presented in **CHAPTER 5** to investigate the impact of the different transport parameters on the transport profile (Figure 1). The results of the simulations are displayed in Figure 2. As expected, I_0 affects tremendously the value of the steady state flux, but it does not affect the shape of the flux profile (Figure 2A). The value of the zero-order mass input is influenced by three factors, the donor concentration, the current density and the electrophoretic mobility. To diminish skin irritation, the current density should be kept as low as possible. Therefore electrophoretic mobility and aqueous solubility for a high donor concentration are the key parameters to increase the iontophoretic transport. Screening different compounds with capillary electrophoresis to determine the electrophoretic mobility is useful to select appropriate candidates for transdermal iontophoresis. In addition improving solubility with the use of prodrugs (**CHAPTER 7**) or by selecting an alternative salt form (**CHAPTER 4**) can merely help to reduce the patch size, without reducing the amount of drug in the patch.

Figure 2B shows the influence of the release constant K_{R1} on the transport profiles. As can be observed, K_{R1} affects the time to steady state during the current

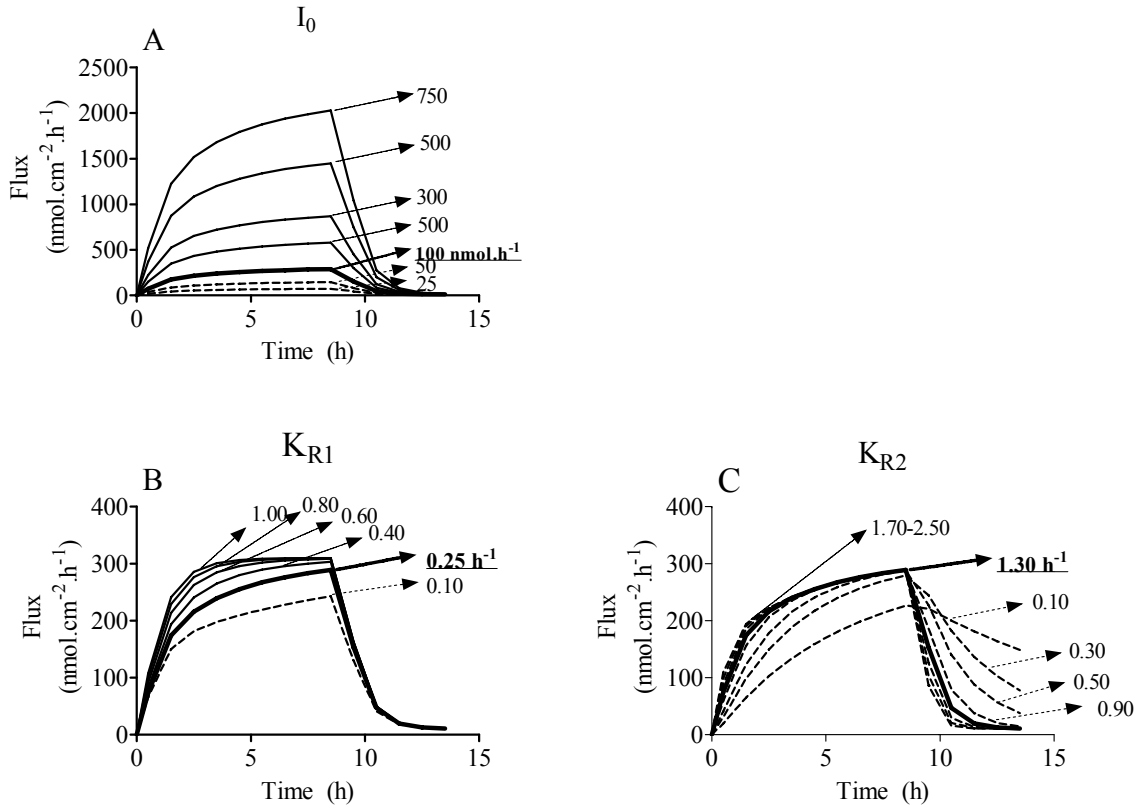

Figure 2: Simulations of iontophoretic transport profiles *in vitro*, changing the zero-order mass input I_0 (**A**), the first order release constants, K_{R1} (**B**) and K_{R2} (**C**). The full thick line is the simulated profile with the transport parameters of 5-OH-DPAT, the intermittent lines and the full lines are the profiles with lower and higher values than of 5-OH-DPAT, respectively. Depicted in every graph are also the values of the parameter used for the simulations. Underlined are the values of transport parameters of 5-OH-DPAT. These values were kept constant when simulations were conducted, changing another transport parameter.

application. The higher K_{R1}, the faster steady state is reached. Therefore a high K_{R1} could be favorable, but K_{R1} is related to the lipophilicity of the compound. Compounds with a higher lipophilicity are less soluble in an aqueous environment and are therefore transported less efficiently with transdermal iontophoresis, as was observed for instance for rotigotine (**CHAPTER 4**). This should be taken into account when screening new compounds. The value of K_{R2} affects the time to steady state and the post-iontophoretic decline of the transport rate (Figure 2C). A lower K_{R2}, attributed to a higher molecular weight, results in a slower release from the skin

into the acceptor phase. Figure 2C, shows also that for K_{R2} values, higher than 1.30, no large differences in transport profiles are observed. This value can be considered as a minimum threshold value for a relatively rapid transport through and a rapid release from the skin. These simulations show that multiple parameters should be taken into account to optimize the iontophoretic transport profile.

A next step is to evaluate the influence of transport parameters K_R and I_0 on the drug profile *in vivo*. Based on the obtained results and using the PK-PD models (Figure 1), as presented in **CHAPTER 6** and **7**, *in vivo* simulations were performed. The results are depicted in Figure 3. The intrinsic zero-order mass driving force I_0 tremendously affects the PK profile as shown in Figure 3A. In a linearly dependent manner the steady-state plasma concentration is augmented with increasing I_0. The corresponding simulations performed to investigate the PD effect with changing I_0 are shown in Figure 3C. From an I_0 value of 50 $\mu g.h^{-1}$ the maximum response remained unchanged when increasing the intrinsic driving force I_0. With increasing dose the duration of maximum effect after patch removal increases. This was also observed for β-ala-(S)-5-OH-DPAT in **CHAPTER 7**, where a higher value of I_0, compared to its parent drug resulted in a prolonged effect. This means that the time to recover to basal dopamine levels increases with increasing dose. On the one hand the prolonged effect can be beneficial for patients who suffer from nocturnal disturbances. Nocturnal disturbances are one of the most common non-motor complications in patients with PD [38]. It is believed that continuous stimulation of the DA receptor during the night can reduce the occurrence of nocturnal disturbances [6]. On the other hand this prolonged effect can be a drawback to initiate therapy to treat Parkinson's disease, since rapid changes in delivery schemes may be required. In addition one should also take into account that with increasing plasma concentrations there is an increasing risk of side effects, such as nausea, vomiting and hallucinations [2]. Therefore it is imperative to achieve constant dopaminergic stimulation with optimized plasma concentrations, based on an understanding of the PK-PD relationship and driven by an acceptable current density. The delivery rate also affects the pharmacodynamic efficiency (EFF), as was observed in **CHAPTER 6**. *EFF* is defined as the pharmacological response per unit of concentration and calculated with the following equation:

$$EFF = \frac{AAEC}{AUC} \tag{1}$$

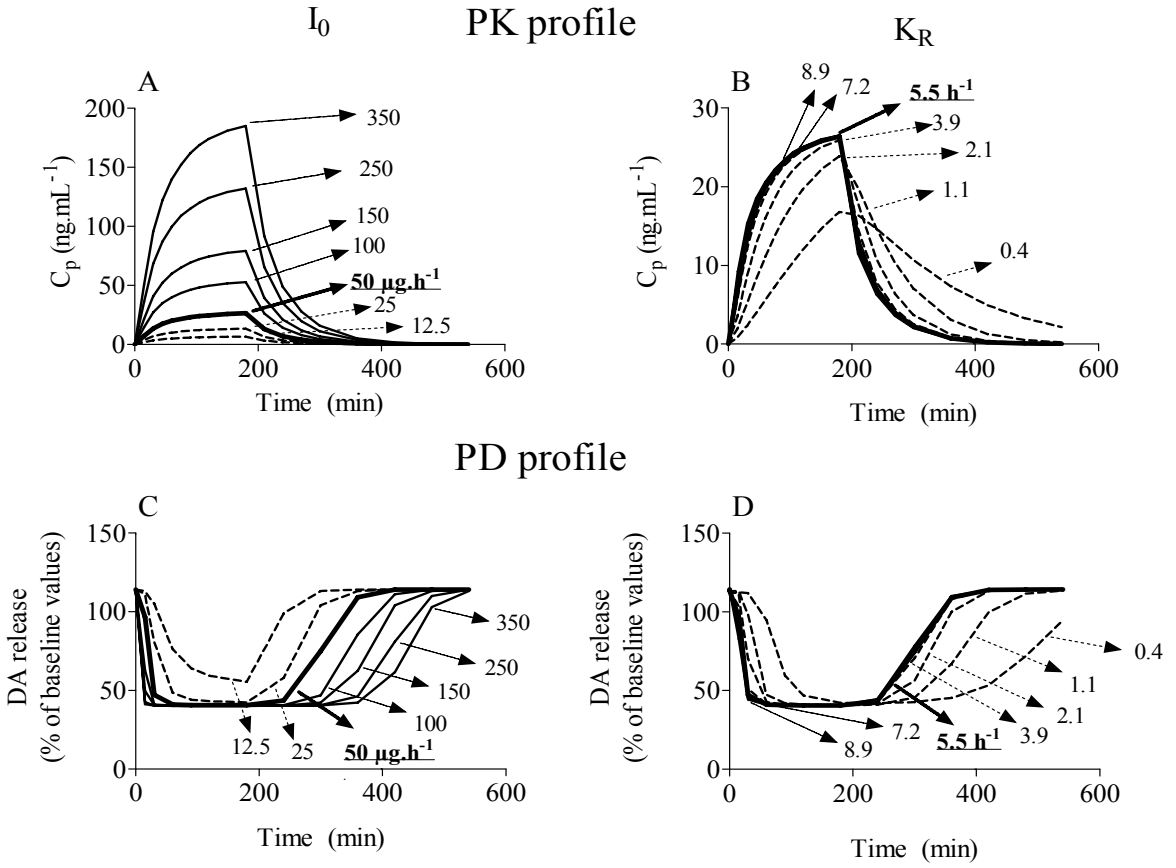

Figure 3: Simulations of transport profiles *in vivo*, changing the different transport parameters. **A**: the plasma concentration profile, simulated with different values of the zero-order mass input I_0. **B**: the plasma concentration profile, simulated with different values of the first order release constants K_R. **C-D**: the corresponding dopamine release (PD endpoint) profile, simulated with different values of I_0 and K_R. The full thick line is the simulated profile with the transport parameters of 5-OH-DPAT, the intermittent lines and the full lines are the profiles with lower and higher values then of 5-OH-DPAT, respectively. Underlined are the values of transport parameters of 5-OH-DPAT. These values were kept constant when simulations were conducted, changing another transport parameter.

Where *AUC* (ng.ml^{-1}.min) is the area under the plasma concentration curve and *AAEC* (DA%.min) is the area above the effect curve (normalized for baseline dopamine levels). Within the range of delivery rates, investigated in **CHAPTER 6**, it was suggested that a higher delivery rate is favorable. By adjusting the current density, the delivery rate can easily be titrated. Therefore with transdermal iontophoresis the design of complicated dosing regimens is possible. For instance, a high initial dose, obtained with a high current density, can be followed by a lower maintenance dose by gradually decreasing the current density. Next to I_0, the release constant K_R also affects the PK-PD profiles. Figure 3B shows that K_R affects the entire plasma profile during and after iontophoresis. K_R values of 3.9 and higher do not change the profile dramatically. If K_R drops below a value of 2.1 h^{-1} however, the PK profile starts to show a slower time to steady state and also a slower decline of the transport post iontophoresis. These profile changes are also found in the PD profile as shown in Figure 3D. Again a K_R value of 3.9 h^{-1} can be considered as the threshold K_R value. 5-OH-DPAT has a K_R of 5.5 and small structural changes, resulting in relative small differences in K_R would not affect the PK and PD profile.

The similarity of the compartmental modeling of the *in vitro* and *in vivo* transport allowed us to examine the *in vitro – in vivo* correlation specifically. For both the analysis of the *in vitro* transport and the *in vivo* plasma profiles kinetic models were used, based on the zero-order mass input from donor patch to skin (I_0) and the first order release constant(s) (K_R) from skin to acceptor (*in vitro*) or plasma (*in vivo*). However, to describe *in vitro* transport 2 release constants were required for all the compounds investigated. In contrast, to describe *in vivo* iontophoretic transport of 5-OH-DPAT 1 release constant was sufficient. In addition, an extra (hydrolysis) compartment was included in the *in vivo* PK model to adequately describe the transport of β-ala-(S)-5-OH-DPAT. This suggests that different transport mechanisms govern the transdermal iontophoretic transport *in vitro* and *in vivo*. These differences can at least partially be attributed to the following factors. Firstly, the structure of human skin differs from the structure of rats. Especially the density of hair follicles will contribute to the difference. Previous studies showed that the appendageal route is believed to be the predominant route during iontophoresis and post-iontophoresis [33]. Therefore it is suggested that that the higher density of hair follicles in rat skin results in a much higher contribution of the appendageal route, reflected by a higher K_{R2}. *In vivo* across rat skin the contribution of K_{R1} might therefore become negligible. This could explain why one K_R is sufficient to describe the skin release *in vivo*. Secondly the clearance of the penetrant by the acceptor flow may be different from the clearance *in vivo* by the microcirculation in the skin [39].

Thirdly, concerning the hydrolysis of β-ala-5-OH-DPAT, the activity of the esterase *in vivo* may be different from the esterase activity in freshly excised skin. Despite these differences the transport parameters *in vitro* and *in vivo* corresponded relatively well.

The estimated *in vivo* steady state flux (J_{ss} *vivo)* is compared with the estimated *in vitro* steady state flux (J_{ss} *vitro*) (Table 1). The absolute value of J_{ss} *vivo* in rats corresponds most closely with the J_{ss} *vitro* across dermatomed human skin for 5-OH-DPAT and to the J_{ss} *vitro* across human stratum corneum for β-ala-5-OH-DPAT. Since K_{R2} describes the release constant post iontophoresis *in vitro*, this

Table 1: Comparison of the transdermal iontophoretic steady state flux (J_{ss}) of 5-OH-DPAT and β-ala-5-OH-DPAT across rat skin *in vivo* and human skin *in vitro*.

			5-OH-DPAT		**β-ala-5-OH-DPAT**	
	Parameter	unit	mean	RSE%	mean	RSE%
Rat skin *in vivo*	J_{ss} *vivo*	$nmol.cm^{-2}.h^{-1}$	174.6	8	221.2	8
	K_R	h^{-1}	2.2[a]-5.5[b]	21-26	0.31[c]-4.8[d]	23-21
HSC *in vitro*	J_{ss} *vitro*	$nmol.cm^{-2}.h^{-1}$	239.4	9	272.5	4
	K_{R2}	h^{-1}	1.39	10	1.69	8
DHS *in vitro*	J_{ss} *vitro*	$nmol.cm^{-2}.h^{-1}$	190.3	1	381.3	7
	K_{R2}	h^{-1}	0.56	11	0.588	5

Note: The transport rates *in vivo* are normalized to a current density of 500 $\mu A.cm^{-2}$. The donor concentration was 3.9 mM and pH was 5.0. [a]This value was obtained from the PK study; [b]This value was obtained from the PK-PD study; [c]This value is the first order release constant K_R value from the skin to central compartment; [d]This value is the first order release constant k_{42} value from the hydrolysis to central compartment

release constant was compared to the *in vivo* release constant. As can be observed, the *in vivo* release constant was more closely related to the *in vivo* release constant across HSC. For both 5-OH-DPAT and the prodrug β-ala-5-OH-DPAT these differences between the *in vitro* and *in vivo* transport parameters are relatively small, certainly considering the interspecies differences. Nugroho *et al.* showed comparable differences between the *in vitro* and *in vivo* transport parameters using the same species [10]. Furthermore in the same study it was demonstrated that by combining the *in vitro* transport parameters with the *in vivo* PK-PD parameters, it was possible to predict the pharmacokinetic transport profile and even the pharmacodynamic effect [10]. In addition, previous studies showed that iontophoresis diminishes the interspecies variations [40]. This emphasizes that *in vitro* transport studies across human skin can provide valuable information for extrapolation towards the *in vivo* situation, even in other species like rats. Modeling and simulations can therefore be very helpful in designing novel experiments.

In conclusion, this thesis presents various potential candidates for the symptomatic treatment of Parkinson's disease with the use of transdermal iontophoresis. Thereby a large framework is constructed to screen new potential candidates for transdermal iontophoretic delivery from physicochemical properties via *in vitro* transport studies towards *in vivo* application. This framework is supported by the application of novel kinetic models to describe the transport profiles during and after iontophoresis. These models can be used to simulate and design new *in vivo* studies and to get a better comprehension about the *in vitro-in vivo* and the PK-PD relationships. Ultimately these models constitute a scientific basis to design a closed-loop self controlled delivery system.

References

1. Hornykiewicz, O., *L-DOPA: from a biologically inactive amino acid to a successful therapeutic agent.* Amino Acids, 2002. **23**(1-3): p. 65-70.
2. Tugwell, C., *Parkinson's disease in focus*. 1st ed. In focus. 2008, London: Pharmaceutical Press. 237.
3. Lim, E., *A walk through the management of Parkinson s disease.* Ann Acad Med Singapore, 2005. **34**(2): p. 188-95.
4. Antonini, A. and P. Barone, *Dopamine agonist-based strategies in the treatment of Parkinson's disease.* Neurol Sci, 2008. **29 Suppl 5**: p. S371-4.
5. Yamamoto, M. and A.H. Schapira, *Dopamine agonists in Parkinson's disease.* Expert Rev Neurother, 2008. **8**(4): p. 671-7.
6. Steiger, M., *Constant dopaminergic stimulation by transdermal delivery of dopaminergic drugs: a new treatment paradigm in Parkinson's disease.* Eur J Neurol, 2008. **15**(1): p. 6-15.
7. Sage, B.H., *Ionotphoresis*, in *Percutaneous penetration enhancers*, E.W. Smith and H.I. Maibach, Editors. 1995, CRC Press: Boca Raton. p. 351-368.
8. Nugroho, A.K., et al., *Compartmental modeling of transdermal iontophoretic transport: I. In vitro model derivation and application.* Pharm Res, 2004. **21**(11): p. 1974-84.
9. Nugroho, A.K., et al., *Compartmental modeling of transdermal iontophoretic transport II: in vivo model derivation and application.* Pharm Res, 2005. **22**(3): p. 335-46.
10. Nugroho, A.K., et al., *Pharmacokinetics and pharmacodynamics analysis of transdermal iontophoresis of 5-OH-DPAT in rats: in vitro-in vivo correlation.* J Pharm Sci, 2006. **95**(7): p. 1570-85.
11. Nugroho, A.K., et al., *Transdermal iontophoresis of the dopamine agonist 5-OH-DPAT in human skin in vitro.* J Control Release, 2005. **103**(2): p. 393-403.
12. *UCB announces The U.S. Launch of Neupro® (Rotigotine Transdermal System) for the Treatment of Early-Stage Parkinson's Disease*. 2007, UCB Milwaukee (USA).
13. *EMEA. European Public Assessment Report (EPAR), annex I: summary of product characteristics for Neupro.* *Available from http://www.emea.europa.eu/humandocs/PDFs/EPAR/neupro/H-626-PI-en.pdf* 2009.
14. Nugroho, A.K., et al., *Transdermal iontophoresis of rotigotine across human stratum corneum in vitro: influence of pH and NaCl concentration.* Pharm Res, 2004. **21**(5): p. 844-50.
15. Nugroho, A.K., et al., *Transdermal iontophoresis of rotigotine: influence of concentration, temperature and current density in human skin in vitro.* J Control Release, 2004. **96**(1): p. 159-67.
16. Lopez, R.F., et al., *Iontophoretic delivery of 5-aminolevulinic acid (ALA): effect of pH.* Pharm Res, 2001. **18**(3): p. 311-5.
17. Schwarz pharma, L. *Neupro®*. 2007.
18. Cawello, W., M. Braun, and R. Horstmann, *Pharmacokinetics of transdermal rotigotine in subjects with impaired renal function* in *ACCP 34th Annual Meeting*. 2005: Rockville, MD.
19. Cawello, W., et al., *Characteristics of Rotigotine Elimination after patch removal.* European Journal of Neurology, 2006. **13(suppl2)**: p. 85.
20. Cawello, W., et al., *Transdermal administration of radiolabelled [14C]rotigotine by a patch formulation: a mass balance trial.* Clin Pharmacokinet, 2007. **46**(10): p. 851-7.
21. Cawello, W., M. Braun, and H. Boekens, *Absorption, disposition, metabolic fate, and elimination of the dopamine agonist rotigotine in man: administration by intravenous infusion or transdermal delivery.* Drug Metab Dispos, 2009. **37**(10): p. 2055-60.
22. Beart, P.M., et al., *Radioreceptor binding reveals the potencies of N,N-disubstituted 2-aminotetralins as D2 dopamine agonists.* Naunyn Schmiedebergs Arch Pharmacol, 1987. **336**(5): p. 487-93.

23. Beaulieu, M., et al., *N,N-disubstituted 2-aminotetralins are potent D-2 dopamine receptor agonists.* Eur J Pharmacol, 1984. **105**(1-2): p. 15-21.
24. Hacksell, U., et al., *N-Alkylated 2-aminotetralins: central dopamine-receptor stimulating activity.* J Med Chem, 1979. **22**(12): p. 1469-75.
25. Horn, A.S., et al., *Synthesis and dopaminergic activity of a new oxygen isostere of the 2-aminotetralins: N,N-dipropyl-8-hydroxy-3-chromanamine.* Eur J Med Chem, 1988. **22**(4): p. 325-328.
26. Thorberg, S.O., et al., *Aminochromans: potent agonists at central dopamine and serotonin receptors.* Acta Pharm Suec, 1987. **24**(4): p. 169-82.
27. van Vliet, L.A., et al., *Affinity for dopamine D2, D3, and D4 receptors of 2-aminotetralins. Relevance of D2 agonist binding for determination of receptor subtype selectivity.* J Med Chem, 1996. **39**(21): p. 4233-7.
28. Vermue, N.A., et al., *Pharmacological profile of N,N dipropyl-8-hydroxy-3-chromanamine, an oxygen isostere of the dopamine agonist N,N dipropyl-5-hydroxy-2-aminotetralin with enhanced presynaptic selectivity.* Arch Int Pharmacodyn Ther, 1988. **293**: p. 37-56.
29. Alvarez-Roman, R., et al., *Visualization of skin penetration using confocal laser scanning microscopy.* Eur J Pharm Biopharm, 2004. **58**(2): p. 301-316.
30. Barry, W., ed. *Dermatological formulations. Percutaneous Absorption.* . 1983: New York: Marcel Dekker.
31. Cullander, C., *What are the pathways of iontophoretic current flow through mammalian skin?* Adv Drug Deliv Rev, 1992. **9**: p. 119-135.
32. Henchoz, Y., et al., *A fast screening strategy for characterizing peptide delivery by transdermal iontophoresis.* J Control Release, 2009.
33. Turner, N. and R.H. Guy, *Iontophoretic transport pathways: dependence on penetration physcicochemical properties.* J Pharm Sci, 1997. **86**(12): p. 1385-1389.
34. Nelson, M.V., et al., *Pharmacodynamic modeling of concentration-effect relationships after controlled-release carbidopa/levodopa (Sinemet CR4) in Parkinson's disease.* Neurology, 1990. **40**(1): p. 70-4.
35. *The Unified Parkinson's Disease Rating Scale (UPDRS): status and recommendations.* Mov Disord, 2003. **18**(7): p. 738-50.
36. Hoehn, M.M. and M.D. Yahr, *Parkinsonism: onset, progression and mortality.* Neurology, 1967. **17**(5): p. 427-42.
37. Sieg, A., R.H. Guy, and M.B. Delgado-Charro, *Noninvasive and minimally invasive methods for transdermal glucose monitoring.* Diabetes Technol Ther, 2005. **7**(1): p. 174-97.
38. Comella, C.L., *Sleep disorders in Parkinson's disease: an overview.* Mov Disord, 2007. **22 Suppl 17**: p. S367-73.
39. Godin, B. and E. Touitou, *Transdermal skin delivery: predictions for humans from in vivo, ex vivo and animal models.* Adv Drug Deliv Rev, 2007. **59**(11): p. 1152-61.
40. Kanikkannan, N., J. Singh, and P. Ramarao, *In vitro transdermal iontophoretic transport of timolol maleate: effect of age and species.* J Control Release, 2001. **71**(1): p. 99-105.

Appendix

Samenvatting

List of abbreviations

List of publications

Curriculum Vitae

Nawoord

Samenvatting

Levodopa (L-DOPA) wordt al 45 jaar beschouwd als de gouden standaard voor de symptomatische behandeling van de ziekte van Parkinson [1]. De eigenschappen van L-DOPA en de pulsatiele stimulatie van de dopamine receptoren bij orale toediening leiden tot bewegingsstoornissen bij chronisch gebruik van dit geneesmiddel [2]. Daarom wordt er gezocht naar andere geneesmiddelen, zoals dopamine agonisten (voorbeelden zijn apomorphine, ropinorole, rotigotine en 5-OH-DPAT). Deze geneesmiddelen activeren rechtstreeks de post-synaptische dopamine receptoren en worden beschouwd als een belangrijk alternatief voor L-DOPA, aangezien dopamine agonisten in mindere mate bewegingsstoornissen veroorzaken na langdurig gebruik [3]. Meer nog, een continue toediening van deze dopamine agonisten zou kunnen zorgen voor een onafgebroken stimulatie van dopamine receptoren. Dit kan leiden tot een verdere afname van bewegingsstoornissen bij chronisch gebruik en kan voordelig voor andere symptomen van deze ziekte, die niet geassocieerd zijn met beweging (o.a. slaapstoornissen) [4-6]. Een continue toediening van dopamine agonisten kan bereikt worden door gebruik te maken van transdermale iontoforese.

Bij transdermale iontoforese wordt door middel van een potentiaalverschil over de huid een zwakke stroom opgewekt, die het mogelijk maakt om de toediening van kleine geladen moleculen via de huid te bevorderen. De toedieningsnelheid en dus de dosis van het geneesmiddel kan nauwkeurig aangepast worden door de stroom te veranderen [7]. Dit kan een groot voordeel zijn bij het opzetten van een behandeling, omdat vaak snelle dosisaanpassingen nodig zijn. Daarom is gedurende de laatste 10 jaar onderzoek verricht naar de haalbaarheid van transdermale iontoforese van verschillende dopamine agonisten: apomorphine, ropinorole, 5-OH-DPAT en rotigotine. Veelbelovende resultaten werden behaald *in vitro* en *in vivo*, zoals beschreven staat in **HOOFDSTUK 1**. Echter om een optimaal therapeutisch effect te bereiken, moet iontoforetische toediening van dopamine agonisten verder geoptimaliseerd en verbeterd worden. Een verdere optimalisatie is vooral gericht op een efficiënter transport. Dit heeft als voordeel dat een kleinere pleister gebruikt kan worden en/of een lager potentiaalverschil over de huid. De klinische toepasbaarheid van transdermale iontoforese kan hiermee aanzienlijk worden verbeterd.

Het doel van het onderzoek, beschreven in dit proefschrift, was het optimaliseren van de transdermale iontoforetische toediening van dopamine agonisten voor de

symptomatische behandeling van de ziekte van Parkinson. Meer specifiek werden de volgende onderwerpen onderzocht:

1. Optimaliseren van transdermale iontoforese *in vitro* van een reeks dopamine agonisten, waaronder rotigotine, 5-OH-DPAT en structureel analoge verbindingen. Ook werden de transport mechanismen onderzocht, die ten grondslag liggen aan iontoforese.
2. Synthese van nieuwe prodrugs van 5-OH-DPAT, met één of meerdere extra positieve ladingen. De chemische en enzymatische stabiliteit van deze verbindingen werd ook onderzocht. Dit deel van het onderzoek werd uitgevoerd door Jeroen De Graan en zal leiden tot een proefschrift aan de Rijks Universiteit Groningen, Groningen, Nederland.
3. *In vitro* transportstudies met geselecteerde prodrugs om te onderzoeken of deze prodrugs geschikt zijn voor toediening met transdermale iontoforese.
4. Farmacokinetiek-farmacodynamiek (PK-PD) studies in een dierenmodel met de meest belovende geneesmiddelen. Tijdens iontoforese werden zowel de plasmaconcentratie alsook het farmacologisch effect gemeten. Deze studies werden uitgevoerd in samenwerking met Jeroen De Graan.
5. Evaluatie en verdere optimalisatie van de kinetische modellen, die ontwikkeld werden door Kharis Nugroho *et al.* voor het beschrijven van transdermaal iontoforetisch transport *in vitro* en *in vivo* [8-10].

Deel I- Optimalisatie van de transdermale iontoforetische toediening van dopaminerge geneesmiddelen *in vitro*

Eerdere studies toonden aan dat transdermale iontoforetische toediening van 5-OH-DPAT zowel *in vitro* [11] als *in vivo* [10] veelbelovend was. Een volledige karakterisatie van de transport mechanismen tijdens iontoforetisch transport ontbrak echter. Het bepalen van de verschillende mechanismen, die een rol spelen bij iontoforese is belangrijk om iontoforetische toediening *in vivo* te begrijpen en verder te verbeteren.

Eerst werden de mechanismen die een rol spelen bij transdermale iontoforese van 5-OH-DPAT *in vitro* onderzocht. Dit is beschreven in **HOOFDSTUK 3**. Er werd vooral gefocusseerd op de elektro-osmose en de invloed van de samenstelling van de donor- en acceptorfase op het transport van 5-OH DPAT tijdens iontoforese. De mogelijkheid om paracetamol (acetaminophen) te gebruiken als een marker voor elektro-osmose werd ook onderzocht. Het totale transport is de som van passief

transport en transport als gevolg van elektro-osmose en elektromigratie. Elektromigratie, het transport als gevolg van het potentiaalverschil en de lading van het geneesmiddel, draagt meer dan 85% bij aan het totale transport, terwijl electro-osmose, het transport als gevolg van de negatieve lading in de huid, ongeveer 15% bijdraagt. Passief transport is nagenoeg te verwaarlozen. Een verlaging van de pH van de donoroplossing van 6.0 naar 5.0 had geen invloed op het totale transport onder stationaire condities ($Flux_{ss}$). Een vermindering van de hoeveelheid Na^+-zout van 78 naar 10 mM in de donorfase resulteerde in een 2.5- tot 3-voudige verhoging van de $Flux_{ss}$. Er was een hyperbolische correlatie tussen de $Flux_{ss}$ en de donorconcentratie van 5-OH-DPAT. Dicht bij de maximale oplosbaarheid van 5-OH-DPAT benaderde het transport een plateauwaarde. Ook vertoonde de $Flux_{ss}$ een lineair verband met de stroomdichtheid. Deze twee factoren tonen aan dat de toegediende dosis heel nauwkeurig getitreerd kan worden met transdermale iontoforese door de donorconcentratie en de stroomdichtheid aan te passen. Het verlagen van de pH van de acceptorfase van 7.4 naar 6.2 zorgde ook voor een afname van de 5-OH-DPAT flux. Dit kan verklaard worden door een verandering van de doorlaatbaarheid van de huid. Bij pH 6.2 is de huid minder negatief geladen, waardoor het elektro-osmotisch transport verlaagd wordt en de competitie van tegenionen (vnl. Cl^-), die migreren van acceptor- naar donorfase, verhoogd wordt. Deze studie toont aan dat 5-OH-DPAT efficiënt door de huid getransporteerd kan worden. Tevens zijn verschillende transportmechanismen die ten grondslag liggen aan deze efficiëntie ontrafeld.

Rotigotine, structureel verwant aan 5-OH-DPAT, is de eerste dopamine agonist, die geformuleerd in een passieve transdermale pleister (Neupro®, UCB Pharma), op de markt is gebracht in Europa [12-13]. Uit *in vitro* studies met rotigotine.HCl bleek, dat in vergelijking met passief transport, door middel van iontoforese een hoger transport met een kortere vertragingstijd kon worden bereikt [14]. In een vervolgstudie werd echter duidelijk dat de oplosbaarheid van rotigotine.HCl in de donoroplossing de beperkende factor was om het transport verder te verhogen.

Eén van de mogelijkheden om de oplosbaarheid van een molecule aan te passen is het gebruik van een ander tegenzout. In **HOOFDSTUK 4** werden transportstudies uitgevoerd onder passieve en iontoforetische condities met een andere zoutvorm van rotigotine, namelijk rotigotine.H_3PO_4. Het transport werd vergeleken met het transport van rotigotine.HCl [14-15]. De oplosbaarheid van rotigotine.H_3PO_4 was respectievelijk 2, 6 en 10 maal hoger dan de oplosbaarheid van het HCl-zout bij pH 6.0, 5.0 en 4.0. Bovendien had de hoeveelheid NaCl geen invloed op de maximale oplosbaarheid bij rotigotine H_3PO_4. Uit de daaropvolgende transportstudies bleek dat

er bij lage concentraties geen verschil was in transport efficiëntie. Echter door de toegenomen maximale oplosbaarheid werd een hoger maximaal transport bereikt met rotigotine.H_3PO_4 (138±12.5 nmol.cm^{-2}.h^{-1}) vergeleken met rotigotine.HCl (80.2± 14.4nmol.cm^{-2}.h^{-1}). Tenslotte werd er met behulp van simulaties onderzocht of iontoforese geschikt is voor rotigotine-toediening *in vivo*. Eerst werd het transdermale transport door humaan stratum corneum (HSC) tijdens iontoforese beschreven met behulp van de kinetische modellen, ontwikkeld door Nugroho *et al.* [8]. Deze modellen zijn gebaseerd op de veronderstelling dat er een 0de orde transport optreedt van het donorcompartiment naar de huid en een 1ste orde transport van de huid naar het acceptorcompartiment (*in vitro*) of de bloedcirculatie (*in vivo*). Het kinetisch model beschreef het iontoforetisch transport nauwkeurig. Daarna werden deze *in vitro* transport parameters gecombineerd met de farmacokinetische parameters, die in de literatuur zijn beschreven [16-21], om de rotigotine plasmaspiegels te simuleren in mensen. Uit de simulaties kon geconcludeerd worden dat toediening met behulp van iontoforese in vergelijking met passieve toediening, twee belangrijke voordelen heeft. Ten eerste was de periode om een bepaalde plasmawaarde te bereiken significant verkort. Ten tweede kon de plasmaconcentratie gemakkelijk getitreerd worden door een aanpassing van de stroomdichtheid. Dit laatste biedt de mogelijkheid om snel en gemakkelijk verschillende toedieningsprofielen te ontwikkelen, aangepast aan de behoefte van de patient.

Naast 5-OH-DPAT en rotigotine zijn andere 2-aminotetralines en structurele analoge verbindingen ook potente agonisten van de D_1- en/of D_2-receptoren in het striatum. Op grond van potentie en moleculaire structuur werden 5 kandidaten geselecteerd: 8-OH-DPAC, 5-OH-EPAT, 5-OH-MPAT, 5,6-di-OH-MPAT and 5,6-di-OH-DPAT [22-28]. Alle verbindingen behoren tot de 2-aminotetralinegroep, behalve 8-OH-DPAC, een chromanamine. In **HOOFDSTUK 5** werden de volgende eigenschappen van deze 5 therapeutische moleculen onderzocht: maximale oplosbaarheid in de donoroplossing, electroforetische mobiliteit, lipofiliteit, en *in vitro* iontoforese transport door HSC en gedermatomiseerde humane huid (DHS). De resultaten werden vergeleken met die van rotigotine en 5-OH-DPAT [11, 14-15]. Hieronder zijn de verbindingen met toenemende oplosbaarheid gerangschikt: rotigotine < 5,6-di-OH-DPAT < 5-OH-DPAT < 5-OH-MPAT < 5-OH-EPAT < 8-OH-DPAC. Uit de daaropvolgende *in vitro* transportstudies bleek dat kleine structurele veranderingen een significante invloed kunnen hebben op de efficiëntie van het transport. 5-OH-EPAT en 5-OH-MPAT hebben een significant hogere flux dan de andere verbindingen door zowel HSC als DHS. Bij alle onderzochte verbindingen bleek dat de flux tijdens iontoforese geen constante waarde bereikte, maar dat de flux gradueel toenam in de tijd. Om dit te beschrijven werd een nieuw kinetisch model

geïntroduceerd. In plaats van 1 afgiftesnelheidsconstante (K_R), zoals eerder gebruikt [8], werden 2 afgiftesnelheidsconstantes (K_{R1}, K_{R2}) geïntroduceerd. Dit model suggereert dat er ten minste 2 transport routes door de huid zijn: 1) een transport route via de haarzakjes, zweet- en talgklieren en 2) een transport route via het stratum corneum [29-33]. Het is daarnaast ook belangrijk om de fysisch-chemische eigenschappen, die verbonden zijn met de verschillende transportparameters, te identificeren. Uit onze studies bleek dat de electroforetische mobiliteit en het moleculair gewicht van de verbindingen gebruikt kunnen worden om het 0^{de} orde massatransport in de huid (I_0) en de afgiftesnelheidsconstante K_{R2} te voorspellen. Ook bleek dat K_{R1} gerelateerd was aan de lipofiliteit, maar verder onderzoek is nodig om deze relatie te bevestigen. Met deze parameters is het mogelijk om flux profielen te simuleren. Bij het selecteren van nieuwe kandidaten kunnen soortgelijke simulaties een grote hulp zijn.

Deel II- De gecontroleerde iontoforetische toediening van (S)-5-OH-DPAT *in vivo*

Uit de *in vitro* transportstudies (**HOOFDSTUK 3)** bleek dat 5-OH-DPAT een geschikte kandidaat is om verder te onderzoeken *in vivo*.

In **HOOFDSTUK 6** werd de gecontroleerde transdermale iontoforetische toediening van het actieve S-enantiomeer van 5-OH-DPAT onderzocht. Deze studies werden uitgevoerd in een rattenmodel. Uit de farmacokinetiek studies bleek dat het iontoforetisch transport *in vivo* een lineair verband vertoonde met de gebruikte stroomdichtheid. Dit komt overeen met de *in vitro* resultaten en bevestigt dat de toegediende dosis gemakkelijk kan worden getitreerd door een aanpassing van de stroomdichtheid. Naast het controleren van de plasmawaarden door middel van iontoforese, was het tweede doel van deze studie om de PK-PD relatie te onderzoeken tijdens een gecontroleerd en omkeerbaar farmacologisch effect. Om de PK-PD relatie te onderzoeken werd eerst een rattenmodel ontwikkeld. Een controle experiment toonde aan dat anesthesie, een potentiaalverschil over de huid en bloedafname geen of slechts een kleine invloed hadden op de dopamine afgifte in het striatum (farmacodynamisch eindpunt). De plasma concentraties en de dopamine afgifte in het striatum werden simultaan in het gevalideerde rattenmodel onderzocht. (S)-5-OH-DPAT werd in de ratten toegediend met transdermale iontoforese of intraveneuze infusie. Intraveneuze en iontoforetische toediening van (S)-5-OH-DPAT resulteerde in een sterke daling van de dopamine afgifte. Dit wijst op een

sterke farmacologische respons. Binnen een periode van 2 uur na het stopzetten van de toediening bereikte de dopamine afgifte weer zijn oorspronkelijke waarde. De experimentele data van deze studies werden uitgebreid geanalyseerd met niet-lineair mixed-effect modellering. De farmacokinetische en farmacodynamische data na transdermale iontoforese en intraveneuze toediening werden simultaan geanalyseerd om de precisie van de schatting van de PK-PD parameters te verhogen. Deze simultane analyse werd ook gebruikt om een onderscheid te maken tussen transport parameters (I_0 en K_R) en geneesmiddel specifieke parameters (V_2, V_3, Cl, Q). De plasmaprofielen tijdens en na iontoforetisch transport werden beschreven met kinetische modellen, ontwikkeld door Nugroho *et al.* [9]. Zoals beschreven voor de *in vitro* situatie, zijn deze modellen ook *in vivo* gebaseerd op de 0^{de} orde massa transfer van donorfase naar de huid en een 1^{ste} orde afgifte van de huid naar de bloedcirculatie. Het bleek dat, in tegenstelling tot de *in vitro* modellen, 1 afgiftesnelheidsconstante (K_R) volstaat om de afgifte van de huid naar de bloedcirculatie nauwkeurig te beschrijven. Wat betreft het farmacodynamische model, werd er een vergelijking gemaakt tussen 2 modellen om de dopamine afgifte in het striatum te beschrijven: 1) indirecte response model type I *vs* 2) effect compartiment model met een sigmoïdaal I_{max} model. Op basis van het Akaike's Information Criterion (AIC) en de visueel voorspellende controle bleek dat het effect compartiment model de dopamine afgifte in het striatum beter beschrijft. Daarnaast bleek uit de covariaat analyse dat de toedieningsnelheid ook een bepalende factor is voor het farmacologisch effect. Het gebruik van een geïntegreerd PK-PD model suggereert dat de plasmaconcentratie vertaald kan worden in een continue stimulatie van de dopamine receptoren in het striatum. Dit kan zeer voordelig zijn voor de symptomatische behandeling van de ziekte van Parkinson. Er wordt namelijk algemeen aangenomen dat continue stimulatie van striatale dopamine receptoren de motor fluctuaties bij chronisch gebruik van dopaminerge geneesmiddelen kan verminderen. Daarnaast kan continue stimulatie ook voordelig zijn voor non-motor complicaties, zoals slaapstoornissen [2].

Deel III- Transdermale iontoforetische toediening van ester prodrugs van 5-OH-DPAT: van synthese tot *in vivo* studies

Door de veelbelovende resultaten van de *in vitro* en *in vivo* studies, uitgevoerd met 5-OH-DPAT, besloten we te onderzoeken of de toepasbaarheid van dit geneesmiddel verder verbeterd kon worden. 5-OH-DPAT werd veresterd met 4 natuurlijk

voorkomende aminozuren: glycine, proline, valine en β-alanine. In vergelijking met het moedermolecule 5-OH-DPAT, bevatten de prodrugs een extra amine-groep. Hierdoor kunnen deze prodrugs in een geselecteerd pH-gebied twee positieve ladingen bezitten. 5-OH-DPAT heeft maximaal slechts 1 positieve lading.

In **HOOFDSTUK 7** werden de volgende eigenschappen van deze prodrugs nauwkeurig onderzocht: chemische stabiliteit, oplosbaarheid en transdermaal iontoforetisch transport. De invloed van pH, temperatuur, iontoforese en HSC op de stabiliteit van de prodrugs werd onderzocht. Een verhoging van de pH en van de temperatuur verminderde de stabiliteit van de prodrugs. Iontoforese en de aanwezigheid van HSC in de oplossing hadden echter geen meetbare invloed op de stabiliteit. Op basis van deze resultaten, werden de meest stabiele verbindingen geselecteerd om verder te onderzoeken: valine- en β-alanine-5-OH-DPAT. Ten opzichte van 5-OH-DPAT, was de maximale oplosbaarheid in de donorfase van valine- en β-alanine-5-OH-DPAT, respectievelijk 4 en meer dan 14 maal groter. Hierdoor kan de pleister aanzienlijk worden verkleind zonder de hoeveelheid beschikbaar geneesmiddel voor iontoforese te verminderen. Uit iontoforetische *in vitro* transportstudies door HSC en DHS bleek dat het lipofielere valine-5-OH-DPAT minder efficiënt door iontoforese werd getransporteerd dan 5-OH-DPAT. De hydrofielere prodrug, β-alanine-5-OH-DPAT werd met dezelfde efficiëntie als 5-OH-DPAT door HSC getransporteerd. Echter wanneer DHS werd gebruikt, werd de prodrug β-alanine-5-OH-DPAT 40% efficiënter getransporteerd. Tijdens transdermaal transport werden beide prodrugs aanzienlijk afgebroken tot het moedermolecule 5-OH-DPAT. De afbraak was prominenter tijdens transport door DHS. Op basis van deze *in vitro* resultaten werd β-alanine-5-OH-DPAT gekozen om verder te onderzoeken *in vivo*. Een reeks iontoforese transportstudies werden uitgevoerd met het actieve S-enantiomeer van β-alanine-5-OH-DPAT en de resultaten van deze studie werden vergeleken met de resultaten van (S)-5-OH-DPAT (**HOOFDSTUK 6**). Ondanks een efficiënter transport *in vitro*, werden lagere plasmawaarden waargenomen tijdens iontoforetische toediening van β-alanine-(S)-5-OH-DPAT dan tijdens de toediening van (S)-5-OH-DPAT. Echter de plasmawaarden post iontoforese waren hoger na toediening van de prodrug. Dit kan wellicht verklaard worden door een vertraagde afgifte van het actief bestanddeel vanuit de huid naar de bloedcirculatie veroorzaakt door hydrolyse en ophoping in de huid. Ondanks dit verschil in farmacokinetiek, bereikte het farmacologisch effect na toediening van β-alanine-(S)-5-OH-DPAT een zelfde maximale waarde, maar het farmacologisch effect hield wel langer aan. De plasma concentraties en de dopamine afgifte werden geanalyseerd met een geïntegreerd PK-PD model. Er werd in het model rekening gehouden met hydrolyse en ophoping van de prodrug in de huid

tijdens iontoforetisch transport. Hiervoor werd een additioneel parallel compartiment geïntroduceerd tussen de huid en het centrale compartiment. Net als bij (S)-5-OH-DPAT werd een effect compartiment model gebruikt om de dopamine afgifte in het striatum te beschrijven. Deze resultaten tonen aan dat met behulp van prodrugs-synthese de fysisch-chemische eigenschappen, het plasma profiel en het farmacologisch effect aangepast kunnen worden. De prodrug β-alanine-(S)-5-OH-DPAT bezit een gebalanceerde stabiliteit en een hoge transportefficiëntie en kan daarom beschouwd worden als een veelbelovende kandidaat voor de symptomatische behandeling van de ziekte van Parkinson.

Conclusie

In dit proefschrift worden verschillende benaderingen beschreven om het iontoforetisch transport van dopamine agonisten te verbeteren. Daarnaast wordt in dit proefschrift ook een raamwerk gepresenteerd om nieuwe kandidaat moleculen te screenen voor transdermale iontoforese. In dit raamwerk werden de fysisch-chemische eigenschappen van de moleculen, de transport eigenschappen *in vitro* en de toepassing *in vivo* met elkaar verbonden. Dit raamwerk wordt ondersteund door kinetische modellen, die de transport profielen beschrijven tijdens en na iontoforese. Deze modellen kunnen gebruikt worden om simulaties uit te voeren en om nieuwe studies te ontwerpen. Deze kinetische modellen kunnen ook helpen om meer inzicht te krijgen in de *in vitro-in vivo* relatie en de PK-PD relaties. Verschillende van de onderzochte moleculen in dit proefschrift lieten veelbelovende resultaten zien *in vitro* en/of *in vivo*. Deze resultaten geven aanleiding tot verdere (pre)klinische ontwikkeling van een geschikte symptomatische behandeling van de ziekte van Parkinson met behulp van transdermale iontoforese.

References

1. Hornykiewicz, O., *L-DOPA: from a biologically inactive amino acid to a successful therapeutic agent.* Amino Acids, 2002. **23**(1-3): p. 65-70.
2. Tugwell, C., *Parkinson's disease in focus*. 1st ed. In focus. 2008, London: Pharmaceutical Press. 237.
3. Lim, E., *A walk through the management of Parkinson s disease.* Ann Acad Med Singapore, 2005. **34**(2): p. 188-95.
4. Antonini, A. and P. Barone, *Dopamine agonist-based strategies in the treatment of Parkinson's disease.* Neurol Sci, 2008. **29 Suppl 5**: p. S371-4.
5. Yamamoto, M. and A.H. Schapira, *Dopamine agonists in Parkinson's disease.* Expert Rev Neurother, 2008. **8**(4): p. 671-7.
6. Steiger, M., *Constant dopaminergic stimulation by transdermal delivery of dopaminergic drugs: a new treatment paradigm in Parkinson's disease.* Eur J Neurol, 2008. **15**(1): p. 6-15.
7. Sage, B.H., *Ionotphoresis*, in *Percutaneous penetration enhancers*, E.W. Smith and H.I. Maibach, Editors. 1995, CRC Press: Boca Raton. p. 351-368.
8. Nugroho, A.K., et al., *Compartmental modeling of transdermal iontophoretic transport: I. In vitro model derivation and application.* Pharm Res, 2004. **21**(11): p. 1974-84.
9. Nugroho, A.K., et al., *Compartmental modeling of transdermal iontophoretic transport II: in vivo model derivation and application.* Pharm Res, 2005. **22**(3): p. 335-46.
10. Nugroho, A.K., et al., *Pharmacokinetics and pharmacodynamics analysis of transdermal iontophoresis of 5-OH-DPAT in rats: in vitro-in vivo correlation.* J Pharm Sci, 2006. **95**(7): p. 1570-85.
11. Nugroho, A.K., et al., *Transdermal iontophoresis of the dopamine agonist 5-OH-DPAT in human skin in vitro.* J Control Release, 2005. **103**(2): p. 393-403.
12. *UCB announces The U.S. Launch of Neupro® (Rotigotine Transdermal System) for the Treatment of Early-Stage Parkinson's Disease*. 2007, UCB Milwaukee (USA).
13. *EMEA. European Public Assessment Report (EPAR), annex I: summary of product characteristics for Neupro.*

Available from http://www.emea.europa.eu/humandocs/PDFs/EPAR/neupro/H-626-PI-en.pdf 2009.

14. Nugroho, A.K., et al., *Transdermal iontophoresis of rotigotine across human stratum corneum in vitro: influence of pH and NaCl concentration.* Pharm Res, 2004. **21**(5): p. 844-50.
15. Nugroho, A.K., et al., *Transdermal iontophoresis of rotigotine: influence of concentration, temperature and current density in human skin in vitro.* J Control Release, 2004. **96**(1): p. 159-67.
16. Cawello, W., M. Braun, and H. Boekens, *Absorption, disposition, metabolic fate, and elimination of the dopamine agonist rotigotine in man: administration by intravenous infusion or transdermal delivery.* Drug Metab Dispos, 2009. **37**(10): p. 2055-60.
17. Cawello, W., M. Braun, and R. Horstmann, *Pharmacokinetics of transdermal rotigotine in subjects with impaired renal function* in *ACCP 34th Annual Meeting*. 2005: Rockville, MD.
18. Cawello, W., et al., *Pharmacokinetics, safety and tolerability of rotigotine after transdermal patch administration in Japanes and Caucasian healthy subjects.* Mov Disord, 2006. **21(S15)**: p. S547.
19. Cawello, W., et al., *Characteristics of Rotigotine Elimination after patch removal.* European Journal of Neurology, 2006. **13(suppl2)**: p. 85.
20. Cawello, W., et al., *Transdermal administration of radiolabelled [14C]rotigotine by a patch formulation: a mass balance trial.* Clin Pharmacokinet, 2007. **46**(10): p. 851-7.
21. Schwarz pharma, L. *Neupro®*. 2007.

22. Beart, P.M., et al., *Radioreceptor binding reveals the potencies of N,N-disubstituted 2-aminotetralins as D2 dopamine agonists.* Naunyn Schmiedebergs Arch Pharmacol, 1987. **336**(5): p. 487-93.
23. Beaulieu, M., et al., *N,N-disubstituted 2-aminotetralins are potent D-2 dopamine receptor agonists.* Eur J Pharmacol, 1984. **105**(1-2): p. 15-21.
24. Hacksell, U., et al., *N-Alkylated 2-aminotetralins: central dopamine-receptor stimulating activity.* J Med Chem, 1979. **22**(12): p. 1469-75.
25. Horn, A.S., et al., *Synthesis and dopaminergic activity of a new oxygen isostere of the 2-aminotetralins: N,N-dipropyl-8-hydroxy-3-chromanamine.* Eur J Med Chem, 1988. **22**(4): p. 325-328.
26. Thorberg, S.O., et al., *Aminochromans: potent agonists at central dopamine and serotonin receptors.* Acta Pharm Suec, 1987. **24**(4): p. 169-82.
27. van Vliet, L.A., et al., *Affinity for dopamine D2, D3, and D4 receptors of 2-aminotetralins. Relevance of D2 agonist binding for determination of receptor subtype selectivity.* J Med Chem, 1996. **39**(21): p. 4233-7.
28. Vermue, N.A., et al., *Pharmacological profile of N,N dipropyl-8-hydroxy-3-chromanamine, an oxygen isostere of the dopamine agonist N,N dipropyl-5-hydroxy-2-aminotetralin with enhanced presynaptic selectivity.* Arch Int Pharmacodyn Ther, 1988. **293**: p. 37-56.
29. Alvarez-Roman, R., et al., *Visualization of skin penetration using confocal laser scanning microscopy.* Eur J Pharm Biopharm, 2004. **58**(2): p. 301-316.
30. Barry, W., ed. *Dermatological formulations. Percutaneous Absorption.* . 1983: New York: Marcel Dekker.
31. Cullander, C., *What are the pathways of iontophoretic current flow through mammalian skin?* Adv Drug Deliv Rev, 1992. **9**: p. 119-135.
32. Henchoz, Y., et al., *A fast screening strategy for characterizing peptide delivery by transdermal iontophoresis.* J Control Release, 2009.
33. Turner, N. and R.H. Guy, *Iontophoretic transport pathways: dependence on penetration physcicochemical properties.* J Pharm Sci, 1997. **86**(12): p. 1385-1389.

List of abbreviations

AAEC	area above the effect curve
ACN	acetonitrile
AIC	Akaike's information criterion
AUC	area under the curve
C.I.	confidence interval
C_{DA}	striatal dopamine concentration
CE	capillary electrophoresis
CL	central clearance
cLogP	calculated logP
C_m	concentration of the molecule
C_{max}	maximum plasma concentration
C_p	plasma concentration
C_s	striatal concentration
CZE	capillary zone electrophoresis
DA	dopamine agonists
DBS	deep brain stimulation
DHS	dermatomed human skin
DLB	dementia with Lewy Bodies
EFF	pharmacodynamic efficiency
F	bioavailability
$Flux_{pss}$	passive steady state flux
$Flux_{ss}$	steady state flux
$Flux_{9h}$	flux after 9h of current application
H	Hill-slope coefficient
HPLC	high pressure liquid chromatography
HSC	human stratum corneum
I_0	zero-order iontophoretic mass transfer
IC_{50}	the concentration of the drug required to produce 50% of I_{max}
I.D.	inner diameter
IDR	indirect response
I_{max}	the maximum inhibition of the dopamine production
IPRED	individual prediction
IV	intravenous
J	flux

J(t)	flux at time t
J_{EM}	electromigrative flux
J_{EO}	electroosmotic flux
J_{pass}	passive flux
J_{ss}	steady state flux
k	elimination rate constant
k_{e0}	distribution rate constant from plasma to effect compartment elimination rate constant from effect compartment
k_{ij}	distribution rate constant from compartment i to compartment j
k_{in}	zero order rate constant for the production of response
k_{out}	first order rate constant fro the loss of response
K_R	first order skin release constant
K_{R1}	first order skin release constant for first (fast) transport route
K_{R2}	first order skin release constant for second (slow) transport route
LC	liquid chromatography
L_{eff}	the distance from the inlet to the detection point
LOD	limit of detection
LOQ	limit of quantification
L_{tot}	total distance of the capillary
MS	mass spectrometry
MSA	multiple system atrophy
MV	molecular volume
Mw	molecular weight
μ_{eff}	electrophoretic mobility
μ_{EOF}	electrophoretic mobility of the electroosmotic marker
μ_{obs}	electrophoretic mobility of the compound
O.D.	outer diameter
Pass	zero-order drug input due to passive diffusion corrected for the surface area (passive flux post iontophoresis)
PBS	phosphate buffered saline
PD	pharmacodynamic(s)
Pd	Parkinson's disease
PK	pharmacokinetic(s)
P_{PI}	zero-order drug input due to passive diffusion
PRED	population prediction
PSP	progressive supranuclear palsy
Q	peripheral clearance
RP	reversed phase

RSE	relative standard error of the estimate
RT	retention time
S	surface area of the patch
SC	stratum corneum
SD	standard deviation
SE	standard error of the estimate
SEM	standard error of the mean
SNc	substantia nigra pars compacta
SPE	solid phase extraction
T	time of current application
TEA	triethylamine
t_{EOF}	time required to reach the detection point for the electroosmotic marker
THF	tetrahydrofuran
t_L	kinetic lag time parameter
T_{max}	time to reach maximum plasma concentration or maximum effect
t_{obs}	the time required to reach the detection point for the analyte
V2	central volume
V3	peripheral volume
V_d/F	apparent volume of distribution
VPC	visual predictive check
V_w	water flow
	volume flow
$X_n(t)$	drug amount at time t in compartment n
λ_{em}	emission wavelength
λ_{ex}	excitation wavelength

List of publications

Papers

O.W. Ackaert, J. Van Smeden, J. De Graan, D. Dijkstra, M. Danhof, J.A. Bouwstra. Mechanistic studies of the transdermal iontophoretic delivery of 5-OH-DPAT *in vitro*. *Journal of Pharmaceutical Sciences.* 2010 Jan;99(1):275-85

O.W. Ackaert, J. Eikelenboom, H.M. Wolff, J.A. Bouwstra. Comparing different salt forms of rotigotine to improve transdermal iontophoretic delivery. *Journal of pharmaceutics and biopharmaceutics.* 2010 Feb;742):304-10

O.W. Ackaert, J. De Graan, R. Capancioni, D. Dijkstra, M. Danhof, J.A. Bouwstra. Transdermal iontophoretic delivery of a novel series of dopamine agonists *in vitro*: physicochemical considerations. *Journal of pharmacy and pharmacology.* 2010. *in press*

O.W. Ackaert[*], J. De Graan[*], R. Capancioni, O.E. Della Pasqua, D. Dijkstra, B.H. Westerink, M. Danhof, J.A. Bouwstra. The *in vitro* and *in vivo* evaluation of new synthesized prodrugs of 5-OH-DPAT for iontophoretic delivery. *Journal of controlled release.* 2010. *in press*

O.W. Ackaert[*], J. De Graan[*], S. Shi, R. Vreeken, O.E. Della Pasqua, D. Dijkstra, B.H. Westerink, M. Danhof, J.A. Bouwstra. Controlling the pharmacokinetics and the pharmacodynamic effect of (S)-5-OH-DPAT with transdermal iontophoresis. 2010. *submitted for publication*

J. de Graan, **O.W. Ackaert**, A. Boltjes, J.A. Bouwstra, B.H. Westerink, D. Dijkstra. Synthesis and evaluation of the chemical and enzymatic stability of a series of novel amino acid prodrugs of the potent dopamine D2 agonist (S)-5-OH-DPAT developed for transdermal iontophoresis. *Manuscript in preparation*

[*]contributed equally as first author.

Curriculum Vitae

Oliver Ackaert was born on June 20th 1981 in Turnhout, Belgium. After his graduation in 1999 at the St-Jozefscollege in Turnhout, Belgium, he started his study pharmacy at the Katholieke Universiteit in Leuven, Belgium. During his study, he specialized in biopharmaceutical sciences. In July 2004 Oliver became a licensed pharmacist and in October of that year he started a research internship at the Department of Drug Delivery Technology at the Leiden\Amsterdam Center for Drug Research (LACDR), University of Leiden, Leiden, The Netherlands. In May 2005 Oliver started at the same department his PhD project under the supervision of Prof. Dr. Joke Bouwstra (Drug Deliver Technology) and Prof. Dr. Meindert Danhof (Pharmacology). This STW project was in collaboration with the department of Medicinal Chemistry of the University of Groningen, The Netherlands. From January 2010 he is working as a consultant Pharmacokinetics-Pharmacodynamics at LAP&P Consultants BV in Leiden, The Netherlands.

Nawoord

Een proefschrift is de samenvatting van het werk van een assistent in opleiding (‘AIO’), waar hij of zij gedurende vier tot vijf jaar van zijn leven aan heeft gewijd. Het tot stand komen van dit proefschrift was enkel mogelijk met de hulp van vele verschillende mensen. Zonder jullie was dit boekje er nooit geweest en daarom wil ik graag mijn dankbaarheid uitdrukken.

Om geneesmiddelen te formuleren en door de huid te transporteren heb je geschikte verbindingen nodig. Hiervoor kon ik rekenen op de deskundigheid en toewijding van Jeroen, mijn collega AIO aan de Universiteit van Groningen. Jeroen, we zijn ongeveer samen gestart met ons promotieonderzoek. De passie voor de organische chemie, je enthousiasme, onze (msn)-conversaties hebben mij steeds geïnspireerd en scherp gehouden. Het was een uitdagende zoektocht die we ook samen geëindigd zijn met de studies in Groningen. Op het einde waren we echt een geoliede machine, die goed op elkaar inspeelde. Ik zal met plezier terugkijken op onze samenwerking en ik denk dat we trots mogen zijn op het resultaat dat we hebben bereikt.

1 tot 2 keer per jaar hadden we een vergadering met de leden van de gebruikerscommissie van het STW-project. Hoewel jullie niet steeds aanwezig konden zijn op alle vergaderingen van de commissie, werd jullie input toch steeds heel sterk gewaardeerd. Speciaal wil ik Ronald van der Geest bedanken. Ronald, jij was bijna altijd aanwezig op de vergaderingen van de gebruikerscommissie. Jouw opmerkingen en aanwijzingen waren heel waardevol en plaatsten het geheel steeds in een ander perspectief. Dit bracht het academische onderzoek dicht bij de farmaceutische toepassing.

Je begint als jonge AIO met weinig ervaring aan je onderzoek. Gelukkig kon ik rekenen op de steun en hulp van de mensen bij de Sectie Drug Delivery Technology van het LACDR. In de beginfase van mijn onderzoek leerden Dirk-Jan en Ferry mij de ‘ins’ and ‘outs’ van iontoforese en HPLC. Dit vormde een goede basis om later zelf met deze technieken verder te gaan. Na het vertrek van Dirk-Jan kon ik steeds rekenen op de assistentie van Stefan, die altijd klaarstond en waarvoor niets te moeilijk of te vervelend was. Stefan, zonder jouw technische hulp bij de HPLC en bij de omschakeling van Adchrom naar Empower stond onze afdeling Drug Delivery Technology (DDT) nu nog in zijn HPLC-kinderschoenen. Ook bij de dierproeven in Leiden en in Groningen was je van onmisbare waarde. Kharis, the ending of your PhD was the beginning of mine. I really appreciate your efforts to help me

understand the principles of iontophoretic transport and how to translate this knowledge into kinetic models.

Thanks to the help of Erik and later Romano I was able to gather the precious results, presented in this thesis. Romano, you started off as a student and continued on the same project as a technician. You performed a lot of transport studies well organized and with care. You were always on top of things and did everything with a smile. Besides your excellent work, I also appreciate very much the time we spent together in and outside the lab. Ik heb ook de hulp van Connie altijd zeer gewaardeerd; jij zorgde er altijd voor dat alles in goede banen werd geleid, dat deadlines op tijd werden gehaald, afspraken niet vergeten werden. En voor een gezellige babbel was ik bij jou ook aan het juiste adres.

Voor de technische aangelegenheden kon ik aan de deur kloppen bij Raphaël Zwier en later ook Mirthe Bergman van de fijn mechanische afdeling (FMD). Ik waardeer jullie bijdrage aan het project door het maken van de ionto-patches en de 'Fill and Twist'. Ook kon ik ook op de kennis rekenen van Rob Vreken en Shanna Shi van ABS voor het analyseren van mijn plasmamonsters.

Daarnaast was de hulp en begeleiding van Oscar Della-Pasqua ook zeer belangrijk, vooral het ontwikkelen en toepassen van de modellen om de *in vitro* en *in vivo* resultaten te beschrijven. Oscar, jij hebt mij geïntroduceerd in de wereld van de PK-PD analyse. Met veel geduld en toewijding heb je de basis gelegd van het modelleren. De bijeenkomsten die we hadden waren steeds heel efficiënt en nuttig. Dankzij jou heb ik ook de smaak te pakken gekregen van het modelleren en ga ik hierin verder.

Het begeleiden van masterstudenten hoort ook bij het AIO-bestaan. Christina en Jeroen, dankzij jullie is het project een heel stuk verder gekomen. Het was niet altijd even gemakkelijk en soms werd er wat meer tijd en inspanning gevraagd van jullie. Maar jullie deden het onderzoek steeds met de glimlach. Jeroen, ik ben blij en trots dat je ook nu zelf als AIO bij DDT aan de slag bent gegaan.

Ook in Groningen werd ik goed ontvangen en opgevangen. Het was niet gemakkelijk om de *in vivo* proeven te plannen en te regelen vanuit Leiden. Maar dankzij de hulp van Gunnar Flik, Thomas Cremers, Karola Jansen en de overige medewerkers van Brains on-Line konden deze proeven netjes ingepland en uitgevoerd worden. Deze hulp werd zeer gewaardeerd.

It is important that technically everything is running smoothly, but it is also very important to have a good working atmosphere. During my time at the DDT-team there always was an inspiring, stimulating, but also relaxed atmosphere. Besides

working, there was also time for a joke, a nice chat, a game of indoor soccer,…. This made the trip from and to Roosendaal a lot less intense. Although at the Division of Drug Delivery Technology people were coming and going, the 'gezellige' atmosphere was constantly present thanks to Miranda & Miranda, Maytal, Julia, Wouter, Marc, Mogjan, Nazmoen, Gert, Jacob, Dennis, Tomo, Diogenes, Tue, Elly, Aat, Sun, Andrea, Robert, Vasco, Varsha, Christophe, Michelle, Wim, Myrra, Basak, Riccardo, Suzanne, Bram, Ana and the many Erasmusstudents that visited our lab. I will look back with great pleasure at our collaborations, the lunch-club, 'lab-uitjes' and various field trips (Biopharmacy Day, GPEN, pubcrawl(s),…). There are three people from the DDT-team I would like to acknowledge in particular. Robert and Ding, around the same time, we started our PhD-adventure in Leiden. And an adventure it was. We dealt with the same hazards, shared the same frustrations, but also enjoyed many nice moments, which I will never forget. Daniel, ik zal de gezellige tijd 'at the office' en daarbuiten niet snel vergeten. Onze theoretische discussies, de senseo-coffee breaks, maar ook de tennis games na het werk waren altijd plezierig. En als de laatste trein richting Roosendaal net iets te vroeg vertrok, kon ik bij jou altijd terecht. I'm very grateful for your friendship and I'm proud that the three of you are my paranimphs today.

Om aan de druk en besognes van het proefschrift te ontsnappen kon ik ook altijd rekenen op mijn familie en vrienden in België. Onze weekends waren tijdens de laatste vier jaar altijd druk bezet met feestjes, dinertjes, of gewoon een gezellig 'after-work-pintje' op vrijdag. Bedankt voor alle mooie momenten, die we samen al hebben beleefd en dat onze vriendschap nog lang mag blijven duren. Ook bij de familie Box in Neerpelt voel ik mij altijd zeer welkom, wat ik heel hard apprecieer.

Lieve paps en mams, Mike en Dons, jullie hebben mij altijd veel liefde, vriendschap, plezier, steun en nog zoveel meer gegeven. Ik ben heel dankbaar voor alle kansen, die ik heb gekregen. Jullie zijn van onschatbare waarde geweest, ook bij het tot stand komen van deze thesis.

Liefste Vienie, we zijn nu bijna vijf jaar geleden samen aan dit 'hollands' avontuur begonnen. Door dik en dun heb je mij gesteund en je hebt mij geleerd wat meer te relativeren. Zonder jouw liefde, onvoorwaardelijke steun, ondernemingszin en organisatietalent zou ik niet zo ver staan als nu. Ik ben blij dat ik elke dag bij jou kan thuiskomen in ons appartementje in Roosendaal. Ik zie je graag.

Ik heb geschreven.

Oliver